universität wien

DISSERTATION

Titel der Dissertation

Drug resistance and virulence of the human fungal pathogen *Candida glabrata*

angestrebter akademischer Grad

Doktor der Naturwissenschaften (Dr. rer. nat.)

Verfasser:	Diplom-Biologe Univ. Tobias Schwarzmüller
Matrikel Nummer:	0409984
Dissertationsgebiet (lt. Studienblatt):	Genetik-Mikrobiologie
Betreuer:	Ao Univ.-Prof. Dr. Karl Kuchler

Wien, am 12. August 2009

“Das Gras wächst nicht schneller, wenn man daran zieht”

from Sambia

TABLE OF CONTENTS

1 Zusammenfassung

Candida glabrata ist ein opportunistischer humanpathogener Pilz. Nach *Candida albicans* stellt er die zweithäufigste Ursache für Pilzerkrankungen durch *Candida* spp. dar. Die Infektion mit *C. glabrata* kann zu Erkrankungen der Haut oder der Schleimhäute bis hin zur lebensbedrohlichen systemischen Infektion bei immunsupprimierten Patienten führen. Hauptvirulenzfaktoren von *C. glabrata* sind sowohl eine erhöhte natürliche Resistenz gegen Azolverbindungen, als auch eine große Anzahl verschiedener Adhesine. Welche molekularen Mechanismen diesen Virulenzfaktoren zu Grunde liegen, ist größtenteils noch unbekannt.

Genomik und phänotypische Analyse von Deletionsmutanten stellen einen Ansatz dar, um neue Virulenzfaktoren pathogener Pilzen zu identifizieren. Für diese Doktorarbeit wurden *C. glabrata* Sequenzdaten verwendet, um nicht essentielle, zu *Saccharomyces cerevisiae* homologe Gene auszuwählen. Mit Hilfe eines revers-genetischen Ansatzes wurde dann eine Kollektion von Deletionsmutanten erstellt. Diese Stammbibliothek diente als Ausgangsbasis für die phänotypische Analyse der Mutanten zur Identifizierung neuer Gene, die die Pathogenität und Azolresistenz von *C. glabrata* beeinflussen. Insgesamt umfasst die Kollektion 476 einzelne, mit einem molekularen Barcode versehene Stämme, bei denen Signaltransduktionsgene, Transkriptionsfaktoren, Zellwandbiosynthesegene, Resistenzgene und *C. glabrata* spezifische Gene deletiert wurden. Es wurden 103 Mutanten identifiziert, die Wachstumsdefekte unter Zellwandstress, in Gegenwart von Antimykotika, bei Temperaturstress, Osmolaritätsänderungen, Kontakt mit Detergenzien oder beim Wachstum auf Minimalmedium aufzeigen.

Die Interaktion zwischen Makrophagen und *C. glabrata* wurde *in vitro* durch die Detektion von reaktiven Sauerstoffmolekülen (ROS) getestet. Dadurch wurden mehrere Zellwandmutanten entdeckt, die eine erhöhte ROS-Produktion durch die Makrophagen verursachen.

Mehrere Deletionsstämme zeigten Phänotypen, die sich von den bekannten *S. cerevisiae* Mutanten unterscheiden. Es konnten Gene identifiziert werden, die noch nicht mit Caspofunginsensitivität assoziiert worden sind. Darunter befanden sich auch Gene, die keine Orthologe in *S. cerevisiae* haben.

Cg*CBK1* wurde aufgrund des schweren Zellteilungsdefekts näher charakterisiert. Die Transkriptionsanalyse des Cg*cbk1*Δ Stammes zeigte, dass bestimmte Zellwandgene unterschiedlich exprimiert werden.

Diese Sammlung von Deletionsstämmen ist eine der größten weltweit und ist somit von sehr großem Nutzen für das Studium der Pathogenität von *C. glabrata*. Zukünftige *in vivo* Experimente werden unter Ausnützung der integrierten „molekularen Barcodes“ die Identifizierung neuer Virulenzfaktoren ermöglichen.

2 Summary

Candida glabrata is an opportunistic human fungal pathogen. It is the second most frequent cause of *Candida*-derived infections after *Candida albicans*. Infection with either one of the two pathogenic fungi can result in diseases ranging from superficial cutaneous or mucosal to life-threatening systemic infections in immunocompromised individuals. Well-documented virulence attributes of *C. glabrata* are the inherent reduced azole susceptibility and a large repertoire of adhesin genes, which are regulated by transcriptional silencing. However, the molecular basis of *C. glabrata* antifungal drug resistance and additional virulence factors is not well understood.

The combination of fungal genomics and large-scale phenotypic profiling of deletion mutants represents a powerful approach to identify new factors contributing to fungal virulence. For this doctoral thesis, the *C. glabrata* genome sequence data were used to select genes with non-essential functional orthologues of the non-pathogenic yeast *Saccharomyces cerevisiae*. Based on this selection, a large-scale reverse genetics approach was initiated to identify novel genes implicated in *C. glabrata* pathogenicity and drug resistance. A bar-coded *C. glabrata* deletion strain collection was engineered comprising some 500 single gene deletion mutants affected in signaling functions, regulation of gene expression, cell wall biogenesis, transport processes, drug resistance, stress response and metabolism. Phenotypic profiling identified a total of 103 *C. glabrata* genes involved in resistance to cell wall-perturbing compounds, antifungal drugs, heat stress, osmosensitivity, metal ion or detergent tolerance, growth on minimal medium and phenotypic switching.

Host-pathogen interaction related phenotypes were analyzed using an *in vitro* assay detecting reactive oxygen species (ROS). Screening for ROS elicited by primary mouse bone-marrow-derived macrophages co-incubated with *C. glabrata* mutants resulted in the identification of mutants lacking cell wall-related genes.

Taken together, numerous deletion strains showed growth phenotypes different from known phenotypes of *S. cerevisiae*. For example, genes were identified, which have previously not been associated with sensitivity to the glucan synthase inhibitor Caspofungin. This also included *C. glabrata* genes, which do not have orthologues in baker's yeast.

The function of Cg*CBK1* gene has been studied in more detail, because it exhibits severe cell separation defects. Transcriptional profiling of this mutant showed differential expression of a distinct set of genes with cell wall-associated functions.

In summary, the generated *C. glabrata* gene deletion strain collection is one of the largest collections of fungal deletion strains in the world and represents a powerful tool to study the virulence of a human fungal pathogen. Future studies based on the *in vitro* results will exploit the signature-tag strategy to identify novel virulence-associated factors *in vivo*.

3 Introduction

3.1 The fungal jungle

Life is divided into three major domains: *Eukaryota*, *Bacteria* and *Archaea*. The idea to classify all living beings into specific groups goes back to the founder of taxonomy, Carolus Linnaeus. He tried to sort the diversity of life into systematic hierarchical categories. In 1969 the ecologist Robert Whittaker proposed a new classification introducing five kingdoms including animalia, plantae, fungi, protista and monera (Whittaker, 1969). Having been considered to be plants for a long time, this classification created an own taxonomic kingdom for fungi. It is estimated that the kingdom of fungi consists of up to 1.5 million different species, which evolved over more than 500 million years. Fungi comprise seven proposed phyla: *Dikarya* (*Ascomycota* and *Basidiomycota*), *Microsporidia*, *Chytridiomycota*, *Neocallimastigomycota*, *Blastocladiomycota* and *Glomeromycota* (Hibbett *et al.*, 2007). The vast number of different fungal species is also vividly reflected in their enormous morphological diversity in nature. Fungi are able to grow in vastly different environments, occupying great many distinct ecological niches. They display numerous different morphologies, and can live as symbionts, commensals and pathogens. They are found in soil or on fruits, as well as on the skin or in the gastro-intestinal tract of many mammals. Commonly known examples for a symbiotic form of fungi are lichens, which consist of a fungal and a photosynthetic organism. Fungi have also been exploited by humans, who benefit from the fungal capability to ferment soy, rice and malt and to synthesize antimicrobial substances.

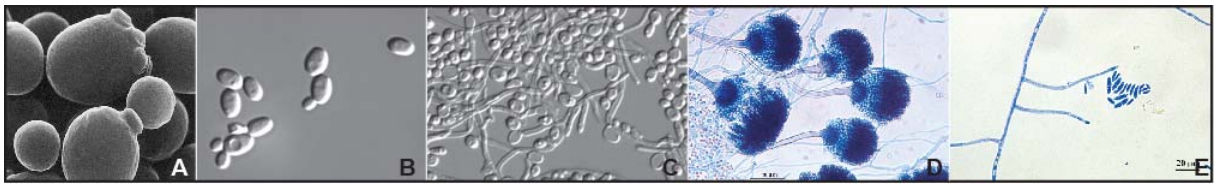

Figure 1. Different fungal organisms A) Electron micrograph of non-pathogenic *S. cerevisiae* (taken from www.bath.ac.uk/bio-sci/research/profiles/wheals-a.html); **B)** DIC image of *C. glabrata*; **C)** Yeast, pseudohyphal, and true hyphal cells of *C. albicans* (Berman & Sudbery, 2002); **D)** *A. fumigatus* **E)** *F. solani* (taken from www.mycology.adelaide.edu.au)

Although fungi are found virtually everywhere, there are only about 300 fungal species causing diseases in humans (Taylor *et al.*, 2001). These pathogenic fungi include organisms across the whole phylum (Figure 1 and 2), including *Ascomycota* such as *Candida* spp., *Aspergillus* spp. and *Fusarium* spp., *Basidiomycota* such as *Cryptococcus neoformans*, *Zygomycetes* such as *Rhizopus oryzae*, and dermatophytes such as *Trichophyton rubrum*.

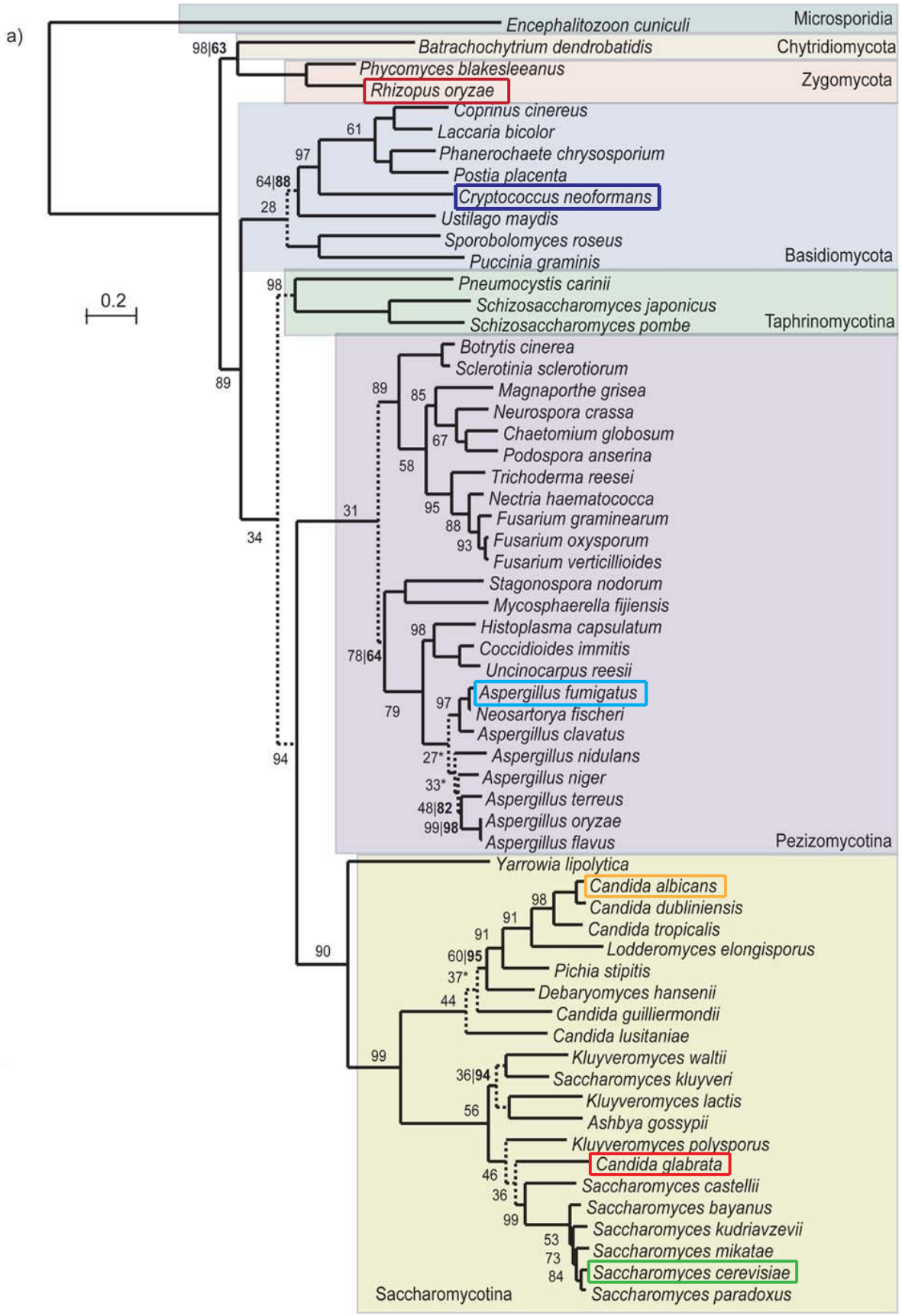

Figure 2. Fungal phylogeny: the phylogeny displays the relationship of 60 taxa, including pathogenic and non-pathogenic fungi such as the *C. glabrata*, *C. albicans*, the non-pathogenic baker's yeast *S. cerevisiae*, as well as more distantly related but medical relevant species such as *A. fumigatus*, *C. neoformans* or *R. oryzae* (taken from (Marcet-Houben & Gabaldon, 2009))

3.2 Medical relevance of fungal pathogens

Fungal organisms can cause a variety of infections, with superficial cutaneous mycoses representing most prevalent infections. A public health problem of increasing importance is the emergence of opportunistic mycoses. *Candida* and *Aspergillus* spp. are the most frequent causes of mycoses-related deaths and are associated with high morbidity and mortality (Horn *et al.*, 2009, Mean *et al.*, 2008, Nace *et al.*, 2009, Neofytos *et al.*, 2009, Pfaller & Diekema, 2007, Wenzel & Gennings, 2005).

The most important causative fungal agent worldwide remain *Candida* spp. *Candida* spp. represent the fourth-leading cause of hospital-acquired infections and account for about 8 to 10% of all nosocomial blood stream infections (Edmond *et al.*, 1999, Wisplinghoff *et al.*, 2004). The overall mortality of systemic *Candida* infections can be as high as 40% (Pfaller & Diekema, 2007, Gudlaugsson *et al.*, 2003, Wenzel & Gennings, 2005). The second most frequent cause of nosocomial infections are *Aspergillus* spp., whereas infections with other molds such as *Mucorales* or *Fusarium* are relatively rare but increasing (Fridkin, 2005, Marr *et al.*, 2002, Pfaller & Diekema, 2004a, Richardson & Lass-Florl, 2008, Nucci & Marr, 2005).

Several factors influence the predisposition to acquire fungal infections. Immunocompromised individuals are at high risk. Well-established risk factors comprise organ or bone marrow transplantation, acquired immune deficiency syndrome, neutropenia, intensive chemotherapy regimens, as well as long-term hospitalization and intensive care unit stays. Additional conditions include mucosal and cutaneous barrier disruptions, neutrophil dysfunctions, and defects in cell-mediated immunity. Further, metabolic disorders, extremes of ages, indwelling vascular catheters, and the increasing use of broad-spectrum antibiotics are considered as risk factors (Safdar *et al.*, 2001, Pfaller & Diekema, 2007, Richardson & Lass-Florl, 2008).

Invasive fungal infections are associated with significant medicare costs and with longer hospital stays (Morgan *et al.*, 2005, Pfaller & Diekema, 2007). Because the incidence and mortality of fungal infections are increasingly frequent problems in the nosocomial setting, the development of new antifungal drugs and diagnostic tools are urgently needed. Recent epidemiological studies also observed a shift to non-*albicans Candida* spp., such *as C. glabrata* and *C. krusei*, both of which display reduced susceptibilities to antifungal drugs (Malani *et al.*, 2005, Safdar et al., 2001, Panackal *et al.*, 2006, Magill *et al.*, 2006). Therefore, the choice of the proper antifungal drug is essential for a successful treatment. In consequence, the correct identification of fungal pathogens to the species level is critical for the initiation of appropriate antifungal therapies (Perlroth et al., 2007, Pfaller & Diekema, 2007). Hence, further research is needed to improve diagnostics, to develop new antifungal strategies, to identify risk factors and to establish common guidelines for prophylactic, pre-emptive, and empirical therapies to effectively combat fungal infections.

3.3 The genus *Candida* – a group of opportunistic fungal pathogens

Candida spp. belong to the phylum *Ascomycota*, which includes a great variety of different fungi pathogenic to plants as well as to humans (see Figure 2). *Candida* spp. are found in diverse habitats and can be isolated from soil, fruits or animals. Furthermore, *Candida* spp. live as commensals on the skin and mucosal layers of otherwise healthy human hosts and commonly colonize the gastro-intestinal tract of healthy individuals (Khatib et al., 2001).

The genus *Candida* consists of more than 100 different species comprising non-pathogenic organisms as well as opportunistic fungal pathogens. With 48% to 58%, *C. albicans* is the most frequently isolated cause of candidemia (Pfaller *et al.*, 2008). However, the distribution of *Candida* spp. varies by geographic regions. Notably, *C. glabrata* ranks second in Northern America and the European Union representing 14% to 24% of all clinical isolates (Pfaller et al., 2008). It is followed by *Candida parapsilosis* and *Candida tropicalis*, which are more prominent in Latin America and the Asian-Pacific region. Other species associated with candidemia are *Candida krusei*, *Candida lusitaniae*, *Candida dubliniensis* and *Candida guilliermondii* (Pfaller *et al.*, 2008, Richardson & Lass-Florl, 2008).

In immunocompetent humans, *Candida* spp. can cause superficial infections of the skin (Odds, 1994). For example, oral thrush and diaper dermatitis are well known infections in infants (Figure 3 A). Further, the majority of healthy women suffer from vaginal candidiasis at least once in a life time (Mardh *et al.*, 2002). Those infections are usually not dangerous for healthy immunocompetent individuals.

Importantly, *Candida* spp. can cause systemic life-threatening disease in immunocompromised patients (Figure 3C, D). In case of systemic and invasive Candidiasis, the causative species is able to penetrate epithelial tissues, to enter the blood stream and to disseminate into different organs (Mavor *et al.*, 2005).

Figure 3. Manifestations of *Candida* infections A) Diaper dermatitis (taken from http://www.doctorfungus.org/); **B)** *C. albicans* infection of skin and nail (taken from http://www.doctorfungus.org/); **C)** Oral Candidiasis caused by *C. albicans* (taken from www.oralcancerfoundation.org/dental/candida.htm); **D)** Esophageal candidiasis in an immunosuppressed patient (taken from www.merck.com/mmpe/sec14/ch180/ch180e.html)

3.4 *Candida glabrata*

3.4.1 General characteristics of *C. glabrata*

The haploid genome of *C. glabrata* has been sequenced and assembled by the Genolevures consortium (http://cbi.labri.fr/Genolevures/) (Dujon *et al.*, 2004). The 12.3 Mb size genome displays a low GC content, containing a total of 5283 putative open reading frames (ORFs) distributed over 13 chromosomes. Taxonomy originally classified both *C. glabrata* and *C. albicans* into the same taxonomic category. However, based on comparative genomic approaches and phylogenetic comparisons, it appears obvious that *C. glabrata* and *S. cerevisiae* share a common ancestor, which underwent whole-genome duplication (WGD) (Fitzpatrick et al., 2006, Scannell *et al.*, 2007). This is supported by the high sequence identity and high degree of gene synteny in both organisms. As shown in Figure 4, *C. glabrata* and *S. cerevisiae* are grouped in the WGD clade (red boxes) whereas *C. albicans* belongs to the CTG clade (grey box). This group comprises species that translate the CTG codon into serine instead of leucine (Santos *et al.*, 1997).

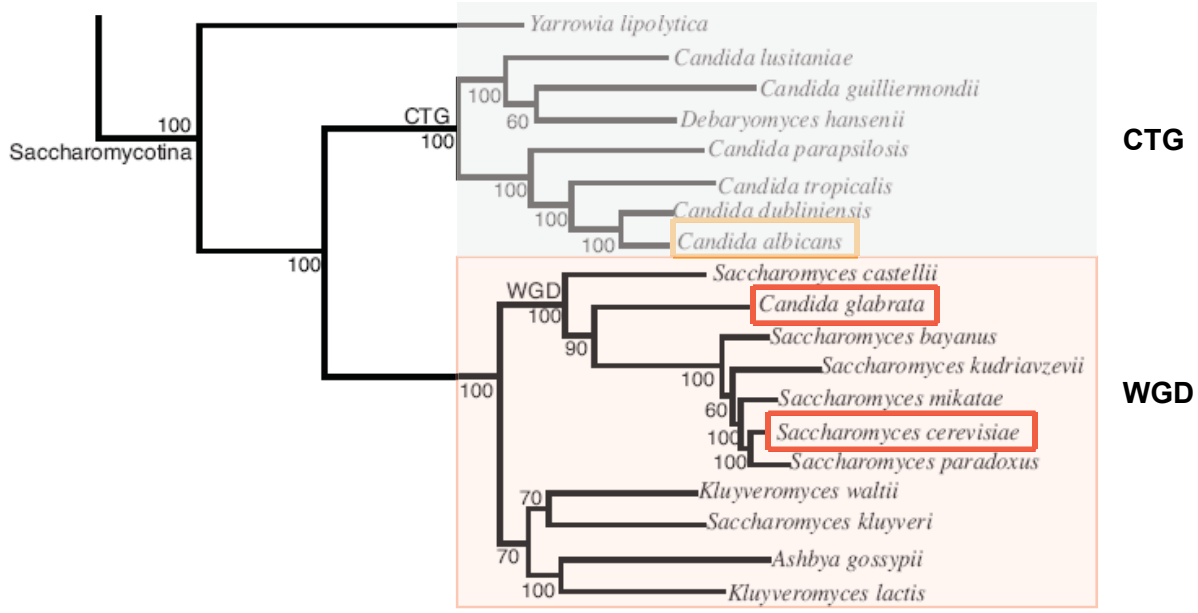

Figure 4. Phylogeny showing the distance between *C. glabrata*, *C. albicans* and their non-pathogenic relative *S. cerevisiae*. *C. glabrata* and *S. cerevisiae* belong to the whole-genome duplication (WGD) clade marked in red, *C. albicans* (orange box) belongs to CTG clade in the grey box (Fitzpatrick et al., 2006).

After the divergence *C. glabrata* may have experienced a greater gene loss than *S. cerevisiae*, resulting in the smaller genome (Dujon et al., 2004, Scannell et al., 2007). A possible explanation for this gene loss is the adaptation of *C. glabrata* to its human host. A total of 29 genes are lost compared to four other hemiascomycete yeast species, including genes implicated in galactose, phosphate, nitrogen and sulfate metabolism, as well as genes involved in cell rescue (Dujon et al., 2004). In total, it is assumed that several hundred genes are not shared between *S. cerevisiae* and *C. glabrata* (Kaur *et al.*, 2005). For example, our

own bioinformatic analysis also showed that homologues of the *S. cerevisiae* MAPK (mitogen-activated protein kinase) pathway genes Sc*SSK22* and Sc*MKK2* are not present in *C. glabrata* (Gregori *et al.*, 2007).

C. glabrata is auxotrophic for thiamine, pyridoxine and nicotinic acid (Domergue *et al.*, 2005, Ma *et al.*, 2007). The nicotinic acid auxotrophy of *C. glabrata* has an important influence on adhesion and host colonization. *C. glabrata* lacks most *BNA* genes (biosynthesis of nicotinic acid), which encode the de novo nicotinic aicd biosynthesis pathway enzymes. Therefore, *C. glabrata* must rely on the uptake of NAD^+ precursors from its environment. However, several different NAD^+ precursors such as nicotinic acid, nicotinamide and nicotinamide riboside can be utilized by *C. glabrata* through uptake and a functional Preiss-Handler salvage pathway (Ma et al., 2007). During infection nicotinamide riboside appears to be a primary source of NAD^+. Interestingly, the histone deacetylase CgHst1 is a major regulator of genes, which are expressed in response to nicotinic acid limitation, including the transporters Cg*TNA1*, Cg*TNR1* and Cg*TNR2* (Ma *et al.*, 2009).

In addition, *C. glabrata* is only able to utilize glucose and trehalose as carbon sources (Land *et al.*, 1996), which is exploited in diagnostic tests to distinguish between different *Candida* isolates.

C. glabrata has been classified as an asexual haploid organism, displaying a pronounced clonal population structure (Dodgson *et al.*, 2005). Nevertheless, the *C. glabrata* genome harbors three mating type-like loci (*MTL1, MTL2, MTL3*) and a- and α-pheromone-expressing strains exist (Srikantha *et al.*, 2003). The expression pattern reflects either the genotype of the *MTL1* or *MTL2* locus. Interestingly, orthologues of the mating pheromone response pathway, as well as of meiotic and recombination genes have been identified in *C. glabrata* (Wong *et al.*, 2003), showing that a large part of the mating machinery in *C. glabrata* may exist. In fact, there is some evidence for recombination, indicating that mating at least occurred during the evolution of *C. glabrata* and may still occur randomly (Dodgson et al., 2005). Recently, expression analysis showed also that pheromone receptor genes are expressed in *C. glabrata*. However, these appear insensitive to synthetic pheromone peptides (Muller *et al.*, 2008).

Although *C. glabrata* and *C. albicans* both live as human opportunistic pathogens, colonize the same host and share similar niches, the phylogenetic studies confirm that both organisms diverged early and underwent distinct evolutionary developments. Therefore, on one hand, both pathogens developed their own specific strategies to colonize the human host. On the other hand, they are likely to share some common virulence features, which may be important for fungal virulence in general. In addition, both pathogens share certain characteristics with the non-pathogenic baker's yeast *S. cerevisiae*. These characteristics are summarized in Table 1 and will be discussed in more detail further below.

	C. albicans	*C. glabrata*	*S. cerevisiae*	Ref.*
Taxonomy	Ascomycota (CTG clade)	Ascomycota (WGD clade)	Ascomycota (WGD clade)	(Marcet-Houben & Gabaldon, 2009)
Genome size	8 chromosomes (n), 6563 ORFs	13 chromosomes (n), 5274 ORFs	16 chromosomes (n), 6607 ORFs	(Dujon et al., 2004)
Ploidy	Diploid/tetraploid	Haploid	Haploid/diploid	-
Codon usage	Alter. yeast (CTG – Ser not Leu)	Standard	Standard	(Santos et al., 1997)
Sexual cycle	Known (cryptic)	Unknown	Known	-
Mating genes	Present	Present	Present	(Srikantha et al., 2003, Wong et al., 2003)
Colony morphology	Smooth (+ wrinkled) colonies	Small, white/creamy colonies	White, round shaped colonies	-
Cell morphology	Dimorphic: yeast, hyphae, pseudohyphae, chlamydospores	Monomorphic: budding yeast (pseudohyphae)	Budding yeast (pseudohyphae)	(Csank & Haynes, 2000)
Biofilm formation	Present	Present	Present	(Iraqui *et al.*, 2005, Shin *et al.*, 2002)
Phenotypic switching	Present (yeast - hyphae; white - opaque)	Present (visible on $CuSO_4$ media)	Absent	(Lachke *et al.*, 2002, Lachke *et al.*, 2000)
Auxotrophy (WT)	Absent	Niacine, thiamine, pyridoxine	Absent	(Domergue et al., 2005)
Sugar utilization	Glucose, maltose, galactose, trehalose	Glucose, trehalose	Glucose, maltose, galactose, sucrose, melibiose	(Land et al., 1996)
Natural habitat	Microbial flora of humans	Microbial flora of humans	Plants, fruits (grapes)	(Khatib et al., 2001)
Adhesins	Lectins (Hwp1, Als family)	Lectins (Epa family)	Sexual agglutinins, lectins (Flo family)	(Cormack *et al.*, 1999)
Azole resistance	Susceptible	Decreased susceptibility	Susceptible	(Pfaller & Diekema, 2004b)
Sites of infection/ isolation	Feces, urine, blood, vagina, oral, disseminated	Feces, urine, blood, vagina, oral, disseminated	-	-
Virulence	Opportunistic pathogen	Opportunistic pathogen	Non - pathogenic	-
Clinical significance	50 % of *Candida* isolates	Up to 25% of *Candida* isolates	No significance	(Horn et al., 2009)

Table 1. Comparison of the main characteristics. The two pathogenic yeast *C. albicans* and *C. glabrata* and the non-pathogenic *S. cerevisiae* are compared. WGD = whole-genome duplication, WT = wild type, ORF = open reading frame; * references refer to *C. glabrata* literature

3.4.2 *C. glabrata* morphology and its influence on virulence

C. glabrata displays a mainly monomorphic morphology, growing as budding yeast with ellipsoid cells of about 2-4 µm in diameter. Under laboratory conditions *C. glabrata* forms smooth, white colored colonies. Clinical isolates of *C. glabrata* from humans are normally also obtained in the budding yeast form. However, pseudohyphae formation of wild type cells has been reported as well as induction of invasive pseudohyphae upon nitrogen starvation *in vitro* (Csank & Haynes, 2000, Odds *et al.*, 1997). Several other morphological traits may influence the pathogenicity of *C. glabrata*, including phenotypic switching, pigmentation, and biofilm formation.

Phenotypic switching. Phenotypic switching is a known attribute of several dimorphic fungal species. In the monomorphic yeast *C. glabrata*, phenotypic switching refers to a high-frequency core switching phenotype and a reversible switching system (Lachke *et al.*, 2000, Lachke *et al.*, 2002). The *C. glabrata* core switching system distinguishes four

phenotypes, according to the intensity of the brown colony color when cultured on $CuSO_4$-containing media. The reversible system is characterized by a spontaneous switch between irregular wrinkled and smooth colonies. *In vivo*, different phenotypes of the core switching system may develop from a single strain, when growth occurs at different anatomical sites of the host (Brockert *et al.*, 2003). In vaginitis patients, phenotypic switching occurs at the site of infection and emphasises the dark-brown phenotype (Brockert *et al.*, 2003). Notably, cells of the dark brown phenotype may have a colonization advantage over cells of other switch phenotypes (Srikantha *et al.*, 2008).

Pigmentation. Several fungi of clinical relevance are able to synthesize colored pigments, which may be associated with their virulence. For instance, the human pathogenic basidiomycetal yeast *Malassezia furfur* displays colored pigmentation, consisting of a variety of different indole compounds (Mayser *et al.*, 1998, Mayser *et al.*, 2004, Hort *et al.*, 2009). Melanin pigments are also described for other human pathogenic fungi such as *Cryptococcus neoformans* or *Aspergillus fumigatus* (Casadevall *et al.*, 2000, Langfelder *et al.*, 2003, Brakhage & Liebmann, 2005). Both fungi are able to synthesize melanins, which have been implicated in pathogenicity (Casadevall et al., 2000). Although the function of melanin as a virulence factor in these fungi remains unclear, it is known that the cAMP-signaling pathway is linked to melanin production (Langfelder et al., 2003).

Interestingly, pigment production can be induced in *C. glabrata* when grown on media containing tryptophan as a sole nitrogen source (Mayser et al., 2007, Brunke). Since virulence factors of *C. glabrata* are weakly defined, it is of certain interest to determine, whether these *C. glabrata* pigments contribute to its pathogenicity.

Biofilm formation. Biofilm formation is another fungal trait, which is implicated in the development of fungal disease and drug resistance. In natural habitats, microbial communities predominantly exist as biofilms rather than planktonic cells (Costerton *et al.*, 1995). A biofilm is a structured community of individual cells, embedded in extracellular matrix developing and growing on a variety of different surfaces (Figure 5 B). Indwelling medical devices, such as catheters or heart valves provide surfaces to which microorganisms can adhere and initiate biofilm formation. A crucial attribute of biofilms is their significantly lower sensitivity to antimicrobial drugs (Mah & O'Toole, 2001).

Several consecutive steps lead to biofilm formation (Douglas, 2003). First, individual cells adhere to a surface. Second, these cells form microcolonies, which produce extracellular matrix. Finally, the biofilm matures, giving rise to hyphal as well as yeast cells embedded by extracellular matrix (Figure 5 B).

Although *C. glabrata* grows in the budding yeast morphology only, it is able to form biofilms (Figure 5 A) (Shin *et al.*, 2002, Iraqui *et al.*, 2005). Two adhesins, Epa6 and Epa7, belonging to the large *EPA* gene family, are required for biofilm formation of *C. glabrata* (Iraqui et al., 2005). Epa6 appears as the major adhesin involved in biofilm formation, since its expression is highly induced in biofilms. Deletion of *EPA6* results in reduced capability to form biofilms *in vitro*. Interestingly, Epa6 and Epa7 expression is regulated by subtelomeric silencing, which in turn may be directly controlled by biofilm formation or via a Yak1 kinase-dependent mechanism (Iraqui et al., 2005). Regulation by silencing is confirmed in Cg*sir4*Δ, Cg*sir3*Δ and Cg*rif1*Δ mutants, which display increased adherence to plastic surfaces. *EPA6* and *EPA7* expression is upregulated in these silencing mutants, connecting the subtelomeric silencing machinery to biofilm formation (Castano *et al.*, 2005, Iraqui et al., 2005). Thus, transcriptional silencing is a distinct mechanism, through which *C. glabrata* controls biofilm formation by adhesins and which may contribute to its virulence.

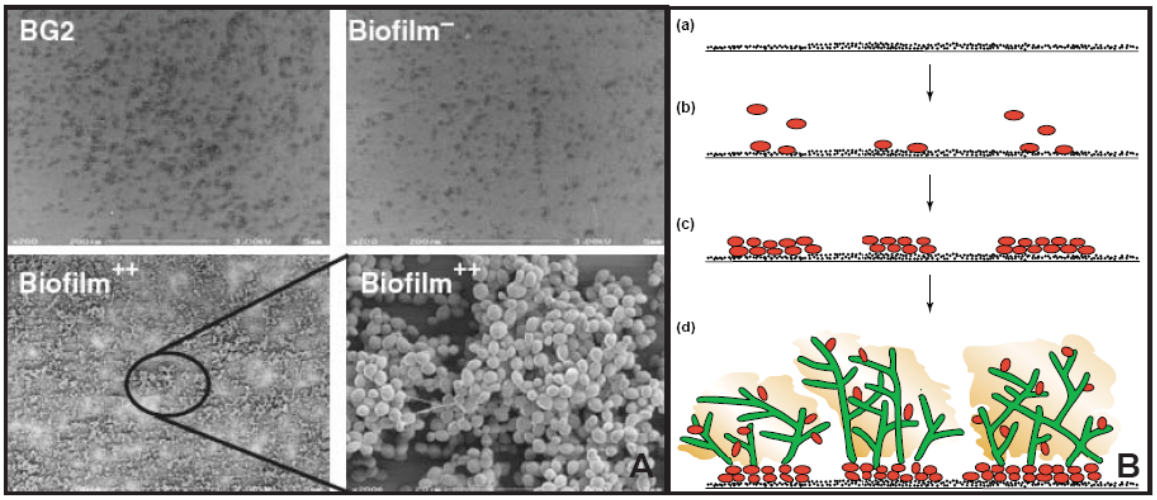

Figure 5. Biofilm formation in *C. glabrata* A) *C. glabrata* BG2 wild type cells form biofilms on plastic surfaces (top left) whereas biofilm negative strains form smaller structures (top right). A Biofilm++ mutant shows extensive biofilm formation (bottom); taken from (Iraqui et al., 2005). **B)** Schematic, showing the steps of biofilm formation (Douglas, 2003).

3.4.3 The hypervirulence factor CgAce2 and the RAM network

Since virulence factors of *C. glabrata* are weakly defined, several attempts have been made to identify novel virulence-associated genes in this organism. A new virulence factor, Cg*ACE2*, was identified by exploiting a library of insertional signature-tagged mutants. The deletion of this transcription factor gene results in a strain defective in cell separation (Figure 6 B) and strongly enhances the formation of large cell aggregates (Kamran et al., 2004). The use of a neutropenic mouse infection model showed that Cg*ace2*Δ mutants are hypervirulent, causing 100% death after only four days. The acute mortality is apparently not due to vascular clogging by the clumpy growth phenotype. Instead, the hypervirulence may at least in part be caused by elevated levels of proinflammatory cytokines (Kamran et al., 2004).

Abnormal exposure of fungal cell wall components may be the cause for this cytokine stimulation.

This is further supported by the analysis of proteomic changes in Cg*ace2*Δ mutants. In total, 123 proteins are identified, including more abundant proteins associated with metabolism and less abundant proteins being related to cellular transport and protein synthesis. Interestingly, the expression of several genes involved in morphogenesis and cell wall remodelling is down-regulated (Stead *et al.*, 2005).

CgAce2 is part of the RAM (Regulation of Ace2 activity and cellular morphogenesis) network, which regulates polarized growth and cell separation, and influences the budding pattern (Figure 6 A). *C. glabrata* harbors homologues of all RAM network genes. The kinase CgCbk1 regulates the transcription factor CgAce2 and deletion of Cg*CBK1* results in a similar clumpy cell morphology as seen for the Cg*ace2*Δ mutant (Schwarzmüller, unpublished results).

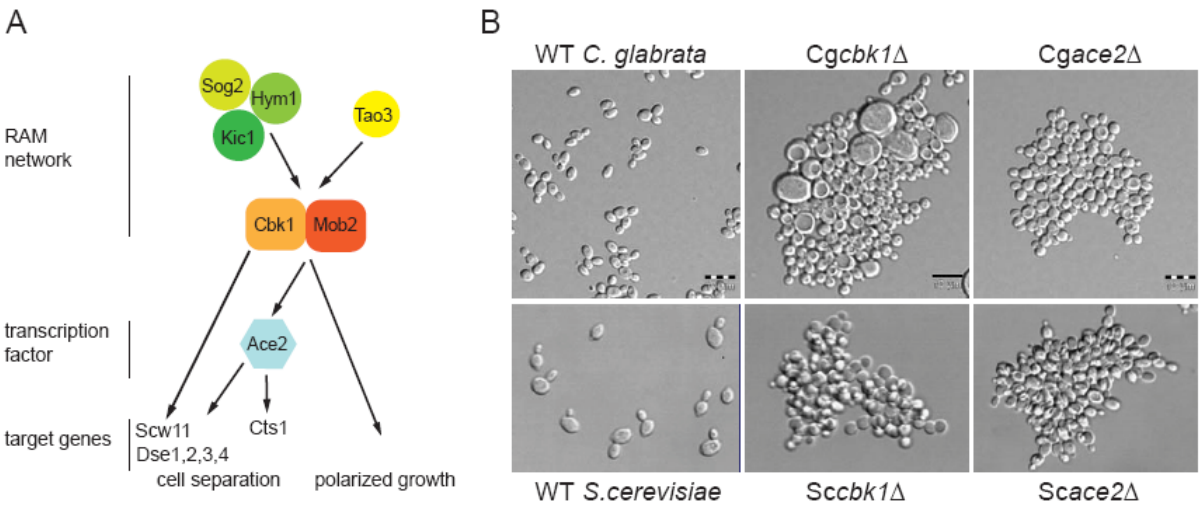

Figure 6. RAM network in *S. cerevisiae* and phenotypes of *cbk1*Δ and *ace2*Δ deletion strains. (A) RAM network components in *S. cerevisiae*. (B) Deletion strain phenotypes of *C. glabrata* and *S. cerevisiae cbk1*Δ and *ace2*Δ strains. *S. cerevisiae* pictures taken from (Bidlingmaier *et al.*, 2001).

Similarly, in *S. cerevisiae* the components of the RAM network regulate polarized growth and ScAce2 activity (Nelson *et al.*, 2003). The network includes several genes, all of which are required for polarized growth. Microarray studies revealed that strains lacking one of the genes including Sc*CBK1*, Sc*MOB2*, Sc*KIC1*, Sc*HYM1* or Sc*TAO3*, show overlapping expression profiles. ScKic1, ScHym1 and ScTao3 regulate the transcription factor ScAce2 via the ScCbk1-ScMob2 complex (Nelson et al., 2003, Bidlingmaier *et al.*, 2001, Colman-Lerner *et al.*, 2001). ScAce2 then localizes to the nucleus of the daughter cell, mediating the separation of mother and daughter cells and activates expression of early G1-phase genes. ScAce2 is required for expression of distinct target genes involved in cell separation such as the chitinase Sc*CTS1,* the putative glucanase Sc*SCW11* and the daughter-specific genes

Sc*DSE1-4* (O'Conallain *et al.*, 1999, Colman-Lerner *et al.*, 2001). Deletion of Sc*ACE2* causes a cell separation defect similar to the phenotype of the Cg*ace2*Δ strain (Figure 6 B), resulting in pseudohyphal growth and agar invasion (King & Butler, 1998).

ScSsd1, a protein involved in cell wall integrity, has been identified by yeast two-hybrid screening as binding partner of ScCbk1 (Racki *et al.*, 2000). Remarkably, deletion of Sc*SSD1* in wild *S. cerevisiae* strains isolated from plants or from clinical isolates results in hypervirulent strains in a mouse model of systemic infection. Alteration in the cell wall composition of the Sc*ssd1*Δ mutant induces proinflammatory cytokines in macrophages, implying that the increased virulence is due to a stronger immune response (Wheeler *et al.*, 2003).

Taken together, the disturbance of the RAM network or associated proteins may lead to perturbations of the cell wall architecture and exposure of otherwise not accessible cell wall components. This exposure may trigger cytokine production by immune cells, thus inducing septicemia. However, the responsible cell wall components still have to be identified although glucans may be the major inducing structural constituent.

3.4.4 Antifungal drugs and drug resistance mechanisms in *C. glabrata*

A particular characteristic phenotype of *C. glabrata* is its reduced susceptibility to clinically used azoles. The inherent resistance against this class of antifungals may be a major virulence factor of *C. glabrata*. This view is supported by the finding that *C. glabrata* is often isolated from patients undergoing azole therapy (Pfaller & Diekema, 2004a, Bouchara *et al.*, 2000). Moreover, the prophylactic use of azoles in treatment of *Candida* infections may actually contribute to the clinical prevalence of *C. glabrata*. However, the increase in *C. glabrata* blood stream infections may not only be due to drug pressure but may also be affected by geographic location, age and other yet ill-defined factors (Pfaller & Diekema, 2007).

The molecular basis of antifungal drug resistance in *C. glabrata* depends on similar mechanisms, also operating in other fungal organisms (Figure 7). These mechanisms comprise reduced uptake, upregulation of drug efflux pumps, sequestration of toxic substances in the vacuole, intracellular drug inactivation, changes in membrane permeability and alteration of drug targets (Cowen & Steinbach, 2008).

The best studied drug resistance mechanism in *C. glabrata* is the upregulation of ABC transporters in response to azole exposure. Azole resistance is rapidly acquired by overexpression of the efflux pumps CgCdr1 and CgPdh1 (CgCdr2), orthologues of the *S. cerevisiae* ABC transporter ScPdr5 and *C. albicans* efflux pumps CaCdr1 and CaCdr2 (Sanglard *et al.*, 1999, Miyazaki *et al.*, 1998, Izumikawa *et al.*, 2003). Interestingly, disruption of Cg*PDH1* alone does not affect azole susceptibility. However, a Cg*cdr1*Δ Cg*pdh1*Δ double

deletion results in drug hypersusceptibility (Sanglard *et al.*, 2001). Both ABC pumps are part of the pleiotropic drug resistance (PDR) network, which has been originally described in baker's yeast (Balzi *et al.*, 1987, Sipos & Kuchler, 2006). Cg*SNQ2* belongs to the *C. glabrata* PDR network as well and mediates resistance to azole drugs (Torelli *et al.*, 2008).

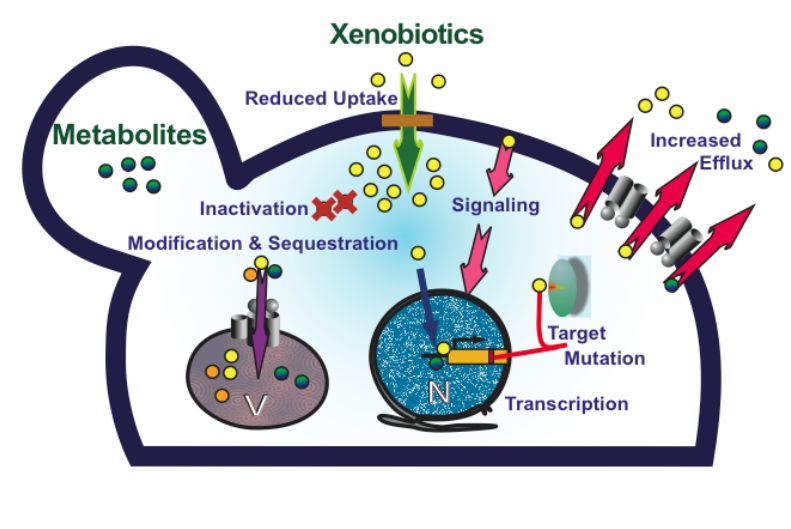

Figure 7. Resistance mechanisms of fungal cells. These include (1) reduced uptake of xenobiotics, (2) increased efflux by upregulation of drug efflux proteins, (3) sequestration of toxic substances to the vacuole, (4) intracellular drug inactivation, (5) alteration of drug targets or their transcriptional activators. Furthermore, signaling and general stress response pathways contribute to drug resistance. Taken from (Kuchler K.).

The transcription factor CgPdr1 is the master regulator of the *C. glabrata* PDR network. It mediates resistance to azoles by controlling Cg*CDR1*, Cg*PDH1* and Cg*SNQ2* gene expression (Vermitsky & Edlind, 2004, Vermitsky *et al.*, 2006, Torelli *et al.*, 2008). Moreover, a putative pleiotropic drug-response element (PDRE) in the promoter region of Cg*PDR1* suggests an autoregulatory loop (Vermitsky et al., 2006, Tsai *et al.*, 2006). In contrast to *S. cerevisiae*, the PDR network of *C. glabrata* is under control of only one transcriptional regulator CgPdr1. In addition, the regulation of drug efflux via CgCdr1 and CgPdh1 is also controlled by phosphorylation of the ABC pumps through protein kinase A activity (Wada *et al.*, 2002, Wada *et al.*, 2005).

Interestingly, strains with Cg*PDR1* gain-of-function mutations are more virulent in a mouse model when compared to strains with wild type alleles (Ferrari *et al.*, 2009). These mutations are not only associated with elevated azole resistance but also with a gain in fitness and virulence. Since these strains show a higher fitness *in vivo*, it is, thus, possible that the increased virulence phenotype is due to the gained fitness.

Recently, the molecular mechanisms underlying Pdr1-mediated resistance have been identified. CgPdr1 directly binds structurally different xenobiotics in a similar manner as known from mammalian PXR nuclear receptors (Thakur *et al.*, 2008, Kliewer *et al.*, 2002). Direct binding of drugs activates the expression of drug efflux pumps. In addition, the mediator complex subunit Gal11 interacts with Pdr1 and is essential for mediating multidrug resistance. Interestingly, *C. glabrata* has two homologues of the baker's yeast Sc*GAL11* gene. Only deletion of Cg*GAL11A* leads to decreased Cg*CDR2* expression, rendering cells

more susceptible to azoles (Thakur et al., 2008). This discovery may open the possibility for the development of new antifungal drugs acting on novel targets.

The regulation of *C. glabrata* ABC transporters is also influenced in so-called petite mutants (Brun *et al.*, 2003, Brun *et al.*, 2004). Petite mutants lack mitochondrial DNA, resulting in mitochondrial dysfunction and respiratory deficiencies (Locker *et al.*, 1979, Slonimski *et al.*, 1968). In *S. cerevisiae*, the petite phenotype leads to up-regulation of Pdr3p function and increased Sc*PDR5* expression (Hallstrom & Moye-Rowley, 2000, Zhang & Moye-Rowley, 2001). Azole-resistant *C. glabrata* petite mutants show elevated Cg*CDR1* and Cg*PDH1* levels and increased drug efflux *in vitro* (Sanglard et al., 2001, Brun et al., 2003, Brun et al., 2004, Defontaine *et al.*, 1999). Interestingly, *C. glabrata* petite mutants appear to be less virulent than the isogenic wild type strain in a mouse model of systemic candidiasis (Brun *et al.*, 2005). In contrast, a clinical isolate from a bone marrow transplant recipient with elevated resistance to several azoles is a petite mutant (Bouchara et al., 2000). This demonstrates that the selective pressure imposed during azole treatment may result in selection of azole-resistant mutants *in vivo*. This mechanism may partially contribute to clinical failures of antifungal azole therapy of *C. glabrata* infections.

A *C. glabrata* strain, lacking Cg*PGS1*, shows overexpression of drug efflux pumps (Batova *et al.*, 2008). Cg*PGS1*, encoding a phosphatidylglycerolphosphate synthase, is an enzyme involved in the synthesis of phospholipids and is essential for functional mitochondria. In this mutant, the absence of anionic phospholipids results in dysfunctional mitochondria, which are associated with increased azole resistance.

C. glabrata also carries a transporter of the major facilitator superfamily (MFS), Cg*FLR1*, which contributes to drug resistance (Chen *et al.*, 2007). Expression of Cg*FLR1* is controlled by the transcriptional regulator CgAp1. CgAp1 mediates resistance to diverse compounds, such as hydrogen peroxide, benomyl, cadmium chloride and fluconazole (Chen *et al.*, 2007).

Most if not all azoles block ergosterol biosynthesis (Figure 8), which leads to a depletion of essential ergosterol in the plasma membrane (Ghannoum & Rice, 1999, Cowen & Steinbach, 2008). The fungal plasma membrane depends on ergosterol, which is the principal sterol component of the fungal cell membrane and required to establish proper membrane function.

A variety of azole drugs selectively inhibit Erg11, a cytochrome P450 lanosterol 14-alpha-demethylase (Akins, 2005). Two possible explanations for the toxic effect of azoles exist. Inhibition of Erg11 leads to accumulation of lanosterol, which is further converted to a toxic intermediate being responsible for growth inhibition (Akins, 2005). On the other hand, the growth inhibitory effect can be explained by the lack of membrane ergosterol. Resistance

to azoles may occur by point mutations in *ERG11*, overexpression or gene amplification, leading to dosage compensation (Henry *et al.*, 2000, Niimi *et al.*, 2002, Redding *et al.*, 2003).

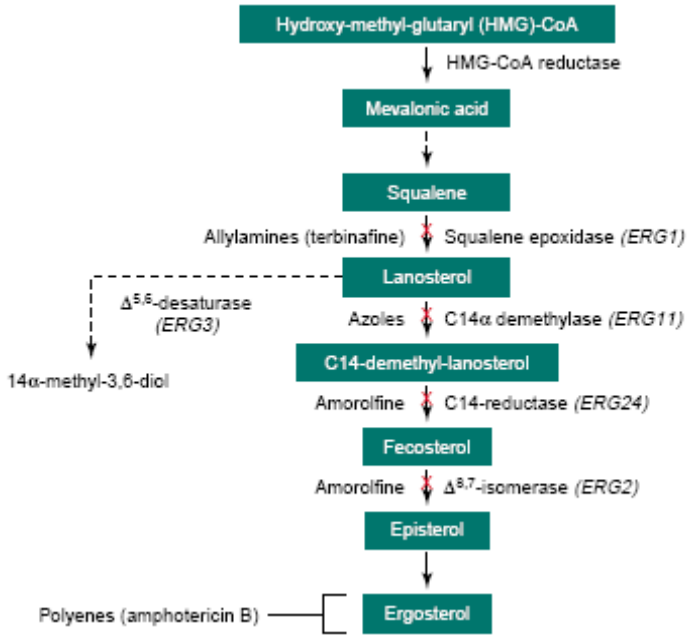

Figure 8. Mechanism of action of the different antifungal drugs targeting the ergosterol biosynthesis pathway. Ergosterol is the major sterol component of the fungal cell membrane and is required for proper membrane fluidity and function. Ergosterol is synthesized from a squalene precursor. Several antifungal drugs selectively inhibit distinct enzymes of this pathway. Terbinafine inhibits the squalene epoxidase Erg1, azoles inhibit the C14α-demethylase, a cytochrome P-450 enzyme, encoded by *ERG11* and amorolfine inhibits Erg24 and Erg2. Amphotericin B leads to cell leakage by binding to ergosterol. Taken from (Lupetti *et al.*, 2002, White *et al.*, 1998)

The contribution of Cg*ERG11* in *C. glabrata* azole resistance is less well understood when compared to *C. albicans*. In azole-resistant clinical isolates, expression levels of Cg*ERG11* are unchanged and no mutations are found in the gene, suggesting that Cg*ERG11* is not involved in *C. glabrata* azole resistance (Henry et al., 2000, Vermitsky & Edlind, 2004, Sanguinetti *et al.*, 2005, Redding et al., 2003).

In *C. glabrata*, Cg*AUS1* is the only homologue of the *S. cerevisiae* ABC transporters ScAus1 and ScPdr11, which are required for sterol uptake from media under anaerobic conditions (Nakayama *et al.*, 2007). In contrast to baker's yeast, *C. glabrata* may be able to take up sterols from serum-supplemented media under aerobic conditions. For instance, growth of a strain lacking Cg*ERG9* can be rescued in medium supplemented with serum. Likewise, when Cg*ERG11* is inhibited by fluconazole growth is restored by serum addition (Nakayama *et al.*, 2000); and Cg*erg1*Δ cells show enhanced uptake of exogenous cholesterol (Tsai *et al.*, 2004). Furthermore, repression of the sterol transporter Cg*AUS1* renders cells hypersensitive to fluconazole in spite of the presence of serum. This effect is not observed for non-azole antifungals such as amphotericin B (Nakayama et al., 2007). Perhaps uptake of serum cholesterol by CgAus1 can compensate for the lack of ergosterol, and thereby protect *C. glabrata* against fluconazole. This may represent a particular drug resistance mechanism of *C. glabrata*.

Many reports suggest that cross-resistance to other drugs commonly occurs in azole-resistant *C. glabrata* strains (Borst *et al.*, 2005, Magill et al., 2006, Panackal et al., 2006,

Pfaller *et al.*, 2004). This is problematic in a clinical setting and may give an explanation for the observed shift from infections with *C. albicans* to other *Candida* spp. (Pfaller & Diekema, 2007). Currently, azole drugs are also mainly used in antifungal therapy because of their efficacy and relatively low toxicity. However, most azoles are fungistatic rather than fungicidal. Therefore, the development of novel antifungal drugs acting on new targets is an important field of research.

Antifungal class	Drug	Mechanism of action	Clinical use	Ref.
Azole	Fluconazole	Inhibition of ergosterol biosynthesis	Systemic opportunistic mycoses	(Richardson *et al.*, 1985, Troke *et al.*, 1985)
	Voriconazole		(yeasts, moulds)	(George *et al.*, 1996)
	Itraconazole			(Heeres *et al.*, 1984)
	Ketoconazole			(Heeres *et al.*, 1979)
Allylamine	Terbinafine	Inhibition of ergosterol biosynthesis	Cutaneous infections (dermatophytes)	(Petranyi *et al.*, 1984)
Poylenes	Amphotericin B	Disruption of membrane by binding of ergosterol	Systemic opportunistic mycoses (yeasts, moulds)	(Donovick *et al.*, 1955)
Nucleoside analog	5-Flucytosine	Inhibition of DNA and RNA synthesis	Combination therapy only (yeasts)	(Heidelberger *et al.*, 1957, Holt & Newman, 1973)
Echinocandins	Caspofungin	Inhibition of β-glucan synthase	Candidiasis, Aspergillosis	(Masurekar *et al.*, 1992)
	Micafungin			(Iwamoto *et al.*, 1994)
	Anidulafungin			(Nyfeler & Keller-Schierlein, 1974)

Table 2. The major classes of antifungal drugs used in clinical antifungal therapy (Chen & Sorrell, 2007, Cowen & Steinbach, 2008, Ghannoum & Rice, 1999, Denning, 2003)

In addition to azoles a variety of other drugs exist for the treatment of fungal infections (Table 2 & Figure 8). The allylamine terbinafine blocks ergosterol biosynthesis by inhibiting the squalene epoxidase Erg1 (Klobucnikova *et al.*, 2003, Ryder, 1992). Terbinafine is mainly used for the treatment of dermatophyte infections. However, the i*n vitro* combination of terbinafine with azoles or calcineurin inhibitors showed a putative extended spectrum of terbinafine action (Jessup *et al.*, 2000, Ryder, 1999). For example, combining terbinafine with the calcineurin inhibitor FK506 resulted in growth inhibition of *C. glabrata* (Onyewu *et al.*, 2003).

Amphotericin B is an effective therapy for fungal infections. The fungicidal effect of the polyene drug amphotericin B is due to its complex formation with membrane ergosterol, leading to permeabilization of the membrane and leakage of cell contents (Table 2, Figure 9). The mode of action also explains the broad antifungal spectrum of amphotericin B on diverse fungal species (Ghannoum & Rice, 1999). Nevertheless, strong side effects, such as nephrotoxicity, are problematic with the clinical use of amphotericin B (Bates *et al.*, 2001).

Flucytosine is a nucleoside analog which develops its antifungal properties after cellular conversion to 5-fluoruracil (Table 2, Figure 9). 5-fluoruracil is incorporated into RNA,

resulting in disruption of protein synthesis. It also affects thymidilate synthase and therefore DNA synthesis (Ghannoum & Rice, 1999). Flucytosine uptake requires a permease. Therefore the use of flucytosine is limited to pathogenic fungi such as *Candida spp.*, which harbor cytosine permeases (Odds *et al.*, 2003).

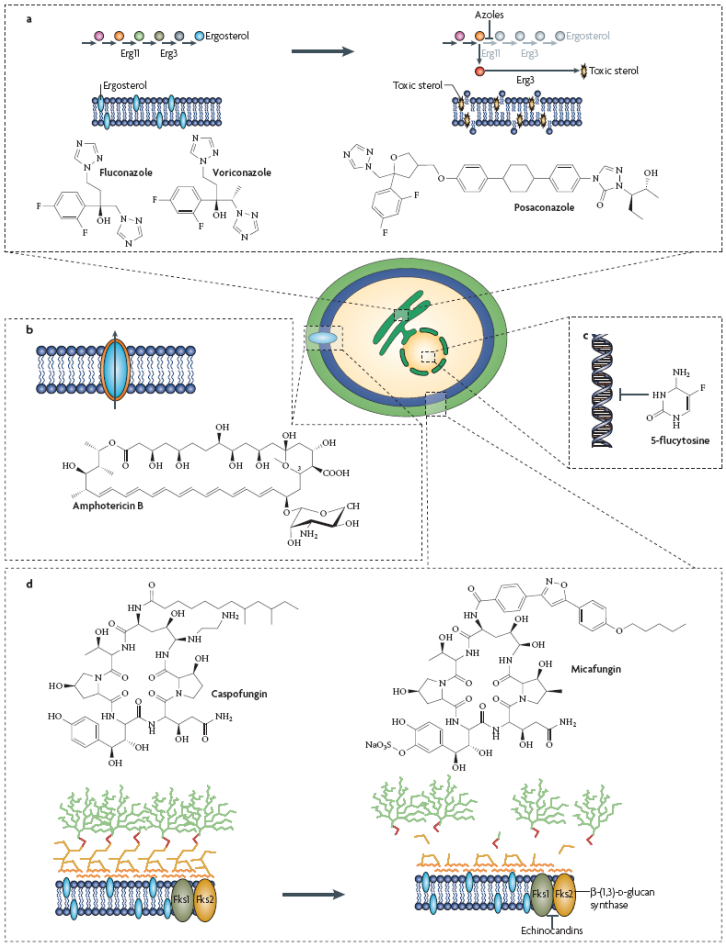

Figure 9. Mechanisms of action of four antifungal drug classes and their targets. Azoles target the ergosterol biosynthesis pathway, Amphotericin B binds to membrane ergosterol forming pores in the membrane, 5-Flucytosine is an inhibitor of DNA and RNA synthesis and echinocandins inhibit β-glucan synthase and interfere with cell wall integrity (Cowen, 2008).

Echinocandins represent a relatively new class of antifungal drugs, targeting the assembly of the fungal cell wall. Three different drugs - Caspofungin, Micafungin and Anidulafungin - have been approved for clinical therapy of candidiasis and aspergillosis (Denning, 2003). The advantage of these antifungal agents is that they target an enzyme specific to fungal organisms, their low toxicity and the absence of cross-resistance with other antimycotic drugs. Echinocandins are fungicidal by inhibiting the fungal glucan synthase complex (Onishi *et al.*, 2000). This enzyme is responsible for the synthesis of β-1,3 glucan, a major constituent of the fungal cell wall. Since echinocandins are poor substrates of ABC transporters, these pumps probably do not contribute to echinocandin resistance (Bachmann *et al.*, 2002, Posteraro *et al.*, 2006). However, overexpression of *C. albicans CDR2* confers caspofungin resistance *in vitro* (Schuetzer-Muehlbauer *et al.*, 2003).

Other known caspofungin resistance mechanisms are based on point mutations in the subunits of the glucan synthase genes, *FKS1* and *FKS2*. Those point mutations have been identified in the glucan synthase genes of clinical isolates of different *Candida spp.*, including *C. glabrata* (Katiyar *et al.*, 2006, Park *et al.*, 2005, Thompson *et al.*, 2008, Cleary *et al.*, 2008, Garcia-Effron *et al.*, 2009). Overall, echinocandins seem to be a good choice for treatment of azole-resistant and cross-resistant pathogenic yeast.

Interestingly, *S. cerevisiae* PKC pathway mutants (i.e. lacking components of the cell integrity pathway) show severe growth defects when exposed to Caspofungin (Reinoso-Martin *et al.*, 2003). Therefore, the ability to sense cell wall damage exerted by cell wall-perturbing drugs is essential for the survival of fungi. Sensing of diverse stress factors and accurate signal transduction is a general theme for adaptation of fungal cells to changing environmental conditions. This may be true in particular for pathogenic yeasts, which have to adapt rapidly to extreme changes in the host environment.

3.4.5 Environmental stress sensing - signaling pathways in *C. glabrata*

Fungal cells are exposed to fluctuating environmental conditions in their natural habitats: temperature, pH, availability of nutrients, osmolarity and oxygen supply. Fungal pathogens have to deal with additional challenges mostly exerted by the host. During the different stages of infection – adhesion, invasion, colonization and dissemination – the fungal pathogen has to adapt to a variety of changing conditions and to counteract or evade immune surveillance. To assure its survival, pathogens must react appropriately and quickly.

Yeast cells possess several different pathways, transducing a signal from the cell surface located sensor to the nucleus. These signaling pathways are involved in nutrient and environmental stress sensing. The protein kinase A (PKA) pathway is involved in metabolism, stress resistance and proliferation related to nutrient availability (Thevelein & de Winde, 1999). The TOR (target of rapamycin) pathway controls cell growth and metabolism in response to environmental cues and regulates protein synthesis at multiple levels (De Virgilio & Loewith, 2006), while the Rim101 pathway is required for growth at alkaline conditions (Lamb *et al.*, 2001). Calcineurin governs gene expression in a species-dependent fashion as a central stress response regulator. It is also implicated in temperature and cell wall stress (Kraus & Heitman, 2003). Further, it may play a virulence-associated role in fungal pathogens (Karababa *et al.*, 2006). Finally, mitogen-activated protein kinase pathways (MAPK) represent an essential part of the cell's ability to sense, respond and communicate with its environment.

The canonical MAPK pathway contains a core module composed of a three-tiered kinase cascade. Upon activation of the MAP kinase kinase kinase (MAPKKK), the MAP kinase kinase (MAPKK) is phosphorylated, which in turn activates the MAP kinase (MAPK).

MAPK signaling drives a diverse set of transcription factors, controlling a multitude of different cellular processes by integration of extracellular and intracellular stimuli. Upstream components include G protein-coupled receptors and a p21-activated protein kinase (PAK) (Chen & Thorner, 2007).

Five MAPK signaling pathways (Figure 10) implicated in stress response and regulation of cellular processes are described in *S. cerevisiae*. The protein kinase C or cell wall integrity pathway (PKC), the high osmolarity glycerol pathway (HOG), the mating pheromone response pathway, the filamentous growth pathway and the spore wall assembly pathway (Chen & Thorner, 2007).

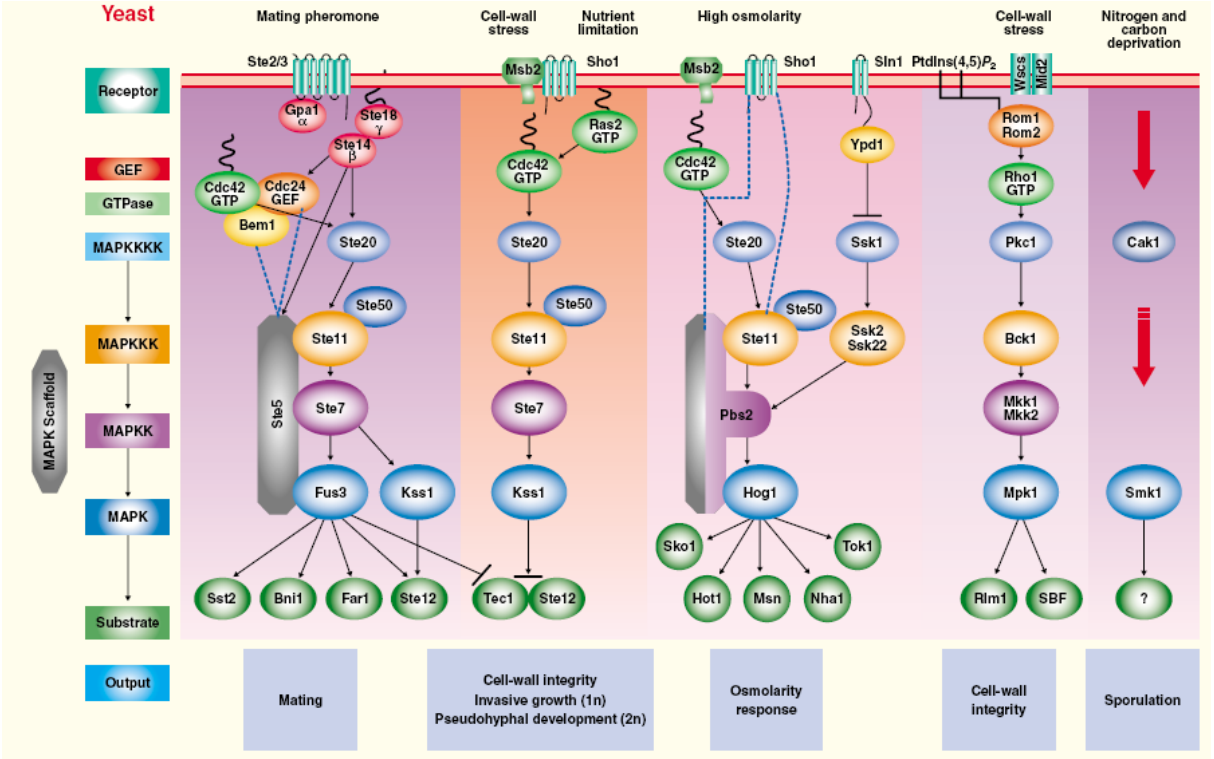

Figure 10. Schematic diagram of MAPK signaling pathways in baker's yeast. The five MAPK signaling pathways in *S. cerevisiae* (PKC, HOG, mating, filamentous growth, sporulation pathway) are principally conserved in *C. glabrata*. Taken from (Qi & Elion, 2005).

C. glabrata harbors putative orthologues of almost any gene of the different *S. cerevisiae* signaling pathways. Several of these genes have already been studied in *C. glabrata* with respect to their influence on growth and virulence properties.

The HOG pathway is a prominent example for a conserved pathway in *C. glabrata*. The HOG pathway consists of two branches, the so-called Sho1 and Sln1 branch (Figure 10). *S. cerevisiae* cells lacking the kinases Sc*PBS2* or Sc*HOG1* are osmosensitive, whereas no obvious phenotype is seen when a single mutation occurs in only one of the branches (Brewster *et al.*, 1993). Remarkably, a *C. glabrata* Cg*sho1*Δ strain displays severe osmosensitivity (Gregori *et al.*, 2007). However, this phenotype is restricted to a mutant in

the ATCC2001 background. The wild type strain ATCC2001 carries a genomic mutation in Cg*SSK2* (Cg*ssk2-1* allele), resulting in the loss of the kinase domain. Since the *C. glabrata* genome does not harbor a Cg*SSK22* gene (a functional redundant homologue of Sc*SSK2* in *S. cerevisiae*), the Cg*ssk2-1* mutation renders the CgSln1 branch inactive. Interestingly, when Cg*ssk2-1* is restored by a fully functional Cg*SSK1* gene, CgHog1 displays increased levels of phosphorylation in strain ATCC2001. This suggests that the Cg*ssk2-1* mutation may be a natural occurring mutation, suppressing associated toxicities of a constitutively activated Hog1 kinase (Gregori et al., 2007).

C. glabrata CgSte11 is required for adaptation to hypertonic stress and is implicated in nitrogen starvation-induced filamentation. Cg*ste11*Δ mutants are attenuated in virulence (Calcagno *et al.*, 2005). CgSte12 shows only a modest influence on virulence. However, it is also required for nitrogen starvation-induced pseudohyphal formation and regulation of cell wall biogenesis (Calcagno *et al.*, 2003). The *C. glabrata* PAK kinase homologue CgSte20 is implicated in cell wall integrity, adaptation to hypertonic stress and wild-type levels of virulence (Calcagno *et al.*, 2004). These studies on different components of signaling pathways demonstrate that sensing of extracellular stresses, which result in transcriptional changes, can influence the morphology and cell wall composition and hence the virulence properties of *C. glabrata*.

Cell wall integrity is a tightly controlled process. In response to various adverse conditions such as heat stress, hypoosmotic shock, cell wall-affecting agents and mating pheromone, the cell wall integrity MAPK pathway is activated (Levin, 2005). In *C. glabrata*, the PKC pathway is involved in resistance to Caspofungin and azole drugs, as well as in cell wall maintenance and regulation of chitin synthesis (Cota *et al.*, 2008, Edlind *et al.*, 2005). Our own studies showed that a *C. glabrata slt2*Δ mutant is sensitive to Caspofungin. However, cells lacking the PKC pathway sensor *WSC1*, display severe growth defects under various stress conditions, such as heat, Calcofluor White, Congo Red, SDS and Caspofungin, all of them affecting cell wall integrity.

During infection, *C. glabrata* has to cope with oxidative and osmotic stress exerted by the host. Environmental stress response (ESR) is accomplished among others by the transcription factors CgMsn2 and CgMsn4. Hyperosmotic shock leads to CgMsn2 mediated activation of specific ESR genes, such as the trehalose genes Cg*TPS1* and Cg*TPS2*. Transcriptional profiling revealed a conserved regulation of *MSN2* in *C. glabrata* and *S. cerevisiae* (Roetzer *et al.*, 2008).

Immune cells produce a variety of different oxygen radicals to fight invading pathogens. Notably, the transcription factors CgYap1 and CgSkn7 are involved in oxidative stress resistance. Together with CgMsn2 and CgMsn4 they regulate CgCta1 catalase activity (Cuellar-Cruz *et al.*, 2008).

C. glabrata can occupy several habitats with ambient changes in pH such as the skin, the gastro-intestinal tract and the vaginal mucosa. Therefore, the ability to adapt to changing pH levels is essential for survival in the host. Although there is no morphological change of *C. glabrata* in response to changing pH conditions, gene expression levels change. A proteomics study revealed four clusters of *C. glabrata* genes regulated in a pH-dependent manner, including amino acid, carbohydrate and lipid metabolism, stress response, and protein synthesis genes (Schmidt *et al.*, 2008). In contrast to other fungal pathogens, such as *C. albicans*, acidic pH levels appear to be less stressful for *C. glabrata* than alkaline pH conditions.

Although many homologues of *S. cerevisiae* and *C. albicans* signaling genes and transcription factors can be identified in *C. glabrata*, differences likely exist in sensing, and signaling mechanisms as well as transcription. New transcription patterns may be formed by different mechanisms such as changes in a transcriptional regulator, resulting in the control over new genes or mutations/loss of promoter sequences, which may put individual genes under control of a different transcriptional regulator. This transcriptional rewiring affects cis-regulatory as well as trans-acting elements and is thought to be a key mechanism by which complexity, diversity and phenotypic novelty can arise (Tsong *et al.*, 2006). By comparison of *S. cerevisiae* and *C. albicans* circuitries, transcriptional rewiring of the mating circuit, of mitochondrial and cytoplasmic ribosomal genes or of ribosomal regulation have been identified (Ihmels *et al.*, 2005, Tanay *et al.*, 2005, Tsong *et al.*, 2006). Therefore, comparison of *C. glabrata* with *S. cerevisiae* or *C. albicans* will probably allow the identification of new regulatory modules and genes influencing stress response patterns and drug resistance.

3.4.6 The yeast cell wall and adhesion in *C. glabrata*

The fungal cell wall is a complex and protective multilayer barrier consisting of polysaccharides and proteins, which together ensure structural integrity of the fungal cell. In spite of its rigid nature and mechanical stability, the cell wall does not resemble an inert structure as its composition continuously changes during growth. Growth, cell division and adaptation to environmental stresses influence biogenesis, assembly and composition of the cell wall. Its unique structure and the differences to the mammalian extracellular matrix, makes the fungal cell wall an excellent target for antifungal drugs. The main constituents are glucan, chitin and mannoproteins (Figure 11) (Klis *et al.*, 2006, Lesage & Bussey, 2006).

The innermost layer consists of chitin, a linear polymer of β-1,4-N-acetyl glucosamine, which is synthesized and deposited by chitin synthases. Chitin represents only a minor part (1 – 3%) of the lateral cell wall and is more abundant at the bud neck and scars (Klis *et al.*, 2006, Lesage & Bussey, 2006).

The core structure of the cell wall consists of long branched β-1,3 glucans (1500 glucose residues), which are covalently linked to β-1,6 glucan and chitin. It makes up to 45 % of the cell wall mass and serves as a three-dimensional scaffold for the outer layer of cell wall proteins (Klis et al., 2006, Lesage & Bussey, 2006). Glucan synthesis is accomplished by two highly homologous transmembrane proteins, ScFks1 and ScFks2, which catalyze the polymerisation of β-1,3 glucan from UDP-glucose. In *S. cerevisiae*, a third homologue ScFks3 appears to be connected to sporulation (Lesage *et al.*, 2004). β-1,6 glucan is a second type of glucan molecule present in the fungal cell wall. It is shorter (150 glucose molecules) and only contributes to about 10% of the total cell wall mass. Covalently linked to β-1,3 glucan, chitin and the mannoproteins, β-1,6 glucan connects the cell wall constituents to each other (Klis et al., 2006). β-1,6 glucan is found in many different fungi with a variable degree of branching (Lesage et al., 2004).

Both, covalently and non-covalently bound mannoproteins are embedded in the glucan network and form the outer mannan layer of the fungal cell wall, being responsible for the majority of the cell wall mass. Cell wall proteins (CWP) usually are heavily glycosylated proteins. Two types of glycosylation exist: protein N-glycosylation adds a complex oligosaccharide to the protein and O-glycosylated CWPs carry short chains of mannosyl residues (Dempski & Imperiali, 2002, Strahl-Bolsinger *et al.*, 1999).

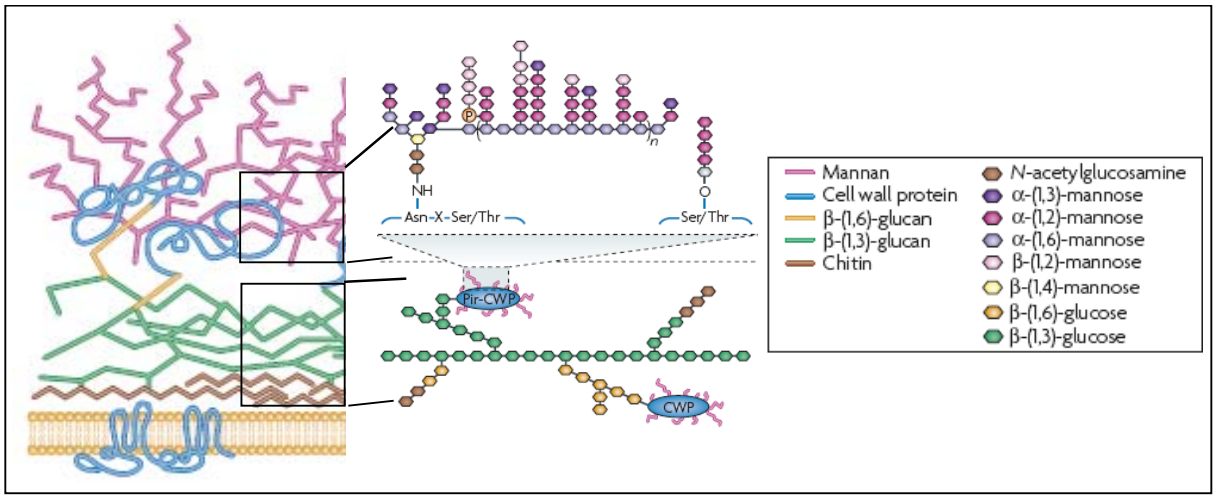

Figure 11. Exemplary structure of the fungal cell wall. Shown are the major cell wall components: chitin, β-1,3 glucan and attached mannoproteins. The magnification shows the structural composition of single polymer components. Modified from (Netea *et al.*, 2008).

The largest group of CWPs consists of glycosyl-phosphatidylinostiol (GPI)-anchored proteins which are attached to β-1,6 glucan. GPI-anchored proteins contain serine/threonine-rich domains, which are highly mannosylated. Flocculins (ScFlo), sexual agglutinins (ScAga), the ScTir protein family (ScTir, ScDan), and the ScGas family are examples for GPI-CWPs (Lesage & Bussey, 2006). GPI-CWPs stabilize the cell wall and mutants often show

hypersensitivity to cell wall-damaging agents (Klis et al., 2006). A second CWP family contains proteins that are released by treatment with mild alkali conditions. This group includes the Pir proteins, which have putative roles in forming a barrier and strengthening the cell wall, thereby influencing cell wall permeability (Mrsa *et al.*, 1997). Several other cell wall proteins execute glycolytic activities. Among those are for example the glucanases ScBgl2 and ScExg1, as well as the chitinase ScCts1 (Klis et al., 2006, Lesage & Bussey, 2006).

The great number of different CWPs demonstrates that the structural composition of the outer cell wall layer can vary significantly among different fungal species. In addition, the cell wall composition depends on growth form, growth stage, cell cycle-dependent expression and environmental influences. The outer layer does not only act as barrier by regulating permeability but may also widely affect hydrophobicity, adhesion, antigenicity and pathogenicity of the fungal cell (Batova *et al.*, 2009, de Groot *et al.*, 2008, Kaur *et al.*, 2007, Netea et al., 2008).

The cell wall composition of *C. glabrata* differs considerably from the cell wall of *S. cerevisiae* or *C. albicans*, although the general constituents are the same (Table 3). The *C. glabrata* cell wall contains almost 50 percent more protein and consists of significantly more mannan than the cell wall of *S. cerevisiae* (de Groot *et al.*, 2008). The amounts of alkali-insoluble glucan as well as chitin levels are relatively low in *C. glabrata*, implying that fewer connections between glucan and chitin exist. The core glucan structure may be thinner whereas the mannan layer is thicker (de Groot *et al.*, 2008). Masking glucans under a dense layer of mannan may be an advantage for *C. glabrata* to successfully escape host immune surveillance. Shielding proinflammatory pathogen-associated molecular patterns (PAMPs) from recognition by the host's immune cells, is generally thought to be an escape mechanism of fungal pathogens (Netea et al., 2008).

Species	Cell wall content[a]						
	Protein (%)	Chitin (%)	Man (%)	Glu (%)	M/G	Alkali-insoluble glucan (%)[b]	
						1,6-β	1,3-β
C. glabrata	6.4 ± 0.1	1.2 ± 0.1	43.8 ± 0.5	54.0 ± 0.2	0.81	4.2 ± 0.1	16.7 ± 1.7
S. cerevisiae	4.0 ± 0.1	1.4 ± 0.2	34.2 ± 1.6	60.3 ± 2.5	0.57	7.1 ± 0.2	26.8 ± 0.9
C. albicans	3.5 ± 0.2	4.2 ± 0.1	26.6 ± 2.3	64.0 ± 4.9	0.42	10.6 ± 0.6	26.2 ± 1.1

Table 3. Cell wall composition of *C. glabrata*, *S. cerevisiae* and *C. albicans*. The *C. glabrata* cell wall contains almost 50 percent more protein and more mannan than *S. cerevisiae*; (de Groot et al., 2008).

Recent studies addressed the distinct composition of the cell wall of fungal pathogens to identify possible components contributing to fungal pathogenicity. An in-silico analysis identified 106 putative GPI-anchored proteins of different functional groups, five CgPir family and five CgBgl2 family members in *C. glabrata* (Weig *et al.*, 2004). A follow-up study revealed a total of 67 adhesin-like proteins in *C. glabrata*, most of which are located in subtelomeric regions. Mass spectrometry analysis identified several known CWPs and

defined Awp1-4 as a new family of adhesin-like wall proteins (de Groot et al., 2008). Remarkably, the presence of adhesins strongly depends on the genetic background and the growth phase. For example, the novel adhesins Awp1 and Awp4 are only expressed in stationary phase cells.

Despite a suspected high number of GPI-linked proteins in *C. glabrata*, only a few have been studied in detail. For instance, the Cg*GAS* gene family shares significant homologies with the *S. cerevisiae* GPI-CWP ScGas1 (Weig *et al.*, 2001). Disruption of Cg*GAS1* or Cg*GAS2* results in cell aggregates, suggesting a cell wall-related function.

The largest group of GPI-anchored adhesins in *C. glabrata* is encoded by the lectin-like *EPA* (epithelial adhesin) gene family. *EPA* homologues are present in several fungal species and share a similar domain structure. The family consists of multiple adhesins of at least 23 related genes (Kaur *et al.*, 2005, De Las Penas *et al.*, 2003). *In vitro* adherence of up to 95 % is largely mediated by the major lectin Epa1. However, its influence on virulence is not fully understood because no difference exists in colonization and persistence between the isogenic wild-type and the *epa1*Δ strain (Cormack *et al.*, 1999). Interestingly, the majority of *EPA* genes are expressed at low levels. This may be partly explained by their localization to subtelomeric regions, where expression is controlled by the silencing machinery (Castano et al., 2005).

The transcriptional silencing machinery of *C. glabrata* involves CgRap1, CgSir2, CgSir3, CgSir4 and CgRif1. *C. glabrata* mutants lacking Cg*SIR3* or Cg*RIF1* show higher expression of *EPA6* and *EPA7*, as well as *EPA1*. In addition, cells with mutations in genes encoding components of the silencing machinery are hyperadherent to epithelial cells in culture and biofilm-positive (Iraqui et al., 2005). These strains also show a more efficient colonization of the kidney when compared to the wild type strain in a murine model of disseminated candidiasis, implying that the silencing machinery is involved in regulation of virulence factors (Castano *et al.*, 2005). The use of glycan microarrays further demonstrated that Epa1, Epa6 and Epa7 bind to a different range of carbohydrates and that the ability to adhere strongly depends on the host cell type (Zupancic *et al.*, 2008).

The regulation of *EPA* genes depends on specific environmental signals, showing that *C. glabrata* closely adapted its physiology to the human host. Limitation of nicotinic acid induces *EPA* expression probably mediated by the silencing machinery (Domergue et al., 2005). Interestingly, nicotinic acid is a precursor for NAD^+, which itself serves as a cofactor of the histone-modifier CgSir2. CgSir2 controls expression of Epa adhesins by transcriptional silencing. In consequence, the low nicotinic acid concentration in the urinary tract leads to decreased CgSir2 activity, resulting in induction of *EPA6* expression. Consistently, a triple *epa1*Δ *epa6*Δ *epa7*Δ mutant shows reduced ability to colonize the bladder (Domergue et al.,

2005). This is a remarkable example of how *C. glabrata* can adapt to a specific ecological host niche.

In addition, *EPA6* expression is induced after exposure to sorbic acid and parabens, which are used as preservatives in food and health products. The induction of *EPA6* transcription upon weak-acid stress is CgFlo8 and Mss11 dependent and leads to increased adherence to vaginal epithelial cells (Mundy & Cormack, 2009).

Another gene family encoding *C. glabrata* GPI-anchored proteins appears upregulated after phagocytosis by macrophages (Kaur *et al.*, 2007). *C. glabrata* has eleven yapsin-like genes, of which Cg*YPS1* and Cg*YPS7* are closely related to the baker's yeast yapsins. Cg*YPS1* and Cg*YPS7* are implicated in cell wall integrity and survival in stationary phase cells (Kaur *et al.*, 2007). Eight *YPS* genes are found in a *C. glabrata* specific cluster, which are transcriptionally induced after coincubation with macrophages. Interestingly, a strain disrupted for Cg*YPS1* and Cg*YPS7* or a strain lacking all eleven Cg*YPS* genes shows reduced virulence in a mouse model of disseminated candidiasis. The strains are highly attenuated in kidney and liver when compared to the wild type. These data imply that Cg*YPS* genes play a role in the infection process and survival of *C. glabrata* in the host (Kaur et al., 2007).

3.5 The host side

To counteract a microbial infection, the host immune system has to mount a rapid response. The vertebrate immune system consists of two major components, the innate and the adaptive arm. The first defence line is composed of cells of the innate immune system. Neutrophils, monocytes, macrophages and dendritic cells are present at tissues, such as mucosal surfaces and epithelial cell barriers (Netea et al., 2008, Romani, 2004). The cells of the innate immunity are equipped with a limited number of surface receptors, so-called pattern recognition receptors (PRR), which enable recognition of conserved microbial structures, collectively termed pathogen-associated molecular patterns (PAMPs) (Kopp & Medzhitov, 2003). These PRRs (Figure 12) enable the host to rapidly recognize a broad range of pathogens and to start coordinating a protective immune response. The immediate innate response involves phagocytosis and secretion of microbial compounds, as well as cytokine production to instruct and modulate the adaptive immune response.

Recognition of fungal pathogens by Toll-like receptors (TLRs), the mannose receptor, complement receptors, scavenger receptors or dectin-1, trigger the uptake of the microbial cell (Netea et al., 2008). Distinct microbial surface molecules serve as ligands for these receptors (Figure 12). For example, the macrophage mannose receptor binds to branched N-bound mannans, whereas O-linked mannan is detected by TLR4 and galectin recognizes β-mannosides (Netea et al., 2008). Further, β-glucans are ligands for the complement receptor

CR3, and dectin-1 specifically recognizes β-1,3 and β-1,6 glucans (Brown, 2006, Taylor *et al.*, 2007). TLRs expressed by phagocytes and dendritic cells recognize different PAMPs, often involving a co-receptor (Gantner *et al.*, 2003). Several receptors also show overlapping functions. For instance, both TLR2 and TLR4 have been implicated in recognition of *C. albicans* (Netea et al., 2002). Notably, immune cells are also able to discriminate between different fungal morphologies such as yeast and hyphae (d'Ostiani *et al.*, 2000, Jouault *et al.*, 2006).

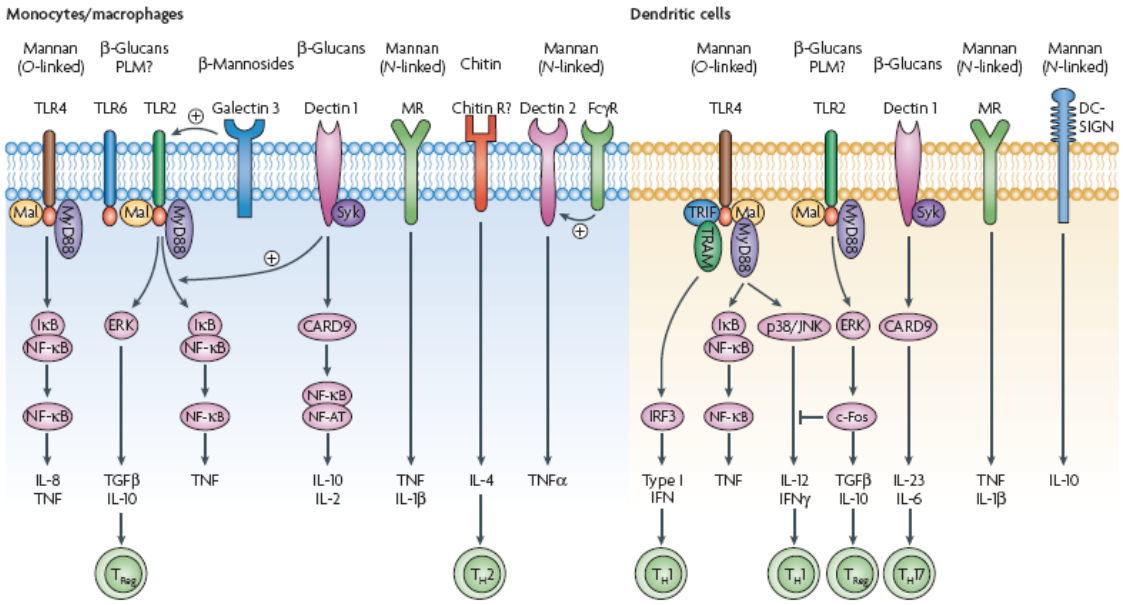

Figure 12. Pattern recognition receptors of innate immune cells. A great variety of pattern recognition receptors of monocytes, macrophages and dendritic cells recognize different fungal cell wall components. Recognition is mediated by Toll-like receptors and lectin receptors such as the mannose receptor (MR), dectin 1 and a putative chitin receptor. Signal transduction is carried out through MAPK and NF-κB pathways (Netea et al., 2008).

TLR-dependent signaling activates innate as well as adaptive immunity to fungi, including the production of proinflammatory cytokines, IL-12 production by dendritic cells and induction of the respiratory burst (Romani, 2004). Other antifungal mechanisms involve degranulation and release of small molecules such as defensins (Romani, 2004).

The respiratory burst is an effective mechanism to fight fungal pathogens. Upon interaction with a pathogen, phagocytic cells produce reactive oxygen species (ROS), involving NADPH oxidase and nitric oxide synthase as key enzymes. ROS include superoxide anions, which are converted to hydrogen peroxide and hydroxyl radicals (Babior, 2000). These radicals can kill microbial pathogens (Missall *et al.*, 2004). However, fungal pathogens developed certain molecular mechanisms to degrade host-derived ROS (Frohner *et al.*, 2009).

The study of the particular defence mechanisms and molecular components of the innate and the adaptive immune response, as well as fungal escape and survival mechanisms will allow to gain a deeper understanding of the interaction between fungal pathogens and their hosts. This may also help to understand the differences between and to

define commensalism and virulence. Exploiting genomic and proteomic studies in both, pathogens and host immune cells, may help to elucidate some of the fundamental processes.

3.6 Genomic studies

A multitude of different methods and techniques have been developed to study all aspects of the biology of the model yeast *S. cerevisiae*. Given the emerging number of fungal opportunistic pathogens, the specific differences between pathogenic and non-pathogenic fungi became an attractive topic. However, specific problems hampered studies of the underlying molecular mechanisms of fungal pathogenesis. For example, *C. albicans* is a diploid organism with a very flexible genome. Therefore, efficient strategies had to be developed to delete both alleles (Berman & Sudbery, 2002, Hibbett et al., 2007). In addition, the use of the auxotrophic *URA3* marker is problematic for virulence studies *in vivo* (Brand *et al.*, 2004, Reuss *et al.*, 2004).

Although being a haploid organism and closer related to baker's yeast, existing tools and techniques from *S. cerevisiae* are of limited applicability for *C. glabrata*. However, a decent methodological repertoire to study virulence properties exists now for *C. glabrata* and for other fungal pathogens, including transformation protocols, auxotrophic strains and corresponding marker cassettes, plasmids for complementation, reporter plasmids, a conditional deletion system and a strain library of insertional mutants (Castano *et al.*, 2003, El Barkani *et al.*, 2000, Frieman *et al.*, 2002, Kitada *et al.*, 1995, Kitada *et al.*, 1997, Nakayama *et al.*, 1998, Willins *et al.*, 2002).

The genomic era allows new approaches for gene profiling. After the full sequencing of the *S. cerevisiae* genome, first attempts were undertaken to precisely delete every single gene, generating complete deletion strain collections (Giaever *et al.*, 2002, Winzeler *et al.*, 1999). These libraries are used to perform functional profiling. The use of signature-tagged (bar-coded) deletion strains, enables the analysis of growth phenotypes and fitness of a large number of strains in parallel. In principle, two possibilities exist for quantification of the upstream and downstream barcode tags, which are introduced during the gene deletion process: quantitative PCR or hybridization of the amplified barcode oligonucleotides to a microarray. Both techniques allow the quantification of the relative abundance of each strain in the input and recovered output pool. This technique makes it possible to assess individual contribution of single genes to the fitness or virulence of an organism.

In recent years, this technology has also been applied for selected fungal pathogens to study their fungal virulence at a genome-wide scale. A strategy for a systematic large-scale gene disruption has been developed to study *C. albicans* virulence (Noble & Johnson, 2005). Recently, a systematic genome-wide study of the pathogenicity in *C. neoformans*

identified many virulence-related genes implicated in capsule formation, melanization, growth and infectivity (Liu *et al.*, 2008). In this study pools of barcoded deletion strains were used to screen a suitable mouse model for pulmonary infection. The relative abundance of each strain was measured after recovery from tissue, using quantitative PCR. This screen of signature-tagged deletion strains identified a number of putative virulence factors, affecting known as well as novel virulence attributes and even the characterization of a transcription factor involved in a previously unknown virulence mechanism.

3.7 Aims of the thesis

C. glabrata represents the second most frequent cause of Candidiasis. However, the specific attributes that turn *C. glabrata* into a successful fungal pathogen remain elusive. Its inherent resistance to azoles is a major characteristic of this monomorphic human fungal pathogen. In contrast to the dimorphic yeast *C. albicans*, which can form true hyphae and possesses virulence-associated secreted proteases and phospholipases, *C. glabrata* lacks most of these putative virulence factors. Interestingly, both opportunistic yeasts are usually found as harmless commensals of immunocompetent hosts, colonizing mucosal surfaces, the skin and the gastro-intestinal tract. Nevertheless, *C. glabrata* displays additional characteristic virulence traits such as a large repertoire of adhesins, which are regulated by transcriptional silencing, the hypervirulence factor CgAce2, and a very dynamic genome, which might influence its virulence and adaptation capabilities.

Understanding the molecular basis, contributing to the pathogenicity and the mutual interaction of *C. glabrata* with the host immune system, may help to better understand its specific virulence. So far, the lack of a full sexual cycle and the low recombination efficiency still hamper efficient genome-wide studies on the specific pathogenicity of *C. glabrata*. However, the availability of the complete genome sequence enables these genome-wide studies.

The aim of this thesis was to identify new putative virulence factors of *C. glabrata*, using a large-scale reverse-genetics approach. This included:

- the selection of categorized candidate genes based on the homology to *S. cerevisiae* genes, using bioinformatics and literature research,
- establishing a protocol for more efficient gene deletion by homologous recombination (fusion PCR approach) to generate a genome-wide signature-tagged *C. glabrata* deletion strain library,
- phenotypic profiling of the generated gene deletion strain library in vitro and ex vivo,
- characterization of single gene deletion mutants.

Approximately 1000 candidate genes have been chosen for gene deletion. The deletion mutants are arranged in sets, each containing some 90 mutants. Every mutant of one set is marked by a unique pair of upstream and downstream barcode sequences, which allow for accurate identification. The generated strain collection was subsequently screened for growth phenotypes on a variety of compounds and media to identify putatively novel virulence and drug resistance-related genes. The deletion strains were also studied for cell and colony morphology phenotypes. Single mutants displaying differences to known *S. cerevisiae* phenotypes were further characterized by microbiological, genetic and biochemical methods for their phenotypes and putative implication in virulence-related functions.

4 Materials and Methods

4.1 Materials

4.1.1 Yeast media

Rich media (YPD) and synthetic media (SC) were prepared essentially as described elsewhere (Kaiser *et al.*, 1994). All media were autoclaved at 121°C. Heat sensitive substances were sterile filtered and added to the media (~50°C) afterwards. For all plates, 250 ml of 4 % agar were added to 250 ml of medium.

Rich medium:

50 ml of 20 % sterile glucose was added to 450 ml 1 x YPD to prepare liquid medium with a final concentration of 2 % glucose. YPD plates contained glucose at a final concentration of 2%.

	1 x YPD	2 x YPD
Yeast extract	10 g/l	20 g/l
Peptone	20 g/l	20 g/l
Glucose (w/v)	2 %	4 %

NAT-plates: Nourseothricin (100 mg/ml, H_2O) was added to a final concentration of 200µg/ml.

Minimal medium:

Minimal medium was prepared with 2 x YNB without amino acids and glucose added to a final concentration of 2 %. MM plates contain glucose at a final concentration of 2 %.

	1 x MM
Bacto-YNB w/o aa	6.7 g/l
Glucose (w/v)	2 %

Drop-out media:

SC medium (500 ml) was prepared with 2 x SC medium and 250 ml sterile H_2O and glucose were added to a final concentration of 2 %. 5 ml of the required amino acids from 100 x stocks were added. SC plates contained glucose at a final concentration of 2 %.

	2 x SC
Bacto-YNB w/o aa and $(NH_4)_2SO_4$	3.4 g/l
Ammonium sulfate	10.0 g/l
Amino acid mix	2.86 g/l

Sterile stock solutions:

Glucose: 20 %

Agar: 4 %

100 x URA: 4 g/l L-Uracil in H_2O

100 x HIS: 6 g/l L-Histidine in H_2O

100 x LEU: 26 g/l L -Leucine in H_2O

100 x TRP: 8 g/l L-Tryptophane in H_2O (filter-sterilized, 4°C)

Amino acid mix (per 29 g):

0.4 g L-arginine	0.6 g L-tyrosine
0.6 g L-isoleucin	8.0 g L-serine
1.0 g L-phenylalanine	2.0 g L-glutamic acid
2.0 g L-aspartic acid	3.0 g L-valine
3.0 g L-methionine	3.6 g L-lysine
4.0 g L-threonine	0.8 g adenine

4.1.2 *E. coli* media

For LB plates, agar was added to a final concentration of 2 % to 2 x LB. For LB-amp plates, ampicillin (100 mg/ml stock, H_2O) was added to a final concentration of 100 µg/ml; for LB-kan plates, kanamycin (50 mg/ml stock, H_2O) i was added to a final concentration of 50 µg/ml; for LB-cam plates, Chloramphenicol (10 mg/ml stock, EtOH) was added to a final concentration of 40 µg/ml.

	1 x LB	2 x LB	SOB
Tryptone	10 g/l	20 g/l	20 g/l
Yeast extract	5 g/l	10 g/l	5 g/l
NaCl	10 g/l	20 g/l	10 mM
KCl	-	-	2.5 mM
$MgCl_2$	-	-	20 mM

4.1.3 Buffer and solutions

Buffer/ solution	Concentration	Chemical
Anode buffer I		
	0.3 M	Tris Base
	20 % (v/v)	Methanol
Anode buffer II		
	25 mM	Tris Base
	20 % (v/v)	Methanol
Blocking buffer	1 x	TBS
	5 %	milk powder
	0.1 %	Tween 20
Cathode buffer		
	25 mM	Tris Base
	40 mM	6-Amino-n-Hexanoic acid
Coomassie staining solution (2 l)	200 ml	Glacial acetic acid
	500 ml	Isopropanol
	0.67 g	Coomassie Blue G250
	1300 ml	
Destaining solution (1 l)		
	250 ml	Methanol
	70 ml	Glacial acetic acid
	680 ml	H_2O
DNA loading buffer (10 x)	100 mM	EDTA pH 8.0
	60 % (v/v)	Glycerol
	0.25 % (w/v)	Bromphenolblau
	0.25 % (w/v)	Xylen Cyanol
Denhardts reagent		
	1% (w/v)	Ficoll 400
	1% (w/v)	Polyvinylpyrrolidone
	1% (w/v)	BSA
		in sterile H_2O, sterile filter
DNA extraction buffer	2% (v/v)	Triton X-100
	1% (v/v)	SDS
	100mM	Tris/HCl pH 8.0
	1mM	EDTA
DTT		
	1 M	dissolved in 0.01M NaOAc pH 5.2
Hybridisation buffer (microarray)		
	4 x	SSC
	0.1 %	SDS
Prehybridisation buffer (microarray)		
	4 x	SSC
	0.1 %	SDS
	10 mg/ml	BSA
PCR buffer (10 x)	500 mM	KCl
	100 mM	Tris-HCl pH 9.0
	1 %	Triton X-100
	15 mM	MgCl2
PBS pH 7,4		
	87.7 g	NaCl
	2.6 g	NaH_2PO_4
	22.5 g	Na_2HPO_4
Prehybridisation solution (Southern Blot)		
	2 ml	50x Denhardts reagent
	1 ml	20x SSC
	1 ml	10% SDS
	5.5 ml	H_2O
	40 µl	ssDNA

Protein sample buffer	40 mM	Tris-HCl pH 6.8
	8 M	Urea
	5 % (w/v)	SDS
	0.1 mM	EDTA
	1 % (v/v)	ß-Mercaptoethanol
	0.1 g/l	Bromphenolblue (freshly added)
	0.1 M	Tris base (freshly added)
RNase A-Lösung (100 x)		
	10mg/ml	RNase A in 1Vol. 10mM NaAc pH 5.2, 15min 100°C, + 0.1 Vol 1M Tris pH 7.5
Running buffer (SDS PAGE, 1l)	1.5 g	Tris
	7.2 g	Glycine
	4.0 g	SDS
Running gel (SDS PAGE, 10 %, 2 gels)	4.2 ml	H_2O
	2.5 ml	1.5 M Tris pH 8.8
	3.3 ml	Acrylamide (30%)
	10 µl	TEMED 0.1 g/l
	100 µl	APS (10%)
	100 µl	SDS (10%)
SSC (20 x, 1l)	175.3g	NaCl
	88.2g	Sodium citrate
		(adjust pH to 7.0 (with 37% HCl), autoclave)
Stacking gel (SDS PAGE, 4,5 %, 4 gels)	3 ml	H2O
	1.25 ml	0.5 M Tris pH 6.8
	0.75 ml	Acrylamide (30%)
	25 µl	SDS (10%)
	10 µl	TEMED
	100 µl	APS (10%)
STET- buffer	8 %	Saccharose
	50mM	Tris/HCl pH 8.8
	50mM	EDTA pH 8.0
	5 %	Triton X-100
Stripping buffer (Western Blot)	62.5 mM	Tris-HCl pH 6.7
	100 mM	ß-Mercaptoethanol
	2 %	SDS
TE	100 mM	Tris-HCl pH 7.5
	10mM	EDTA pH 8.0
TB		PIPES
	10 mM	$MnCl_2$
	55 mM	$CaCl_2$
	15 mM	KCl (dissolved in H_2O, pH adjusted to pH 6.7
	250 mM	with KOH, $MnCl_2$ added & filter sterilised, stored at 4°C)
TBE (10 x)	108 g/l	Tris base
	55 g/l	Boric acid
	40 ml	0.5 M EDTA pH 8.0
TBS (10 x)	1.44 M	NaCl
	0.5 %	Tween 20
	250 mM	Tris-HCl pH 7.5
TBS-T	1 x	TBS
	0.1 %	Tween 20
Yex-lysis buffer	1.85 M	NaOH
	7.5 %	ß-Mercaptoethanol (v/v) (freshly added)
	50% (w/v)	TCA

Table 4. Buffer compositions and solutions used in this study. Buffers were autoclaved or sterile filtered, when necessary.

4.1.4 Chemicals and computing software

Manufacturer	Location	Chemicals
Becton Dickinson	USA	Bacto Peptone, Yeast extract, Yeast Nitrogen Base, Tissue Culture plates, Casamino acids
Dako GmbH	Austria	Fluorescent mounting medium
Discovery Fine Chemicals	United Kingdom	Fluconazole, Ketoconazole, Itraconazole, Voriconazole, Amphotericin B
Eurogentec	Belgium	Oligonucleotides, Mesa green qPCR MasterMix plus dTTP
Fermentas	Austria	Restriction enzymes, PageRuler PLUS protein ladder, RiboLock RNase inhibitor, dNTPs, M-MuLV Rev. Transcriptase, DNaseI
GE Healthcare Europe	Austria	Hybond-N+ Membrane, Cy5 dCTP (25nmol), Cy3 dCTP (25nmol), DNA probe Labeling Kit, Klenow polymerase
Greiner Bio-One	Austria	96 well cell culture plates
Hanke Lab Products	Austria	α^{32}P dCTP
Harvard Apparatus	USA	96 well electroporation plates
Invitrogen (Molecular Probes)	USA	FCS, HBSS, Superscript III Reverse Transcriptase, β-mercatpoethanol
Lonza (Cambrex)	Belgium	TaKaRa ExTaq, Mighty Ligation Mix, Agarose
Merck	Austria	Glucose, $CuSO_4$, $MgCl_2$, $ZnCl_2$, KCl, Tris, Sodium Citrate, NaOH
NEB	Germany	Phospho-p44/42 MAPK (T202/Y204) Antibody
PAA Laboratories	Austria	DMEM w L-glutamine
Promega	Austria	pGEM cloning kit, RNA extraction kit
Santa Cruz Biotech.	Germany	BSA
Seikagaku	Japan	Zymolyase 100T, 20T
Sigma, Fluka	USA	Calcofluor White, Congo Red, 5'-Flucytosine, DMSO, Triton X-100, Tween 20, Anitbiotics, SDS, Lithiumacetate, PEG 3500, TEMED, APS, EDTA, , NaCl, Luminol,Isoluminol, Zymosan, Amino acids, PCI, IPTG, Ampicillin, Kanamycin, DTT, D-Sorbitol, Ammonium sulfate, $MnCl_2$, LiCl, Phenol, glass beads, Ficoll400, Polyvinylpyrolidone,
Singer Instruments	UK	PlusPlates, RePads (short and long pins)
THP Medical Products	Austria	CL-XPosure Film 5x7 inches
VWR	Austria	Electroporation cuvettes, Petri dishes, Falcon tubes, Ammonium sulfate, 96 deep well plates
Werner Bioagents	Germany	Nourseothricin

Software	Manufacturer	Location	Resource
Gene Pix Pro4.1	Molecular Devices	USA	CD, license
Photoshop CS3, Illustrator CS3	Adobe	USA	ZID, license
ApE v1.12	Davis M. W.	USA	www.biology.utah.edu/jorgensen/wayned/ape/
Realplex 2.0	Eppendorf	Austria	CD, license
Filemaker 9.0	FileMaker	USA	ZID, license
GraphPad Prism 4	GraphPad	USA	ZID, license
Vector NTI 10	Invitrogen	USA	license
Perlprimer v1.1.14	Marshall O.	USA	perlprimer.sourceforge.net
Soft Imaging Viewer 5.0	Olympus	Germany	www.olympus-sis.com
FlowJo 7	TreeStar	USA	CD, license

Table 5. **Chemicals and software used in this study.**

4.1.5 Organisms

4.1.5.1 Bacterial strains

Strain	Genotype	Reference
DH5α	*F⁻, λ⁻, endA1, hsdR17(r_k^-, m_k^+), supE44, thi-1, recA, gyrA96, relA1, Φ80lacZΔM15*	(Hanahan, 1983)
TOP10	F- *mcr*A Δ(*mrr-hsd*RMS-*mcr*BC) φ80*lac*ZΔM15 Δ*lac*X74 *rec*A1 *ara*D139 Δ(*araleu*)7697 *gal*U *gal*K *rps*L (StrR) *end*A1 *nup*G	Invitrogen

Table 6. **Bacterial strains used in this study.**

4.1.5.2 *S. cerevisiae* strains

Strain	Genotype	Reference
BY4741	MATa *his3*Δ1 *leu2*Δ0 *met15*Δ0 *ura3*Δ0	(Brachmann *et al.*, 1998)
*slt2*Δ	BY4741 Mat a *his3*Δ1 *leu2*Δ0 *met15*Δ0 *ura3*Δ0 YHR030c::kanMX4	(Brachmann et al., 1998)

Table 7. ***S. cerevisiae*** **strains used in this study.**

4.1.5.3 *C. glabrata* strains

Strain	Genotype	Reference
ATCC2001	*C. glabrata* wild type strain	www.attc.org
HTL	*his3*Δ::FRT l*eu2*Δ::FRT *trp1*Δ::FRT	Jungwirth H., Lechner S.
H	Isogenic to ATCC2001; *his3*Δ::FRT	Jungwirth H., Lechner S.
T	Isogenic to ATCC2001; *trp1*Δ::FRT	Jungwirth H., Lechner S.
L	Isogenic to ATCC2001; *leu2*Δ::FRT	Jungwirth H., Lechner S.
HT	Isogenic to ATCC2001; *his3*Δ::FRT *trp1*Δ::FRT	Jungwirth H., Lechner S.
TL	Isogenic to ATCC2001; *trp1*Δ::FRT *leu2*Δ::FRT	Jungwirth H., Lechner S.
HL	Isogenic to ATCC2001; *his3*Δ::FRT *leu2*Δ::FRT	Jungwirth H., Lechner S.
HTL reference	*his3*Δ::FRT *leu2*Δ::FRT *trp1*Δ::*NAT1* (barcode)	this study
All deletion strains	All strains isogenic to HTL; *gene*Δ::*NAT1*	this study
Cg*fks1*Δ	Isogenic to HTL; *fks1*Δ::*HIS3*	this study
Cg*ace2*Δ	Isogenic to HTL; *ace2*Δ::*HYGr*	this study

Table 8. ***C. glabrata*** **strains used in this study.** For better reading, the addition of "Cg" has been skipped in the results and discussion chapters. Only where necessary to underline the difference between genes/proteins of *C. glabrata* and other organisms "Cg" is added. Genes and proteins of *S. cerevisiae* are marked with "Sc", of *C. albicans* with "Ca".

4.1.5.4 Cell lines and primary cells

Cell line	Genotype	Reference
BMDM WT	C57BL/6 mice	(George-Chandy *et al.*, 2008)
gp91phox-/-	C57BL/6 mice	(Frohner et al., 2009) (Lundqvist & Dahlgren, 1996)

Table 9. **Mammalian primary cells used in this study.**

4.1.6 Plasmids

Name	Marker	Description	Insert	Reference
pGEM-T	ampR	ampR, cloning of PCR products	-	Promega
pACT	Cg*TRP1*	ampR, CEN, ARS	-	(Gregori et al., 2007)
pBM51	Sc*HIS3*	CEN, ARS	-	from Biao Ma
pJK863	*NAT1*	ampR, *NAT1*, recombinase	*NAT1*	(Shen *et al.*, 2005)
pTS50	ampR	Carries *NAT1* with U2 & D2 adaptor seq.	U2-*NAT1*-D2	this study
pSFS2a	ampR	ampR, *SAT1* marker, recombinase	*SAT1*-ca*FLP*	(Reuss et al., 2004)
pGRB2.0	ampR, Sc*URA3*	CEN, ARS	-	(Frieman et al., 2002)
pGRB2.3	ampR, Sc*URA3*	CEN, ARS, GFP	-	(Frieman et al., 2002)
pGRB2.0HIS	ampR, Sc*HIS3*	CEN, ARS	-	this study
pGRB2.3HIS	ampR, Sc*HIS3*	CEN, ARS, GFP	-	this study
pGRB2.0HIS-*SLT2*	ampR, Sc*HIS3*	CEN, ARS, Cg*SLT2* (own promotor)	Cg*SLT2*	this study
pBM51-*CBK1*	ampR, Sc*HIS3*	CEN, ARS, Cg*CBK1* (Sc*PGK1* promotor)	Cg*CBK1*	this study
pBM51-*DSE2*	ampR, Sc*HIS3*	CEN, ARS, Cg*DSE2* (Sc*PGK1* promotor)	Cg*DSE2*	this study
pACT-*DSE2*	ampR, Sc*TRP1*	CEN, ARS, Cg*DSE2* (own promotor)	Cg*DSE2*	this study
pBM51-*ACE2*	ampR, Sc*HIS3*	CEN, ARS, Cg*ACE2* (Sc*PGK1* promotor)	Cg*ACE2*	this study

Table 10. **Plasmids used and generated in this study.**

4.1.7 Oligonucleotides

Name	Sequence	Description
fp_NAT1-U2	5'-***CGTACGCTGCAGGTCGAC***agcttgcctcgtccccgccg-3'	forward primer to add U2 marker; ready to add barcode
rp_NAT1-D2	5'-***CTACGAGACCGACACCG***ctggatggcggcgttagtatcg-3'	reverse primer to add U2 marker; ready to add barcode
Heukan2	5'-CGTCAAGACTGTCAAGGAGGG-3'	Internal 5' reverse control primer
Heukan3	5'-CATCATCTGCCCAGATGCGAAG-3'	Internal 3' forward control primer
5M-marker	5'-**ccgctgctaggcgcgccgtg**BARCODE-UP***cgtacgctgcaggtcgac***-3'	Forward primers to add unique barcode sequences
3M-marker	5'-**gcagggatgcggccgctgac**BARCODE-DOWN***ctacgagaccgacaccg***-3'	Reverse primers to add unique barcode sequences
f_ctrl_pGRB	5'-aggctgcgcaactgttgg-3'	Control primer for pGRB plasmids
r_ctrl_pGRB	5'-gcggataacaatttcacacagg-3'	Control primer for pGRB plasmids
pGRBctrl	5'-CACACAGGAAACAGCTATGACC-3'	Control primer for pGRB plasmids
pGRB2.3ctrl	5'-CGTAGTTTTTCAAGTTCTTAGATGC-3'	Control primer for pGRB plasmids
fCBK1_BamH	5'-agt**GGATCC**atgtttggtggcgagtatgatcac-3'	Clone Cg*CBK1* into pBM51
rCBK1_EcoRI	5'-atc**GAATTC**ttataatgcattctttctcgtcaagtag-3'	Clone Cg*CBK1* into pBM51
fCBK1_EP_EcoRI	5'-tca**GAATTC**gcattggcggctatgactgtg-3'	Clone Cg*CBK1* into pGRB2.0*HIS3*
rCBK1_EP_EcoRI	5'-tga**GAATTC**acacacatgcataggcacacag-3'	Clone Cg*CBK1* into pGRB2.0 *HIS3*
fDSE2_Xba	5'-agtc**TCTAGA**atgcaattccgtgccgctacac-3'	Clone Cg*DSE2* into pBM51
rDSE2_Xho	5'-gact**CTCGAG**ttaattagcagaaacagttttgtataccg-3'	Clone Cg*DSE2* into pBM51
fDSE2_EcoRI	5'-agtc**GAATTC**aacccctatgaaatcaggggc-3'	Clone Cg*DSE2* into pGRB2.0 *HIS3*
rDSE2_EcoRI	5'-gact**GAATTC**ggacagtgaatagaatgctggc-3'	Clone Cg*DSE2* into pGRB2.0 *HIS3*
fACE2_EcoRI	5'-agtc**GAATTC**atgaatactttccaggcggattgg-3'	Clone Cg*ACE2* into pBM51
rACE2_SalI	5'-agtc**GTCGAC**tatactactcctcaatcgtccc-3'	Clone Cg*ACE2* into pBM51
fp-CBK1	5'-TGATATACCTCAGTTACACCCTTCC-3'	qRT-PCR
rp-CBK1	5'-GTTGTTCATGTTACTTGTGCTCGG-3'	qRT-PCR
fp-ACE2	5'-GACAGGAGAGCATCAACATCGT-3'	qRT-PCR
rp-ACE2	5'-GACAGGAGAGCATCAACATCGT-3'	qRT-PCR
fp-DSE2	5'-ATCTGCTTCCTCTAGTAGTGTTTCC-3'	qRT-PCR
rp-DSE2	5'-TACACTTGAGCTATCGTTGTCTAGG-3'	qRT-PCR
fp-CTS1	5'-AATGTCCATACCCAGATGCCTC-3'	qRT-PCR
rp-CTS1	5'-GAAATTCTTCCAGTCGTCCCAG-3'	qRT-PCR
fp-PGK1	5'-TCATTGCTGACGCTTTCTCC-3'	qRT-PCR
rp-PGK1	5'-CGAACAACTTTCTGGACTCTGG-3'	qRT-PCR
fp_cgFLO9	5'-GTGAGTAAGACTATTTCCAGCGG-3'	qRT-PCR
rp_cgFLO9	5'-GGTCCCACCATCACTTACAG-3'	qRT-PCR
fp_cgSED1	5'-ACTACCACTGTCTCTTCTACTACC-3'	qRT-PCR
rp_cgSED1	5'-GTAAGCAGTAACAACTTCGATCTC-3'	qRT-PCR
fp_cgMUC1	5'-GCTAACAAATCCGTCATCTACTG-3'	qRT-PCR
rp_cgMUC1	5'-ATTGTCAGGTCCCGTAATATAGG-3'	qRT-PCR

fp_cgKSS1	5'-CATCCTTTCTTAGCAACATACCAC-3'	qRT-PCR
rp_cgKSS1	5'-CTGTCGTCTGTCCCATATCC-3'	qRT-PCR
fp-cgSCW4	5'-ATGCTCATGCTTACTTTGACCA-3'	qRT-PCR
rp-cgSCW4	5'-CTTTCTTACCGTCACAAGCAGTC-3'	qRT-PCR
fp-EPA1	5'-GCGTAATCAAGGAAACCAAAGAC-3'	qRT-PCR
rp-EPA1	5'-GTTCCACCTAAAGACTCATAACTG-3'	qRT-PCR
fp-EPA7	5'-AGATCCGAACCCTGTAATAGAC-3'	qRT-PCR
rp-EPA7	5'-TCAACACCGATGATTGTAGATGAG-3'	qRT-PCR
fp-EXG1	5'-CCGCTTTAACCGATTGTACCA-3'	qRT-PCR
rp-EXG1	5'-TGAACCTATGTAAGAAGAGCCC-3'	qRT-PCR

Table 11. Single primers used in this study. Primers used for generation of deletion cassettes are deposited in the *C. glabrata* gene deletion collection. Oligonucleotides **fp_NAT1-U2** and **fp_NAT1-D2** were used to amplify the dominant marker *NAT1* and addition of the constant regions U2 and D2 (italic, bold). Oligonucleotides **Heukan2** and **Heukan3** were used as control primers for colony PCR binding inside the *NAT1* marker. Oligonucleotides **5M-marker** and **3M-marker** were used to amplify the *NAT1* marker from plasmid pTS50 adding the unique individual barcode sequences and the constant regions U1 and D1 (bold) which are used for fragment fusion as well as amplification of barcodes. BARCODE-UP/BARCODE-DOWN are placeholders for the unique barcode sequences listed in Table 12.

4.1.8 Barcode sequences used for signature tags

well	UPTAG	Sequence Uptag 5'-3'	DOWNTAG	Sequence Downtag 5'-3'
A1	BC_UP_A1	5'-CGCCTAAGACCGGATAAAGC-3'	BC_DN_A1	5'-GGGCTCGAGATTTAAACGGC-3'
A2	BC_UP_A2	5'-CGATTCGATAAATGACGCGA-3'	BC_DN_A2	5'-CGGCCTAAGTTTCGGTTCGT-3'
A3	BC_UP_A3	5'-GCTACAAACATAAGTGCGGC-3'	BC_DN_A3	5'-CCGAGTTCTACTAGGTGTTA-3'
A4	BC_UP_A4	5'-ATCGAACGTGTGTCAAACGC-3'	BC_DN_A4	5'-ATAGCCGACTAACGAGCGTC-3'
A5	BC_UP_A5	5'-AAGATAGTCGCCGAACTCGC-3'	BC_DN_A5	5'-AATCGACGCTAACGACTGAG-3'
A6	BC_UP_A6	5'-ATCGAGCACGTAACCGTTGC-3'	BC_DN_A6	5'-ATATGATACTCACGACCCGG-3'
A7	BC_UP_A7	5'-AATGTCGCGTAATGGCTTAG-3'	BC_DN_A7	5'-ACCTTATGTGTAATGAGCGG-3'
A8	BC_UP_A8	5'-AGGCAGATACGATTAGTACG-3'	BC_DN_A8	5'-AAGTCTATATCAGTAGCGGG-3'
A9	BC_UP_A9	5'-AAGCATCGTTAAGGCTGCCG-3'	BC_DN_A9	5'-ATTGGTCAGCGAGCCCTACT-3'
A10	BC_UP_A10	5'-ATAGATGACTACCGCGTCCG-3'	BC_DN_A10	5'-ACTTGAGGCGTAGACCTGCT-3'
A11	BC_UP_A11	5'-AATCGACTGTAAGTATCGCG-3'	BC_DN_A11	5'-AACGTGGGATCACTCGTGCT-3'
A12	BC_UP_A12	5'-ATAGCCTTCTAAGAGCGGCG-3'	BC_DN_A12	5'-AATCGGCGCTCACGCTTAGT-3'
B1	BC_UP_B1	5'-ATCGGCCTGTAATCGGATCG-3'	BC_DN_B1	5'-ACGATTGCGCGATTCGAGTT-3'
B2	BC_UP_B2	5'-AATTAGCACTGACGGCCTCG-3'	BC_DN_B2	5'-ATGCGACCTTGTGGCAATTT-3'
B3	BC_UP_B3	5'-ATAGTTCCCGCAGCTCGTTG-3'	BC_DN_B3	5'-CGCCGTGTGAAACATACTAA-3'
B4	BC_UP_B4	5'-ACAGCTATTAGGACGTGTTG-3'	BC_DN_B4	5'-ATGACGGATGTATGACGACT-3'
B5	BC_UP_B5	5'-AGTAGTACAGCCCGCGTCAT-3'	BC_DN_B5	5'-CCCATTAGTCGCAAGAGTTA-3'
B6	BC_UP_B6	5'-ATGCCCGAGTTGTCGCCATT-3'	BC_DN_B6	5'-CGCGTTATGCAATACGGTTA-3'
B7	BC_UP_B7	5'-CCGCGTCGTAAATGATTAGA-3'	BC_DN_B7	5'-ATACACCGGCATAATCTGTC-3'
B8	BC_UP_B8	5'-CGCCCGAACGGAAGATATGA-3'	BC_DN_B8	5'-ATGTACCGAGCATTGCACGG-3'
B9	BC_UP_B9	5'-CCATATTTGCGAAGGTCGGC-3'	BC_DN_B9	5'-CGCATTCAGTACATTTACCG-3'
B10	BC_UP_B10	5'-CGGATATGTACTAATTGGGC-3'	BC_DN_B10	5'-CCGCGTCTAGTATAGTATGT-3'
B11	BC_UP_B11	5'-CGGCCTAACTGTAATTGATC-3'	BC_DN_B11	5'-CTCGACGCTGGACGTTATGT-3'
B12	BC_UP_B12	5'-CCCTGTTATGAACCTTGATC-3'	BC_DN_B12	5'-CGCTTCGAGTATGGGATATT-3'
C1	BC_UP_C1	5'-CGCGCAGAGGTTAGATAAAT-3'	BC_DN_C1	5'-CTGTACGTGCGATACTCGTT-3'
C2	BC_UP_C2	5'-CGACCCTGATGATCCTTTAT-3'	BC_DN_C2	5'-GCCTATACCCAACTAATGGA-3'
C3	BC_UP_C3	5'-CGGACGGTATTCATTCATCT-3'	BC_DN_C3	5'-GCCGAACCTTCAACAGAGTA-3'
C4	BC_UP_C4	5'-GTGAGCGAAACACCGCGTAA-3'	BC_DN_C4	5'-GCGTGTGAATAATACGGAAC-3'
C5	BC_UP_C5	5'-GTGCGAACCAACGTACTACA-3'	BC_DN_C5	5'-GGTCGATAATAACACGCCAC-3'
C6	BC_UP_C6	5'-GGGTACTCCACAACATTACA-3'	BC_DN_C6	5'-GAAGTACGCTCAAGACCGAC-3'
C7	BC_UP_C7	5'-GCTAATCGCTAATTCGTTCC-3'	BC_DN_C7	5'-GCGACCCTATAATTCTTGAC-3'
C8	BC_UP_C8	5'-GCATTAACGGGAACTAGAGC-3'	BC_DN_C8	5'-GTTAGGTCCATCCGCCATTG-3'
C9	BC_UP_C9	5'-GCCATTCGTATAACCGTGTC-3'	BC_DN_C9	5'-GCGAGACCGCTTTACCAGAT-3'
C10	BC_UP_C10	5'-GATTATACGCTATCCGAGGT-3'	BC_DN_C10	5'-GACTCCGTACTCACTAGGAT-3'
C11	BC_UP_C11	5'-GTATTCCGACTGCGGCACTT-3'	BC_DN_C11	5'-TCGGTTAGAACAGTAGAGAC-3'
C12	BC_UP_C12	5'-TAATACCCGATCACTGGTGG-3'	BC_DN_C12	5'-TACACTCGACGACACGGTAG-3'
D1	BC_UP_D1	5'-AAATTGGTCGTAATGCGTCG-3'	BC_DN_D1	5'-TATGTCGGACGCCGTAGACT-3'
D2	BC_UP_D2	5'-ATTACGAGGTACGCGCTTCG-3'	BC_DN_D2	5'-TTTGCGTACTGAGGACCGCT-3'
D3	BC_UP_D3	5'-ATTACCTAGTCGGAGACAGG-3'	BC_DN_D3	5'-TATCAGTTCCGCAGACGGGT-3'
D4	BC_UP_D4	5'-ATTAGCGTCTCGACTACCTT-3'	BC_DN_D4	5'-ACGGACCTTGTACGCGATCT-3'
D5	BC_UP_D5	5'-ACCGACGGCTTAGCGATCTT-3'	BC_DN_D5	5'-ACCCGAGCGTTGATAATTCT-3'
D6	BC_UP_D6	5'-ACTAGATACACATGCGTGCC-3'	BC_DN_D6	5'-ATTATCCTTAGGCGCGGCGT-3'
D7	BC_UP_D7	5'-CCGACCGTATAAGTTCTATC-3'	BC_DN_D7	5'-AATTCGTATGCACCGGGCGT-3'
D8	BC_UP_D8	5'-CCGTTATACGAATATCGACC-3'	BC_DN_D8	5'-CCCGGTACTACAATACGAGA-3'
D9	BC_UP_D9	5'-CAGAGTAAGTAACGGTTCGC-3'	BC_DN_D9	5'-ATCGCGCAGGTCGGACATAT-3'
D10	BC_UP_D10	5'-CCGGCTAGTTAATTTGACTC-3'	BC_DN_D10	5'-GGCTCCACTAAATAGACGCA-3'
D11	BC_UP_D11	5'-GGCTAACCGAAACCGTGACA-3'	BC_DN_D11	5'-TCATAGCCAACACAGGGCGA-3'
D12	BC_UP_D12	5'-GGTGTACCTCCAACTTACTA-3'	BC_DN_D12	5'-GCTCCTAGAGTATGAGAGAT-3'
E1	BC_UP_E1	5'-TAGTGACTTAGACCCTCCGT-3'	BC_DN_E1	5'-ATTGCGACCTCGTCATGGCT-3'
E2	BC_UP_E2	5'-TATAGTTCGGGCCATACGGT-3'	BC_DN_E2	5'-GGTATTCCATAATCGCTCTC-3'
E3	BC_UP_E3	5'-TAAGGCGTCGTCACTACGGT-3'	BC_DN_E3	5'-TCTATTAGTGGACAGTACGG-3'

E4	BC_UP_E4	5'-TTACTTGCCCGAGCCGGATT-3'	BC_DN_E4	5'-CACCCGAGTTACGATCAAAT-3'
E5	BC_UP_E5	5'-TATTAGTGCGGACCCGGCTT-3'	BC_DN_E5	5'-CGGGAGGATTTATACTCAGT-3'
E6	BC_UP_E6	5'-TTCTACCGTCGGAGGCAGTT-3'	BC_DN_E6	5'-TTACGACCAGAACGGGACAC-3'
E7	BC_UP_E7	5'-TTTAGTGTCCGCGCCACGTT-3'	BC_DN_E7	5'-TATACTTGCGTAACGGGCCG-3'
E8	BC_UP_E8	5'-TATTCTCCGTGACGCGGGTT-3'	BC_DN_E8	5'-AATTTAGGTGCGACCGCCCT-3'
E9	BC_UP_E9	5'-AATCGGTACTAAGTCGGTTC-3'	BC_DN_E9	5'-CGGGTGTAGAAACCGACTAA-3'
E10	BC_UP_E10	5'-CCCGATTGGTTAATACCGAT-3'	BC_DN_E10	5'-AAGAAGGTTTAATTCGCCCG-3'
E11	BC_UP_E11	5'-GGACCGACTATTCCCTAAAT-3'	BC_DN_E11	5'-GCGCGGTCAGAACTAATATA-3'
E12	BC_UP_E12	5'-GCGCTGCAATCAGAAAGGTA-3'	BC_DN_E12	5'-CCAATGTACGCCAAGGTATA-3'
F1	BC_UP_F1	5'-AGCATGTCTCTAACTGGACG-3'	BC_DN_F1	5'-TCTATTCGGCGAGGCTGACT-3'
F2	BC_UP_F2	5'-ATATAGCGTGACAGAGTACG-3'	BC_DN_F2	5'-AAGTCAGGTCAATCATGCCC-3'
F3	BC_UP_F3	5'-ATATACGTGGAATGACTGGC-3'	BC_DN_F3	5'-TGACTCCTACGAGGTGCGAT-3'
F4	BC_UP_F4	5'-ACATGGTTGAAAGCGCGTCA-3'	BC_DN_F4	5'-TATGACTGCGGACGTTCGCT-3'
F5	BC_UP_F5	5'-CGACTATTGTGACATACCTG-3'	BC_DN_F5	5'-ACGTTGATCGCATGAGATTG-3'
F6	BC_UP_F6	5'-TGGATTCGACTCGCTCGCAT-3'	BC_DN_F6	5'-CATTACGTCAGATAGGGCTG-3'
F7	BC_UP_F7	5'-ATTTCGGCACGCTCACGATG-3'	BC_DN_F7	5'-TAACGCGACAGACGATATGC-3'
F8	BC_UP_F8	5'-GAGCTTGACTCACCGTCTTG-3'	BC_DN_F8	5'-TAACTCGTACTAGCGATCTG-3'
F9	BC_UP_F9	5'-GCGGCGGATATGCTATAAAT-3'	BC_DN_F9	5'-AATAGAGACGGCTCGATCTG-3'
F10	BC_UP_F10	5'-TACTCGGCAACAGGTCGGTA-3'	BC_DN_F10	5'-ATTCTCGATAGAGCGTGCTG-3'
F11	BC_UP_F11	5'-TATGGCACCACACGAAGGAC-3'	BC_DN_F11	5'-GACGCGAGTCGATGATACCT-3'
F12	BC_UP_F12	5'-GGGCTACCTCTCAATTATAC-3'	BC_DN_F12	5'-CGCTCCTAAGACATTGTTAC-3'
G1	BC_UP_G1	5'-GCCCACATGGATAACATTAC-3'	BC_DN_G1	5'-CGTAATAAGTGGGTAGAACC-3'
G2	BC_UP_G2	5'-AGACTAAGACCATTGTACCC-3'	BC_DN_G2	5'-GGTAACACTATCTCAAGACC-3'
G3	BC_UP_G3	5'-TAGCCAGTAACAGTAGGCCC-3'	BC_DN_G3	5'-GGTATGACGATAACCCATCC-3'
G4	BC_UP_G4	5'-GCCCAAATAAGACGTGAGCC-3'	BC_DN_G4	5'-AGCACACGTAGGAACTATCC-3'
G5	BC_UP_G5	5'-TAAGAATCGTTAGCAAGGCC-3'	BC_DN_G5	5'-CACGACGTAACATGAGGTCC-3'
G6	BC_UP_G6	5'-AGAGATTCGCTTAACGCCCG-3'	BC_DN_G6	5'-ATTCCGAGCGGCAGCGATAT-3'
G7	BC_UP_G7	5'-CATAAGCGTTGTGAATCGCG-3'	BC_DN_G7	5'-TATACTGCGCGACATGCGAG-3'
G8	BC_UP_G8	5'-TGCGCGGTCAAACCAAGCAA-3'	BC_DN_G8	5'-TAATCGCTACGAATGCTACC-3'
G9	BC_UP_G9	5'-TTCACCGAGACAAGGCGAGA-3'	BC_DN_G9	5'-AATAGGACGGAACGCCATCC-3'
G10	BC_UP_G10	5'-TCCATACCGATAAAGCTCGA-3'	BC_DN_G10	5'-ATATACGGGTAACCAGCCGC-3'
G11	BC_UP_G11	5'-TACTGACGCGGGACTGACTT-3'	BC_DN_G11	5'-CGGAGAGACAGATTACACGC-3'
G12	BC_UP_G12	5'-TAACTGCCGCGAGTCGTCTT-3'	BC_DN_G12	5'-AGTATCACACGAGCTTACGC-3'
H1	BC_UP_H1	5'-TATCCTGTCGGAGCGCGTTT-3'	BC_DN_H1	5'-TTAGGTACACTACACGTCGC-3'
H2	BC_UP_H2	5'-ACGGACACGACAGTAGTTCC-3'	BC_DN_H2	5'-CCAGGGCGTGTTCATAAATA-3'
H3	BC_UP_H3	5'-GGGTACATACGCATATTAGC-3'	BC_DN_H3	5'-TCATCCGAGCGACTTAGTGG-3'
H4	BC_UP_H4	5'-AAGCCAAACGAACTTGCGGC-3'	BC_DN_H4	5'-ATACCTTACTCAGCGGGTGG-3'
H5	BC_UP_H5	5'-CCGAGTTAGGAATGTTATGC-3'	BC_DN_H5	5'-TACGGAATTCGTACGTGCTC-3'
H6	BC_UP_H6	5'-TACCTATTGACCAGTGGGCG-3'	BC_DN_H6	5'-TACGGATGTCGACTAACCAT-3'
H7	BC_UP_H7	5'-ATTGAGCCTGACCACATGCG-3'	BC_DN_H7	5'-TAGGTTGAGGCGATCGCGAT-3'
H8	BC_UP_H8	5'-CCTAGAGACGTAGATATGCG-3'	BC_DN_H8	5'-ATACACATCGGGTTAAGCGG-3'
H9	BC_UP_H9	5'-ACACCGTATTTAAGACTGCG-3'	BC_DN_H9	5'-GTTATTACCCTACATCGTCG-3'
H10	BC_UP_H10	5'-ATCTCGCGTGACGATAGGCT-3'	BC_DN_H10	5'-TACCTTAGGAGGCGTAAATG-3'
H11	BC_UP_H11	5'-GATGCGGCACTATCGCTCAT-3'	BC_DN_H11	5'-CAGCGCGTACTAGACTGGAT-3'
H12	BC_UP_H12	5'-AGGAGCTTGTCTAATATCGG-3'	BC_DN_H12	5'-CAGCATTGTAAATAGGCGGA-3'

Table 12. Unique barcode sequences used to label *C. glabrata* deletion strains with a unique signature tag. 2 x 96 upstream and downstream barcodes are reused for every set of 96 gene deletion strains and can be amplified from the constant regions (U1 + U2; D1 + D2). Barcode sequences from the systematic *S. cerevisiae* gene deletion project were adopted (http://www-sequence.stanford.edu/group/yeast_deletion_project/deletions3.html; (Giaever et al., 2002, Winzeler et al., 1999)). The reference strain carries a unique barcode not used for any other strain.

Reference strain barcodes: The reference strain contains the following barcodes to be tracked as a positive control during parallel experiments:

uptag 5'-CGATGCAGGTTATAGACGAT-3' downtag 5'-GGCACTACTCAAGCATCTTA-3'

Constant and overlap sequences, flanking unique barcodes:

U1 overlap	5'-ccgctgctaggcgcgccgtg-3'	(overlap sequence for fusion PCR)
U2 marker	5'-cgtacgctgcaggtcgac-3'	(amplification of marker + addition of barcode)
D1 overlap	5'-gcagggatgcggccgctgac-3'	(overlap sequence for fusion PCR)
D2 marker	5'-ctacgagaccgacaccg-3'	(amplification of marker + addition of barcode)

4.2 Methods

4.2.1 Cultivation and storage of organisms

4.2.1.1 Cultivation and storage of *E. coli*

E. coli strains were cultured in liquid or on solid LB medium, when necessary supplemented with antibiotics for selection and incubated at 37°C. For long term storage the cells were suspended in 15% sterile glycerol, frozen in liquid nitrogen and stored in cryotubes at -80°C.

4.2.1.2 Competent bacteria and *E. coli* transformation

E. coli strain DH5α was grown in 250 ml SOB medium at 18°C or RT to an OD_{600} of 0.6. The bacterial culture was chilled on ice for 20 minutes and harvested (1000g, 4°C, 10 min). The pellet was resuspended in 15 ml ice-cold TB buffer, further incubated on ice for 10 minutes and pelleted again (1000g, 4°C, 10 min). The pellet was resuspended in 15 ml of ice cold TB buffer, DMSO added to a final concentration of 7% (v/v) and incubated on ice for 10 minutes. 400 µl aliquots were prepared, frozen in liquid nitrogen and stored at -80°C.

4.2.1.3 Transformation of competent *E. coli* – heat shock

Competent cells were slowly thawed on ice. 1 to 10 µl of DNA (e.g. 100 ng DNA) were added to 100 µl of cells and incubated on ice for 30 minutes. The cells were heat-shocked at 42°C for 45 sec, cooled on ice for 2 minutes and after addition of 900 µl of LB medium incubated on a shaker at 37°C for one hour. The cells wer plated on a LB plate containing the appropriate antibiotic and incubated at 37°C overnight.

4.2.1.4 Cultivation and storage of *C. glabrata* strains

Cells were routinely grown in rich media (YPD) and synthetic media (SC), prepared essentially as described elsewhere (Kaiser *et al.*, 1994). Unless otherwise indicated, all strains were grown routinely at 30°C. For solid media, 2% agar (w/v) was added. For

selection of nourseothricin resistant transformants, plates were supplemented with 200 µg/ml nourseothricin (Werner Bioagents, Jena, Germany). Supplements were filter sterilized prior to be added to the autoclaved media at appropriate concentrations.

For short term storage strains were kept on YPD plates at RT in the dark. For long term storage the cells were suspended in 15% sterile glycerol, frozen in liquid nitrogen and stored in cryotubes at -80°C. Strains of the deletion collection were stored in triplicates in 200µl 15% sterile glycerol in 96 well plates as well as in single cryotubes.

4.2.2 General genetic and molecular techniques

Standard methods (restriction digestion, dephosphorylation, ligation, agarose gel-electrophoresis, standard PCR, determination of nucleic acid concentration) were performed according to Sambrook et al. (Sambrook *et al.*). Plasmid preparations from *E. coli* were routinely done by boiling preparation (STET method) or with the Quiagen Miniprep kit according to the manufacturer's instructions. For elution of DNA fragments from agarose gels after preparative gel-electrophoresis the Peqlab gel extraction kit was used according to the manufacturer's instructions.

4.2.2.1 DNA precipitation

DNA precipitation was carried out by adding 1/10 of the volume 3 M Na-acetate (pH 5,3) to the DNA solution. After addition of 3 volumes of cold 100% ethanol the solution was incubated at - 80°C for 60 minutes, centrifuged for 15 minutes at 18.000g and washed with cold 70% ethanol. The DNA pellet was dried at 55°C and resuspended in sterile water (bidest.).

4.2.2.2 Sequencing analysis

DNA sequencing was carried out using the BigDye Terminator Cycle Sequencing Kit Ver. 3.0 according to the manufacturer's instructions and the ABI PRISM Sequencing System 310 (Applied Biosystems, Germany), or using the sequencing service of the institutes IMP/IMBA.

4.2.2.3 Generation of deletion cassettes by fusion PCR

The dominant marker *NAT1* was amplified from plasmid pJK863 (Shen *et al.*, 2005) with primers fp_NAT1-U2 and rp_NAT1-D2 to add the constant 20 bp sequences U2 and D2. The PCR product was ligated into pGEM-T vector (Promega), generating plasmid pTS50. ***Fusion PCR*****:** Deletion cassettes were generated using a modified fusion PCR protocol (Noble & Johnson, 2005, Wach, 1996) (see Figure 14 A). Briefly, 500bp long flanking homology regions were amplified from ATCC2001 genomic DNA with primer pairs 5'5'/5'3'

and 3'5'/3'3' adding the constant overlap sequence (U1/D1) of 20 bp and purified by ethanol precipitation. The conditions for a 50 µl reaction were as follows: 1x Taq buffer (50 mM KCl, 10 mM Tris-HCl (pH 9.0, 25°C), 0.1% TritionX-100, 1.5 mM $MgCl_2$), 0.2 µM dNTPs, 0.5 µM each primer, 1 µl Taq-Polymerase and genomic wild type DNA from strain ATCC2001; 93°C for 5 minutes, 35 cycles 93°C for 30s, 45°C for 30s, 72°C for 90s, finally 10 minutes at 72°C. The dominant marker *NAT1* was amplified from plasmid pTS50 in a separate PCR reaction using primers 5M and 3M, adding unique barcode tags and constant complementary U1 and D1 sequences. The marker fragment was gel-purified over a 0.7% agarose gel. The conditions for a 50 µl reaction were as follows: 1 x Taq buffer, 0.2 µM dNTPs, 0,5 µM each primer, 1 µl Taq-Polymerase and plasmid TS50; 93°C for 3 minutes, 32 cycles 93°C for 30s, 49°C for 30s, 72°C for 2,5 minutes, finally 10 minutes at 72°C. Fusion PCR was carried out in a 50 µl volume with the same conditions as above: 1x ExTaq buffer, 0.2 µM dNTPs, 0.5 µM each primer, 0.5 µl ExTaq-Polymerase (TaKaRa) and 3 µl marker fragment, 1.25 µl each flanking homology fragment; 93°C for 3 minutes, 35 cycles 93°C for 30s, 45°C for 30s, 72°C for 3 minutes, finally 10 minutes at 72°C. The final deletion construct was purified by ethanol precipitation.

4.2.2.3 Transformation of *C. glabrata* by electroporation

For transformation of the background strain HTL, we used a modified electroporation protocol (Reuss et al., 2004). 50 ml of a *C. glabrata* culture in YPD at an optical density of 600nm (OD_{600}) of 1.3 were harvested, washed with H_2O, resuspended in 1x TE buffer, 100mM LiAc and incubated at 30°C for 30 minutes with slow shaking (130rpm). After addition of 250 µl 1M DTT and further incubation at 30°C for 60 minutes (130rpm), 40 ml of H_2O were added and the cells were harvested at 1000g for 5 minutes at 4°C. The cells were washed with 25 ml H_2O, subsequently with 5 ml 1 M cold sorbitol, finally resuspended in 550 µl 1 M sorbitol and kept on ice until use. Sterile electroporation cuvettes were precooled on ice and loaded with a mix of 40 - 45 µl electrocompetent cells and 5 - 10 µl linear DNA deletion construct (app. 2 - 3 µg DNA). Cells were left on ice for 10 minutes and electroporation was carried out with a BioRad GenePulser (200Ω, 1.5kV, 25µF). For recovery, 950 µl YPD was added and cells incubated for 4 h shaking at 30°C, before plating on YPD supplemented with 200 µg/ml Nourseothricin (Werner Bioagents, Jena). The plates were incubated for 48 hours at 30°C. For auxotrophic marker constructs the cells were recovered for 1 h at 30°C before plating on selective SC medium. Transformants were patched on YPD/Nourseothricin plates for colony PCR. For 96 well parallel electroporation, 300 ml of culture were grown to OD_{600} of 1.3, split into 50 ml aliquots and treated as described above. For electroporation, a BTX Harvard Apparatus ECM630 electroporation device with a HT-100 plate handler was used.

4.2.2.4 Transformation of *C. glabrata* by heat shock

For heat shock transformation a modification of the LiAc method was used (Gietz *et al.*, 1992). Cells were grown to early log phase in YPD (OD=1 to 2), harvested (3 minutes, 1000g) and washed with 25 ml sterile H_2O. Cells were resuspended in 1 ml 100 mM LiAc, transferred into an Eppendorf tube and pelleted 15 seconds at 1000g. The supernatant was removed completely, the cells resuspended in 400 µl 100mM LiAc and distributed in 50 µl aliquots. The cells were pelleted again, the supernatant removed completely and following solutions were added: 240 µl 50% PEG (3500), 36 µl 1 M LiAc, 50 µg of heat-denatured salmon sperm DNA and transforming DNA dissolved in 50 µl of sterile water. After mixing the cells were incubated for 30 minutes at 30°C. Then 45 µl DMSO was added, mixed immediately and the cells heat shocked for 15 minutes at 42°C. The cells were pelleted (2 minutes, 3400g), resuspend in 200 µl sterile H_2O and plated on selective plate.

4.2.2.5 Verification by yeast colony PCR

Strains were verified by colony PCR and “loss-of-gene” PCR according to the following protocol (Figure 14 C). Transformants were patched on selective plates and incubated at 30°C for 24h. Cells were resuspended in 40 µl PCR mix 1 (0.2µM dNTPs, 0.5 µM of each gene specific primer 5c/3c up-/downstream of the homology region and marker specific primer 5M/3M) and heated for 10 minutes at 93°C. After cooling on ice, 10 µl polymerase mix (5 µl 10 x PCR buffer and 1 µl Taq-Pol.) were added per reaction and a regular PCR was performed (93°C for 5 min, 25 cycles 93°C for 30s, 45°C for 30s, 72°C for 90s, final 10 min 72°C). To verify the loss of the coding sequence (CDS), colony PCR was essentially performed the same way. Oligonucleotides used to screen for CDS loss bind inside the CDS to generate a product of 500bp. All internal primers were also checked for functionality in a separate PCR reaction, amplifying the fragment from genomic wild type DNA.

4.2.2.6 Isolation of genomic DNA from yeast

Genomic DNA was isolated according to a modified protocol as described in Sambrook et al (Sambrook et al.). Cells from 10 ml of overnight culture in YPD were harvested by centrifugation, washed once with 10 ml sterile water and then resuspended in 500 µl H_2O. The cell suspension was transferred into a screw cap tube and resuspended in 200 µl of DNA lysis buffer. One volume of glass beads (Sigma 425-600 µm, acid-washed) and 200µl phenol-chloroform-isoamylalcohol (PCI, 25:24:1, Fluka) were added and the cells were broken, using a Vibrax vortex (15 minutes, 4°C) or alternatively a Fastprep (40s, 5m/s, RT; MPBiomedicals). 200 µl sterile water were added and the suspension was centrifuged (5 minutes, 16000 g, 4°C). The aqueous top layer was transferred into a new tube and the DNA

was ethanol precipitated. The pellet was resuspended in 400 µl 1 x TE buffer + 3 µl RNase A (10µg/ml) and incubated at 55°C for 50 minutes to digest the RNA. The PCI step was repeated, the DNA precipitated again and resuspended in 50 µl H_2O. DNA quality was checked on an agarose gel and the DNA concentration was determined at 260 nm.

4.2.2.7 Isolation of RNA from yeast

RNA was extracted from yeast cells by the hot phenol method according to Sambrook et al. (Sambrook et al.). Cells from a 50 ml culture with an optical density of 1 (OD_{600}) were harvested, washed with sterile water and resuspended in 400 µl 50 mM sodium acetate (pH 5.3) and 10 mM EDTA (pH 8.0). 40 µl of 10% SDS were added, mixed and incubated with 400 µl acid phenol (pH 4.3) at 65°C for 15 minutes. After rapidly chilling on ice the broken cell suspension was centrifuged (5 minutes, 16000g, room temperature (RT)) and the aqueous phase transferred into a new tube. An equal volume of PCI was added, incubated for 5 minutes at RT, centrifuged and the aqueous phase was transferred into a new tube. This step was repeated once more, followed by two steps of chloroform extraction. The purified RNA was precipitated with 1/10 volume of 3 M sodium acetate (pH 5.3) and 2.5 volumes of cold 100% ethanol. The pellet was washed with 70% ethanol, dried at 55°C and resuspended in 100 µl TE buffer. RNA was stored in aliquots at minus 80°C until use. RNA concentration was determined using a UV/Vis spectrophotometer (Nanodrop - Thermo Scientific) and the quality was checked using a Bioanalyzer 2100 (Agilent). For RT-PCR the RNA was incubated with 2U of DNaseI (Fermentas) for 15 minutes at 37°C and the DNaseI was inactivated by PCI extraction. RNA for microarrray analysis was precipitated with 2 M LiCl.

4.2.2.8 Southern blot analysis

Southern blot analysis was performed according to Sambrook et al (Sambrook et al.). 25 µg of genomic DNA were digested overnight at 37°C with appropriate restriction enzymes and separated by gel electrophoresis (70 V) on 0.7% agarose gel in TBE. The DNA was denatured in 0.5 M sodium hydroxide, 1.5 M sodium chloride for one hour and neutralised for one hour in 0.5 M Tris/HCl pH 7.5, 1.5 M NaCl. Capillary blotting onto a nylon membrane (Hybond N+, Amersham) using 20 x SSC buffer was carried out over night and crosslinked on the membrane using a Stratagene UV Crosslinker. The membrane was incubated at 65°C for at least 3 h in prehybridisation solution. Probes were obtained by PCR internally labelled with [α-^{32}P]dCTP (Megaprime DNA Labelling Systems, GE Healthcare) for 2 hours at 37°C (20-100ng DNA, 5µl primer solution, x µl sterile H_2O, 33 µl total volume, 10µl labelling buffer, 5µl [α-^{32}P]dCTP (6000Ci/mmol), 2µl Klenow polymerase). The labelled DNA was purified with NICK columns (GE Healtcare) according to the manufacturer's instructions and the activity of

the eluates was measured with a scintillation counter. Prior to hybridisation the probe was denatured for 5 minutes at 95°C. The radio-labelled probe was added to the prehybridisation solution and incubated overnight at 65°C. The membrane was washed twice with 2 x SSC, 1% SDS for one hour each, twice with 1xSSC, 1% SDS for one hour each and detected on X-ray film (CL-Xposure Film 5x7 inches, Pierce). For stripping, the membrane was incubated in 0.3% SDS, 0.1 x SSC at 65°C for 20 minutes and prehybridised again before adding a new probe.

4.2.3 Quantitative real-time PCR

Primers for quantitative real-time PCR were designed using PerlPrimer according to recommendations and tested in a gradient PCR. RNA was extracted by the hot phenol method and treated with DNaseI as described above. Three independent biological replicates were prepared. Reverse transcription was performed in triplicates on 2 µg of total RNA each according to the manufacturer's instructions (Fermentas First-strand cDNA synthesis Kit) with 100 pmol oligo$(dT)_{18}$ and 100 pmol random hexamer primer. The sample mixes (4 µl 5 x reaction buffer, 0,5 µl RiboLock Rnase inhibitor (20U), 2 µl 10 mM dNTP mix, 1 µl M-MuLV Rev. Transcriptase (200U)) were incubated for 10 minutes at 25°C followed by 60 minutes at 42°C and final 10 minutes at 72°C, diluted 1:10 in H_2O and stored at -20°C. All cDNA and RNA samples were tested in a regular PCR for DNA amplification with specific primers. Quantitative PCR was carried out in triplicates on a Realplex Mastercycler (Eppendorf), monitoring cDNA amplification quantitatively by SYBR Green incorporation. The conditions for a 20 µl reaction were as follows: 2 µl cDNA template, 7 µl H_2O, 0.75 µl each primer (375 nM), 10 µl 2 x Mastergreen mix (Eurogentec); 95°C 5 minutes, 40 cycles 95°C 10 s, 62°C 10 s, 72°C 20 s; melting curve 95°C 20 s, 62°C – 94°C gradient, 95°C 15 s. For analysis the Realplex data analysis program was used.

4.2.4 Microarray analysis

50 ml cultures of the HTL *C. glabrata* background strain and the Cg*cbk1*Δ deletion strain were grown in YPD to an OD_{600} of 1, harvested, washed and immediately frozen. Total RNA was prepared by hot phenol method and treated with DNaseI. RNA was additionally precipitated with 2 M LiCl and RNA concentration was measured and quality checked as described above. Three independent biological replicates were prepared. Samples of 25 µg total RNA were used for cDNA synthesis using 200 U of Superscript II reverse transcriptase (Invitrogen, USA) with either Cy3-dCTP or Cy5-dCTP. Labelled cDNAs were pooled, and RNA was hydrolyzed for 20 minutes in 50 mM NaOH at 65°C, followed by neutralization with acetic acid and probe clean-up with CyScribe GFX purifiaction kit (Amersham). Microarrays were incubated for at least 45 minutes at 42°C in prehybridization solution (4 x SSC, 0,1%

SDS, 10 mg/ml BSA). Hybridization to *C. glabrata* whole-genome cDNA microarrays was done in hybridisation solution (4 x SSC, 0.1% SDS) at 37°C overnight. Microarrays were washed for one minute in 2 x SSC, 0.1% SDS at 42°C, followed by a 5 minutes wash in 2 x SSC, 0.1% SDS at 42°C and a 10 minutes wash in 0,1 x SSC, 0,1% SDS at room temperature. Microarrays were washed for two minutes in 0.1 x SSC, 0.1% SDS at room temperature and in 0.01 x SSC for 30 seconds. Glass slides were dried for 3 minutes at 500 rpm in a tabletop centrifuge, scanned on an Axon 4000B scanner (Molecular Devices), analyzed and normalized using Gene Pix Pro4.1 software (Molecular Devices). Custom made DNA microarrays and protocols were obtained from the laboratory of Dr. Steffen Rupp, Fraunhofer Institute, Stuttgart. Oligonucleotides were obtained from Dr Ken Haynes, Imperial College, London. All microarray experiments were carried out with three independent RNA preparations.

4.2.5 Protein-biochemical methods

4.2.5.1 Preparation of whole cell TCA extracts

5 ml of a yeast culture with OD_{600} of 0.8 was harvested (5 min, 1000g) and the cells resuspend in 1 ml H_2O. 150 µl Yex-lysis buffer was added, mixed and incubated for 10 minutes on ice before adding 150 µl of cold 50% TCA (trichloracetic acid) and further incubation on ice for at least 10 minutes. The solution was centrifuged (5 min, 16100 g, 4°C), the supernatant discarded and residual liquid was carefully removed. The pellet was resuspended in protein sample buffer (20 µl/1 OD_{600}), incubated for 15 minutes at 37°C on a shaker and centrifuged (5 min, 16100 g) to pellet cell debris. 10 µl (equivalent to 0.5 OD_{600}) were loaded on a SDS PAGE and the gel was run at 200 V.

4.2.5.2 Preparation of cell extracts and immunoblotting

To investigate phosphorylation of CgSlt2 protein wild type and deletion strain cultures were grown to exponential phase with and without stress (10 ng/ml caspofungin). Cells were harvested at 5, 10, 30, 60 minute time points and trichloroacetic acid (TCA) extracts were prepared as described elsewhere (Gregori *et al.*, 2007). Aliquots corresponding to 0.5 OD of cells were separated by 10% SDS-PAGE and transferred to nitrocellulose membranes. Immunoblotting was carried out using a phosphospecific anti-phospho p44/42 antibody MAPK (Erk1/2) (Cell Signaling Technologies, USA) for detection of phosphorylated CgSlt2. Anti-ScPgk1 antibodies recognizing CgPgk1 were used as loading control (Kuchler *et al.*, 1993).

4.2.6 Phenotypic profiling

4.2.6.1 Screening conditions for growth phenotypes using robotics

For ***large-scale phenotypic analysis***, cells were restreaked from frozen stock and grown for 48 h at 30°C on fresh YPD plates. Each of the three plates containing independent transformants of the same set of genes was arrayed into 384 spot array formats serving as source plates. Phenotypic profiling of the deletion collection was performed using a robot (RoToR HDA, Singer Ltd., Roadwater, UK) on media plates supplemented with compounds at the following final concentrations: 50 µg/ml Calcofluor White (Sigma-Aldrich), 250 µg/ml Congo Red (Sigma-Aldrich), 0.02% SDS (Sigma-Aldrich), 7 mM Caffeine (Sigma-Aldrich), 150 ng/ml Caspofungin, 1 mM CuSO4 (), 1.1 M NaCl, 500 mM $CaCl_2$, 600 mM $MgCl_2$, 8 mM $ZnCl_2$, 2 mM $CdCl_2$, 5 mM $MnCl_2$, 40 mM LiCl (Merck). Plates were routinely incubated at 30°C for up to 3 days and scanned with a HPScanjet G3010, using Adobe Photoshop CS3 software or photographed with S&P Imaging system (S&P Imaging, Canada), after 24, 48 and 72h for documentation.

Primary hits were manually rescreened for confirmation. Exponentially growing cells were adjusted to an OD_{600} of 0.1. Equal volumes of serial dilutions (1:10, 1:100 and 1:1000) were spotted on YPD plates containing drugs and incubated as described above. For identification of mutants displaying differences in phenotypic switching, cells were spotted and dilutions were plated on YPD containing 1mM $CuSO_4$ and grown for 4 days at 25°C.

Media plates used for large-scale phenotypic screening and manual confirmation of growth phenotypes contained compounds listed in Table 13:

Compound	Stock conc.	Solvent	Screening conc.	Confirmation conc.	Manufacturer
NaCl	5 M	H_2O	1.1 M	1.1 M	Merck
Calcofluor White	10 mg/ml	H_2O	50 µg/ml	50 µg/ml	Fluka
Congo Red	10 mg/ml	H_2O	250 µg/ml	250 µg/ml	Sigma
SDS	10 %	H_2O	0.02 %	0.02 %	Fluka
Caffeine	300 mM	H_2O	7 mM	7 mM	Sigma
Caspofungin	50 µg/ml	H_2O	200 ng/ml	150 ng/ml	Merck
Fluconazole	10 mg/ml	DMSO	4 µg/ml	1.5 µg/ml	Discovery Fine Chemicals
Voriconazole	10 mg/ml	DMSO	100 ng/ml	75 ng/ml	Discovery Fine Chemicals
Ketoconazole	10 mg/ml	DMSO	100 ng/ml	-	Discovery Fine Chemicals
Itraconazole	10 mg/ml	DMSO	100 ng/ml	-	Discovery Fine Chemicals
Amphotericin B	10 mg/ml	DMSO	3 µg/ml	1.5 µg/ml	Discovery Fine Chemicals
5-Flucytosin	10 mg/ml	H_2O	5 µg/ml	5 µg/ml	Discovery Fine Chemicals
$CuSO_4$	1 M	H_2O	1 mM	1 mM	Merck
$CaCl_2$	5 M	H_2O	500 mM	400 mM	Merck
$ZnCl_2$	1 M	H_2O	8 mM	8 mM	Merck
$MgCl_2$	5 M	H_2O	600 mM	600 mM	Merck
$CdCl_2$	1 M	H_2O	2 mM	2 mM	Merck
$MnCl_2$	1 M	H_2O	5 mM	5 mM	Sigma
LiCl	1 M	H_2O	40 mM	40 mM	Sigma

Table 13. **Compounds used for profiling analysis in the primary and conformational screen.**

Azole susceptibility screenings were carried out by a modified endpoint method (Rex *et al.*, 1997) in liquid culture in microtiter plates, using the following drug concentrations: 4 µg/ml Fluconazole, 0.1 µg/ml Voriconazole, 0.1 µg/ml Ketoconazole, 0.1 µg/ml Itraconazole (all azoles from Discovery Fine Chemicals), 3 µg/ml Amphotericin B (Discovery Fine Chemicals), 5 µg/ml 5-Flucytosine (Sigma-Aldrich). Cells were grown overnight in deep well plates to stationary phase, diluted 100-fold in sterile water and 100 µl suspension mixed with 100 µl of 2 x YPD containing a 2 x drug concentration (app. 10^5 cells/well). After incubation at 30°C for 24 h and 48 h, cells were resuspended and the OD_{600} was measured with a Victor plate reader (Perkin Elmer, USA).

4.2.6.2 Microbroth dilution assay for IC_{50} determination

To determine the IC_{50} of antifungal drugs a modified protocol of the microbroth dilution assay was used (Sanglard *et al.*, 1995). Briefly, an overnight culture was diluted 1:100 in YPD, regrown to an OD_{600} of 1 and an inoculum of 2.5 x 10^4 cells/ml was prepared. Antifungal stock solutions were prepared in DMSO. Two fold serial dilutions of the drugs were then prepared in water in a deep well plate and stored at -20°C until use. 100 µl of two fold serial drug dilutions were distributed in triplicates into a flat bottom microtiter plate. The last wells free of antifungal drugs served as a growth control. After adding 100 µl of the inoculum (200 µl total volume), plates were incubated at 30°C for 24h and 48h in a humid environment to avoid evaporation. OD_{600} was determined with a plate reader. Endpoint readings were set as the antifungal concentrations, causing at least 90% growth inhibition after 24 h of growth when compared to the control. The IC_{50} was determined by linear regression using Graph Pad Prism software.

4.2.7 *In vitro* interaction studies

4.2.7.1 Cultivation of cell lines and primary bone marrow-derived macrophages

BMDM (bone marrow-derived macrophages) media contained DMEM, 10% heat-inactivated FCS, 20% L-conditioned medium. L-conditioned medium was produced as described: Ten confluent 10 cm dishes of L929 cells were divided into 20 bottles and 50 ml of medium (DMEM, 10% FCS) per bottle added. When the cells were 70% confluent, the medium was replaced with 100 ml starving medium (DMEM without FCS, no antibiotics) and incubated for 10 days, filter sterilized and aliquots were stored at -20°C.

4.2.7.2 Preparation of bone-marrow derived macrophages from mice

BMDMs were prepared and cultured as described elsewhere (Frohner et al., 2009). Briefly, bones from 7- to 9-week-old C57BL/6 wild-type mice were dissected and stored in cold sterile PBS buffer on ice. Bone marrow was collected from femur and tibia treated with

red blood lysis buffer (8.29 g l-1 NH4Cl, 1 g l-1 KHCO3, 0.0372 g l-1 EDTA, pH 7.2–7.4) and resuspended either in macrophage media to induce differentiation into BMDMs as described elsewhere (Hume & Gordon, 1983, Inaba *et al.*, 1992). Frozen bone marrow of 6-to 8-week-old gp91phox-/- C57BL/6 mice was kindly provided by Kristina Erikson (George-Chandy et al., 2008). Fresh medium was added after three days in culture. At day seven, BMDMs cultures were split 1:3 and further cultured until day 10 to 12 and used between day 10 and day 13 of differentiation.

4.2.7.3 Detection of reactive oxygen species by chemiluminescent assay

For detection of accumulated reactive oxygen species after incubation of primary macrophages with *C. glabrata* cells, the deletion strain library was screened with the ROS assay essentially as described in (Frohner et al., 2009). Total and extracellular ROS were detected using luminol and isoluminol (Sigma, USA). Briefly, 100 µl of BMDMs in prewarmed HBSS at a density of 4 x 10^5 cells/ml were distributed to a 96-well luminometer plate (Nunc, Roskilde, Denmark). 50 µl HBSS medium containing zymosan (100 µg/ml) or the *C. albicans* wild type strain SC5314 (MOI 5:1) were used as positive controls. Mutant strains were added at the indicated cell numbers, usually at a MOI of 10:1. Immediately afterwards, 50 µl HBSS containing either 200 µM luminol or 600 µM isoluminol and 50 µl HBSS containing 16 U horse radish peroxidase (HRP) were transfered to each well. Chemiluminescence was measured with a plate reader (Wallac VictorV3, PerkinElmer) at 2.5 minute intervals at 37°C for four hours. Data are expressed as relative luciferase units/min/1000 BMDM cells over time, or as total relative luciferase units under the curve over a period of 90 minutes. Primary hits were confirmed in triplicates in three independent experiments.

4.2.8 Microscopy

Microscopy was done on an Axioplan 2 (Zeiss, Germany) or Olympus CellR life imaging station microscope (Olympus, Austria). Pictures were captured with a Spot Pursuit camera (Sony). Cells were grown to exponential growth phase, harvested and washed with water before transferring them onto microscopy slides. For chitin staining, cells in the early exponential growth phase were incubated with calcofluor white (Fluorescent Brightener 28, Sigma-Aldrich) at a final concentration of 50 µg/ml in medium for 1 hour at room temperature in the dark. Cells were washed twice with water and transferred to a microscopy slide and observed with a DAPI filter. Colony pictures were taken with a Discovery.V12 Stereomicroscope and a AxioCam MRc5 (Zeiss, Germany). Cells were grown in liquid YPD to logarithmic phase to take pictures of the cell morphology.

4.2.9 Bioinformatic analysis

Gene selection. Genes of different functional categories were manually selected based on potential function in virulence and drug resistance. The categories involved genes of signaling pathways, kinases, ABC transporters and permeases, GPI-anchored proteins, cell wall associated genes, genes involved in glycosylation, phospholipid biosynthesis, histone modification, iron metabolisms and several genes with no obvious homologue in *S. cerevisiae*.

The genes were selected by their homology to *S. cerevisiae* based on these functional categories (SGD annotations; http://www.yeastgenome.org/). *C. glabrata* orthologues were identified using a BLAST approach. The three best aligned hits for each gene were saved. These orthologues have been remapped with the help of T. Gabaldon (Barcelona, Spain), using a tree-based approach applying the algorithm described in (Huerta-Cepas *et al.*, 2007).

Primer generation. Oligonucletide sequences for generation of the deletion cassettes and strain verification were automatically designed, using a custom written perl script called PrimerList (W. Glaser, Vienna). PrimerList utilizes Bioperl (Stajich *et al.*, 2002) to read and process nucleotide sequences and uses the EMBOSS (Rice *et al.*, 2000) programs *eprimer 3* and *stssearch* to find suitable primersets. The parameters used by PrimerList for primerdesign were: Upstream and downstream fragments were chosen to have a size between 450 and 550 nucleotides. 5'5' (forward) and 3'3' (reverse) primers were chosen to have a length of 20 to 30 bp, a GC content between 30 and 60% and a melting temperature of 50°C ± 4°C with a GC clamp. 5'3', 3'5' primers were chosen to have a length of 20 to 30 bp plus the 20 bp constant overlap sequence (Figure 14, Table 11), a GC content between 30 and 60% and a melting temperature of 50°C ± 4°C. 5'3' (reverse), 3'5' (forward) primers were chosen to bind exactly adjacent to the coding sequence, including the start codon ATG or the stop codon, respectively. 5c and 3c control primers have a length of 20 to 25 bp, a GC content between 40 and 60% and a melting temperature between 50°C to 60°C. The product size of the control PCR is between 750 and 900 bp. Internal control primers (5i and 3i) were designed to bind inside the coding sequence and to give a product of 400 to 500 bp in size. The primers have a length of 20 to 25 bp, a GC content between 40 and 60% and a melting temperature between 55°C to 60°C.

Oligonucleotides were ordered from Eurogentec, Belgium in 96 well plate format. Six plates were needed per set. Each of the six plates (5'5', 5'3', 3'5', 3'3', 5c, 3c) contained the primers for a specific gene at the exact same well position (eg.: well A1 contains the different primers needed to generate the deletion cassette of a specific gene; plate 5'5' contains all forward primers for the 5' region upstream to the gene to be deleted).

5 Results

5.1 Construction of the triple-auxotrophic background strain HTL

ATCC2001 is a wild type isolate routinely used in many laboratories to study the drug resistance profile and virulence properties of *C. glabrata*. We generated a novel triple-auxotrophic strain in the ATCC2001 wild type background to use as the recipient strain for a genome-wide gene deletion approach. The introduction of three auxotrophies should allow for the creation of double deletion strains, while still having two additional markers for complementation, if necessary. This is useful because the lack of a full sexual cycle in *C. glabrata* hampers the exploitation of genetic methods such as genetic crossing of two strains to yield double deletion strains. Also used as auxotrophic markers in the model organism *S. cerevisiae*, we selected the *C. glabrata HIS3*, *LEU2* and *TRP1* genes by homology to these amino acid biosynthesis genes. We avoided the use of an auxotrophic *URA3* marker in the new *C. glabrata* background strain, because it is known to influence the virulence properties of *C. albicans* (Brand *et al.*, 2004, Lay *et al.*, 1998).

We used the dominant recyclable nourseothricin resistance marker *SAT1* (Reuss et al., 2004) to precisely replace each of the three coding sequences from start to stop codon. The repeated use of this marker allowed us to create the new *C. glabrata* background strain referred to as HTL (*his3*Δ::FRT l*eu2*Δ::FRT *trp1*Δ::FRT), as well as all single deletion and all combinations of double deletion strains (Figure 13A and Table 14) (Jungwirth H. et al., unpublished).

Strain	Genotype	Reference
ATCC2001	*C. glabrata* wild type strain	www.attc.org
HTL	*his3*Δ::FRT *leu2*Δ::FRT *trp1*Δ::FRT	Jungwirth H., Lechner S.
H	Isogenic to ATCC2001; *his3*Δ::FRT	Jungwirth H., Lechner S.
T	Isogenic to ATCC2001; *trp1*Δ::FRT	Jungwirth H., Lechner S.
L	Isogenic to ATCC2001; *leu2*Δ::FRT	Jungwirth H., Lechner S.
HT	Isogenic to ATCC2001; *his3*Δ::FRT *trp1*Δ::FRT	Jungwirth H., Lechner S.
TL	Isogenic to ATCC2001; *trp1*Δ::FRT *leu2*Δ::FRT	Jungwirth H., Lechner S.
HL	Isogenic to ATCC2001; *his3*Δ::FRT *leu2*Δ::FRT	Jungwirth H., Lechner S.
HTL reference	*his3*Δ::FRT *leu2*Δ::FRT *trp1*Δ::*NAT1* (barcode)	this study
deletion strains	All isogenic to HTL; *gene*Δ::*NAT1*	this study
*fks1*Δ	Isogenic to HTL; *fks1*Δ::*HIS3*	this study
*ace2*Δ	Isogenic to HTL; *ace2*Δ::*HYGr*	this study

Table 14. ***C. glabrata*** **strains used in this study.** All strains of the deletion strain collection are deposited in the *C. glabrata* deletion strain library (http://funpath.cdl.univie.ac.at/)

Moreover, a HTL reference strain was generated by deletion of the *TRP1* gene in the HL double deletion strain using a signature-tagged *NAT1* marker cassette. This reference strain can serve as a tractable wild type control for fitness and *in vivo* virulence tests, exploiting the barcoded mutant strain pools. All strains were verified for correct genomic integration, for the subsequent loss of the selection marker after induction of the recombinase and for the loss of the coding sequence by colony PCR and Southern blot analysis (data not shown).

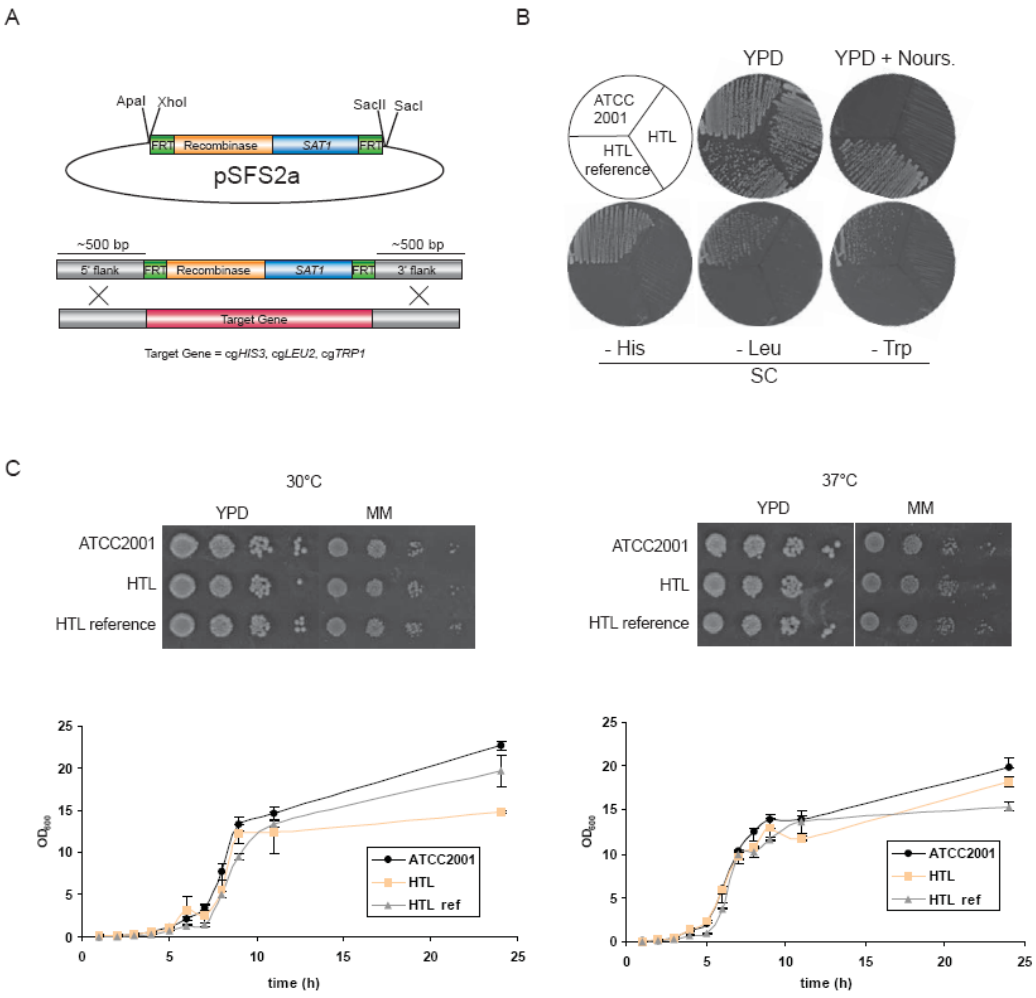

Figure 13. Generation of new triple auxotrophic strain HTL. (A) Cloning strategy using the *SAT1* flipper for recyclable deletion cassettes of *C. glabrata TRP1*, *LEU2* and *HIS3* genes. 500bp homology flanking regions were ligated into ApaI/XhoI and SacII/SacI restriction sites in pSFS2a, the deletion cassette excised with ApaI/SacI and the resulting fragment used to transform *C. glabrata* ATCC2001. (B) Growth of ATCC2001 wild type strain, HTL and HTL reference strain on YPD alone, supplemented with 200 µg/ml Nourseothricin and SC plates lacking Histidine, Leucine or Tryptophan. (C) Growth of ATCC2001 wild type strain, HTL and HTL reference strain at 30°C and 37°C on solid and in liquid YPD and minimal medium (YNB, ammonium sulfate, glucose, Histidine, Leucine or Tryptophan). OD_{600} was measured every hour in triplicates.

As expected, the new background strain HTL is unable to grow on medium lacking one of the amino acid, whose biosynthesis gene has been disrupted. On YPD medium, the strain grew normally, and did not display any resistance against nourseothricin (Figure 13B). The growth defects indirectly confirmed correct targeting of the deletion constructs.

In addition, we examined the growth properties of strain HTL in comparison to ATCC2001 on minimal medium supplemented with histidine, leucine and tryptophan and at different growth temperatures (30°C and 37°C). Both strains grew as predicted on full and minimal medium and showed similar growth rates when cultured in liquid media (Figure 13C).

The reference strain showed the same growth properties on YPD and minimal medium. It was unable to grow on medium lacking histidine, leucine or tryptophan but grew on nourseothricin supplemented growth medium (Figure 13B).

5.2 Generation of a signature-tagged deletion strain library

To identify novel *C. glabrata* genes implicated in drug resistance and virulence, we selected 868 *C. glabrata* orthologous genes based on their homology to *S. cerevisiae* and assigned functional categories, using a BLAST approach. These orthologues were also remapped by a tree-based approach, using the algorithm described in (Huerta-Cepas et al., 2007) (performed by Marcet-Houben M. and Gabaldon T.). The selected genes represent a heterogeneous group of putative non-essential genes, some of which might be implicated in virulence or drug resistance. Genes were assigned to the following categories: signaling pathways (MAPK, RIM101/pH, PKA, TOR, calcineurin pathways), zinc-finger transcription factors, ABC transporters, permeases, genes involved in cell wall biogenesis (glucan synthesis, glycosylation, GPI-anchor, adhesion), genes involved in metabolism (glyoxylate cycle, iron metabolism), peroxisomal genes, phospholipid biosynthesis and histone modification genes. Also genes with no obvious homology to *S. cerevisiae* genes were selected.

Targeted gene disruption with short homology flanking regions is rather inefficient in *C. glabrata*. Highest targeting efficiency was obtained using 500 bp long homology flanking regions (Ueno et al., 2007). To achieve more efficient gene replacement suitable for a large-scale gene deletion project, we modified a fusion PCR technique (Noble & Johnson, 2005), which enabled us to generate gene deletion constructs with long homology flanking regions in a large-scale approach. The first step involved individual PCR reactions of the homology flanking regions from genomic DNA and the amplification of the dominant marker *NAT1* from plasmid pTS50 (pGEMT-U2-*NAT1*-D2). Vector pTS50 carries the *NAT1* marker flanked by the constant U2 and D2 sequences needed for addition of the unique barcode sequences (Shen et al., 2005). The resulting three fragments were combined via the complementary tails (U1 and D1) in the fusion PCR reaction. The product is a deletion construct with a dominant selectable marker flanked by 500 bp gene-specific upstream and downstream sequences (Figure 14A, B and Material & Methods).

For future high-throughput parallel analysis of mutant strains, we adopted the signature-tagged mutagenesis approach (Giaever et al., 2002, Hensel *et al.*, 1995, Liu et al., 2008, Saenz & Dehio, 2005). For this purpose, individual mutant strains are labeled with two unique DNA barcode sequences to allow for the identification and quantification of each strain from a mixed strain pool. This way it is possible to test a large number of strains at the same time for their virulence properties *in vivo* or their fitness *in vitro*. We employed two times 96 barcode sequences originally created for the *S. cerevisiae* genome deletion project (Giaever et al., 2002, Winzeler *et al.*, 1999). This is convenient, because the same arrays can be used for identification and quantification of *C. glabrata* mutants. These 192 tag sequences, as well as the constant sequences to amplify the barcodes were also checked for their sequence homology against the *C. glabrata* genome to avoid false primer binding (Table 9 Materials and Methods). Thus, each gene deletion cassettes consisted of a the dominant *NAT1* marker flanked by unique upstream and downstream barcode sequences and 500 bp long homology regions for targeted gene replacement by homologous recombination.

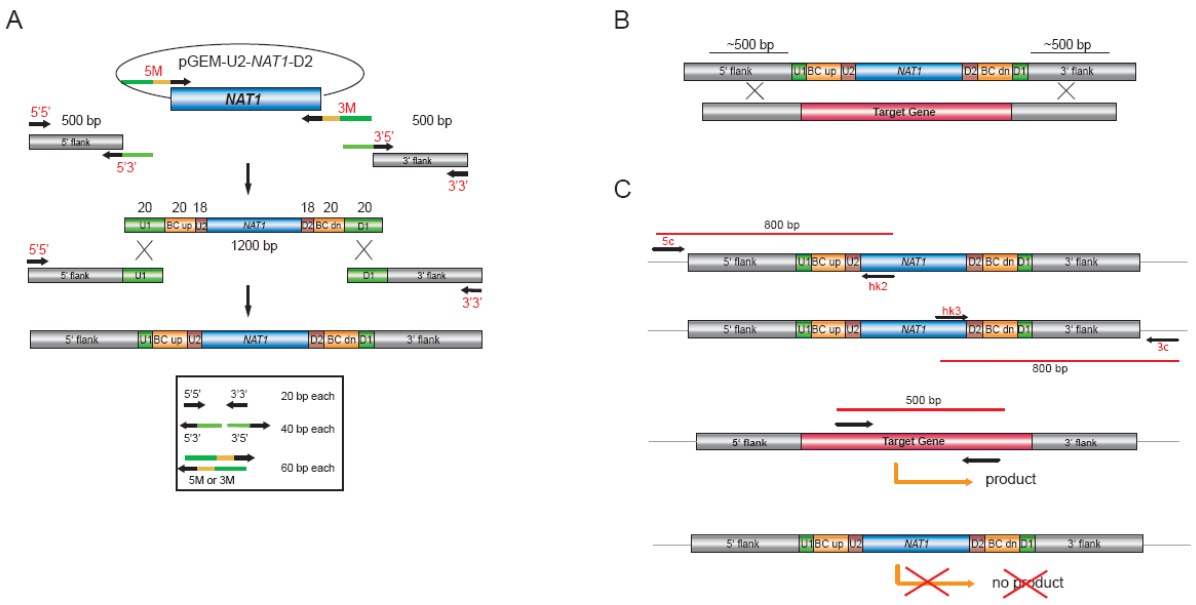

Figure 14. The sequential steps for generation of *C. glabrata* gene deletion cassettes. (A) Fusion PCR using the dominant selectable marker *NAT1* was applied to generate barcoded gene deletion cassettes. A set of two times 96 unique barcode sequences was integrated in oligonucleotides to amplify the marker fragment and to add overlap sequences. (B) Gene disruption by replacement of the target gene based on homologous recombination. *C. glabrata* strain HTL was transformed by an electroporation method. (C) Verification of correct integration of the deletion cassette by colony PCR (forward primer outside flanking region, reverse primer inside marker) checking both junctions. Loss-of-gene PCR (internal primer pair) was used to confirm that the coding sequences has not reintegrated in the genome. Reintegration, indicating that the CDS remained in the genome, gave a 500 bp PCR product.

For gene disruption, the background strain HTL was transformed with a modified parallel 96-well format electroporation protocol (Reuss et al., 2004). About 12 to 16 transformants per transformation and targeted gene were grown on selective medium and each was tested for correct genomic integration by colony PCR verifying both 5' and 3'

junctions (Figure 14C). With a maximum of three transformation rounds per gene, we were able to delete 476 genes representing 55 % of the selected genes and 9 % of the entire *C. glabrata* genome. Because illegitimate recombination can take place in *C. glabrata* (Cormack & Falkow, 1999), we also tested the deletion strains for the absence of the open reading frame (ORF) with a primer pair binding inside the ORF sequence (Figure 14C). Applying this loss-of-gene PCR on all transformants verified by colony PCR (297 genes, 852 deletion strains), we were able to exclude 13 strains (4.4% of targeted genes), yielding a PCR product in all three independent transformants. In 20 other strains, only one or two of the three independent transformants gave a PCR product, indicating that at least one generated deletion strain is correct. Deletion strains used for more detailed functional studies were confirmed for correct integration of the deletion cassette by Southern analysis (data not shown).

5.3 Efficient deletion of *PBS2*, *CDR1*, *PDR1* and *SLT2* in strain HTL

To validate the method of using long homology flanking regions for more efficient gene targeting in *C. glabrata*, gene deletion strains with well-described phenotypes were generated. Genes involved in osmosensitivity (*PBS2*), drug resistance (*CDR1*, *PDR1*), and cell wall stress (*SLT2*) were targeted and the mutants tested for growth under restrictive conditions.

Survival of *S. cerevisiae* under hyperosmotic conditions requires the HOG pathway. Deletion of the MAPKK Sc*PBS2* renders cells unable to grow on high osmolarity medium (Brewster *et al.*, 1993). Recently, it was demonstrated that the HOG pathways of *S. cerevisiae* and *C. glabrata* share similar functions in osmostress adaptation (Gregori et al., 2007). The deletion of *PBS2* - generated in the large-scale deletion project – also resulted in a sodium chloride (NaCl) sensitive deletion strain (Figure 15A).

C. glabrata is known to be inherently more tolerant to azoles. This resistance is mainly mediated by the ABC transporter Cdr1, Cdr2 and the transcription factor Pdr1 (Sanglard *et al.*, 1999, Vermitsky *et al.*, 2006). Cdr1 and Cdr2 are homologues of *S. cerevisiae* ScPdr5, and Pdr1 is the only homologue of the baker's yeast PDR transcription factors ScPdr1 and ScPdr3, the master regulators of pleiotropic drug resistance (PDR) (Balzi *et al.*, 1987, Delaveau *et al.*, 1994). Disruption of the *C. glabrata CDR1* or *PDR1* gene leads to drastically increased susceptibility to azoles (Sanglard *et al.*, 1999, Vermitsky *et al.*, 2006). With the *C. glabrata cdr1*Δ and *pdr1*Δ deletion strains of the library we reproduced the phenotypes of elevated azole susceptibility (Figure 15B).

The conserved yeast protein kinase C (PKC) or cell wall integrity pathway (Figure 15E) is activated in response to various stimuli such as heat stress, hypo-osmotic shock, mating pheromone and cell wall affecting agents (Levin, 2005). We reasoned that the PKC

pathway may have a strong influence on the pathogenicity and survival of *C. glabrata in vivo,* because it regulates cell wall integrity in response to external stresses (i.e. exerted by the host). Deletion of several PKC pathway genes in *C. glabrata*, including *SLT2*, resulted in a growth defect on medium supplemented with the fungal β-glucan synthase inhibitor caspofungin (CF) (Figure 15C). Also a *mkk1*Δ deletion strain showed CF sensitivity, which could be predicted by the lack of a redundant *MKK2* gene (Figure 15E). The lack of *C. glabrata MKK2* is also confirmed by a computational study, which found only one orthologue of the baker's yeast MAPKK pair ScMkk1/ScMkk2 (Byrne & Wolfe, 2005). However, in contrast to *S. cerevisiae*, *C. glabrata slt2*Δ mutants are not sensitive to calcofluor white (CW) or congo red (CR) (data not shown) (Reinoso-Martin *et al.*, 2003).

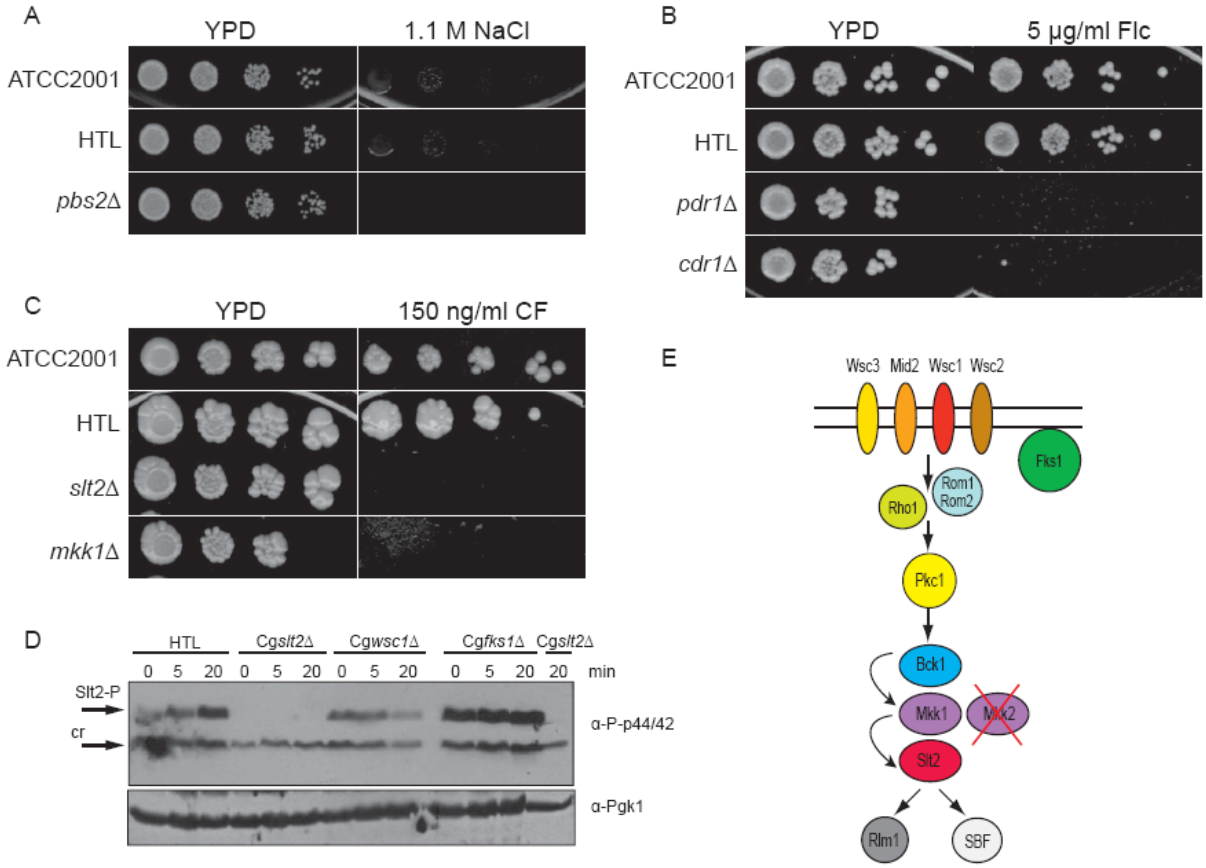

Figure 15. Sensitivity of *C. glabrata* deletion strains to antifungals and osmostress. Deletion strains were grown to OD_{600} of 1.0, serial diluted to OD_{600} of 0.1, 0.01, 0.001 and 0.0001 and spotted onto YPD and YPD agar plates containing the indicated amounts of NaCl (A), fluconazole (B) and caspofungin (C). Plates were incubated at 30°C for 2 days and scanned. (D) Cultures of strain HTL and the indicated isogenic deletion strains were grown to the early-exponential-growth phase before adding caspofungin at a final concentration of 10 ng/ml. Samples were taken at the indicated time points and crude trichloroacetic acid (TCA) extracts prepared. Aliquots corresponding to 0.5 OD_{600} equivalents per lane were separated through 10% SDS-PAGE gel. Immunoblotting was carried out using polyclonal anti-phospho p44/42 MAPK or anti-ScPgk1 antibodies. Detection of Pgk1 served as loading control. (E) Schematic drawing of the PKC cell wall integrity pathway. *S. cerevisiae* harbors two redundant MAPKKs (*MKK1* and *MKK2*), whereas in *C. glabrata* only one homologue exists. cr = cross reaction

Using a phospho-specific antibody raised against the dually phosphorylated p44/42 MAP kinase, we showed that Slt2 of *C. glabrata* is rapidly phosphorylated upon CF stress (Figure 15D). Phosphorylation of Slt2 increased already after five minutes of stress. In a

*wsc1*Δ deletion strain, no increase of Slt2 phosphorylation was observed, indicating that Wsc1 is necessary for stress sensing and/or signal transduction. In contrast, in a *fks1*Δ strain Slt2 is constitutively phosphorylated. The loss of a fully functional glucan synthase Fks1 probably leads to cell wall defects resulting in a constant activation of the cell wall integrity pathway.

These data indicate that the PKC pathways in *S. cerevisiae* and *C. glabrata* share several similar functions in response to CF. However, sensitivity to other cell wall affecting agents such as CW or CR differs. In *S. cerevisiae*, the deletion of Sc*SLT2* results in hypersusceptibility to CF as well as to CR, CW, and caffeine (Reinoso-Martin *et al.*, 2003). Interestingly, a Sc*mkk1*Δ deletion strain is not sensitive, because Sc*MKK2* can functionally compensate for the loss of Sc*MKK1*. The loss of the redundant *C. glabrata* homologue of Sc*MKK2* is one example for a so-called “stream-lined” *C. glabrata* genome, which means that *C. glabrata* lost redundant genes during its evolution possibly due to the close adaptation to its mammalian host (Kaur *et al.*, 2005).

Taken together, these data demonstrate that the employed fusion PCR approach combined with the adapted electroporation protocol and the use of the dominant selection marker comprise a reliable and efficient method of targeted gene deletion in *C. glabrata*.

5.4 Large-scale phenotypic profiling of the *C. glabrata* gene deletion library

With a few exceptions, virulence factors of *C. glabrata* are not well understood. For identification of genes that modify the virulence properties and alter the drug resistance profile of *C. glabrata*, the complete gene deletion strain library was screened for growth phenotypes under various stress conditions. The large-scale robotic-based primary screening scored for growth sensitivity to cell wall affecting compounds (calcofluor white (CW), congo red (CR), sodium dodecyl sulfate (SDS)), to temperature stress (25°C, 37°C, 42°C), to hyperosmotic conditions (NaCl), for tolerance to metal ions (LiCl, $MgCl_2$, $CaCl_2$, $MnCl_2$, $CdCl_2$, $ZnCl_2$), antifungal susceptibility (fluconazole (FLC), voriconazole (VOR), amphotericin B (AMB), 5-flucytosine (5FLU)) and growth on minimal medium as well as the identification of morphological differences on cell and colony level. These stress conditions were chosen, because they may mimic stress, to which *C. glabrata* is exposed during colonization and infection in the host.

In total, we screened all 476 generated strains for growth defects or phenotypic changes on solid and in liquid media. For plate assays, cells were spotted from a source plate onto plates supplemented with the diverse compounds or drugs and routinely grown at 30°C. After 24, 48 and 72 hours, the plates were inspected for the colony phenotypes and scanned for documentation. For liquid assays, cells were grown in microtiter plates, using the endpoint dilution method, the OD_{600} was determined after 24 and 48 hours for each strain

and compared to the growth of the untreated cells. Some 103 strains (22 % of all 476 gene deletion strains) showed phenotypic differences or sensitivities to the tested compounds under at least one condition (Table 15, Figure 16 A, Table 16). The high number of mutants displaying various growth defects is most likely due to the gene selection, which shows a bias towards cell wall and signaling mutants. Six of the 103 strains showed sensitivities to more than six tested conditions (*wsc1*Δ, *cdc12*Δ, *cwh41*Δ, *ypk1*Δ, *tpk2*Δ and *bcy1*Δ deletion strains). The former three genes are implicated in cell wall biogenesis and morphology. The latter three are signaling components. Notably, all six mutants already displayed slower growth on full medium, which putatively also influences growth under all stress conditions.

Stress condition	Primary screen	Confirmation screen
Temperature	50	46
CW, CR, SDS	18, 16, 30	13, 15, 28
Caffeine	14	11
NaCl	24	22
Metal ions	49	34
$CuSO_4$ (phenotypic switching)	50	17
Minimal medium	8	5
Caspofungin	41	33
Azoles	26	14
Amphotericin B	26	13
5-Flucytosin	9	3
Altered cell morphology	-	11
Altered colony morphology	12	13
Total	144	103

Table 15. Summary of strains identified in primary and confirmation screenings.
The primary screen was done in 96- or 384-well format, using a replica plating robot or microtiter plate assays. Primary hits were manually rescreened by spot assays on solid plates with serial dilutions. For liquid drug susceptibility assays, sensitivities were confirmed in triplicates. Strains that displayed aberrant growth (slow growth, different colony morphology) were inspected under the microscope. Numbers are not additive, because many mutants displayed several phenotypes. CR = congo red, CW = calcofluor white, SDS = sodium dodecyl sulfate, morph. = morphology

A remarkably high number of mutants (46 strains) displayed growth defects at elevated temperatures (37°C and 42°C). We noticed that many of these strains are affected in cell wall assembly or biogenesis. The second largest group (34 strains) identified, included mutants with metal ion sensitivity, although about one third of those strains were susceptible to cadmium chloride only. The third group contained deletion strains showing CF hypersensitivity (33 strains) (Figure 16A).

Some 22 mutants showed osmosensitivity phenotypes, 13 strains were sensitive to CW, 15 strains to CR and 28 strains to SDS followed by azole- (14 mutants) and amphotericin B- (13 mutants) susceptible strains. Notably, 17 strains did not stain brown on $CuSO_4$-containing media, suggesting changes in the switching phenotypes. The smallest groups were comprised of caffeine-sensitive deletion strains (11 strains) and mutants unable

to grow on minimal medium (5 strains). A set of 13 strains showed altered colony morphology or color and 11 strains aberrant cell morphologies.

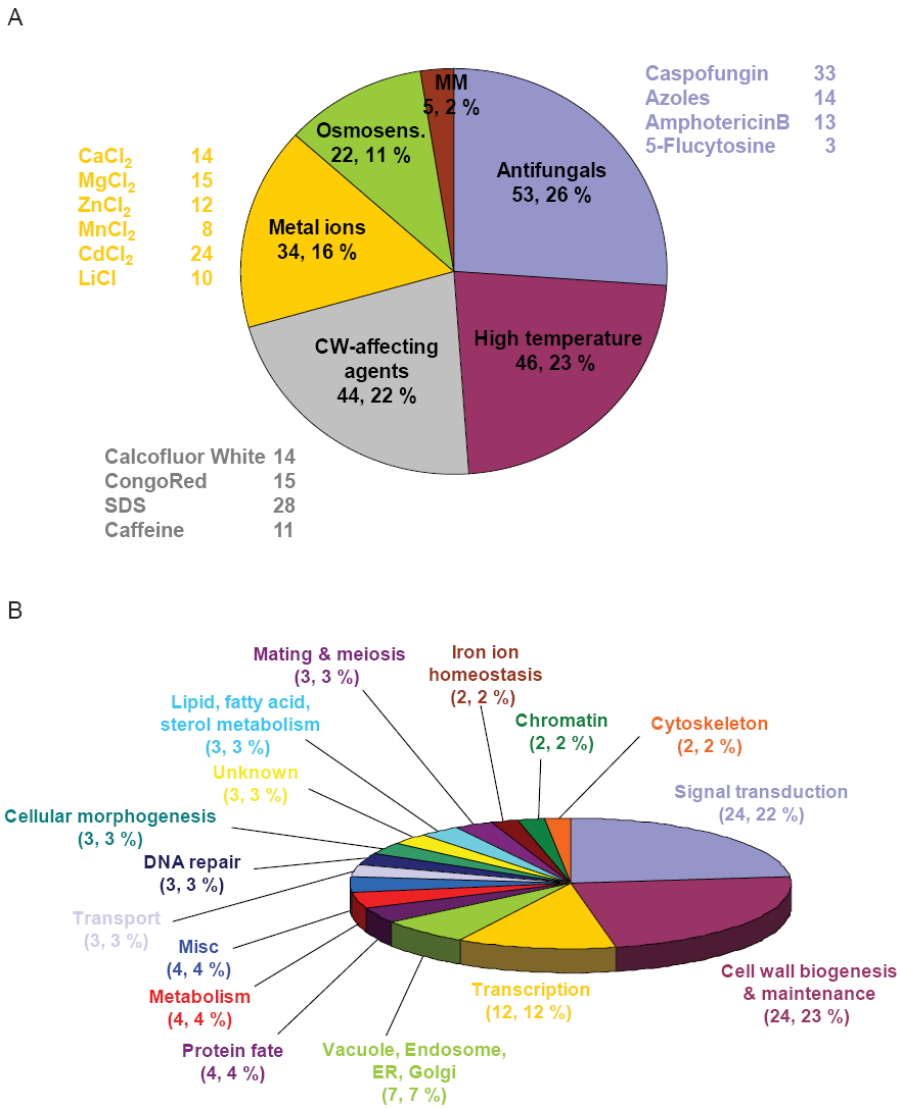

Figure 16. Summary of phenotypic analysis of all *C. glabrata* deletion strains. All 476 strains of the collection were tested for their sensitivity to cell wall-perturbing agents and metal ions, as well as heat- and osmostress, growth on minimal medium and antifungal susceptibility. (A) Shown are the absolute numbers of deletion mutants found to be sensitive under the indicated growth conditions. (B) Distribution of identified *C. glabrata* genes by functional categories according to the GO annotation of homologues in *S. cerevisiae* (numbers correspond to mutants per category; % is the percentage of the total number of identified sensitive strains).

All 103 sensitive mutants were classified into functional categories based on the *Saccharomyces* Genome Database (http://www.yeastgenome.org/), including signal transduction, cell wall biogenesis and maintenance, transcription, vacuolar, endosomal, ER- and Golgi functions, protein fate, metabolism, transport, DNA-repair, cellular morphogenesis, lipid, fatty acid and sterol metabolism, mating and meiosis genes, iron homeostasis, chromatin, cytoskeleton, miscellaneous and unknowns (Figure 16B).

Sorting the identified genes by the functional categories of *S. cerevisiae* homologues (Figure 16B) showed that one quarter of the genes is involved in signalling functions, one quarter is implicated in cell wall biogenesis and maintenance (including glycosylation), and 12 % of

genes play roles as transcriptional regulators. This distribution reflects the bias in the gene selection, with the exception of transcriptional regulators. The transcriptional regulators are underrepresented in our gene selection, because they were supposed to be deleted by a collaboration partner.

To be able to compare the growth defects of each mutant to the wild type control strains and to distinguish qualitative differences in the strength of the defect, we introduced a simple scoring system for the confirmation screenings. This scoring system differentiated four grades: not affected or no difference to wild type growth relates to zero (full growth in all dilutions as wild type), a slight or weak growth defect relates to one (•, no growth at highest dilution), an intermediate growth defect relates to two (••, growth only at two lowest dilutions), and a pronounced and strong growth defect or no growth relates to three (•••, no growth a any dilution or weak growth only at the lowest dilution). The following Table 16 gives an overview of all mutants, showing growth phenotypes. It lists all 103 mutants of the deletion strain collection, which exhibited one or more different growth phenotypes under the tested conditions. The *S. cerevisiae* gene and ORF is assigned to every *C. glabrata* ORF, as well as the cellular location and a functional description.

In the following chapters, the results of the different screenings, including the identified strains, are described in more detail.

Table 16. *C. glabrata* deletion mutants displaying growth deficiencies on media supplemented with various compounds.

Cg ORF	Sc Gene	Sc ORF	42°C	CW	CR	SDS	Caf	NaCl	CF	Azole	AmpB	5-Flu	MM	Metal ion	Loc.	Description
CAGL0M04565g	*ACF2*	YLR144C										•			C	Intracellular beta-1,3-endoglucanase
CAGL0L08910g	*AEP3*	YPL005W				••									M	Peripheral mitochondrial inner membrane protein, located on the matrix face of the membrane
CAGL0G09042g	*AFT2*	YPL202C	•												N	Iron-regulated transcriptional activator; required for iron homeostasis & resistance to oxidative stress
CAGL0E06028g	*ALG5*	YPL227C	•••						•••					Cd	ER	UDP-glucose:dolichyl-phosphate glucosyltransferase, asparagine-linked glycosylation
CAGL0E02629g	*ALG6*	YOR002W	•••						•••					Cd	ER	Alpha 1,3 glucosyltransferase, transfer of oligosaccharides from dolichyl-PP to asp residues during N-glycosylation
CAGL0L01331g	*ANP1*	YEL036C			•••			•••	•••					•	G	Subunit of the alpha-1,6 mannosyltransferase complex
CAGL0C02343g	*ARB1*	YER036C		•	•	•••		•••							C	ATPase of the ATP-binding cassette (ABC) family involved in 40S and 60S ribosome biogenesis
CAGL0H06875g	*ARG81*	YML099C											•••		N	Zinc-finger transcription factor, Zn(2)-Cys(6) binuclear cluster, regulation of arginine-responsive genes
CAGL0M13739g	*ATM1*	YMR301C				•••		•••							M	Mitochondrial inner membrane ABC transporter, exports mitochondrially synthesized precursors of Fe/S clusters
CAGL0J02288g	*BAR1*	YIL015W				••									CW	Aspartyl protease secreted into the periplasmic space of mating type a cells
CAGL0L03520g	*BCK1*	YJL095W							•••						C	MAPKKK of the protein kinase C signaling pathway, which controls cell integrity
CAGL0I05236g	*BCY1*	YIL033C	•	••	••	•••		•••	•••				•		C/N	Regulatory subunit of the cAMP-dependent protein kinase (PKA), controls a variety of cellular processes
CAGL0L11528g	*BIG1*	YHR101C	•••		•••									Cd	ER	Integral membrane protein of the ER, required for normal content of cell wall beta-1,6-glucan
CAGL0J06072g	*CBK1*	YNL161W				•••			••						C	S/T protein kinase, regulates cell morphogenesis; involved in cell wall BS, apical growth and cell separation
CAGL0G06754g	*CDC10*	YCR002C	•••					••							CW	Septin ring component of mother-bud neck, required for cytokinesis; septins can act as diffusion barrier
CAGL0I01188g	*CDC12*	YHR107C	•••	••	••	•••	••	••							CW	Septin ring component of mother-bud neck, required for cytokinesis; septins can act as diffusion barrier
CAGL0E03476g	*CDC25*	YLR310C	••												C/PM	Membrane bound GEF; indirectly regulates adenylate cyclase through activation of Ras1p and Ras2p
CAGL0J11506g	*CHS1*	YNL192W	•			•									PM	Chitin synthase I; required for repairing the chitin septum during cytokinesis
CAGL0G02035g	*CKA2*	YOR061W					•			•	••			•	C/N	Alpha' catalytic subunit of casein kinase 2, a Ser/Thr protein kinase with roles in cell growth and proliferation
CAGL0I00946g	*CKB2*	YOR039W	••						•••					Cd	C/N	Beta' regulatory subunit of casein kinase 2, a Ser/Thr protein kinase with roles in cell growth and proliferation
CAGL0L11110g	*CNA1*	YLR433C		•••		•••			••	•				•	C	Calcineurin A; catalytic subunit of calcineurin, a Ca++/calmodulin-regulated protein phosphatase, regulates Crz1p
CAGL0L00605g	*CNB1*	YKL190W		•••		••				•				•	C	Calcineurin B; regulatory subunit of calcineurin
CAGL0D00242g	*CNE1*	YAL058W	•••			•••									ER	Calnexin; integral membrane ER chaperone involved in folding and quality control of glycoproteins
CAGL0M06831g	*CRZ1*	YNL027W							•••						N/C	Transcription factor that activates transcription of genes involved in stress response
CAGL0J06490g	*CUE1*	YMR264W							•••						ER	ER membrane protein that recruits the ubiquitin-conjugating enzyme Ubc7p, functions in protein degradation

Table 16. continued

Cg ORF	Sc Gene	Sc ORF	42°C	CW	CR	SDS	Caf	NaCl	CF	Azole	AmpB	5-Flu	MM	Metal ion	Loc.	Description
CAGL0A01452g	*CWH41*	YGL027C	●●●	●●●	●●	●	●	●●		●●	●				ER	Processing alpha glucosidase I, involved in assembly of cell wall β-1,6 glucan and asp-linked protein glycosylation
CAGL0L07854g	*CWH43*	YCR017C	●●●												ER	Putative sensor/transporter protein involved in cell wall biogenesis; null mutation is synthetically lethal with pkc1Δ
CAGL0H06347g	*DEP1*	YAL013W									●●				N	Transcriptional modulator, regulation of structural phospholipid BS genes & metabolically unrelated genes
CAGL0K02827g	*DID4*	YKL002W												•	C	Class E Vps protein of the ESCRT-III complex, sorting of integral membrane proteins, involved in endocytosis
CAGL0G05896g	*DSE2*	YHR143W					●		●●						CW	Daughter cell-specific protein, similarity to glucanases, degrades cell wall from the daughter cell side
CAGL0L07326g	*DUN1*	YDL101C							●						N	Cell-cycle checkpoint serine-threonine kinase required for DNA damage-induced transcription
CAGL0M07656g	*ERG5*	YMR015C							●						ER	C-22 sterol desaturase, cytochrome P450 enzyme, ergosterol biosynthesis; may be a target of azoles
CAGL0H09460g	*FAA2*	YER015W	●●●			●●●								•	P	Long chain fatty acyl-CoA synthetase
CAGL0I06138g	*FAR1*	YJL157C												•	N/C	Cyclin-dependent kinase inhibitor that mediates cell cycle arrest in response to pheromone
CAGL0G01034g	*FKS1*	YLR342W							●●●						PM	Catalytic subunit of 1,3-beta-D-glucan synthase, involved in cell wall synthesis and maintenance
CAGL0K05841g	*HAP1*	YLR256W								●●					N	Zinc finger TF involved in the complex regulation of gene expression in response to levels of heme and oxygen
CAGL0L06226g	*HEK2*	YBL032W				●									N	RNA binding protein involved in the asymmetric localization of ASH1 mRNA
CAGL0M04169g	*KRE1*	YNL322C		●●●		●●●					●		●		CW	Cell wall glycoprotein involved in beta-glucan assembly; serves as a K1 killer toxin membrane receptor
CAGL0F04873g	*KRE6*	YPR159W											●●●		G	Protein required for beta-1,6 glucan BS; putative beta-glucan synthase; appears functionally redundant with Skn1p
CAGL0L00627g	*KRH1*	YAL056W	●●●												C	Regulator of cAMP-PKA signaling; inhibits PKA downstream of Gpa2p and Cyr1p increasing cAMP dependency
CAGL0B04565g	*KTR1*	YOR099W							●●●						G	Alpha-1,2-mannosyltransferase involved in O- and N-linked protein glycosylation
CAGL0M05841g	*KTR2*	YKR061W	●●●		●●●					●●	●●			Cd	G	Mannosyltransferase involved in N-linked protein glycosylation
CAGL0M07381g	*KTR6*	YPL053C								●					PM	Probable mannosylphosphate transferase involved in synthesis of core oligosaccharides in protein glycosylation
CAGL0J05236g	*LAS21*	YJL062W	●●											Cd	ER	Integral plasma membrane protein involved in the synthesis of the glycosylphosphatidylinositol (GPI) core structure
CAGL0D02442g	*LEM3*	YNL323W												•	PM/ER	Membrane protein of PM and ER, translocation of phospholipids & alkylphosphocholine drugs across PM
CAGL0E01683g	*MCK1*	YNL307C			●●									Cd	C/N	Protein serine/threonine/tyrosine kinase involved in control of chromosome segregation & regulating entry into meiosis
CAGL0I10769g	*MCM1*	YMR043W				●●●									N	Transcription factor involved in cell-type-specific transcription and pheromone response
CAGL0A01133g	*MDL2*	YPL270W						●							M	Mitochondrial inner membrane half-type ATP-binding cassette (ABC) transporter
CAGL0I08503g	*MET16*	YPR167C				●●●							●●●		C	3'-phosphoadenylsulfate reductase, involved in sulfate assimilation and methionine metabolism
CAGL0J03828g	*MKK1*	YOR231W							●●●						C	MAPKK involved in protein kinase C signaling pathway that controls cell integrity

Table 16. continued

Cg ORF	Sc Gene	Sc ORF	42°C	CW	CR	SDS	Caf	NaCl	CF	Azole	AmpB	5-Flu	MM	Metal ion	Loc.	Description
CAGL0K11231g	*MNN10*	YDR245W	•		•••				•••					•	G	Subunit of a Golgi mannosyltransferase complex containing Anp1p, Mnn9p, Mnn11p, & Hoc1p, elongation of mannan
CAGL0C04048g	*MNT3*	YIL014W							•						G	Alpha-1,3-mannosyltransferase, adds 4.& 5. α-1,3-linked mannose residues to O-linked glycans, O-glycosylation
CAGL0G06864g	*MPS3*	YJL019W	••					•••						•	N	Nuclear envelope protein required for SPB duplication and nuclear fusion
CAGL0F00671g	*MYO2*	YOR326W										•			C	Type V myosin motors, actin-based transport, polarized delivery of sec. vesicles, vacuole, late Golgi, peroxisomes
CAGL0D02750g	no sim.	-	•••				••			••				•	?	
CAGL0A01892g	no sim.	-							••					•	?	
CAGL0J11308g	*NPR1*	YNL183C				•••						•			C	Protein kinase that stabilizes several PM amino acid transporters by antagonizing ubiquitin-mediated degradation
CAGL0J08569g	*OST3*	YOR085W	•••		••				•••					Cd	ER	Subunit of oligosaccharyltransferase complex of the ER, catalyzes N-glycosylation of newly synthesized proteins
CAGL0L05632g	*PBS2*	YJL128C	••	•		••		•••						•	C	MAPKK that plays a pivotal role in the osmosensing signal-transduction pathway, activated under osmotic stress
CAGL0K09944g	*PDE2*	YOR360C	•••												C/N	High-affinity cyclic AMP phosphodiesterase, component of the cAMP-dependent protein kinase signaling system
CAGL0A00451g	*PDR1*	YGL013C								•••					N	Zinc cluster TF, master regulator of pleiotropic drug response
CAGL0M01760g	*PDR5*	YOR153W								•••					PM	Plasma membrane ABC transporter,involved in steroid transport and cellular detoxification during exponential growth
CAGL0I01012g	*PEP12*	YOR036W	••											•	G	t-SNARE for vesicular intermediates traveling between the Golgi apparatus and the vacuole
CAGL0F08041g	*PFK1*	YGR240C	••			•••								•	C	Alpha subunit of phosphofructokinase involved in glycolysis, indispensable for anaerobic growth
CAGL0I07513g	*PKH2*	YOL100W	•••				••	••							N	S/T protein kinase, sphingolipid-mediated signaling pathway, activates Ypk1p & Ykr2p, cell wall integrity
CAGL0J08734g	*PMT2*	YAL023C	•••						•••						ER	Protein O-mannosyltransferase, transfers mannose residues from dolichyl phosphate-D-mannose to S/T residues
CAGL0M00220g	*PMT4*	YJR143C	•••						•						ER	Protein O-mannosyltransferase, transfers mannose residues from dolichyl phosphate-D-mannose to S/T residues
CAGL0D01034g	*PSA1*	YDL055C	•••	••	••		•••	••							C	GDP-mannose pyrophosphorylase, synthesizes GDP-mannose from GTP and mannose-1-phosphate in cell wall BS
CAGL0L02827g	*PTP2*	YOR208W						•••						•	N/C	Protein phosphatase involved in MAPK inactivation during osmolarity sensing; dephosporylates Hog1
CAGL0I09130g	*PTR3*	YFR029W									•				PM	Component of the SPS plasma membrane amino acid sensor system, senses external amino acid concentration
CAGL0A04587g	*ALG3*	YBL082C	••											Cd	ER	Dolichol-P-Man dep. α(1-3) mannosyltransferase, synthesis of dolichol-linked oligosaccharide donor
CAGL0H05621g	*RLM1*	YPL089C							•••						N	TF of the PKC pathway involved in the maintenance of cell integrity, activated by the MAP-kinase Slt2
CAGL0K06963g	*ROT2*	YBR229C	•••		•••									•	ER	Glucosidase II catalytic subunit required for normal cell wall synthesis
CAGL0D05434g	*ROX1*	YPR065W									•				N	Heme-dependent repressor of hypoxic genes
CAGLB01441g	*RPD3*	YNL330C							•••					Cd	N	Histone deacetylase; regulates transcription and silencing; plays a role in regulating Ty1 transposition

Table 16. continued

Cg ORF	Sc Gene	Sc ORF	42°C	CW	CR	SDS	Caf	NaCl	CF	Azole	AmpB	5-Flu	MM	Metal ion	Loc.	Description
CAGL0D03850g	*RSC3*	YDR303C	•												N	Component of RSC chromatin remodeling complex, maintenance of ploidy, regulation ribosomal genes, stress response
CAGL0M01628g	*SAC7*	YDR389W									•				C	GTPase activating Rho1p, involved in signaling to the actin cytoskeleton
CAGL0J08778g	*SEC13*	YLR208W	•••						••						G	Component of nuclear pore sub-complex and of the COPII complex, important for the formation of ER to Golgi vesicles
CAGL0G03597g	*SHO1*	YER118C	•••	••		••		•••						•	PM	Transmembrane osmosensor, activation of both the Cdc42p- and MAPK-dependent filamentous growth & HOG pathway
CAGL0L03377g	*SIP4*	YJL089W				••									N	Zinc cluster TF, binds to carbon source-responsive element of gluconeogenic genes, pos. regulator of gluconeogenesis
CAGL0F09097g	*SKN7*	YHR206W	•					••							N	Nuclear response regulator & TF, induction of heat-shock genes in response to oxid. stress, involved in osmoregulation
CAGL0E02783g	*SLA1*	YBL007C									••				N/C	Cytoskeletal protein required for assembly of cortical actin, interacts with proteins regulating actin dynamics
CAGL0J00539g	*SLT2*	YHR030C							•••	•					C/N	S/T MAPK involved in regulating the maintenance of cell wall integrity and progression through the cell cycle
CAGL0F02079g	*SMC1*	YFL008W	••												N	Subunit of the multiprotein cohesin complex, involved in chromosome segregation and in double-strand DNA break repair
CAGL0E03718g	*SNF6*	YHL025W							•		••				N	Subunit of SWI/SNF chromatin remodeling complex involved in transcriptional regulation
CAGL0D01936g	*SNF7*	YLR025W	••					••			•			•	C	Subunit of ESCRT-III,sorting of transmembrane proteins into multivesicular body pathway
CAGL0C02717g	*SPO7*	YAL009W				•••									ER/N	Regulatory subunit of phosphatase, regulates nuclear growth, required for normal nuclear envelope morph. & sporulation
CAGL0M02585g	*SPP1*	YPL138C							•						N	Subunit of COMPASS, a complex which methylates histone H3 on lysine 4, required in telomeric transcriptional silencing
CAGL0H01287g	*SSD1*	YDR293C	•••					••	••	•	•				C	Role in maintenance of cellular integrity, interacts with components of the TOR pathway
CAGL0K02673g	*STE20*	YHL007C				•••		•••							C	Signal transducing kinase of the PAK family, involved in pheromone response and pseudohyphal/invasive growth
CAGL0B00858g	*STE50*	YCL032W				••		•••						•	C	Involved in mating response, invasive/filamentous growth, and osmotolerance, acts as an adaptor
CAGL0M08778g	*SWM1*	YDR260C	•••												N	Subunit of anaphase-promoting complex, regulates metaphase-anaphase transition and exit from mitosis
CAGL0D03146g	*SYS1*	YJL004C	••			••									G	Integral membrane protein of the Golgi required for targeting of the Arf-like GTPase Arl3p to the Golgi
CAGL0C01463g	*TCO89*	YPL180W	••				•••								V/PM	Subunit of TORC1, regulates growth in response to nutrient availability, deletion strains hypersensitive to rapamycin
CAGL0F08371g	*TNA1*	YGR260W												•	PM	High affinity nicotinic acid plasma membrane permease, responsible for uptake of low levels of nicotinic acid
CAGL0M03773g	*TOS6*	YNL300W					•								CW	GPI-dep. CW protein, expression is periodic & decreases in respone to ergosterol perturbation or entry into stationary phase
CAGL0G09020g	*TPK2*	YPL203W	•••	••	••	•		•							N	cAMP-dep. protein kinase catalytic subunit; promotes vegetative growth in response to nutrients via Ras-cAMP signaling
CAGL0H08437g	*VPS15*	YBR097W									•••				G	S/Tprotein kinase for vacuolar protein sorting, membrane-assoc. complex with Vps34, recruits Vps34 to Golgi membrane
CAGL0F01507g	*WSC1*	YOR008C	•••	•••	••	•••	••	•••	•••	•				•	PM	Sensor of stress-activated PKC/cell wall integrity pathway, involved in organization of the actin cytoskeleton

Table 16. continued

Cg ORF	Sc Gene	Sc ORF	42°C	CW	CR	SDS	Caf	NaCl	CF	Azole	AmpB	5-Flu	MM	Metal ion	Loc.	Description
CAGL0M05643g	*YFH1*	YDL120W	••	•	•				•				•••	•	M	Mitochondrial matrix iron chaperone; oxidizes and stores iron, interacts with Isu1p to promote Fe-S cluster assembly
CAGL0K03399g	*YPK1*	YKL126W	•••				••		•••	•	••			•	C	S/T protein kinase required for receptor-mediated endocytosis, sphingolipid-mediated and cell integrity signaling pathways
CAGL0K08272g	*YSR3*	YKR053C							•						ER	Dihydrosphingosine 1-phosphate phosphatase, membrane protein involved in sphingolipid metabolism
CAGL0E01353g	*ZRT2*	YLR130C	•					•							PM	Low-affinity zinc transporter of the PM, transcription induced under low-zinc conditions by the Zap1p transcription factor
Total # of genes	**103**		**46**	**13**	**15**	**28**	**11**	**22**	**33**	**14**	**13**	**3**	**6**	**34**		

Table 16. Summary of all 103 mutants displaying growth phenotypes. The scoring system differentiates four grades: Dots correspond to ••• pronounced, •• intermediate or • slight growth defect. CW = calcofluor white, CR = congo red, SDS = sodium dodecyl sulfate, Caf= caffeine, NaCl = sodium chloride, CF = caspofungin, Azole = fluconazole or voriconazole, AmpB = amphotericin B, 5-Flu = 5-Flucytosine, MM = minimal medium, Metal ion = $CaCl_2$, $MgCl_2$, $ZnCl_2$, $MnCl_2$, $CdCl_2$, LiCl. Loc. = cellular localization (M = mitochondrium, C = cytoplasm, ER = endoplasmic reticulum, PM = plasma membrane, G = golgi, N = nucleus, CW = cell wall, V = vacuole).

5.4.1 Sensitivity to cell wall-perturbing agents and elevated temperatures

The cell wall ensures structural integrity and forms a barrier against environmental changes. It is further important for adhesion to host tissue and represents the structural cell component, which is recognized by the host's immune cells (Brown, 2006, de Groot *et al.*, 2008, De Las Penas *et al.*, 2003, Iraqui et al., 2005, Kopp & Medzhitov, 2003). Cell wall defects can change these properties, resulting in a different cell wall composition.

In a primary screening for CW, CR and SDS sensitivity, we identified deletion mutants exhibiting cell wall defects. The fluorescent dye CW binds to chitin and interferes with its polymerisation; CR interferes with the cell wall glucan, thereby inhibiting growth (Ram *et al.*, 1994, Roncero & Duran, 1985); and the detergent SDS putatively acts on the plasma membrane and surface proteins, which play a role in cell wall assembly. Defective cell walls may also facilitate the access of SDS to the membrane, causing cell lysis (Bickle *et al.*, 1998, Igual *et al.*, 1996). In addition, we screened for growth at elevated temperatures (37°C and 42°C), since cells deficient of a normal cell wall often display cell lysis under high temperature conditions.

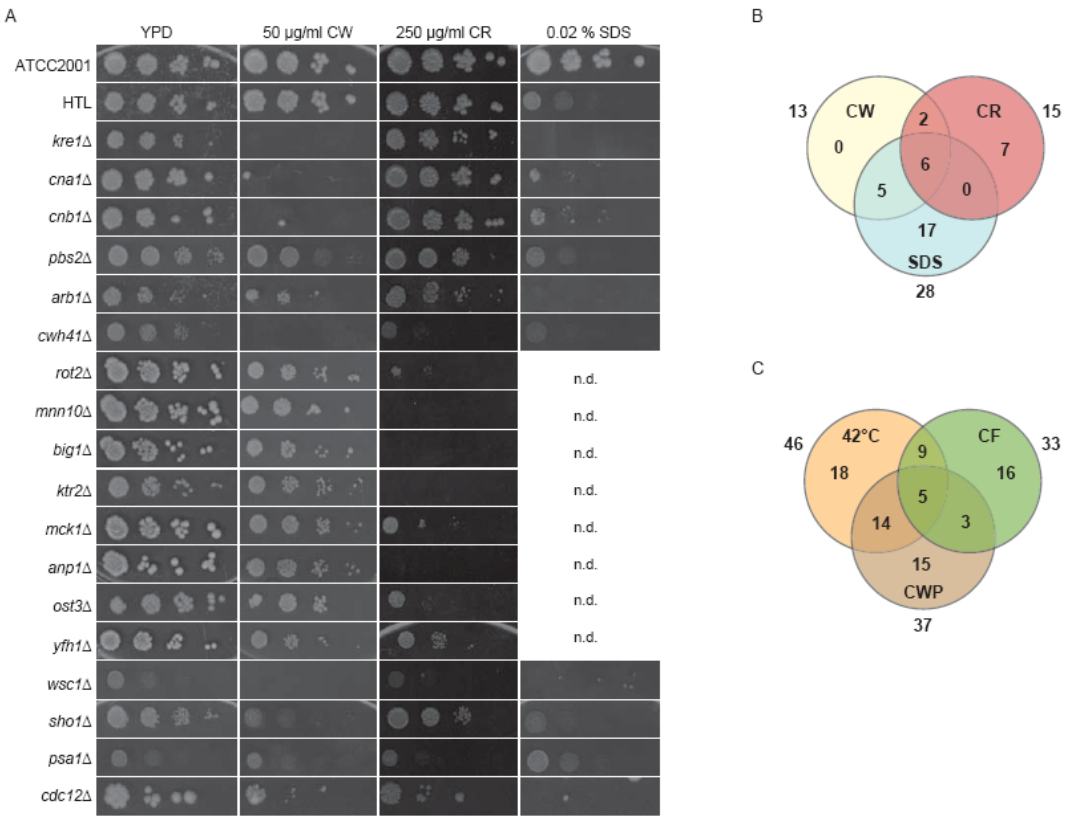

Figure 17. Sensitivity of *C. glabrata* deletion mutants to cell wall-perturbing agents. Cells were spotted on medium supplemented with calcofluor white (CW), congo red (CR) or sodium dodecyl sulfate (SDS) at the indicated concentrations and incubated for 48 hours at 30°C. Strains that did not show any SDS sensitivity in the large-scale screening were not screened in confirmation tests; n.d. = not determined, because the strains didn't show a growth defect in the large-scale primary screening. (B) Venn diagram showing correlation of deletion strains exposed to different cell wall perturbing agents (CW = Calcofluor White, CR = Congo Red). (C) Correlation of growth deficient mutants under heat stress, exposed to Caspofungin or to cell wall-perturbing agents (CWP).

A large group of mutants displayed hypersensitivity to cell wall-perturbing agents (44 strains, Figure 18A), mainly affected in signaling transduction and cell wall biogenesis and maintenance. Most of the 46 identified temperature-sensitive deletion strains also lack genes implicated in signaling pathways and cell wall biogenesis (Figure 18B).

Some 13 mutants were confirmed to be hypersensitive to CW, 15 to CR and 28 to SDS (Table 15, Figure 17 B). Several mutants displayed growth defects under all three stress conditions, indicating that their cell wall integrity is severely affected. Interestingly, five mutants (*kre1*Δ, *cna1*Δ, *cnb1*Δ, *pbs2*Δ, *arb1*Δ) were sensitive to CW and SDS but not to CR and seven mutants (*rot2*Δ, *mnn10*Δ, *big1*Δ, *ktr2*Δ, *mck1*Δ, *anp1*Δ, *ost3*Δ) were only sensitive to CR but not to the other two substances, indicating that CR has another impact on the cell wall than CW or SDS. Interestingly, the overlap between mutants sensitive to cell wall-perturbing compounds and elevated temperatures was higher, than the overlap of cell wall-perturbing compounds and CF-susceptible mutants (Figure 17C).

Most of the mutants sensitive to cell wall-perturbing agents as well as to increased temperature are involved in glycosylation and cell wall biogenesis. Based on their homology to *S. cerevisiae* genes, identified *C. glabrata* mutants lacking *KTR2*, *PSA1*, *CWH41*, and *MNN10* are involved in glycosylation and mannosylation (Ballou *et al.*, 1989, Hashimoto *et al.*, 1997, Lussier *et al.*, 1996, Jiang *et al.*, 1996). *KRE1* is a cell wall constituent implicated in β-1,6 glucan synthesis (Boone *et al.*, 1990). Lack of *KRE1* results in reduced fitness as well as CW and SDS sensitivity. Lack of the septin homologue *CDC12* results in improper cell separation and growth sensitivity to various cell wall-perturbing stresses (Figure 17 and 31D) similar as in *S. cerevisiae* (Cid *et al.*, 2001). *OST3*, *BIG1*, *ROT2* and *ANP1* function in cell wall biogenesis (Azuma *et al.*, 2002, Burda & Aebi, 1999). Remarkably, *C. glabrata* deletion mutants of the former three genes underwent cell lysis at 37°C, suggesting that their cell wall is severely weakened. In contrast to *C. glabrata*, a growth defect is documented for the *S. cerevisiae rot2*Δ mutant (Trombetta *et al.*, 1996). Cell wall mutants lacking the protein O-mannosyltransferase genes *PMT2, PMT4* and *LAS21*, which are implicated in synthesis of the GPI-anchor core structure (Benachour *et al.*, 1999, Girrbach & Strahl, 2003) and *CWH43*, encoding a putative transporter protein involved in cell wall biogenesis (Ram et al., 1994), displayed temperature and CF but no CW, CR or SDS sensitivity.

A *C. glabrata* mutant lacking *SSD1* was heat sensitive and additionally showed growth defects on NaCl and CF. The growth phenotype of the *C. glabrata* deletion strain suggests an altered cell wall composition. Likewise, the baker's yeast *ssd1*Δ mutant is unable to grow at high temperatures and displays an altered cell wall phenotype resulting in flocculation (Wheeler *et al.*, 2003). Remarkably, the *S. cerevisiae SSD1* gene is connected to virulence, because this mutant is more virulent causing rapid death of the mice in a murine infection model (Wheeler *et al.*, 2003).

Out of 28 mutants, 17 were hypersensitive to the detergent SDS only. Some of these mutants are rather involved in metabolism and membrane functions than in cell wall biogenesis. For example, ScFaa2 is involved in lipid metabolism and functions as a long chain fatty acyl-CoA synthetase (Johnson *et al.*, 1994). A *C. glabrata faa2*Δ strain displayed growth deficiencies on SDS and at increased temperature. A *cne1*Δ deletion strain was also unable to grow on media containing SDS and under elevated temperatures. *CNE1* is a homologue of the mammalian calnexin, an ER-located integral membrane chaperone which is involved in quality control of glycoproteins (Parlati *et al.*, 1995). This suggests that, on one hand, SDS indirectly affects the cell wall by acting on membrane lipids and proteins, but that, on the other hand lipid biosynthesis-deficient mutants also become hypersensitive for SDS.

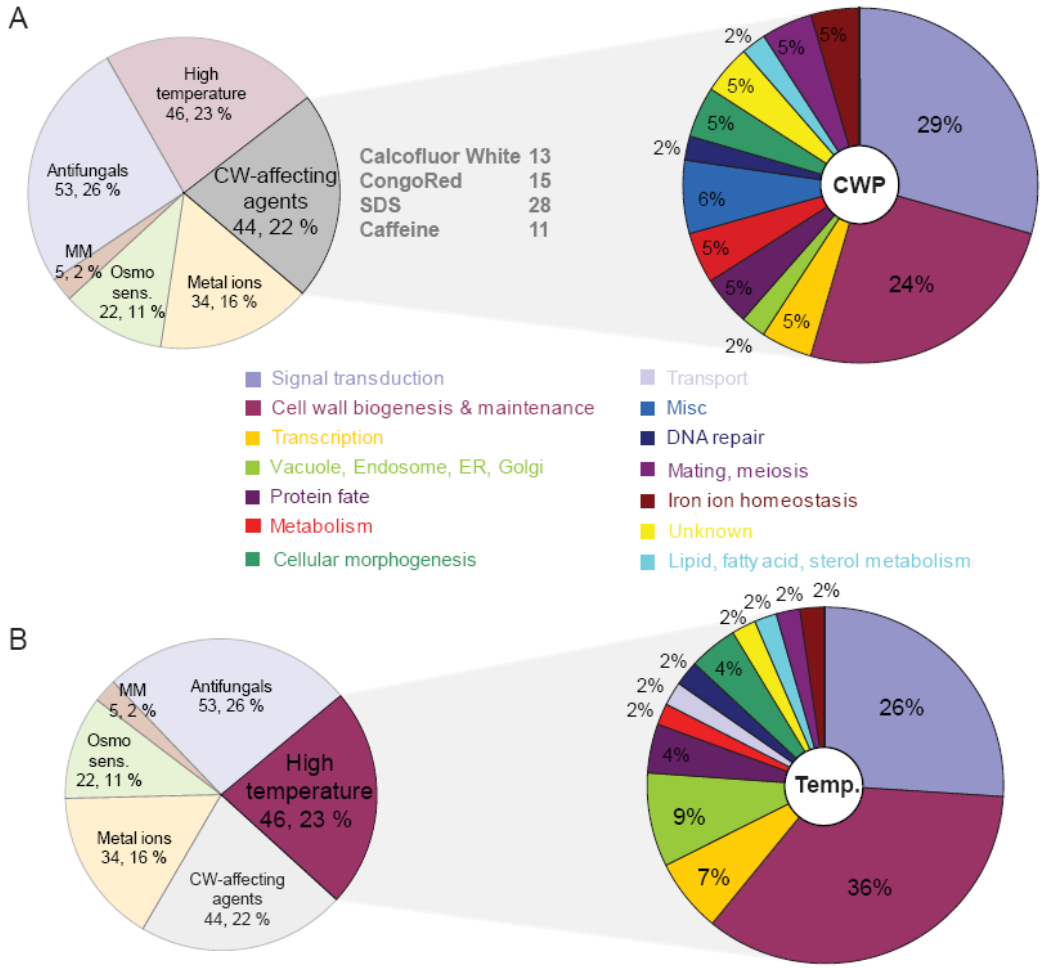

Figure 18. Distribution of mutants sensitive to cell wall-perturbing agents and temperature stress. Functional categories were assigned using the *Saccharomyces* Genome Database GO data (http://www.yeastgenome.org/). (A) Mutants sensitive to the cell wall-perturbing agents CW, CR, SDS and Caffeine. (B) Mutants sensitive to elevated temperatures (37°C, 42°C). CWP = cell wall-perturbing agents; Temp. = temperature stress.

In addition to cell wall mutants, many *C. glabrata* signaling pathway mutants displayed growth defects when exposed to cell wall-perturbing agents or temperature stress. These genes involve the PKA pathway regulatory subunit Bcy1, the cAMP-dependent protein kinase Tpk2, the two calcineurin subunits (Cna1 and Cnb1) and the HOG pathway

components Pbs2 and Sho1. Further, the *wsc1*Δ mutant, lacking the PKC pathway sensor, was very sensitive to all tested growth conditions affecting the cell wall. The PKA-pathway associated genes *KRH1* and *PDE2* (Thevelein & de Winde, 1999) and the sphingolipid-mediated pathway signaling components Pkh2 and Ypk1 (Levin, 2005) were only sensitive to heat stress but not to CR, CW or SDS.

In summary, most of the detected *C. glabrata* deletion mutants with decreased tolerance to cell wall perturbing agents or growth deficiencies at elevated temperatures showed similar phenotypes as described for *S. cerevisiae* mutants. However, not all *C. glabrata* mutants showed an identical susceptibility pattern, suggesting that basic functions and regulation are similar but specific differences exist between the pathogenic *C. glabrata* and the non-pathogenic *S. cerevisiae*.

5.4.2 Caffeine sensitivity

In *S. cerevisiae*, exposure to the alkaloid caffeine activates the cell wall integrity pathway. PKC pathway mutants display an altered sensitivity to caffeine, implying that caffeine affects cell wall assembly or composition (de Groot *et al.*, 2001, Martin *et al.*, 1996, Martin *et al.*, 2000). Recent findings disclosed TORC1 (target of rapamycin complex) as one of the major caffeine targets (Reinke *et al.*, 2006, Wanke *et al.*, 2008). The TOR pathway regulates cellular growth in response to stresses and nutrient availability (Cardenas *et al.*, 1999, Loewith *et al.*, 2002). Therefore, we screened for growth on caffeine-supplemented medium, because the caffeine-affected TOR pathway and other caffeine targets may have an impact on virulence.

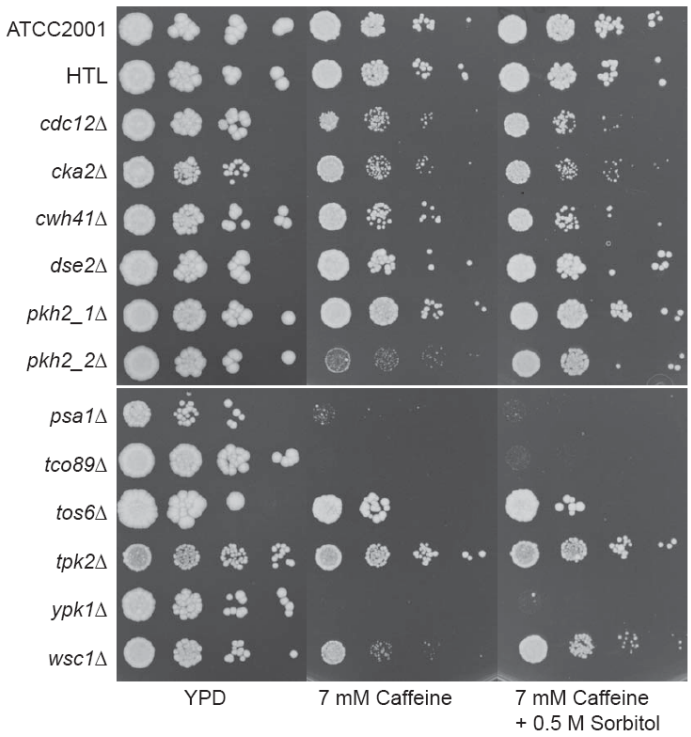

Figure 19. Caffeine sensitivity of *C. glabrata* deletion strains. Deletion strains were grown to OD_{600} of 1.0, serial diluted to OD_{600} of 0.1, 0.01, 0.001 and 0.0001 and spotted onto YPD and YPD agar plates containing the indicated amounts of caffeine and caffeine + sorbitol. Plates were incubated at 30°C for 2 days and pictures taken with the spImager system (S&P Robotics, Canada).

Only a small set of eleven *C. glabrata* genes showed caffeine sensitivity. Although we were not able to delete *TOR1* of *C. glabrata*, a mutant lacking *TCO89*, a TORC1 subunit, was unable to grow on YPD supplemented with 7 mM of caffeine. The hypersusceptible phenotype of a *tco89*Δ mutant confirms that the TOR pathway is also a major target of caffeine in *C. glabrata*.

Several strains lacking cell wall-related genes (*cdc12*Δ, *cka2*Δ, *cwh41*Δ, *dse2*Δ, *tos6*Δ) showed a slight to intermediate caffeine sensitivity. A *psa1*Δ mutant was severely affected by caffeine, similar as the cell wall-related signaling pathway genes (*wsc1*Δ, *ypk1*Δ, *pkh2*Δ (CAGL0I07513g); Figure 19). Some caffeine-sensitive mutants were osmoremedial as addition of 0.5 M sorbitol rescued *wsc1*Δ and *pkh2*Δ strains. The osmoremedial growth phenotype of these two mutants is consistent with their implication in cell wall biogenesis. The *tco89*Δ, *ypk1*Δ and *psa1*Δ deletion strains were unable to grow on caffeine and were not rescued by sorbitol. A sensitive strain lacking *TPK2* was detected in the primary screening for caffeine sensitivity but could not be confirmed. The identification of caffeine-sensitive mutants (*dse2*Δ, *cwh41*Δ, *tos6*Δ, *cdc12*Δ), which additionally displayed altered cell morphologies (see Figure 29) supports the idea that caffeine indeed influences cell wall integrity in *C. glabrata*.

5.4.3 Susceptibility to the fungal β-glucan synthase inhibitor caspofungin

The fungal cell wall is a potential target of antifungal drugs. Caspofungin (CF) is a potent inhibitor of the fungal β-glucan synthase (Onishi *et al.*, 2000). Expression of the glucan synthase subunits depends on the cell cycle and is regulated in response to cell wall integrity (Levin, 2005). Remarkably, cell wall integrity pathway mutants of *S. cerevisiae* are unable to grow on CF-supplemented medium (Reinoso-Martin et al., 2003).

The known mechanisms for caspofungin resistance are mainly based on hot-spot mutations in one of the β-glucan synthase subunits (Cota *et al.*, 2008, Park *et al.*, 2005, Katiyar *et al.*, 2006, Thompson *et al.*, 2008, Cleary *et al.*, 2008, Garcia-Effron *et al.*, 2009). Additional data demonstrate that the calcineurin pathway might act in synergy with the PKC pathway to regulate the cell wall-dependent stress response (Steinbach *et al.*, 2007, Wiederhold *et al.*, 2005, Perlin, 2007).

We performed a plate based screen on solid medium, scoring for CF-susceptible mutants, to identify novel *C. glabrata* genes implicated in CF sensitivity. The screen revealed a large number of genes, mainly involved in cell wall-associated and signaling functions or acting as transcriptional regulators (Figure 20 & 21, Table 16). As expected the glucan synthase mutant *fks1*Δ and the MAP-kinase mutant *slt2*Δ were susceptible to CF but also many novel genes not previously associated with CF sensitivity were identified. For instance, many cell wall biosynthesis mutants implicated in glycosylation (*alg5*Δ, *alg6*Δ, *ost3*Δ) and

mannosylation (*pmt2*Δ, *pmt4*Δ, *mnn10*Δ, *anp1*Δ, *mnt3*Δ, *ktr1*Δ), as well as other cell wall-associated functions (*ssd1*Δ, *dse2*Δ, *cbk1*Δ) displayed growth defects on CF-supplemented media.

The strong effect on cell wall-defective mutants suggests that CF may also target other cell wall components or associated proteins than the fungal β-glucan synthase. However, the only validated CF target so far, is the fungal glucan synthase (Perlin, 2007). Therefore, it appears that a functional cell wall is necessary for CF tolerance. In other words, a functional cell wall may buffer the negative effects of glucan synthase inhibition by CF. This view is confirmed by a study on *C. albicans* cell wall genes (Plaine *et al.*, 2008). Mutants with thin cell walls were found to be more sensitive to CF, while those with thicker cell walls are more resistant. In addition, the transcriptional profiling of *C. albicans* exposed to CF performed in our (Gregori C., unpublished data) and other labs (Liu *et al.*, 2005) identified several cell wall genes upregulated in response to CF. Expression profiling of *S. cerevisiae* also demonstrated CF-induced upregulation of many cell wall genes (Agarwal et al., 2003).

Taken together, a weakened cell wall may result in higher CF sensitivity, while a cell wall strengthened with other components such as chitin helps to compensate the lack of glucan and to survive CF stress (Walker *et al.*, 2008).

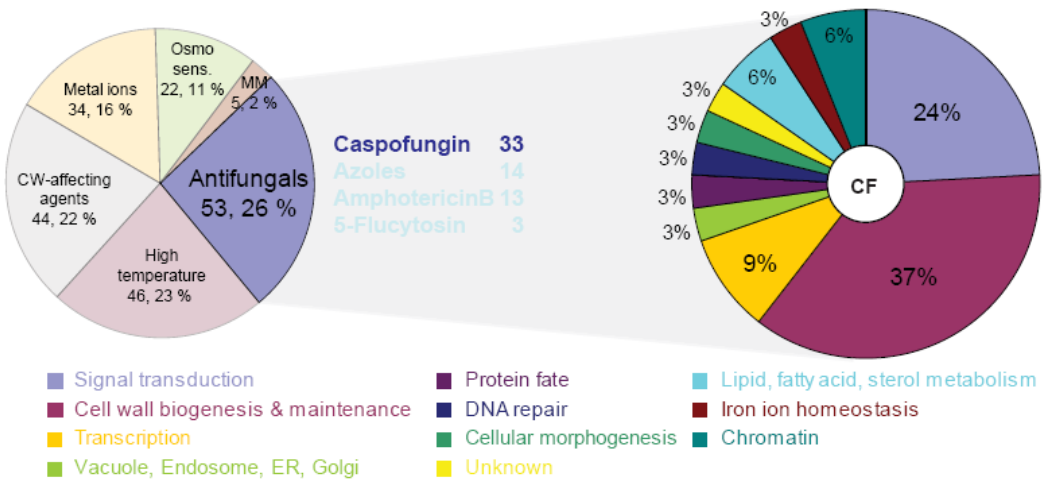

Figure 20. Distribution of CF-sensitive mutants. Gene annotations were assigned as in Figure 18. A total of 33 mutants displayed CF sensitivity, which differ largely from the genes found to be sensitive to the other tested antifungals.

The screen for CF susceptibility also identified several signaling components implicated in CF-stress sensing, such as the PKC (*WSC1*, *BCK1*, *MKK1*, *SLT2*, *RLM1*) and calcineurin (*CNA1*, *CNB1*, *CRZ1*) pathway components (Figure 21, Table 16). *C. glabrata* mutants lacking the PKC stress sensor protein Wsc1 showed a pronounced susceptibility to CF. In general, Wsc1 appeared to be essential for sensing a variety of stresses, which affect cellular integrity. Thus, Wsc1 may represent an essential surface stress sensor of *C. glabrata* and may also signal via several different pathways. Therefore, Wsc1 is also likely to be

involved in virulence and adaptation to diverse host niches, because it appears to be involved in sensing various environmental changes that affect the cell wall.

Interestingly, the *C. glabrata* genes encoding the MAP-kinases of the PKC pathway are almost exclusively sensitive to CF. In contrast, *S. cerevisiae* MAPK-kinase mutants are sensitive to CF, CR and CW (Reinoso-Martin et al., 2003). This difference may provide an indication for a transcriptional rewiring of the cell wall integrity pathway in *C. glabrata*, controlling the expression of a differing set of cell wall genes.

Remarkably, the *C. glabrata YPK1* homologue was also essential for growth on CF, indicating a putative connection of the sphingolipid-mediated signaling and the PKC pathway. Ypk1 as well as Pkh2 are kinases acting in the sphingolipid-mediated signaling pathway (Levin, 2005). In addition, *ypk1*Δ and *pkh2*Δ mutants exhibited cell lysis at elevated temperatures, suggesting an implication in cell wall integrity. Furthermore, the *ypk1*Δ strain was also sensitive to a variety of metal ions, caffeine and the antifungal drug amphotericin B. These growth phenotypes suggest that Ypk1 functions in a second parallel cell integrity pathway of *C. glabrata*, which may be connected to the PKC pathway.

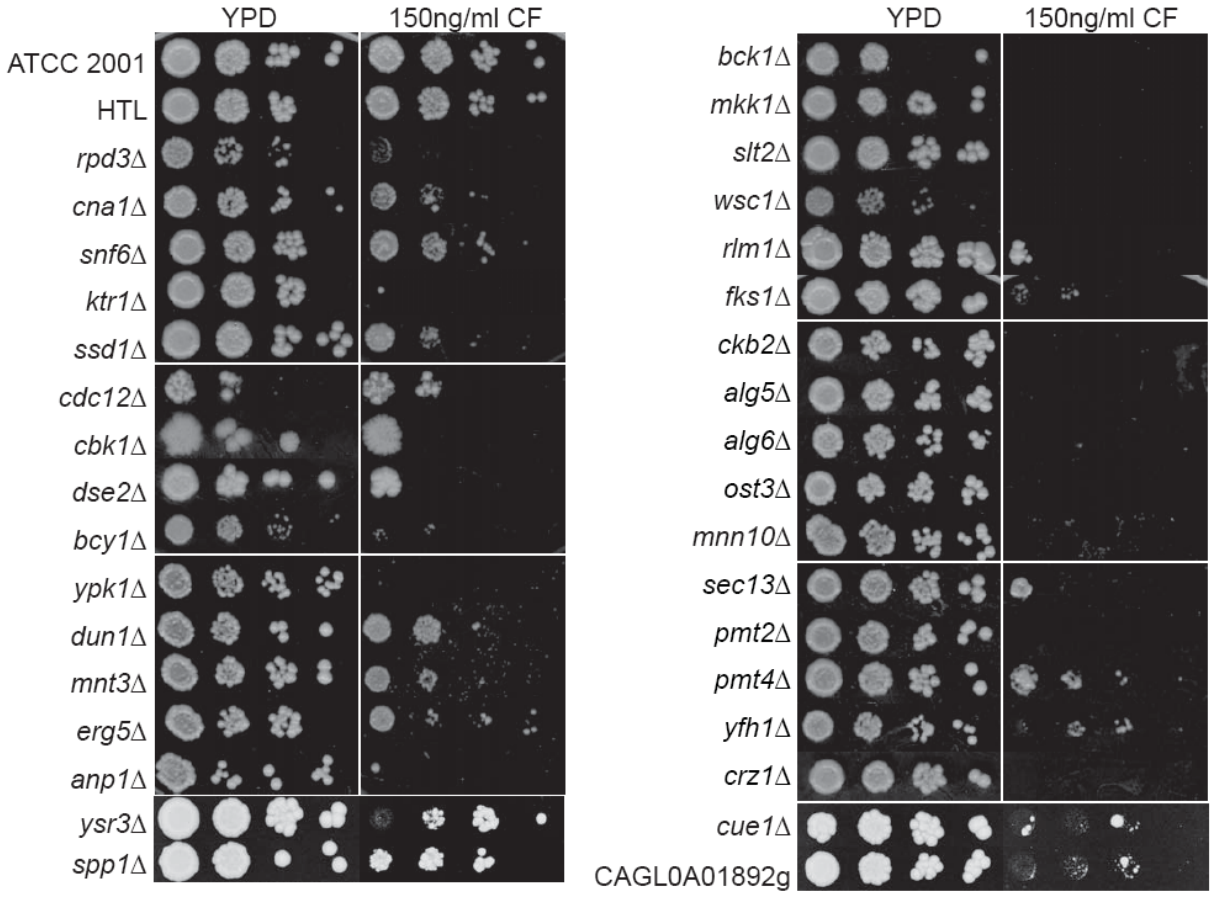

Figure 21. Sensitivity of *C. glabrata* deletion strains to caspofungin. Wild type ATCC2001, HTL and isogenic deletion strains were grown to OD_{600} of 1.0, serial diluted to OD_{600} of 0.1, 0.01, 0.001 and 0.0001 and spotted onto YPD and YPD agar plates containing the indicated amount of caspofungin. Plates were incubated at 30°C for 2 days and scanned or photographed.

In *S. cerevisiae* the ScYpk1/Ypk2 sphingolipid-mediated pathway is thought to function as a putative second cell integrity pathway, which cross-talks to the PKC pathway (Levin, 2005). Involvement of Sc*YPK2* in CF response was demonstrated by induced Sc*YPK2* expression upon CF exposure (Agarwal et al., 2003). Yeast cells lacking Sc*YPK1* grow slowly and show severe actin polarization defects. ScYpk2 and ScYpk1 are redundant kinases, both of which can be activated by ScPkh1 and ScPkh2, functional equivalents of the mammalian 3-phosphoinositide-dependent protein kinase-1 (PDK1) (Levin, 2005). Cellular targets of ScYpk1 and -2 are not clear but ScSmp1 may be a target of ScYpk1 (Roelants *et al.*, 2002). ScSmp1is related to the PKC pathway transcription factor ScRlm1.

Moreover, mutants affected in the calcineurin pathway displayed growth defects on CF-supplemented media. Lack of the transcriptional regulator *CRZ1* resulted in a severe defect on CF-supplemented media, cells lacking the catalytic calcineurin subunit *CNA1* displayed a slight growth deficiency (Figure 21). Calcineurin components may buffer for the cell wall stress exerted by CF, suggesting that inhibition of calcineurin signaling in *C. glabrata* may act synergistic with CF. This is consistent with studies in *A. fumigatus*, where inhibition of calcineurin signaling enhances the effect of cell wall inhibitors (Steinbach et al., 2007). In *C. albicans*, this synergistic effect influences the so-called paradoxical effect at high CF concentrations (Wiederhold et al., 2005).

A variety of other genes (*RPD3*, *CDC12*, *SEC13*, *CKB2*, *CUE1*, *YSR3*, *SPP1*, *ERG5*, *DUN1*, *YFH1*, *SEC13*,) implicated in various unrelated functions also showed CF sensitivity, indicating that the activity of many different genes is necessary for a full response to CF.

Comparison of our list of CF-sensitive mutants with the data set of a CF sensitivity screening, using the *S. cerevisiae* deletion strain collection, revealed only a small overlap of genes (Lesage *et al.*, 2004). The *fks1*Δ, *slt2*Δ, *mnn10*Δ mutants were found in both data sets to be sensitive to CF. Some other genes (Cg*ERG5* and Sc*ERG6*, Cg*SNF6* and Sc*SNF2*, Cg*CKB2* and Sc*CKA2*) found in both sets are implicated in corresponding functional pathways. Interestingly, two genes displayed different sensitivity patterns. The lack of *CRZ1* and *WSC1* resulted in CF susceptibility of *C. glabrata* mutants, while in *S. cerevisiae* the mutants were more resistant. Unexpectedly, the chitin synthase mutants showed no growth defect on CF-supplemented plates. In *S. cerevisiae* it was shown that cell wall stress leads to upregulation of chitin synthesis and deletion of chitin synthases results in CF hypersensitivity (Lesage et al., 2004).

Comparison of our data set to an expression profile analysis in *S. cerevisiae* exposed to CF showed an overlap of several genes as well (Agarwal et al., 2003). PKC pathway genes (*SLT2*, *RLM1*) and several cell wall genes were identified in both studies. The overlap between the *C. glabrata* set and a data set of the genomic response to CF in *C. albicans*

gave only two similarly regulated genes, *ERG5* and a glucan synthase subunit (Liu *et al.*, 2005).

5.4.4 Azole susceptibility

Reduced susceptibility to azole drugs is considered one of the major virulence factors of *C. glabrata*. Its resistance is mediated by upregulation of the ABC transporter genes *CDR1* and *PDH1*. These genes are controlled by the transcription factor Pdr1 (Sanglard et al., 1999, Miyazaki *et al.*, 1998, Izumikawa *et al.*, 2003, Vermitsky & Edlind, 2004).

To determine which genes further contribute to the decreased susceptibility of *C. glabrata*, we screened the mutant strain collection to commonly used antifungals in liquid medium containing either 6 µg/ml Fluconazole or 100 ng/ml Voriconazole, using an endpoint dilution assay in a 96-well microtiter plate format. The optical density was determined after 24 and 48 hours of incubation at 30°C. Strains showing reduced growth of more than 50 % when compared to the wild type control were scored and rescreened in triplicates. Positive hits were used to perform a broth microdilution assay to determine the IC_{50} as described in Material and Methods.

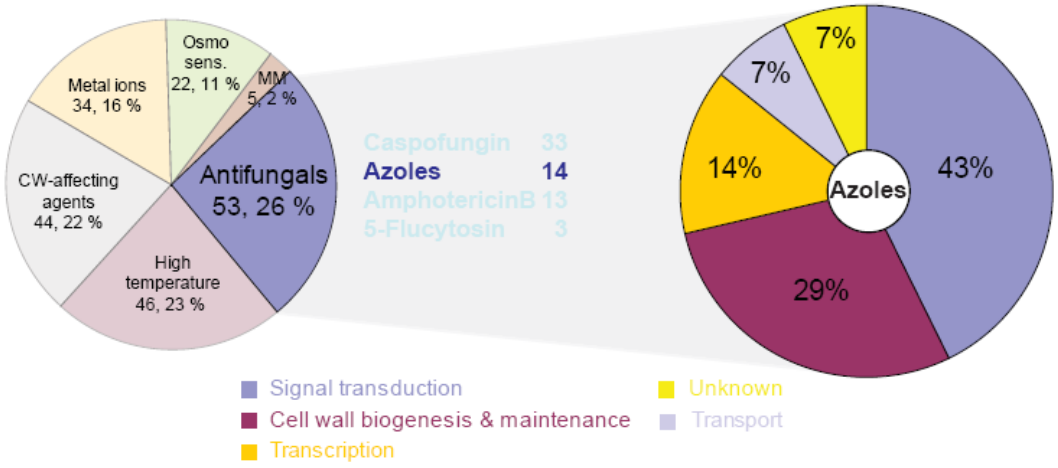

Figure 22. Distribution of azole-susceptible mutants. Gene annotations were assigned as in Figure 18. A total of 14 mutants displayed azole susceptibility (fluconazole, voriconazole), which differ largely from the set of genes found to be sensitive to CF, AMB, and 5FLU.

As expected, deletion of *PDR1* and *CDR1* resulted in a severe growth deficiency of the mutants exposed to azole stress (Figure 23 and 15B) (Sanglard et al., 1999, Vermitsky et al., 2006). A strain lacking *PDH1* (*CDR2*) was not susceptible, which is consistent with the data that Cdr1 is more potent to confer azole resistance (Sanglard *et al.*, 2001).

We identified four cell wall mutants (*ktr2*Δ, *cwh41*Δ, *ssd1*Δ, *ktr6*Δ) with intermediate sensitivity to azoles (Figure 23B). This suggests that azole inhibition of ergosterol biosynthesis affects the cell wall due to perturbation of the fungal plasma membrane. Thus, inhibition of ergosterol biosynthesis may act synergistic with certain cell wall defects, perhaps because a perturbed cell wall facilitates the access of azoles to the plasma membrane.

A

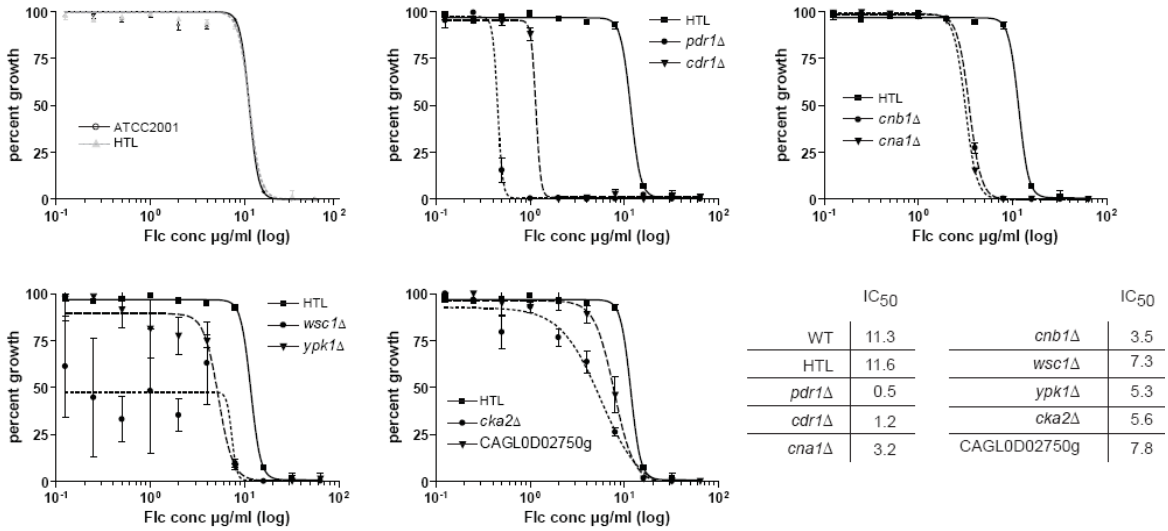

	IC_{50}
WT	11.3
HTL	11.6
pdr1Δ	0.5
cdr1Δ	1.2
cna1Δ	3.2

	IC_{50}
cnb1Δ	3.5
wsc1Δ	7.3
ypk1Δ	5.3
cka2Δ	5.6
CAGL0D02750g	7.8

B

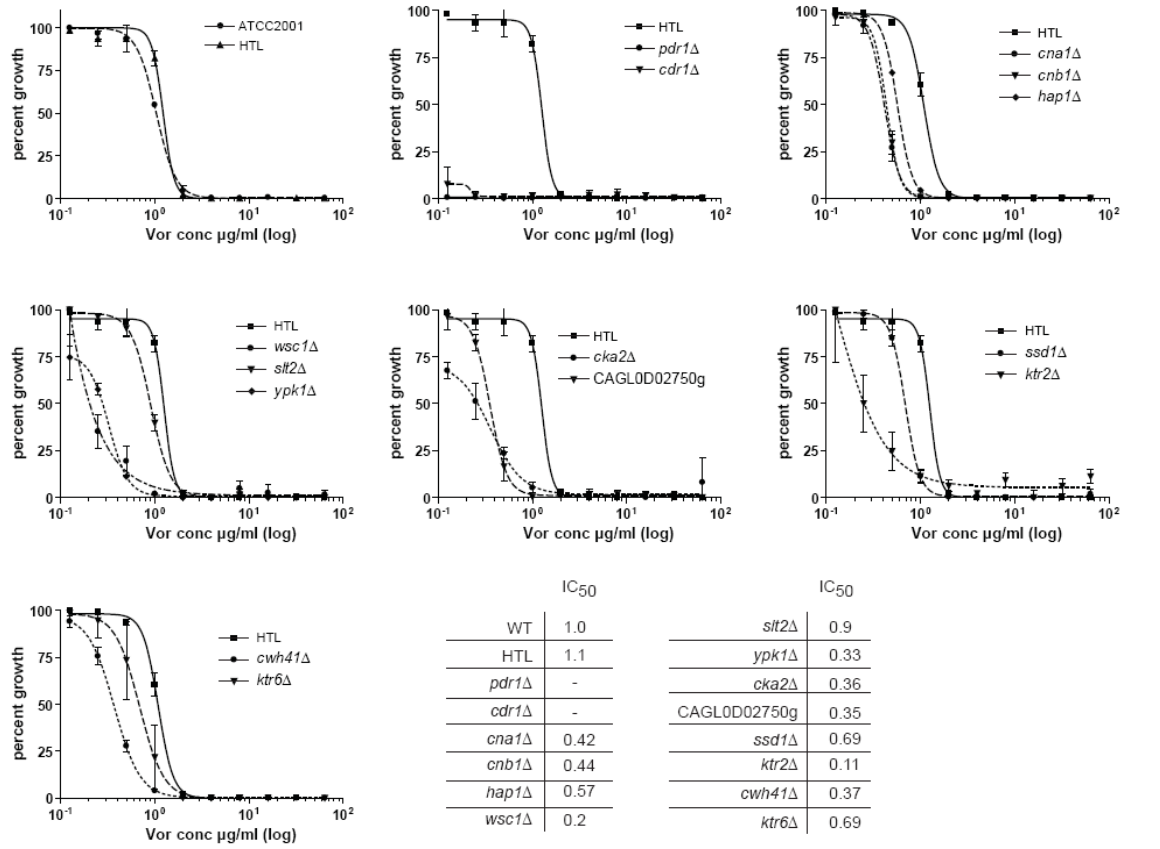

	IC_{50}
WT	1.0
HTL	1.1
pdr1Δ	-
cdr1Δ	-
cna1Δ	0.42
cnb1Δ	0.44
hap1Δ	0.57
wsc1Δ	0.2

	IC_{50}
slt2Δ	0.9
ypk1Δ	0.33
cka2Δ	0.36
CAGL0D02750g	0.35
ssd1Δ	0.69
ktr2Δ	0.11
cwh41Δ	0.37
ktr6Δ	0.69

Figure 23. Growth susceptibilities of *C. glabrata* mutants to azole derivatives. Susceptible strains identified in the primary screenings were subjected to IC_{50} determination. Overnight cultures were grown to OD_{600} of 1.0 and a microdilution assay was carried out in YPD to determine IC_{50} as described in Materials and Methods. The optical density (OD) of each well was determined at 600 nm on a microplate reader after 24 h and 48 h of incubation at 30°C. Each strain was tested in triplicates and mean values normalized to the untreated control were plotted against the antifungal concentration. The IC_{50} was calculated by nonlinear regression (curve fit), using GraphPadPrism. (A) Fluconazole, (B) voriconazole. Shown are data of 24 h measurement. Bars denote standard deviations.

Interestingly, several stress signaling mutants (*slt2*Δ, *wsc1*Δ, *ypk1*Δ, *cna1*Δ, *cnb1*Δ, *cka2*Δ) displayed also slight to intermediate azole sensitivities. Whereas *wsc1*Δ and *ypk1*Δ mutants showed intermediate susceptibilities to azoles, the *slt2*Δ strain was only very slightly affected. All three genes participate in cell wall integrity pathways, further indicating that azoles influence the cell wall integrity of *C. glabrata*.

Both calcineurin pathway mutants *cna1*Δ and *cnb1*Δ also displayed azole sensitivity, supporting the idea that several signaling pathways participate in the response to azole drugs. Recent data show that calcineurin inhibitors may have a synergistic effect with azoles in *C. glabrata* (Kaur *et al.*, 2004, Onyewu et al., 2003). The synergism between calcineurin inhibitors and azoles is also well-documented for *C. albicans* (Onyewu *et al.*, 2003, Sanglard *et al.*, 2003).

In addition, a strain lacking CAGL0D02750g displayed increased azole sensitivity. CAGL0D02750g is a gene of unknown function. Also a deletion strain lacking the zinc finger transcription factor gene *HAP1* was slightly sensitive to voriconazole. *S. cerevisiae* ScHap1 is involved in regulation of gene expression in response to oxygen and heme levels (Kwast et al., 1998).

5.4.5 Amphotericin B and 5-Flucytosine susceptibility

The polyene amphotericin B (AMB) interferes with membrane ergosterol, resulting in cell leakage due to perturbation of the plasma membrane (Akins, 2005). Some 13 mutants showed increased sensitivities to AMB (Figure 22 & 23). The most sensitive strains lack genes, which play diverse roles in phospho- and sphingolipid regulation (*ypk1*Δ), signaling (*cka2*Δ), transcriptional regulation (*dep1*Δ, *rox1*Δ, *snf6*Δ) and endocytosis (*vps15*Δ).

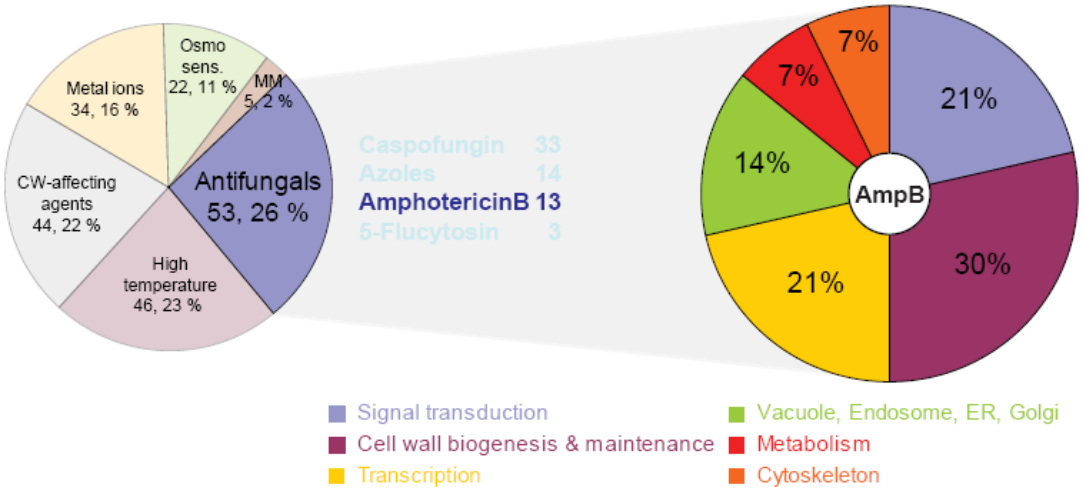

Figure 22. Distribution of amphotericin B-susceptible mutants. Gene annotations were assigned as in Figure 18. A total of 13 mutants displayed amphotericin B susceptibility.

The *vps15*Δ, *ypk1*Δ and *cka2*Δ strains showed the most pronounced susceptibilities (Figure 23). Deletion of *CKA2* in *C. glabrata* caused intermediate sensitivity to AMB. Cka2 is

the catalytical subunit of the casein kinase and plays a role in cell growth and viability (Ahmed *et al.*, 2002). Thus, *C. glabrata* Cka2 may function in general stress response needed for survival under plasma membrane stress conditions.

A mutant lacking *VPS15* was severely affected in growth on media containing AMB. Exposure to azoles or other drugs did not affect the *vps15*Δ mutant. Interestingly, the *S. cerevisiae* homologue of *VPS15* is involved in membrane trafficking, vacuole segregation and endocytosis (Stack *et al.*, 1995). Thus, *VPS15* may be essential for maintenance of the *C. glabrata* plasma membrane under AMB stress conditions. The *vps15*Δ deletion strain may be unable to counteract the perturbation of the plasma membrane caused by AMB due to a membrane trafficking defect.

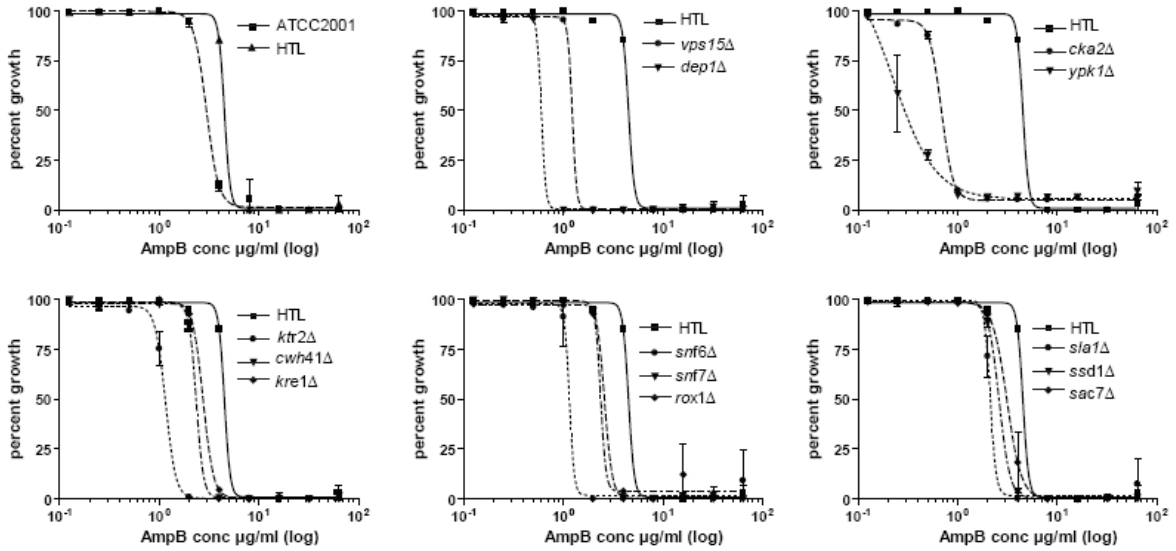

	IC_{50}
WT	3.0
HTL	4.5
vps15Δ	0.6
dep1Δ	1.2

	IC_{50}
cka2Δ	0.7
ypk1Δ	0.2
ktr2Δ	1.2
cwh41Δ	2.4

	IC_{50}
kre1Δ	2.8
snf6Δ	1.2
snf7Δ	2.6
rox1Δ	2.4

	IC_{50}
sla1Δ	2.1
ssd1Δ	2.6
sac7Δ	3.1

Figure 23. Growth susceptibilities of *C. glabrata* mutants to amphotericin B. Susceptible strains identified in the primary screening were subjected to IC_{50} determination. Over night cultures were grown to OD_{600} of 1.0 and a microdilution assay carried out in YPD to determine IC_{50} as described in Materials and Methods. The optical density (OD) of each well was determined at 600 nm on a microplate reader after 24 h and 48 h of incubation at 30°C. Each strain was tested in triplicates and mean values normalized to the untreated control were plotted against the antifungal concentration. The IC_{50} was calculated by nonlinear regression (curve fit), using GraphPadPrism. Shown are data of 24 h measurement. Bars denote standard deviations.

Three mutants (*acf2*Δ, *myo2*Δ, *npr1*Δ) were found in the 5'-Flucytosine (5FLU) screening. 5FLU is a DNA and RNA synthesis inhibitor. In the cell, 5FLU is converted into 5-fluorouracil and incorporated into RNA, leading to the disruption of protein synthesis (Ghannoum & Rice, 1999). In *S. cerevisiae*, genes implicated in sensitivity or resistance to 5FLU are involved in protein synthesis, DNA synthesis and DNA repair functions as identified by genome-wide expression profiling (Agarwal *et al.*, 2003).

The identified *C. glabrata* genes (*acf2*Δ, *myo2*Δ, *npr1*Δ) showed slight sensitivities only after 24 hours of growth. They are functionally unrelated and thus, might have to be studied in more detail to investigate their role in 5FLU sensitivity.

5.4.6 Growth on minimal medium

C. glabrata is able to colonize different host environments with variable supplies of nutrients. A mutant defective in metabolic functions may be impaired in establishing full virulence. Increased expression of metabolic genes after internalization by macrophages shows that *C. albicans* is able to adapt its metabolism to different host environments (Lorenz *et al.*, 2004). To test if some of the mutant strains depend on exogenous nutrient supply, we screened for growth on minimal medium.

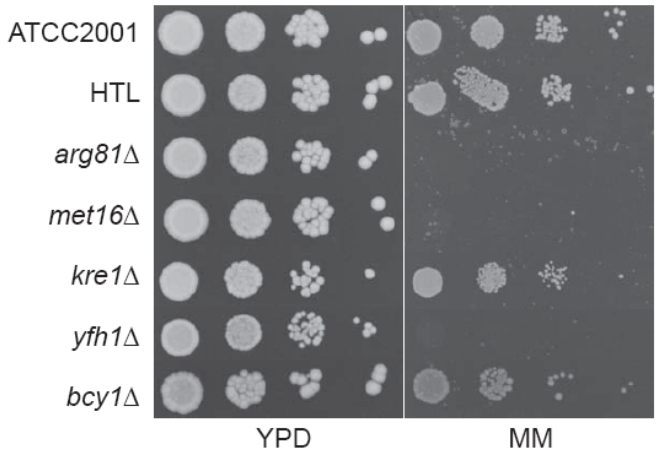

Figure 24. Growth on minimal medium.
Deletion strains were grown to OD_{600} of 1.0, serial diluted to OD_{600} of 0.1, 0.01, 0.001 and 0.0001 and spotted onto YPD agar plates and minimal medium plates (YNB, ammonium sulfate, glucose, Histidine, Leucine and Tryptophan). Plates were incubated at 30°C for 2 days and pictures taken with spImager system (S&P robotics, Canada).

Four strains (*arg81*Δ, *met16*Δ, *yfh1*Δ, *kre6*Δ) were unable to grow on minimal medium, and two showed slightly reduced growth (*bcy1*Δ, *kre1*Δ) (Figure 24). The deletion strains *arg81*Δ, *met16*Δ lack genes involved in arginine biosynthesis and methionine metabolism. These genes may have an influence on colonization of host niches with low nutrient availability or for survival in the nutrient-depleted phagosome. Cells impaired in certain metabolic reactions may fail in adapting to the harsh phagosomal conditions.

The identification of a *kre6*Δ mutant in this screen was likely due to its overall very slow growth phenotype and was not further tested.

5.4.7 Sensitivity to high osmolarity conditions

As a unicellular opportunistic pathogen, *C. glabrata* is also exposed to fluctuations in the osmolarity of the host environment. Depending on the colonization of a certain host niche (e.g. gastro-intestinal or urogenital tract) and the course of disease (*C. glabrata* in blood stream, organ colonization, phagosome), environmental parameters such as osmolarity are likely to change.

In *S. cerevisiae*, the HOG pathway is essential to adapt to high-osmolarity conditions. This canonical MAPK pathway mediates adaptation through regulation of intracellular glycerol levels (Gustin *et al.*, 1998). The two sensory branches ScSln1 and ScSho1 converge into one pathway, transmitting the signal to several transcription factors (Hohmann, 2002). Deletion of the MAPK Sc*HOG1* and the MAPKK Sc*PBS2* renders cells osmosensitive (Brewster et al., 1993).

To identify *C. glabrata* genes involved in the adaptation to hyperosmolarity, we screened the mutant collection against high concentrations of NaCl (1.1 M), yielding 22 NaCl sensitive strains (Table 16).

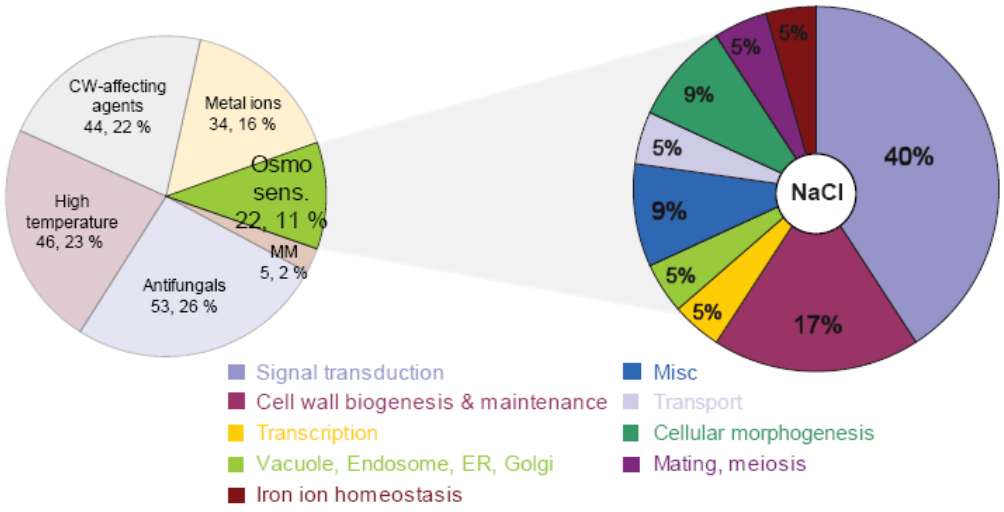

Figure 25. Distribution of osmosensitive mutants. Gene annotations were assigned as in Figure 18. A total of 22 mutants displayed growth defects on NaCl-supplemented media.

Deletion strains lacking homologous genes of the HOG pathway (*pbs2*Δ, *ste20*Δ, *ste50*Δ, *sho1*Δ) were unable to grow on NaCl-supplemented medium. A strong osmosensitive phenotype was also found for a mutant lacking the protein phosphatase *PTP2*, supporting the notion that the *C. glabrata* HOG pathway is indeed similarly regulated as the one in *S. cerevisiae*. ScPtp2 regulates ScHog1 localization in baker's yeast. Its overexpression suppresses the toxic effect of constitutively hyperactivated ScHog1 (Mattison & Ota, 2000, Wurgler-Murphy *et al.*, 1997). *PTP2* is essential for adaptation to osmostress of *C. glabrata* as the *ptp2*Δ deletion strain is inviable under salt stress conditions.

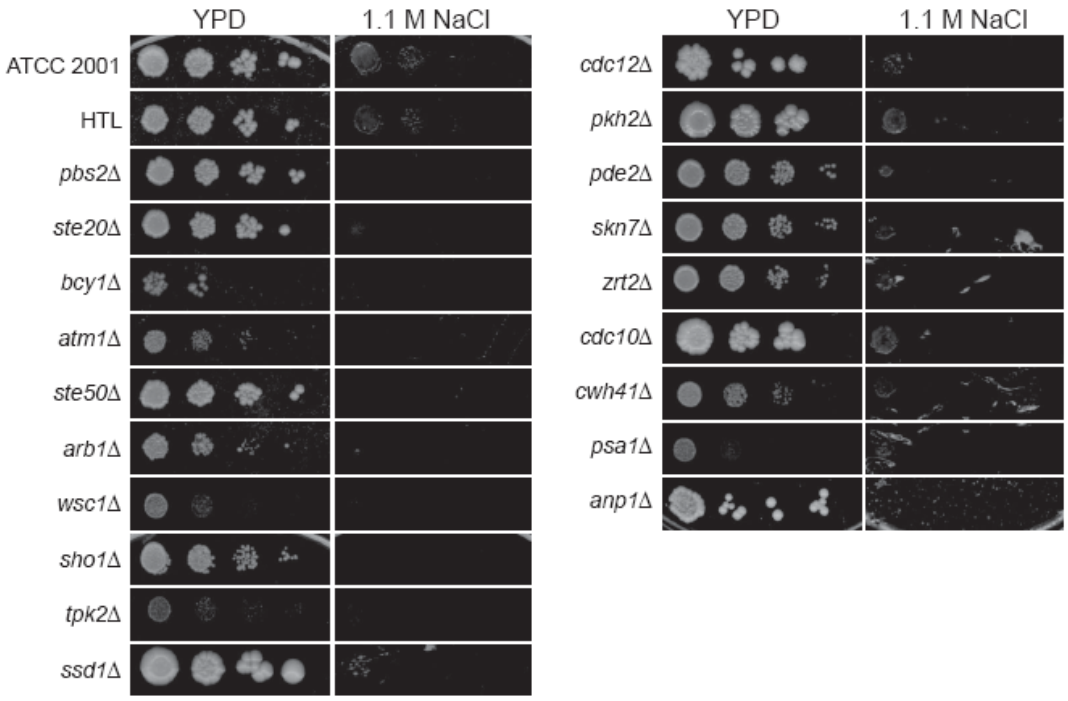

Figure 26. Osmosensitivity of *C. glabrata* mutants. Deletion strains were grown to OD_{600} of 1.0, serial diluted to OD_{600} of 0.1, 0.01, 0.001 and 0.0001 and spotted onto YPD and YPD agar plates supplemented with NaCl at the indicated concentrations. Plates were incubated at 30°C for 2 days and scanned for documentation.

The baker's yeast PKC pathway is also involved in sensing osmolarity changes, activating ScPkc1 in response to hypotonic shock (Davenport *et al.*, 1995). In contrast, we found that a *C. glabrata wsc1*Δ mutant is incapable to grow under high osmolarity conditions.

Other signaling pathway mutants (*bcy1*Δ, *tpk2*Δ, *skn7*Δ) showed also sensitivities to hypertonic conditions. In addition, several cell wall mutants were restricted in growth on NaCl, indicating that the weakened cell wall may not be able to compensate the stress exerted by hyperosmolar conditions.

In summary, most *C. glabrata* deletion strains with high osmolarity phenotypes lack genes, which have already been associated with osmoregulation in baker's yeast. This confirms that the high osmolarity stress response of *C. glabrata* is similar to *S. cerevisiae* (Gregori et al., 2007). However, osmosensitive *C. glabrata* mutants may exhibit altered virulence because of their inability to adapt to osmolarity changes in the host environment.

5.4.8 Sensitivity to metal ions

Several metal ions are essential trace elements for all organisms. Cu^{2+}, Co^{2+}, Zn^{2+}, Fe^{3+} and Mn^{2+} act as enzyme cofactors involved in a variety of redox reactions. However, accumulation of these ions or heavy metals such as Cd^{2+}, Pb^{2+} and Hg^{2+} are toxic to cells, because they can interfere with biological or catalytical protein activity (Mendoza-Cozatl *et al.*, 2005, Dichtl *et al.*, 1997, Lapinskas *et al.*, 1996, Rosen, 2002). Accumulation beyond physiological concentrations of ions such as Ca^{2+}, perturbs the natural calcium ion

homeostasis, interfering with cell signaling and stress response (Kraus & Heitman, 2003). Therefore, organisms have developed several mechanisms to control metal ion homeostasis.

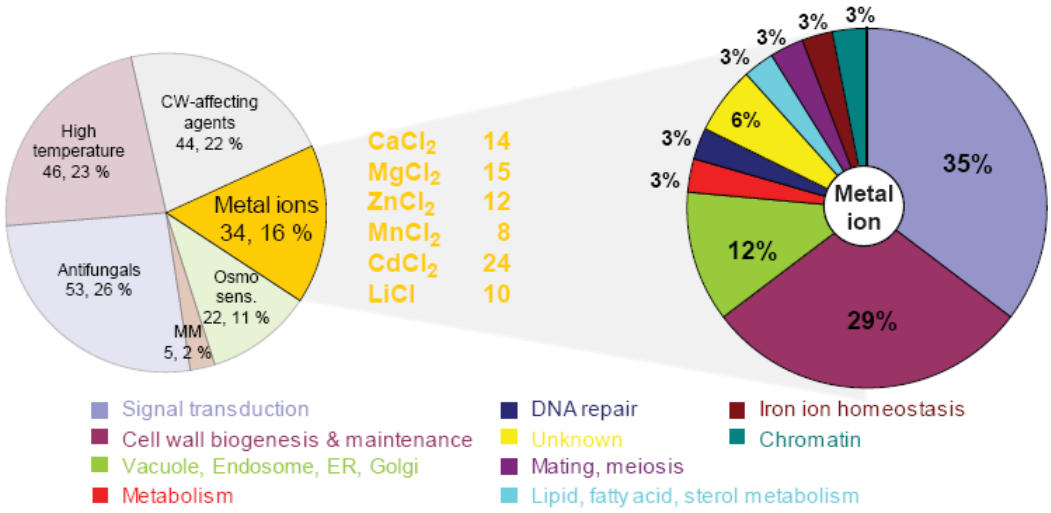

Figure 27. Distribution of metal ion-sensitive mutants. Gene annotations were assigned as in Figure 18. A total of 34 mutants displayed growth defects on various metal ion-supplemented media. A large number of strains was sensitive to $CdCl_2$ only and several showed overlapping sensitivities to NaCl stress.

To identify *C. glabrata* genes involved in tolerance to metal ion stress, the deletion strain library was screened for growth on high concentrations of various (heavy) metal ions, including $CaCl_2$, $MgCl_2$, $ZnCl_2$, $MnCl_2$, $CdCl_2$, and LiCl. Out of 49 primary hits, 34 strains were confirmed to be sensitive to the various ions (Table 16 & 17). Some 24 mutants were unable to grow on cadmium containing medium. Out of these, 10 strains showed cadmium sensitivity only, and were not inhibited by any other metal ion.

Many of these metal-ion sensitive strains lack cell wall biosynthesis genes. Osmosensitive *C. glabrata* mutants lacking *STE50*, *SHO1*, *PBS2*, *WSC1* and calcineurin showed additional growth deficiencies on media containing calcium, magnesium, zinc and lithium.

Deletion of the metabolic genes *PFK1* and *FAA2* led to severely reduced growth on any of the tested metal ions. Mutants lacking genes involved in vesicular transport processes (*PEP12*, *DID4*) also displayed decreased metal ion sensitivity.

CgORF	Gene	500 mM $CaCl_2$	600 mM $MgCl_2$	8 mM $ZnCl_2$	2 mM $CdCl_2$	40 mM LiCl	5 mM $MnCl_2$
CAGL0A04587g	*ALG3*				••		
CAGL0E06028g	*ALG5*				••		
CAGL0E02629g	*ALG6*				••		
CAGL0L01331g	*ANP1*	•••	•••	•••	•••		
CAGL0L11528g	*BIG1*				•••		
CAGL0G02035g	*CKA2*		••				
CAGL0I00946g	*CKB2*				•••		
CAGL0L11110g	*CNA1*	••					
CAGL0L00605g	*CNB1*	••			•••		
CAGL0K02827g	*DID4*			•••			
CAGL0H09460g	*FAA2*	•••	•••	•••	•••	•••	•••
CAGL0I06138g	*FAR1*	••	••				•
CAGL0M05841g	*KTR2*				•••		
CAGL0B03025g	*LAS21*				•••		
CAGL0D02442g	*LEM3*			••			
CAGL0E01683g	*MCK1*				•••		
CAGL0K11231g	*MNN10*		•		•••		
CAGL0G06864g	*MPS3*	•••	•••	••			
CAGL0A01892g	-				•••		
CAGL0D02750g	-					•••	
CAGL0J08569g	*OST3*				•••		
CAGL0L05632g	*PBS2*	•••	•••		•••		
CAGL0I01012g	*PEP12*	••	•	•••	•••		
CAGL0F08041g	*PFK1*	••	••	•••	•••	•••	•••
CAGL0L02827g	*PTP2*	•••	•••		•••	•••	•••
CAGL0K06963g	*ROT2*				•••		•
CAGL0B01441	*RPD3*				•••		
CAGL0G03597g	*SHO1*	•••	•••	•••	•••	••	
CAGL0D01936g	*SNF7*	•••	••	••			
CAGL0B00858g	*STE50*	•••	•••	•••		•••	
CAGL0D03146g	*SYS1*					••	•••
CAGL0F01507g	*WSC1*	••	•••	••	•••	•••	••
CAGL0M05643g	*YFH1*		•••		••	•••	
CAGL0K03399g	*YPK1*			••	•••	•••	••
Total	**34**	**14**	**15**	**12**	**24**	**10**	**8**

Table 17. Summary of metal ion-sensitive *C. glabrata* mutants. Cells were spotted on medium supplemented with metal ions at the indicated concentrations and incubated for 48 hours at 30°C. Plates were scanned with a HP scanner. Dots correspond to ••• pronounced, •• intermediate or • slight growth defect. Blue labelled genes were only sensitive to $CdCl_2$.

The mitochondrial matrix iron chaperone *YFH1* is implicated in cellular iron homeostasis (Foury & Talibi, 2001). Deletion of the *C. glabrata* homologue renders cells sensitive to Mg^{2+}, Cd^{2+} and Li^{+}, suggesting that it probably influences also metal ion homeostasis. Its essential role in de novo Fe/S cluster biogenesis (Gerber *et al.*, 2003) makes it an interesting candidate to analyse its survival in macrophages.

In summary, many mutants were extremely sensitive to the heavy metal cadmium, probably due to its pleiotropic toxicity. Osmosensitive mutants were clearly affected by several ions, which change osmolarity and interfere with associated signaling pathways.

Thus, the ion composition of the environment influences the viability of *C. glabrata* and may possibly modify also its virulence properties.

5.5 Phenotypic switching

The virulence of *C. albicans* has been associated with the ability to switch between different morphologies (Berman & Sudbery, 2002). In response to different stimuli, *C. albicans* is able to switch between these morphological forms (hyphae, pseudohyphae, yeast) (Sudbery *et al.*, 2004). In addition, *C. albicans* has to undergo the white-opaque transition to become mating competent (Miller & Johnson, 2002, Slutsky *et al.*, 1987). Moreover, opaque cells are more efficient in colonizing the skin, while white cells are more virulent in a mouse model of systemic infection (Kvaal *et al.*, 1999).

Phenotypic switching in *C. glabrata* has been implicated in virulence just recently (Lachke *et al.*, 2000, Srikantha et al., 2008). On $CuSO_4$-containing media four different core switching phenotypes of wild type cells can be distinguished: white (Wh), light brown (LB), dark brown (DB) and very dark brown (vDB). The core switching phenotypes can also be differentiated by growth on medium supplemented with phloxine B, where Wh cells stain dark pink and vDB cells white (Lachke *et al.*, 2002).

Interestingly, DB cells are more prevalent in natural isolates. It has been demonstrated that these cells have a competitive advantage over other switch phenotypes and may even be more virulent (Srikantha et al., 2008). Differential expression of genes in DB versus Wh cells include sulphur metabolism, copper assimilation and stress response genes (Srikantha *et al.*, 2005). Furthermore, evidence exists that different switch phenotypes are able to colonize different host niches (Brockert *et al.*, 2003).

For identification of new virulence-associated genes related to this phenotypic switching, the mutant collection was screened for phenotypic differences on $CuSO_4$-containing media. Most of the strains stained DB after four days of growth at 25°C. Due to the robotic primary screening, it was only possible to distinguish between clear differences (i.e. Wh or DB). This way, we scored for white colonies only, identifying a large number of mutants in the primary screening. Dilutions of these strains were then plated on $CuSO_4$ and phloxine B medium for further analysis. We identified 17 strains, which predominantly did not stain brown and thus, showed staining patterns different from wild type colonies (Figure 28).

Colonies of the wild type ATCC2001 cells and the triple-auxotrophic background strain stained predominantly DB on $CuSO_4$ and as expected, light pink on phloxine B. Importantly, all but three strains showed only one phenotype as assessed by growth on $CuSO_4$ medium and did not switch between the different phenotypes. Strains lacking *BCY1* and *ARG81* showed a LB phenotype, whereas on phloxine B medium, they stained medium to light pink. This is similar to the staining pattern of wild type cells.

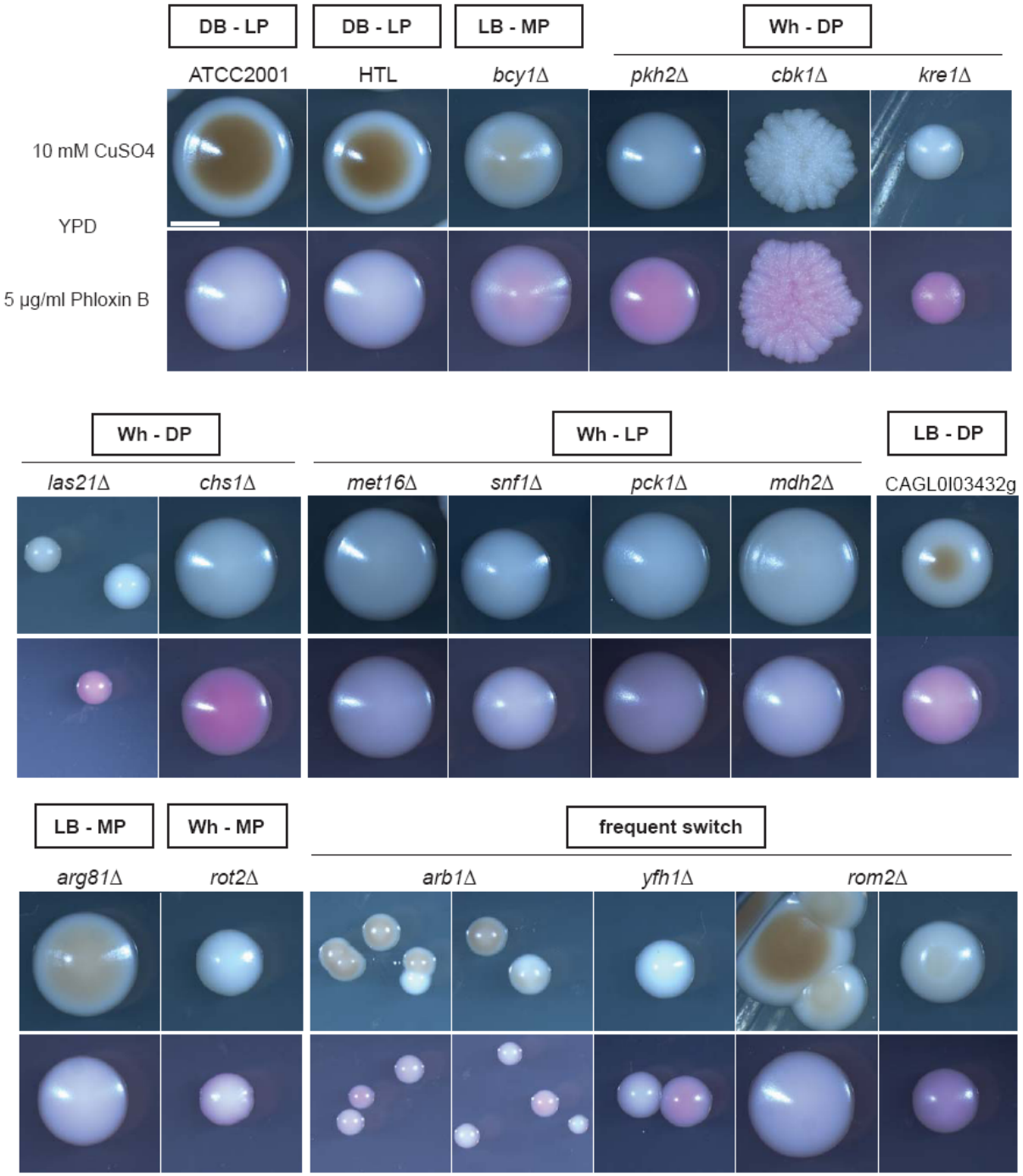

Figure 28. Switching phenotypes of *C. glabrata* deletion strains. Primary screening on 1mM $CuSO_4$-containing plates scored for Wh colonies. Overnight cultures of the strains were grown to OD_{600} of 1.0, diluted to 500 cells per ml and 100 µl were plated on YPD plates containing 1 mM $CuSO_4$ or 5 mg/l phloxine B. Plates were incubated at 25°C for 4 days and colony pictures were taken with a Zeiss Axio Stereomicroscope (9 x magnification). Core switching phenotypes are white (Wh), light brown (LB), dark brown (DB) and very dark brown (vDB) (Lachke et al., 2002). Growth on Phloxine B results in an inverse staining, Wh cells stain dark pink (DP), LB stain intermediate (MP), DB stain light pink (LP) and vDB cells do not stain pink. ATCC2001 and the background strain HTL stain DB and conversely, light pink.

Single colonies of five strains (*pkh2*Δ, *cbk1*Δ, *kre1*Δ, *las21*Δ, *chs1*Δ) exclusively displayed a Wh phenotype on $CuSO_4$ medium and dark pink on phloxine B. No switching to another phenotype was observed. Remarkably, all genes are implicated in cell integrity signaling, cell wall biogenesis or morphogenesis. Also a *rot2*Δ strain displayed a different

phenotype (Wh colonies on $CuSO_4$ but medium pink on phloxine B). Thus, an intact cell wall may be involved in the determination of the switching phenotype.

Mutants lacking *MET16, SNF1, PCK1* and *MDH2* showed Wh colonies on $CuSO_4$ and light pink on phloxine B. All plated colonies of these deletion strains were white on $CuSO_4$. Phloxine B stained colonies were only light pink, which differs from the expected staining of wild type colonies (DB and LP). Interestingly, several phenotypic Wh deletion strains lacked metabolic genes (*ARG81*, *MET16*, *PCK1*). This is in agreement with an earlier study, demonstrating that several metabolism genes are upregulated in DB versus Wh cells (Srikantha et al., 2005).

A strain lacking CAGL0I03432g showed LB and DP colonies. CAGL0I03432g has no homologue in *S. cerevisiae*. Finally, strains lacking *ARB1*, *YFH1* or *ROM2* displayed many differently stained colonies, suggesting that they frequently switch phenotypes.

Since wild type *C. glabrata* cells display a specific switching frequency it will be of importance to determine the switching frequency of the mutants compared to wild type cells to give a detailed statement about the influence of the single genes on the switching phenotypes.

5.6 Phenotypic differences in cell shape, size and colony morphology

Mutants that showed different fitness or slow growth on YPD were investigated more closely for phenotypic differences in colony and cell morphology. Five types of distinct cell morphologies different from the wild type were found. Wild type cells grew as typically ellipsoidal budding yeast (Figure 29a). Some mutants formed cell chains, others large cell clumps or showed defective budding patterns and irregular growth size. Again other mutants formed regular sized but round cells. Some mutants grew in a very large and round cell morphology (Figure 29).

The *bni1*Δ mutant showed a round cell morphology (Figure 29e). Formins are essential for the assembly of actin filaments and their deletion perturbs cytokinesis (Lew, 2002).

Deletion of the daughter cell-specific gene *DSE2* resulted in improper cell separation and formation of cell chains (Figure 29l). The colonies looked slightly wrinkled after a several days of growth. ScDse2 is a daughter cell-specific putative glucanase involved in mother-daughter cell separation (Colman-Lerner *et al.*, 2001).

Similarly, *tos6*Δ mutants had cell separation defects, displaying a pseudohyphal growth and causing colonies to show a slightly wrinkled morphology (Figure 29k). Tos6 of *S. cerevisiae* is a GPI-anchored cell wall protein (Hamada *et al.*, 1998).

Cells of the *kre6*Δ mutant were round, showed indications of cell lysis and were much larger than wild type cells (Figure 29h). Indeed, growth of *kre6*Δ mutants is severely affected,

which was also seen by its very slow growth phenotype. ScKre6 is required for synthesis of β1-6 glucans and also displays a round cell shape. However, no such severe growth defect is described in a *S. cerevisiae* Sc*kre6*Δ mutant (Roemer & Bussey, 1991).

C. glabrata cells lacking *KRE1* were unable to separate properly and displayed budding defects (Figure 29g). ScKre1 is a glycoprotein involved in β -glucan assembly (Boone et al., 1990).

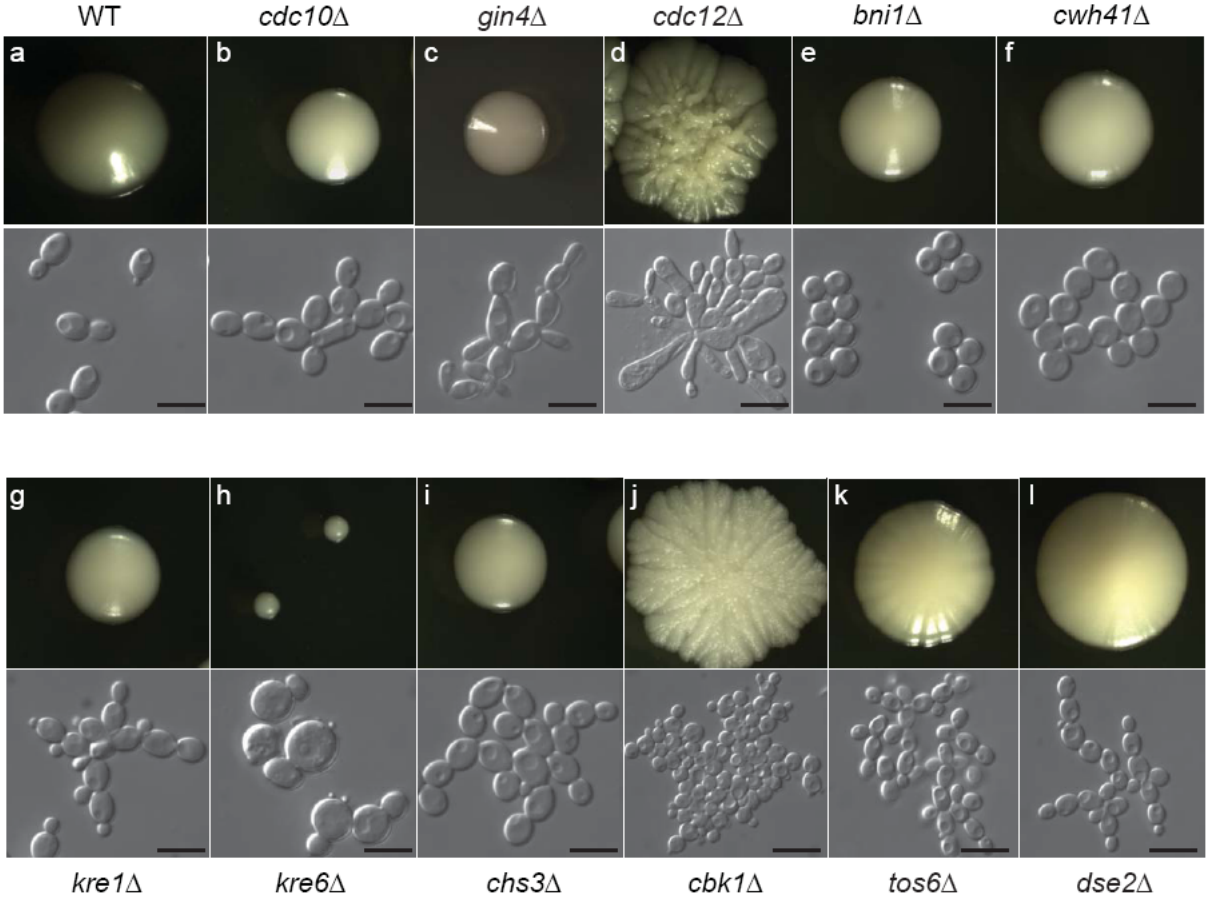

Figure 29. Colony and cell morphologies of *C. glabrata* deletion strains. Five types of distinct cell morphologies and four different colony morphologies were found. Cell morphology classes: ellipsoid (a), chains (b, f, g, i, k, l), elongated (c, d), large clumps (j), round (e), large and round (h); colony morphologies: smooth (a, b, c, e, f, g, i), small (h), slightly wrinkled (k, l), wrinkled (d, j). WT = HTL background strain; colony pictures 9 x magnification, black bars correspond to 10 µm.

The cell wall mutants *chs3*Δ and *cwh41*Δ also displayed impaired cell separation and *cwh41*Δ cells grew as round cells (Figure 29f, i). *CHS3* encodes one of the chitin synthases (Pammer *et al.*, 1992). Cwh41 is a glucosidase, which is involved in β1,6-glucan assembly (Jiang et al., 1996).

Deletion of *CBK1* resulted in a cell aggregation phenotype (Figure 29j), which was very similar to an *ace2*Δ deletion strain (Kamran *et al.*, 2004). Some cells of the *cbk1*Δ mutant were very large (see Figure 30). The kinase ScCbk1 is part of the RAM network and controls morphogenesis, cell separation and polarised growth via the transcription factor ScAce2 (Nelson *et al.*, 2003).

Deletion of the *C. glabrata* septin homologues of Sc*CDC12*, Sc*CDC10* and Sc*GIN4* resulted in cells unable to separate properly, often forming very long cells (Figure 29b, c, d). Septins are essential for septum formation and influence cytokinesis (Gladfelter *et al.*, 2001). The lack of *CDC12* led to a very pronounced morphology. The cells looked malformed, showed elongated shapes and uncontrolled budding, thereby forming large cell aggregates. This severe growth defect was also reflected in the heavily wrinkled colony morphology (Figure 29d). Interestingly, a second homologue of Sc*CDC12* is found in *C. glabrata*. Deletion of this ORF (CAGL0A02552g) has no influence on cell separation or growth (data not shown).

Not unexpected, most of the mutants displaying morphological defects, were sensitive to a variety of different growth conditions, mainly affecting the cell wall (Figures 17, 19, 21, 26).

To investigate the altered cell morphologies in more detail, the mutants were treated with Calcofluor White to visualize the chitin distribution in the cell wall. Chitin mainly localizes to the bud scars and bud necks, and only little to the lateral cell wall. The *kre6*Δ, *kre1*Δ, *cwh41*Δ, *dcw1*Δ, *fks1*Δ and *dse2*Δ mutants showed increased chitin levels (Figure 30). All six mutants have defects in glucan synthesis and play a role in cell wall assembly and maintenance. Chitin probably compensates for the lack of other essential cell wall components such as glucans to assure proper growth. Therefore, increased integration of chitin into the cell wall confirms the cell wall defects of these mutants. The chitin distribution in the *cbk1*Δ and *cdc12*Δ cells appeared to be dislocalized, indicating a defect in correct targeting of chitin to its correct destination in the cell wall.

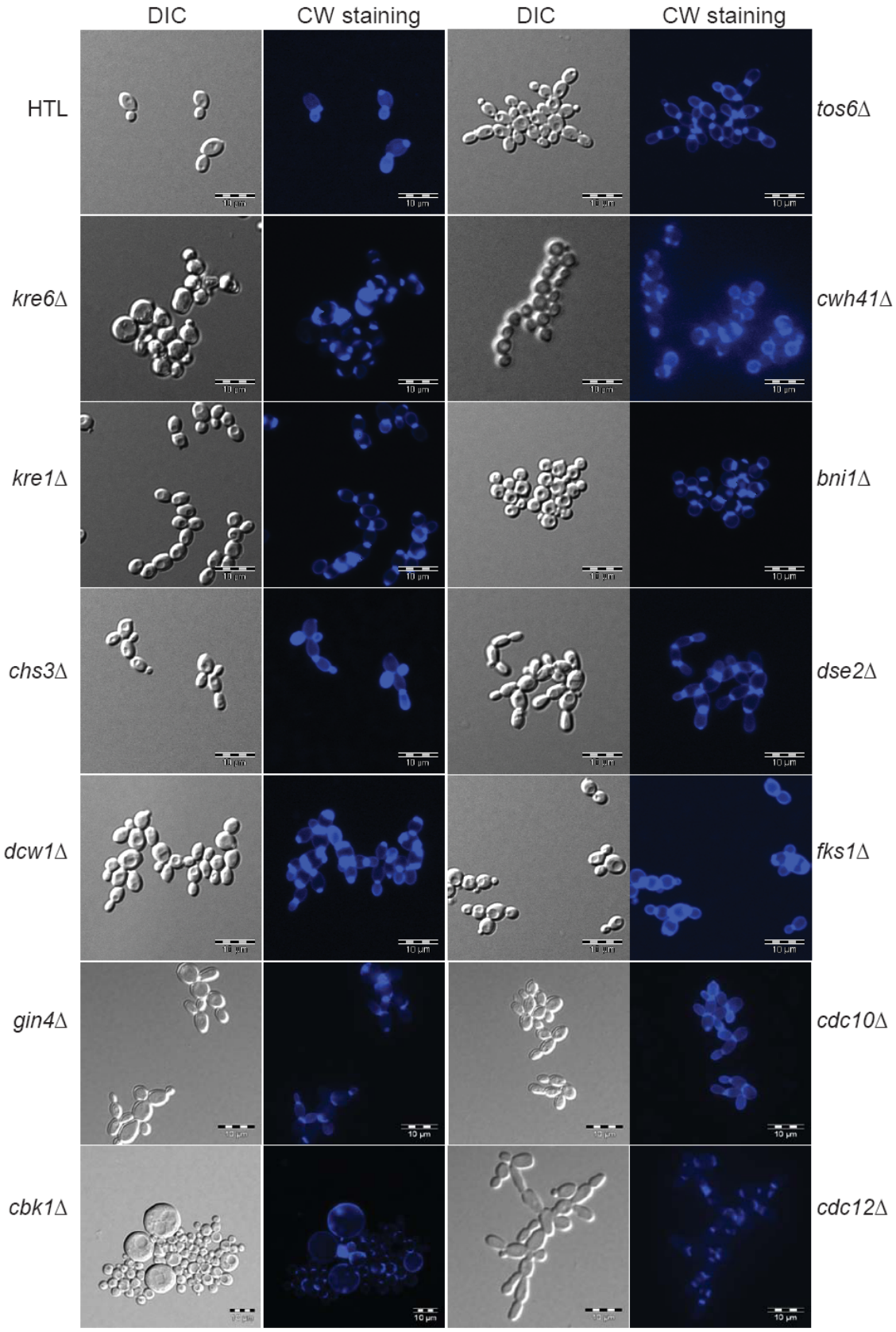

Figure 30. Chitin staining of *C. glabrata* cell wall mutants. Overnight cultures were grown to the early exponential growth phase and incubated with calcofluor white (CW) at a final concentration of 50 µg/ml in medium for 1 hour at room temperature in the dark. Cells were extensively washed twice with water, transferred to a microscopy slide and observed with a DAPI filter using the Olympus Cell R Life Imaging microscope (Olympus, Austria). Bars correspond to 10 µm.

5.7 *C. glabrata* mutants displaying phenotypes different from baker's yeast

The overall synteny and homology between the *C. glabrata* and *S. cerevisiae* genome is high. However, some studies revealed differences for several genes. For example, *C. glabrata* is a nicotinic acid auxotroph, because it lacks most of the *BNA* synthesis genes (Kaur *et al.*, 2005). Also genes of the galactose, phosphate, nitrogen and sulfate metabolism are lost in *C. glabrata* (Dujon et al., 2004). Moreover, genes with redundant functions such as Sc*SSK22*, Sc*PDR3* or Sc*MKK2* are not present in the genome (Gregori et al., 2007, Vermitsky & Edlind, 2004). Overall, it is estimated that several hundred genes are not shared between *S. cerevisiae* and *C. glabrata (Kaur et al., 2005)*.

One explanation for the gene reduction in *C. glabrata* is its close adaptation to its human host. This adaptation might also have led to the evolution of new genes by chromosomal rearrangements or gene duplications, which do not have any homologous *S. cerevisiae* genes. As shown recently, chromosomal rearrangements are indeed prevalent in clinical *C. glabrata* isolates (Polakova et al., 2009).

A prominent example of a gene family, which is absent in *S. cerevisiae*, are the *EPA* genes (Kaur et al., 2005). However, *EPA*-related genes of *S. cerevisiae* exist, such as the flocculin (*FLO*) genes. We included a total of 39 *C. glabrata* genes for deletion, of which no homologue has been identified in any of the post-whole genome duplication (WGD) organisms. In addition, 32 genes were identified, which have recently been duplicated in *C. glabrata* but lack the same duplication in *S. cerevisiae*.

Two of these *C. glabrata* ORFs showed growth defects in the large-scale phenotypic screenings. The deletion mutant lacking CAGL0D02750g displayed growth defects at increased temperatures, on Caffeine and LiCl-supplemented media and was susceptible to azole drugs (Figure 31A, B). The ORF encodes a small protein of 125 amino acid residues (MW=14.7 kDa) with a theoretical pI of 9.75. It shows a weak homology to myosin based on the homology to the myosin motor domain identified by a BLAST search. Using the Interpro database, a fatty acid binding motif was also found. From the phenotypic and the homology data together, on can speculate that the protein may function in an essential transport process (vesicular transport), putatively involved in plasma membrane maintenance.

A mutant lacking CAGL0A01892g was sensitive to caspofungin (Figure 31C). It encodes a small 88 residue protein located between an unspecified ORF and a gene coding for a homologue of Sc*TRA1*, which is a subunit of the SAGA and NuA4 histone acetyltransferase complexes (Grant *et al.*, 1998).

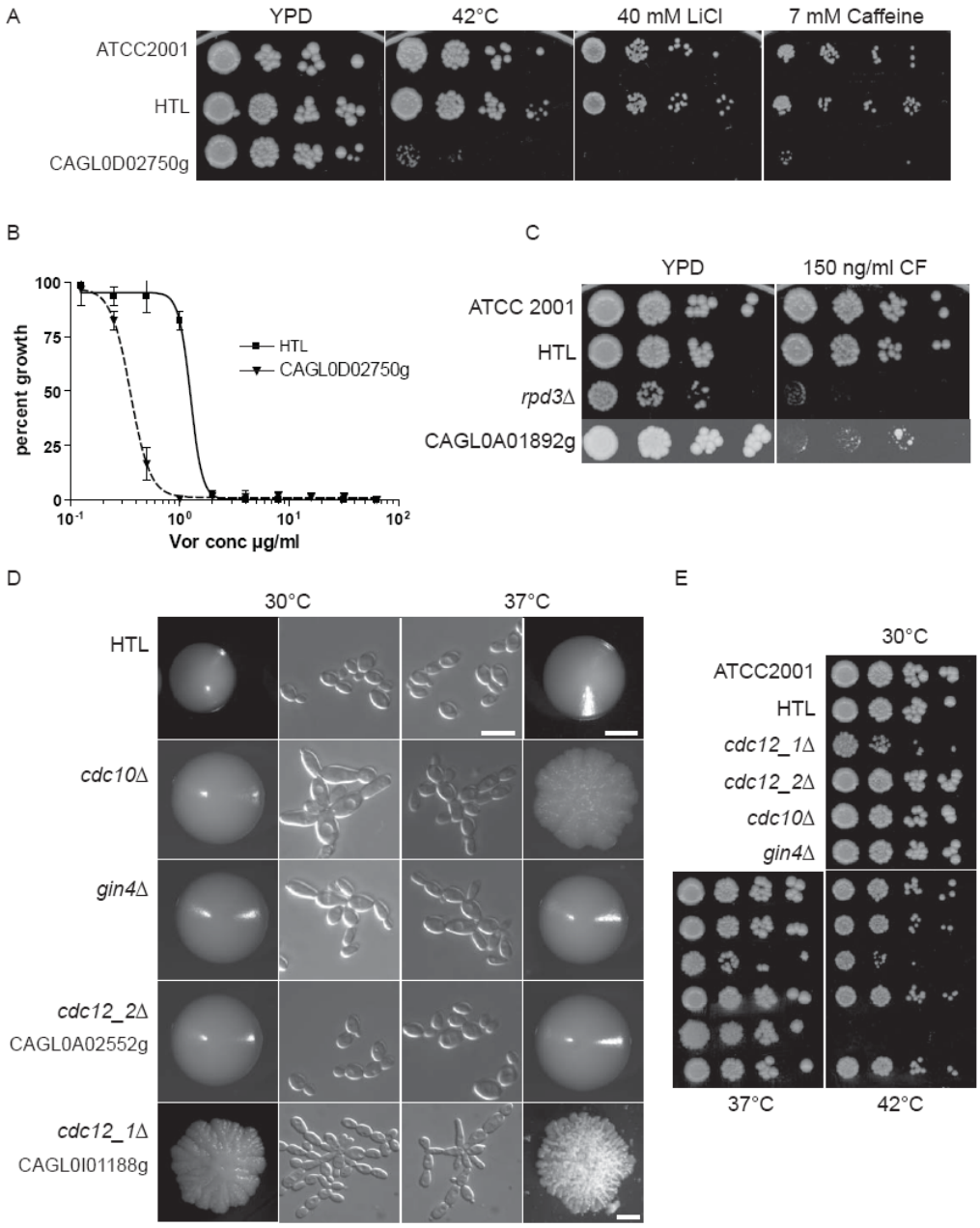

Figure 31. Growth phenotypes of mutants lacking *C. glabrata* specific genes. (A, C, E) Deletion strains were grown to an OD_{600} of 1.0, serial diluted to OD_{600} of 0.1, 0.01, 0.001 and 0.0001 and spotted onto YPD and YPD agar plates containing the indicated amounts of LiCl, Caffeine, caspofungin. Plates were incubated at 30°C, 37°C or 42°C as indicated for 2 days and scanned. (B) For IC_{50} determination of the mutant lacking CAGL0D02750g a broth microdilution assay was carried out, containing voriconazole concentrations as indicated and as described in Materials and Methods. (D) *C. glabrata* septin mutants were grown in YPD to OD_{600} of 1.0 at the indicated temperatures, washed twice with water before taking DIC pictures taken (Olympus CellR microscope).

Interestingly, a *C. glabrata rpd3*Δ mutant showed growth defects on CF (Figure 31C). *RPD3* of *S. cerevisiae* encodes a histone deacetylase involved in many processes, including transcriptional silencing, telomeric repression of transcription (Rundlett *et al.*, 1996), and modulating extension of life span in yeast (Kim *et al.*, 1999). Cells deleted for Sc*RPD3* are sensitive to cycloheximide (Colina & Young, 2005). Recently, it has also been implicated in the regulation of resistance to various antifungal drugs, including azoles but not CF (Borecka-Melkusova *et al.*, 2008).

Gene regulation by sirtuin-mediated transcriptional silencing is well-established for the *EPA* gene family and many adhesins are found in subtelomeric regions (Castano et al., 2005). As a transcriptional regulator, Rpd3 may also control the expression of cell wall-associated genes. Therefore, lack of Rpd3 may indeed result in reduced expression of cell wall genes essential to cope with CF stress. In addition, the downregulation of important cell wall genes may also explain the slow growth phenotype observed for the *rpd3*Δ deletion strain. Hence, the severe growth defect of a *rpd3*Δ mutant on CF-supplemented medium suggests an additional level of regulation of drug resistance in *C. glabrata*.

Finally, the *cdc12*Δ mutant was identified by the formation of heavily wrinkled colonies (Figure 31D, 29). The *cdc12*Δ strain lacks the homologue of the baker's yeast septin ScCdc12. Septins are a family of evolutionary widely conserved proteins required for cytokinesis by mediating septum and chitin ring formation, as well as recruitment of the necessary enzymes (Gladfelter *et al.*, 2001). With the exception of one gene (Sc*KCC4*), *C. glabrata* harbors all homologues of *S. cerevisiae* septin genes. Interestingly however, two *CDC12* homologues exist in *C. glabrata*. The lack of CAGL0I01188g resulted in cells incapable to separate properly and showing aberrant chitin localization, while deletion of the second ORF CAGL0A02552g did not affect cell morphology. The deletion of the septin genes such as *CDC12* and *CDC10* resulted in temperature-sensitive phenotypes (Figure 31E). Although the *gin4*Δ strain was not temperature-sensitive, it showed a similar defect in cell morphology. Hence, mutations in *C. glabrata* septin genes cause phenotypes similar to those found in *S. cerevisiae*, although regulation and function of the single genes may differ in *C. glabrata*.

In summary, *C. glabrata* harbors numerous genes, which do not have any obvious homologues in baker's yeast. Several of these genes have been identified in this study. Other genes show (partly) functional differences, which may have evolved due to the opportunistic lifestyle of *C. glabrata*. Alteration of gene function or evolution of novel genes may be a consequence of the adaptation to its human host.

5.8 *In vitro* macrophage-yeast interactions

Innate immune cells such as macrophages and dendritic cells are the first defence line against invading pathogens. Their recognition by specific pattern recognition receptors (PRRs) initiates defence mechanisms and phagocytosis of pathogens. One mechanism to fight pathogens upon interaction is the rapid production of reactive oxygen species (ROS) by immune cells. Different ROS species are thought to eliminate microbial cells (Missall *et al.*, 2004). However, to cope with oxidative stress, fungi as well as host cells express protective catalase and superoxide dismutases (SOD) (Chauhan *et al.*, 2006). Recently, our group demonstrated that *SOD5* of *C. albicans* is able to decay host-derived ROS and to escape the

oxidative burst exerted by the host. Using a chemiluminescent assay, it was possible to detect the accumulation of total ROS produced by macrophages infected with *C. albicans* (Frohner et al., 2009).

This assay was adapted to a 96-well microtiter format to screen the *C. glabrata* deletion strain library for mutants, which induce high accumulation of ROS in mouse bone marrow-derived macrophages (BMDM). We reasoned that mutants with altered cell walls or mutants lacking enzymes to counteract ROS may elicit accumulation of ROS. Wild type *C. glabrata* ATCC2001 cells and the triple-auxotrophic background strain HTL induced very low ROS accumulation, when compared to BMDMs stimulated with zymosan, a cell wall preparation of *S. cerevisiae*, or the different cell wall mutants (Figure 32A & B).

The screening revealed twelve mutants, which caused a higher accumulation of ROS than wild type cells. Ten mutants could be confirmed using the original ROS assay, testing each strain in triplicates (Figure 32A, D, E). Wild type *C. albicans* and zymosan served as positive controls for ROS induction. Interestingly, all identified strains lack cell wall genes. The lack of these genes leads to a defective cell wall or affects the cell morphology as shown by microscopic analysis. The identified genes comprised the septin genes *CDC10* and *CDC12*, the chitin synthase *CHS3*, the formin *BNI1*, genes involved in β-glucan assembly (*KRE1*, *KRE6*, *CWH41*, *DSE2*) and two GPI-anchored proteins (Dcw1, Tos6).

The *dse2*Δ, *tos6*Δ and *cdc12*Δ mutants were analysed in more detail (Figure 32C-F). All three deletion strains showed cell separation defects and it was difficult to compare the strains to the wild type by OD measurement (Figure 29). Therefore, we related the number of cells used for infection to the amount of DNA, which corresponded to the wild type inoculum ($4x10^5$ cells/well; MOI 10:1). Total ROS accumulation in the presence of either one of the mutants was higher than those due to wild type infection.

It is assumed that the NADPH-oxidase is assembled in the plasma or the phagosomal membrane (Hampton *et al.*, 1998). Therefore, ROS may be concentrated in the phagosome but can also be released into the environment. To discriminate the location of ROS accumulation, ROS was measured, using isoluminol (Frohner et al., 2009). In contrast to luminol, which detects total ROS in the system, the membrane-impermeable isoluminol detects extracellular ROS only (Lundqvist & Dahlgren, 1996). For all tested mutants, the extracellular ROS levels were lower than total accumulated ROS, indicating that extracellular ROS partly accumulated outside of the cells (Figure 32A).

To clarify if ROS was produced by the BMDMs or by the *C. glabrata* mutants, we used macrophages derived from *gp91phox*$^{-/-}$ mice. These mice lack an essential subunit of the NADPH oxidase required for ROS production (George-Chandy *et al.*, 2008). Thus, *gp91phox*$^{-/-}$ BMDMs can be used as a control to determine the source of ROS (Frohner et al., 2009). As expected, ROS could not be detected when the *gp91phox*$^{-/-}$ BMDMs were infected

with zymosan or the *C. glabrata* cell wall mutants, suggesting that a functional NADPH oxidase is required for ROS accumulation and that the detected ROS is mainly derived from the BMDMs.

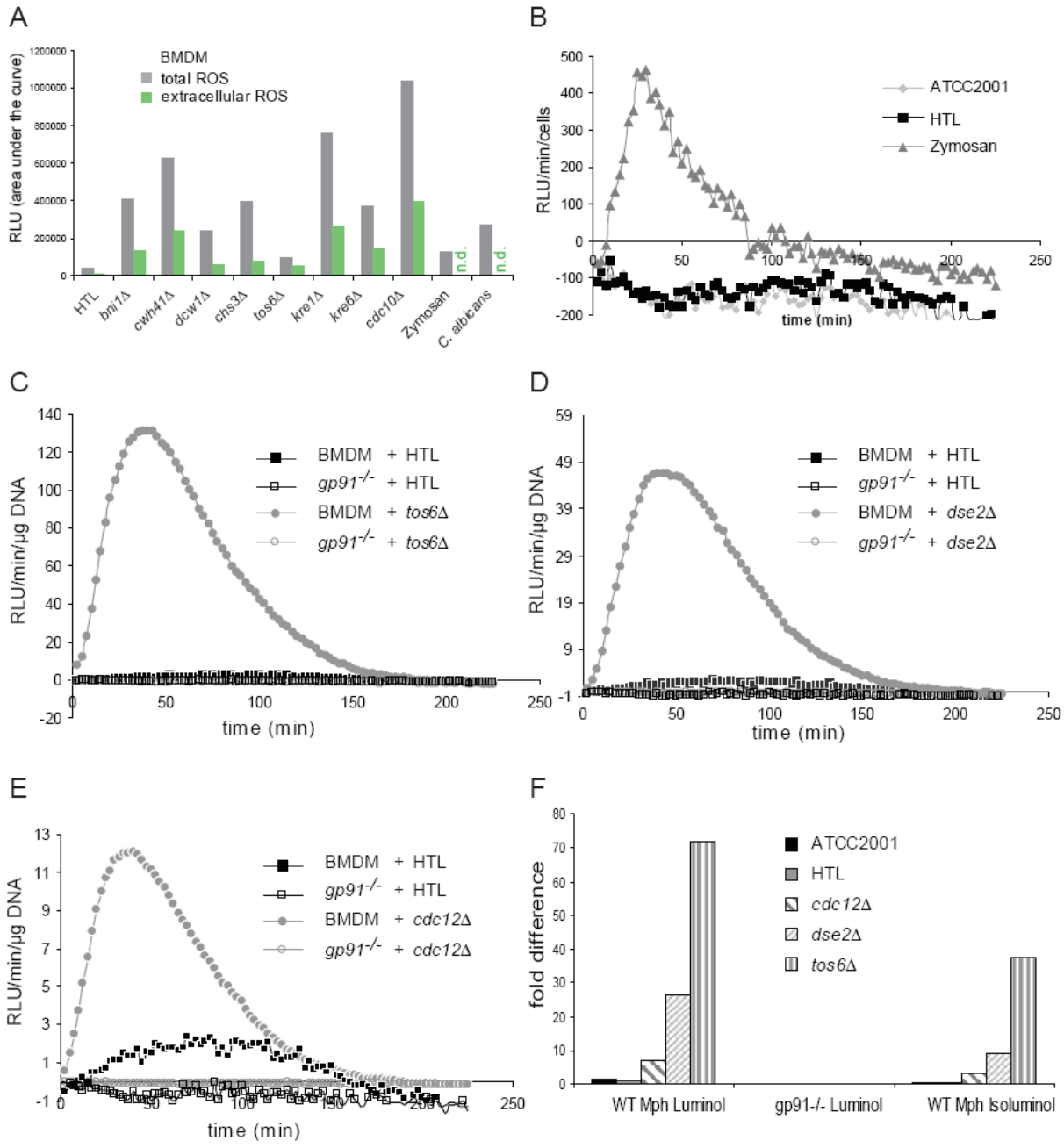

Figure 32. ROS accumulation upon incubation of wild type BMDMs with *C. glabrata* cell wall mutants. (A) Deletion strains of the primary screening inducing ROS in BMDM were retested (37°C in 2.5 min intervals over a 90 min period, MOI 10:1) in triplicates using the standard assay for luminol- and isoluminol-dependent chemiluminescence (Frohner et al., 2009). The area under the curve was calculated and plotted for each mutant. Zymosan (20 µg/well) and *C. albicans* (MOI 5:1) were used as positive controls. Examples of indicated deletion strains are shown in B – D. Stimulation of ROS production of wt BMDM or gp91phox$^{-/-}$ with *C. glabrata* HTL strain and isogenic mutants *tos6*Δ (B), *dse2*Δ (C), *cdc12*Δ (D) was measured with luminol-dependent chemiluminescence. Due to clumping/pseudohyphal cell phenotypes the RLU/min were referred to the amount of genomic DNA of the wild type HTL strain. (E) RLUs under the curve were calculated for B – D and fold ROS induction compared to the HTL strain were plotted.

In conclusion, it appears that changes in the cell wall composition lead to ROS accumulation, when *C. glabrata* interacts with host immune cells. These changes may lead

to exposure of certain cell wall constituents, which are recognized more easily by the PRRs of the macrophages, eliciting host defence mechanisms. Thus, the mutants identified by the ROS screening assay may be interesting for further *in vitro* and *in vivo* studies to determine their virulence potential.

6 Discussion

C. glabrata is the second most frequent human fungal pathogen, causing systemic candidiasis (Pfaller et al., 2008). Inherent resistance against azole drugs and a large repertoire of adhesins are major virulence attributes, yet the understanding of other basic molecular mechanisms regulating its pathogenicity remains elusive.

Systematic functional genomics represent a powerful tool to dissect the specific virulence traits of *C. glabrata*. In this thesis, I describe the exploitation of a new *C. glabrata* triple-auxotrophic for the generation of a gene deletion strain library as a tool to study fungal pathogenicity and drug resistance.

This strain is derived from the sequenced strain ATCC2001 and was used as the background strain for all gene deletions. It was decided to use a strain with three auxotrophies (*his3*Δ, l*eu2*Δ, *trp1*Δ), which should allow the engineering of single and double gene deletion mutants, while having markers left for complementation of the gene deletions. Because the use of an auxotrophic *URA3* marker influences the virulence properties of *C. albicans* (Brand *et al.*, 2004, Lay *et al.*, 1998), the introduction of the *ura3*Δ auxotrophy in the new *C. glabrata* background strain was avoided. I further demonstrate that the application of fusion PCR is suitable for the large-scale generation of disruption cassettes with long homology flanking regions, which enables sufficient efficiency for targeted gene deletion in *C. glabrata*. During the course of the work, a total of 476 *C. glabrata* gene deletion mutants were generated and phenotypically analysed. The phenotypic profiling of this deletion strain collection gives new insights in gene functions, differing from baker's yeast and reveals putative factors involved in drug resistance and virulence of *C. glabrata*.

Targeted gene deletion in *C. glabrata*. To understand the specific virulence factors of *C. glabrata*, targeted gene deletion is a suitable reverse-genetics approach. However, the gene targeting efficiency in this organism is much lower than in the model organism *S. cerevisiae*, which hampers this strategy. A few studies tried to circumvent these problems, using modified techniques such as the conditional expression of *YKU80* to reduce non-homologous end joining during transformation (Ueno et al., 2007). The use of long homology flanking regions was considered as the method of choice to be independent of the *YKU80* modification, which may have an unknown effect on the virulence properties of *C. glabrata*. Long homology flanking regions for more efficient gene replacement has also been successfully employed for gene deletion in *C. albicans*, (Noble & Johnson, 2005). Further, I decided to use the dominant marker *NAT1*, conferring resistance against nourseothricin. The *NAT1* marker has been proofed useful for gene disruption in several *Candida* spp., including *C. glabrata* (Shen et al., 2005).

Based on the results on recombination efficiency (Ueno et al., 2007), it seemed reasonable to use 500 bp long flanking homology regions to achieve proper gene targeting. Although 55% of the selected genes could be deleted successfully, it was not possible to obtain correct transformants for the remaining targeted genes, despite the preselection for non-essential *S. cerevisiae* homologues. Moreover, the efficiency seems to depend strongly on the targeted gene in spite of the use of long homology flanking regions.

For many genes a transformation efficiency of approximately more than 50% was achieved (i.e. every second transformant gave a positive signal in both colony PCR reactions), whereas for a number of genes the efficiency was as low as 1% or even none of the transformants was correct. Several explanations may exist for the differences in recombination efficiency. First, DNA repair and DNA regulatory mechanisms seem to be different in *C. glabrata* when compared to *S. cerevisiae*, including the machinery necessary for non-homologous end joining (Ueno et al., 2007). Second, illegitimate recombination (Cormack & Falkow, 1999) and chromosomal rearrangements (Polakova et al., 2009) are frequently observed in *C. glabrata*. For many transformants, only a single signal was detected in the colony PCR reaction, indicating that the deletion construct did not integrate correctly or replace the complete coding sequence. The reason for a partial integration remains unknown. Interestingly, a recent study reports that the *C. glabrata* genome is very dynamic (Polakova et al., 2009). The authors suggest that these events may be due to some sort of telomere dysfunction. The occurring chromosomal rearrangements include chromosome fusions, possible circularizations, nonreciprocal translocations and generation of novel chromosomes. Remarkably, they even speculate that *C. glabrata* might had to sacrifice its sexual life cycle to better tolerate these genome dynamics (Polakova et al., 2009).

In approximately 10% of the transformations, a very large number of small transformant colonies arose. None of these tested transformants was positive upon restreaking, although being able to grow on selective media. A possible explanation is that autonomously replicating sequences (ARS) are located on the flanking regions, resulting in the formation of episomal DNA (Castano *et al.*, 2003). Linear transforming DNA, containing ARS may recircularize after transformation and form episomes, giving rise to a high number of marker containing transformants. Eventually the episomes get lost because they lack a *CEN* sequence (Castano *et al.*, 2003). Shortening the flanking regions may result in a non-functional ARS, but at the expense of reduced recombination efficiency.

Interestingly, the choice of the marker gene may also influence the recombination efficiency. For some targets, the generation of a correct deletion strain was impossible, when using the *NAT1* marker construct. For example, repeated attempts to delete the glucan synthase gene *FKS1* failed with a *NAT1* disruption cassette. Using the auxotrophic *HIS3*

marker with the same flanking regions instead, resulted in several correct transformants lacking *FKS1*. Notably, many other putatively non-essential cell wall genes also could not be deleted. Likewise, deletion of *ACE2* was only successful, using a hygromycin B instead of the *NAT1* resistance marker. Thus, the choice of the marker gene may have an influence on the gene targeting efficiency in *C. glabrata*.

As shown by “loss-of-gene” PCR, not all nourseothricin resistant transformants, giving a positive signal in the colony PCR actually lost the coding sequence. This may be explained by replacement of the coding sequence by the deletion construct followed by a random genomic reintegration of the coding sequence somewhere else in the genome. Since it is not possible to control the reintegration, I decided to generate three independently verified transformants for every gene. The same phenotypes of all three independent transformants would additionally confirm that the gene replacement was successful. However, this implicates that the deletion strains should be checked by Southern analysis, before being used for follow-up studies. This was done for several mutants, proofing a very high number of transformants to be correct.

There is one caveat with the use of the triple-auxotrophic strain. As described recently, the *C. glabrata* ATCC2001 wild type strain carries a truncated *ssk2-1* allele, which interrupts one branch of the high osmolarity glycerol (HOG) pathway (Gregori et al., 2007). Thus, the triple-auxotrophic strain and all generated gene deletions in this background carry the *ssk2-1* mutation. The generation of the triple-auxotrophic *C. glabrata* strain for the deletion project was started before this mutation was identified. In consequence, every deletion strain generated by the project actually represents a double deletion strain and stress-related phenotypes may be due to synthetic genetic interactions. This is most important for the mutants displaying osmostress-related phenotypes but may also affect other mutants.

Phenotypic analysis of the deletion strain collection. A major goal was to identify factors, which contribute to the specific pathogenicity and drug resistance of *C. glabrata*. Applying a number of various *in vitro* phenotypic screens, I identified 103 gene deletion strains, displaying one or more different growth sensitivities. The largest groups of sensitive mutants were unable to grow at elevated temperature conditions, under CF or metal ion stress. Many of the identified genes show similar functions as observed for their homologues in *S. cerevisiae* or *C. albicans*. For instance, functions in chitin synthesis, cell wall integrity signaling and cell wall biosynthesis (Munro *et al.*, 2007, Reinoso-Martin et al., 2003, Lesage & Bussey, 2006, Levin, 2005). In general, the generated deletion strain collection shows a bias towards genes implicated in cell wall biogenesis, stress signaling and drug resistance, since I preselected these genes under the assumption that they may have an impact on

virulence and drug resistance of *C. glabrata*. It is thus not unexpected that a large number of cell wall and signaling mutants have been identified in the different screenings.

Growth defects of cell wall mutants. Many mutants display sensitivities to more than one stress condition. Among all 103 mutants, six mutants are striking because they are sensitive to more than six different tested growth conditions. These genes are involved in cell wall biogenesis and morphogenesis (*WSC1*, *CWH41* and *CDC12*) and/or signaling (*YPK1*, *TPK2* and *BCY1*). This indicates that the maintenance of the cell wall and stress signaling play an important role and are essential for *C. glabrata* to cope with various external stresses.

A number of mutants are affected in their growth by cell wall-perturbing agents such as CW, CR and SDS. Interestingly, the correlation between mutants sensitive to heat stress and one of the cell wall perturbing agents is quite high, while the overlap between mutants sensitive to cell wall-perturbing agents and CF-susceptible mutants is much lower. Only three *C. glabrata* mutants (*wsc1*Δ, *bcy1*Δ, *mnn10*Δ) display major growth deficiencies under CF or cell wall-perturbing stress conditions. In contrast, 14 mutants show sensitivities to temperature stress as well as stress exerted by cell wall-perturbing agents. Thus, similar cell wall constituents appear to be affected by heat or cell wall perturbing agents, while CF seems to affect a different set of genes. However, several strains display overlapping sensitivities to CF as well as temperature stress. Not unexpectedly, many deletion strains (*cwh41*Δ, *cbk1*Δ, *cdc12*Δ, *cdc10*Δ, *dse2*Δ) affected by cell wall-perturbing conditions display morphological differences, independently confirming cell wall-related defects.

Several *C. glabrata* cell wall mutants show sensitivities differing from the described phenotypes of the *S. cerevisiae* mutants. This may hint at differences in individual gene functions, although the cell walls of both organisms principally consist of the same basic components. Detailed studies of the functional differences may allow the identification of *C. glabrata* specific mechanisms.

The susceptibility of many cell wall mutants to CF establishes a chemical-genetic interaction between CF and several cell wall biogenesis genes of *C. glabrata*. The susceptibility of the mutants may be due to the inability to compensate cell wall defects when exposed to additional stresses, such as the inhibition of glucan synthesis. This view is confirmed by a recent study, showing that *C. albicans* mutants with thin cell walls are more sensitive to CF, while a thick cell wall renders cells more resistant (Plaine et al., 2008). The identification of cell wall genes also demonstrates a chemical-genetic interaction between CF and cell wall biogenesis genes (mannosylation, glycosylation) other than the known PKC pathway and glucan synthase genes. In addition, it has been shown that calcineurin signaling and the PKC pathway also synergize to regulate the cell wall-dependent stress response

(Steinbach et al., 2007, Wiederhold et al., 2005, Perlin, 2007). This notion is confirmed by the identification of a CF-sensitive *cna1*Δ mutant. The increased CF susceptibility of several cell wall mutants might serve as a basis to identify alternative drug targets. Novel compounds interfering with fungal-specific enzymes of the cell wall biogenesis may synergize with CF and potentiate its antifungal effect. Therefore, the identified cell wall biogenesis genes implicated in CF sensitivity may represent putative new drug targets.

***In vitro* macrophage and *C. glabrata* interactions.** Interestingly, the *C. glabrata* mutants, which stimulated high ROS accumulation when coincubated with BMDMs were cell wall-deficient strains. In contrast to these mutants, ROS induction by *C. glabrata* wild type strains with intact cell walls was very low. These observations support the hypothesis that certain cell wall components such as glucans and chitin are normally hidden from direct surface exposure in the wild type cells. These components may only be accessible to the pattern recognition receptors of the immune cells at certain sites, such as bud scars and bud necks (Gantner *et al.*, 2005). Alterations in the cell wall structure due to mutations in cell wall biogenesis or morphogenetic genes for example, can lead to increased exposure of cell wall constituents and consequently result in recognition of the fungal cell by the cells of the host immune system.

As observed for several mutants, some mutants display severe cell separation defects. Those mutants display altered morphologies, forming pseudohyphal structures or large cell clumps. Remarkably, most of the ten identified mutants, which induce ROS accumulation show these morphologies associated with cell separation defects. Thus, stimulation of ROS production may be triggered by the increased exposure of normally hidden cell wall components or by the abnormal size and appearance of the fungal cells.

Interestingly, BMDMs have problems to phagocytose the large cell clumps formed by the *cbk1*Δ and *ace2*Δ mutants (see *CBK1* manuscript). In addition, the *ace2*Δ mutant is hypervirulent and causes not only acute mortality but also drastically changed levels of the cytokines TNFα, IL-6 and IFNγ (Kamran et al., 2004). It has also been shown that large particles can not be internalized by macrophages (Hernanz-Falcon *et al.*, 2009). The inability to internalize large particles triggers a cytokine release in a Dectin-1-dependent manner. This shows the important role of phagocytosis in clearance and modulation of PRP signaling (Hernanz-Falcon *et al.*, 2009). Therefore, it may be interesting to study phagocytosis of the *C. glabrata* mutants and the cytokine release of the immune cells, inducing ROS accumulation, *in vitro* and *in vivo*. The exposure of otherwise inaccessible cell wall components of the cell wall mutants may facilitate the recognition by and stimulate the phagocytosis by immune cells. If the mutant cells can not be internalized due to size

restrictions, this may finally not result in clearance but rather in a dramatic cytokine release, leading to septicemia as it was observed for the *ace2*Δ mutant (Kamran et al., 2004).

A small number of mutants were unable to grow on minimal medium. These strains are affected in certain metabolic genes. The inability to grow under nutrient-depleted conditions certainly affects the virulence capabilities of a fungal pathogen. Studies in *C. albicans* demonstrated that the expression of metabolism genes changes upon internalization by macrophages. For example, the expression of glyoxylate, gluconeogenic and fatty acid metabolism genes increased in fungi recovered from phagocytic cells (Barelle *et al.*, 2006, Fernandez-Arenas *et al.*, 2007, Lorenz *et al.*, 2004). Identified genes include arginine biosynthesis genes and the mitochondrial matrix iron chaperone *YFH1* (Lorenz et al., 2004). Notably, Yfh1 of *C. glabrata* is essential for growth on minimal medium, as shown by the screening for growth defects on minimal medium. Thus, survival of the *yfh1*Δ or the metabolic deficient mutants in a phagosomal nutrient-depleted environment may also be diminished. This implies that, for example, *YFH1* may play a role in the pathogenicity of *C. glabrata*. However, this speculation must be interpreted with care, because these phenotypes may be the result of the deletion of one of the identified genes in the triple-auxotrophic parental strain. In other words, deletion of each of these genes in the auxotrophic background strain may act synergistic with the impaired amino acid biosynthesis pathways.

Azole-susceptible mutants. Several mechanisms are implicated in fungal drug resistance, including reduced uptake, upregulation of drug efflux pumps, sequestration of toxic substances in the vacuole, intracellular drug inactivation, changes in membrane permeability and alteration of drug targets (Cowen & Steinbach, 2008). ABC transporters have been characterized as the major drug efflux pumps in baker's yeast and other *Candida* spp. (Holland *et al.*, 2003).

Besides the *cdr1*Δ and *pdr1*Δ deletion strains, screening for genes implicated in azole drug resistance yielded several signaling and cell wall mutants, showing elevated azole susceptibility. Among them, the *cna1*Δ and *cnb1*Δ mutants were susceptible to fluconazole and voriconazole. Remarkably, increasing data demonstrate synergistic effects of calcineurin inhibitors and azoles on different *Candida* species (Cruz *et al.*, 2002, Onyewu et al., 2003, Uppuluri *et al.*, 2008). For instance, calcineurin is essential for survival of *C. albicans* during membrane perturbation caused by azole inhibition of ergosterol biosynthesis (Cruz et al., 2002, Onyewu et al., 2003, Uppuluri et al., 2008). The azole sensitivity of the *C. glabrata cna1*Δ and *cnb1*Δ deletion strains is consistent with these data, suggesting that calcineurin buffers azole stress in *C. glabrata*.

A *C. glabrata* mutant lacking *YPK1* is sensitive to voriconazole, linking the sphingolipid-mediated signaling pathway to proper membrane function. Ypk1 seems to play an essential role for *C. glabrata* viability and counteracting membrane perturbations because the *ypk1*Δ mutant is severely affected by several diverse drugs such as azoles, amphotericin B and caffeine. Ypk1 is also implicated in cell wall integrity, as the *ypk1*Δ mutant is sensitive to CF. Ypk1 pathway-mediated activation of the PKC pathway has been demonstrated in *S. cerevisiae* (Inagaki *et al.*, 1999). Interestingly, several *C. glabrata* cell wall mutants also show increased susceptibility to azoles. This sensitivity may be caused by an indirect effect of ergosterol biosynthesis inhibition on the cell wall structure. On one hand, a debilitated cell wall may facilitate azole uptake, thereby potentiating the fungistatic effect. On the other hand, the inhibition of ergosterol biosynthesis may act synergistic with certain cell wall defects and, consequently, cell wall mutants are unable to compensate for azole stress.

Further, the integration of the cell wall integrity pathway in response to azole stress is supported by the reduced azole resistance of the *wsc1*Δ deletion strain. In addition, a *slt2*Δ mutant also displays slight azole sensitivity. Although the PKC pathway has not been clearly implicated in azole resistance yet, these data hint at a contribution of cell wall integrity signaling in *C. glabrata*. So far, only one genome-wide expression study found a down-regulation of the PKC pathway sensor *WSC1* in the resistant strain, when comparing a fluconazole-resistant mutant with its parent strain (Vermitsky et al., 2006).

Taken together, perturbation of the plasma membrane by azole drugs may lead to growth deficiencies of certain cell wall mutants due to a synergistic effect. Likely, cell wall deficient mutants are unable to compensate for additional membrane perturbations and consequently lose viability. Cell wall integrity signaling via the PKC or the sphingolipid-mediated Ypk1 pathways appears to be involved in counteracting azole stress. Alterations of the cell wall as an indirect effect of exposure to azole drugs may lead to activation of the *C. glabrata* cell integrity pathways.

Phenotypic switching. Phenotypic switching is a common attribute of dimorphic fungi such as *C. albicans* (Sudbery et al., 2004). Phenotypic switching in *C. glabrata* has been implicated in virulence just recently (Lachke *et al.*, 2000, Srikantha et al., 2008). On $CuSO_4$-containing media four different core switching phenotypes of wild type cells can be distinguished. Interestingly, DB cells are more prevalent in natural isolates and seem to have a colonization advantage over other switching phenotypes (Srikantha et al., 2008).

Screening on $CuSO_4$-containing media revealed cell wall and metabolism-deficient mutants of *C. glabrata*, displaying only the Wh phenotype. Since DB cells are thought to be more virulent than Wh cells (Srikantha et al., 2008), the identified genes responsible for the Wh phenotype may represent new factors attenuating the virulence of *C. glabrata*.

Remarkably, the core switching phenotype differs between *C. glabrata* cells isolated from different host niches (Brockert et al., 2003). While a Wh phenotype dominated in the oral cavity, DB was more prevalent in vaginal samples. One explanation for this observation is that the selection of the switching phenotype may occur in response to differences in environmental factors, such as the nutrient composition, nutrient availability, the pH or the cell type of the host niche. Efficient colonization of different host niches may require differently equipped fungal cell surfaces. Thus, the expression of adhesins may vary, depending on the tissue or the host niche (i.e. oral cavity, intestinal tract, vaginal tract) and cell wall changes leading to altered adhesion properties may be beneficial for the best possible adhesion to a specific cell type. Wh cells, for example, may reflect the rearrangement of its cell wall to adapt to specific environmental host conditions. Since Wh cells were found to predominate the oral cavity, the specific environmental conditions of this host niche may favour a distinct state of *C. glabrata*, which becomes manifested in the Wh phenotype. Thus, an intact cell wall biogenesis and a functional metabolism may both contribute to the determination of the switching phenotype, reflecting a specific state of the fungal cell for a specific host niche.

Novel *C. glabrata* genes. The screening of the deletion collection revealed many *C. glabrata* genes involved in stress response and drug resistance. Many gene functions and phenotypes are similar to *S. cerevisiae*. However, several genes have been identified, which show distinct phenotypes. Thus, further studies on *C. glabrata*-specific genes will be fruitful and may help to answer, which attributes turn *C. glabrata* into a successful fungal pathogen.

One example is the mutant lacking CAGL0D02750g, which encodes a protein with homology to a myosin motor domain and a fatty acid binding motif. The protein may be involved in transport processes important for plasma membrane or cell wall maintenance, since it is essential to maintain viability under such diverse conditions as heat, caffeine and azole stress. The lack of CAGL0A01892g is a second example, which renders *C. glabrata* sensitive to CF. However, BLAST and protein motif searches did not lead to the identification of a homologue.

Finally, the histone deacetylase Rpd3 is an interesting candidate for further detailed studies on the drug resistance mechanisms of *C. glabrata*. Sc*rpd3*Δ mutants are sensitive to cycloheximide (Colina & Young, 2005) and ScRpd3 has been implicated in the regulation of azole drug resistance in yeast (Borecka-Melkusova et al., 2008). The *C. glabrata rpd3*Δ mutant displays a different susceptibility profile, showing slow growth and high CF sensitivity. Thus, Rpd3 of *C. glabrata* may regulate a different set of genes than its orthologue in *S. cerevisiae*. Since regulation of cell wall genes by transcriptional silencing is a well-described

phenomenon in *C. glabrata* (*EPA* gene family (Castano et al., 2005)), it may be possible that Rpd3 also plays a role in chromatin-dependent regulation of cell wall genes.

In summary, the generation and phenotypic characterization of the generated *C. glabrata* gene deletion library described in this thesis mainly revealed new insights about the implication of *C. glabrata* genes in drug resistance, stress sensing and putative virulence-associated factors. The expansion of the mutant collection and further *in vitro* screenings, for example, for host-pathogen interactions, such as phagocytosis, survival in phagocytes or the determination of cytokine production by immune cells upon interaction with fungal cells, will lead to a deeper understanding of the specific virulence attributes of *C. glabrata*. Furthermore, the future exploitation of the signature-tagged deletion strains in a suitable animal model will define novel *C. glabrata*-specific virulence factors. Therefore, this *C. glabrata* gene deletion collection represents a highly valuable tool for the future study of fungal pathogenicity.

7 Literature

Agarwal, A. K., P. D. Rogers, S. R. Baerson, M. R. Jacob, K. S. Barker, J. D. Cleary, L. A. Walker, D. G. Nagle & A. M. Clark, (2003) Genome-wide expression profiling of the response to polyene, pyrimidine, azole, and echinocandin antifungal agents in *Saccharomyces cerevisiae*. *J Biol Chem* **278**: 34998-35015.

Ahmed, K., D. A. Gerber & C. Cochet, (2002) Joining the cell survival squad: an emerging role for protein kinase CK2. *Trends Cell Biol* **12**: 226-230.

Akins, R. A., (2005) An update on antifungal targets and mechanisms of resistance in *Candida albicans*. *Med Mycol* **43**: 285-318.

Azuma, M., J. N. Levinson, N. Page & H. Bussey, (2002) *Saccharomyces cerevisiae* Big1p, a putative endoplasmic reticulum membrane protein required for normal levels of cell wall beta-1,6-glucan. *Yeast* **19**: 783-793.

Babior, B. M., (2000) Phagocytes and oxidative stress. *Am J Med* **109**: 33-44.

Bachmann, S. P., T. F. Patterson & J. L. Lopez-Ribot, (2002) In vitro activity of caspofungin (MK-0991) against clinical isolates displaying different mechanisms of azole resistance. *J Clin Microbiol* **40**: 2228-2230.

Ballou, L., E. Alvarado, P. K. Tsai, A. Dell & C. E. Ballou, (1989) Protein glycosylation defects in the *Saccharomyces cerevisiae mnn7* mutant class. Support for the stop signal proposed for regulation of outer chain elongation. *J Biol Chem* **264**: 11857-11864.

Balzi, E., W. Chen, S. Ulaszewski, E. Capieaux & A. Goffeau, (1987) The multidrug resistance gene *PDR1* from *Saccharomyces cerevisiae*. *J Biol Chem* **262**: 16871-16879.

Barelle, C. J., C. L. Priest, D. M. Maccallum, N. A. Gow, F. C. Odds & A. J. Brown, (2006) Niche-specific regulation of central metabolic pathways in a fungal pathogen. *Cell Microbiol* **8**: 961-971.

Bates, D. W., L. Su, D. T. Yu, G. M. Chertow, D. L. Seger, D. R. Gomes & R. Platt, (2001) Correlates of acute renal failure in patients receiving parenteral amphotericin B. *Kidney Int* **60**: 1452-1459.

Batova, M., S. Borecka-Melkusova, M. Simockova, V. Dzugasova, E. Goffa & J. Subik, (2008) Functional characterization of the CgPGS1 gene reveals a link between mitochondrial phospholipid homeostasis and drug resistance in *Candida glabrata*. *Curr Genet* **53**: 313-322.

Batova, M., V. Dzugasova, S. Borecka, E. Goffa, Z. Oblasova & J. Subik, (2009) Molecular and phenotypic analysis of mutations causing anionic phospholipid deficiency in closely related yeast species. *Folia Microbiol (Praha)* **54**: 30-36.

Benachour, A., G. Sipos, I. Flury, F. Reggiori, E. Canivenc-Gansel, C. Vionnet, A. Conzelmann & M. Benghezal, (1999) Deletion of *GPI7*, a yeast gene required for addition of a side chain to the glycosylphosphatidylinositol (GPI) core structure, affects GPI protein transport, remodeling, and cell wall integrity. *J Biol Chem* **274**: 15251-15261.

Berman, J. & P. E. Sudbery, (2002) *Candida albicans*: a molecular revolution built on lessons from budding yeast. *Nat Rev Genet* **3**: 918-930.

Bickle, M., P. A. Delley, A. Schmidt & M. N. Hall, (1998) Cell wall integrity modulates *RHO1* activity via the exchange factor *ROM2*. *EMBO J* **17**: 2235-2245.

Bidlingmaier, S., E. L. Weiss, C. Seidel, D. G. Drubin & M. Snyder, (2001) The Cbk1p pathway is important for polarized cell growth and cell separation in *Saccharomyces cerevisiae*. *Mol Cell Biol* **21**: 2449-2462.

Boone, C., S. S. Sommer, A. Hensel & H. Bussey, (1990) Yeast *KRE* genes provide evidence for a pathway of cell wall beta-glucan assembly. *J Cell Biol* **110**: 1833-1843.

Borecka-Melkusova, S., Z. Kozovska, I. Hikkel, V. Dzugasova & J. Subik, (2008) *RPD3* and *ROM2* are required for multidrug resistance in *Saccharomyces cerevisiae*. *FEMS Yeast Res* **8**: 414-424.

Borst, A., M. T. Raimer, D. W. Warnock, C. J. Morrison & B. A. Arthington-Skaggs, (2005) Rapid acquisition of stable azole resistance by *Candida glabrata* isolates obtained before the clinical introduction of fluconazole. *Antimicrob Agents Chemother* **49**: 783-787.

Bouchara, J. P., R. Zouhair, S. Le Boudouil, G. Renier, R. Filmon, D. Chabasse, J. N. Hallet & A. Defontaine, (2000) *In-vivo* selection of an azole-resistant petite mutant of *Candida glabrata*. *J Med Microbiol* **49**: 977-984.

Brachmann, C. B., A. Davies, G. J. Cost, E. Caputo, J. Li, P. Hieter & J. D. Boeke, (1998) Designer deletion strains derived from *Saccharomyces cerevisiae* S288C: a useful set of strains and plasmids for PCR-mediated gene disruption and other applications. *Yeast* **14**: 115-132.

Brakhage, A. A. & B. Liebmann, (2005) *Aspergillus fumigatus* conidial pigment and cAMP signal transduction: significance for virulence. *Med Mycol* **43 Suppl 1**: S75-82.

Brand, A., D. M. MacCallum, A. J. Brown, N. A. Gow & F. C. Odds, (2004) Ectopic expression of URA3 can influence the virulence phenotypes and proteome of *Candida albicans* but can be overcome by targeted reintegration of *URA3* at the RPS10 locus. *Eukaryot Cell* **3**: 900-909.

Brewster, J. L., T. de Valoir, N. D. Dwyer, E. Winter & M. C. Gustin, (1993) An osmosensing signal transduction pathway in yeast. *Science* **259**: 1760-1763.

Brockert, P. J., S. A. Lachke, T. Srikantha, C. Pujol, R. Galask & D. R. Soll, (2003) Phenotypic switching and mating type switching of *Candida glabrata* at sites of colonization. *Infect Immun* **71**: 7109-7118.

Brown, G. D., (2006) Dectin-1: a signalling non-TLR pattern-recognition receptor. *Nat Rev Immunol* **6**: 33-43.

Brun, S., C. Aubry, O. Lima, R. Filmon, T. Berges, D. Chabasse & J. P. Bouchara, (2003) Relationships between respiration and susceptibility to azole antifungals in *Candida glabrata*. *Antimicrob Agents Chemother* **47**: 847-853.

Brun, S., T. Berges, P. Poupard, C. Vauzelle-Moreau, G. Renier, D. Chabasse & J. P. Bouchara, (2004) Mechanisms of azole resistance in petite mutants of *Candida glabrata*. *Antimicrob Agents Chemother* **48**: 1788-1796.

Brun, S., F. Dalle, P. Saulnier, G. Renier, A. Bonnin, D. Chabasse & J. P. Bouchara, (2005) Biological consequences of petite mutations in *Candida glabrata*. *J Antimicrob Chemother* **56**: 307-314.

Brunke, S., personal communication.

Burda, P. & M. Aebi, (1999) The dolichol pathway of N-linked glycosylation. *Biochim Biophys Acta* **1426**: 239-257.

Byrne, K. P. & K. H. Wolfe, (2005) The Yeast Gene Order Browser: combining curated homology and syntenic context reveals gene fate in polyploid species. *Genome Res* **15**: 1456-1461.

Calcagno, A. M., E. Bignell, T. R. Rogers, M. Canedo, F. A. Muhlschlegel & K. Haynes, (2004) *Candida glabrata* Ste20 is involved in maintaining cell wall integrity and adaptation to hypertonic stress, and is required for wild-type levels of virulence. *Yeast* **21**: 557-568.

Calcagno, A. M., E. Bignell, T. R. Rogers, M. D. Jones, F. A. Muhlschlegel & K. Haynes, (2005) *Candida glabrata* Ste11 is involved in adaptation to hypertonic stress, maintenance of wild-type levels of filamentation and plays a role in virulence. *Med Mycol* **43**: 355-364.

Calcagno, A. M., E. Bignell, P. Warn, M. D. Jones, D. W. Denning, F. A. Muhlschlegel, T. R. Rogers & K. Haynes, (2003) *Candida glabrata* STE12 is required for wild-type levels of virulence and nitrogen starvation induced filamentation. *Mol Microbiol* **50**: 1309-1318.

Cardenas, M. E., N. S. Cutler, M. C. Lorenz, C. J. Di Como & J. Heitman, (1999) The TOR signaling cascade regulates gene expression in response to nutrients. *Genes Dev* **13**: 3271-3279.

Casadevall, A., A. L. Rosas & J. D. Nosanchuk, (2000) Melanin and virulence in *Cryptococcus neoformans*. *Curr Opin Microbiol* **3**: 354-358.

Castano, I., R. Kaur, S. Pan, R. Cregg, L. Penas Ade, N. Guo, M. C. Biery, N. L. Craig & B. P. Cormack, (2003) Tn7-based genome-wide random insertional mutagenesis of *Candida glabrata*. *Genome Res* **13**: 905-915.

Castano, I., S. J. Pan, M. Zupancic, C. Hennequin, B. Dujon & B. P. Cormack, (2005) Telomere length control and transcriptional regulation of subtelomeric adhesins in *Candida glabrata*. *Mol Microbiol* **55**: 1246-1258.

Chauhan, N., J. P. Latge & R. Calderone, (2006) Signalling and oxidant adaptation in *Candida albicans* and *Aspergillus fumigatus*. *Nat Rev Microbiol* **4**: 435-444.

Chen, K. H., T. Miyazaki, H. F. Tsai & J. E. Bennett, (2007) The bZip transcription factor Cgap1p is involved in multidrug resistance and required for activation of multidrug transporter gene Cg*FLR1* in *Candida glabrata*. *Gene* **386**: 63-72.

Chen, R. E. & J. Thorner, (2007) Function and regulation in MAPK signaling pathways: lessons learned from the yeast *Saccharomyces cerevisiae*. *Biochim Biophys Acta* **1773**: 1311-1340.

Chen, S. C. & T. C. Sorrell, (2007) Antifungal agents. *Med J Aust* **187**: 404-409.

Cid, V. J., L. Adamikova, M. Sanchez, M. Molina & C. Nombela, (2001) Cell cycle control of septin ring dynamics in the budding yeast. *Microbiology* **147**: 1437-1450.

Cleary, J. D., G. Garcia-Effron, S. W. Chapman & D. S. Perlin, (2008) Reduced *Candida glabrata* susceptibility secondary to an *FKS1* mutation developed during candidemia treatment. *Antimicrob Agents Chemother* **52**: 2263-2265.

Colina, A. R. & D. Young, (2005) Raf60, a novel component of the Rpd3 histone deacetylase complex required for Rpd3 activity in *Saccharomyces cerevisiae*. *J Biol Chem* **280**: 42552-42556.

Colman-Lerner, A., T. E. Chin & R. Brent, (2001) Yeast Cbk1 and Mob2 activate daughter-specific genetic programs to induce asymmetric cell fates. *Cell* **107**: 739-750.

Cormack, B. P. & S. Falkow, (1999) Efficient homologous and illegitimate recombination in the opportunistic yeast pathogen *Candida glabrata*. *Genetics* **151**: 979-987.

Cormack, B. P., N. Ghori & S. Falkow, (1999) An adhesin of the yeast pathogen *Candida glabrata* mediating adherence to human epithelial cells. *Science* **285**: 578-582.

Costerton, J. W., Z. Lewandowski, D. E. Caldwell, D. R. Korber & H. M. Lappin-Scott, (1995) Microbial biofilms. *Annu Rev Microbiol* **49**: 711-745.

Cota, J. M., J. L. Grabinski, R. L. Talbert, D. S. Burgess, P. D. Rogers, T. D. Edlind & N. P. Wiederhold, (2008) Increases in *SLT2* expression and chitin content are associated with incomplete killing of *Candida glabrata* by caspofungin. *Antimicrob Agents Chemother* **52**: 1144-1146.

Cowen, L. E., (2008) The evolution of fungal drug resistance: modulating the trajectory from genotype to phenotype. *Nat Rev Microbiol* **6**: 187-198.

Cowen, L. E. & W. J. Steinbach, (2008) Stress, drugs, and evolution: the role of cellular signaling in fungal drug resistance. *Eukaryot Cell* **7**: 747-764.

Cruz, M. C., A. L. Goldstein, J. R. Blankenship, M. Del Poeta, D. Davis, M. E. Cardenas, J. R. Perfect, J. H. McCusker & J. Heitman, (2002) Calcineurin is essential for survival during membrane stress in *Candida albicans*. *Embo J* **21**: 546-559.

Csank, C. & K. Haynes, (2000) *Candida glabrata* displays pseudohyphal growth. *FEMS Microbiol Lett* **189**: 115-120.

Cuellar-Cruz, M., M. Briones-Martin-del-Campo, I. Canas-Villamar, J. Montalvo-Arredondo, L. Riego-Ruiz, I. Castano & A. De Las Penas, (2008) High resistance to oxidative stress in the fungal pathogen *Candida glabrata* is mediated by a single catalase, Cta1p, and is controlled by the transcription factors Yap1p, Skn7p, Msn2p, and Msn4p. *Eukaryot Cell* **7**: 814-825.

d'Ostiani, C. F., G. Del Sero, A. Bacci, C. Montagnoli, A. Spreca, A. Mencacci, P. Ricciardi-Castagnoli & L. Romani, (2000) Dendritic cells discriminate between yeasts and hyphae of the fungus *Candida albicans*. Implications for initiation of T helper cell immunity in vitro and in vivo. *J Exp Med* **191**: 1661-1674.

Davenport, K. R., M. Sohaskey, Y. Kamada, D. E. Levin & M. C. Gustin, (1995) A second osmosensing signal transduction pathway in yeast. Hypotonic shock activates the *PKC1* protein kinase-regulated cell integrity pathway. *J Biol Chem* **270**: 30157-30161.

de Groot, P. W., E. A. Kraneveld, Q. Y. Yin, H. L. Dekker, U. Gross, W. Crielaard, C. G. de Koster, O. Bader, F. M. Klis & M. Weig, (2008) The cell wall of the human pathogen *Candida glabrata*: differential incorporation of novel adhesin-like wall proteins. *Eukaryot Cell* **7**: 1951-1964.

de Groot, P. W., C. Ruiz, C. R. Vazquez de Aldana, E. Duenas, V. J. Cid, F. Del Rey, J. M. Rodriquez-Pena, P. Perez, A. Andel, J. Caubin, J. Arroyo, J. C. Garcia, C. Gil, M. Molina, L. J. Garcia, C. Nombela & F. M. Klis, (2001) A genomic approach for the identification and classification of genes involved in cell wall formation and its regulation in *Saccharomyces cerevisiae*. *Comp Funct Genomics* **2**: 124-142.

De Las Penas, A., S. J. Pan, I. Castano, J. Alder, R. Cregg & B. P. Cormack, (2003) Virulence-related surface glycoproteins in the yeast pathogen *Candida glabrata* are encoded in subtelomeric clusters and subject to *RAP1*- and *SIR*-dependent transcriptional silencing. *Genes Dev* **17**: 2245-2258.

De Virgilio, C. & R. Loewith, (2006) The TOR signalling network from yeast to man. *Int J Biochem Cell Biol* **38**: 1476-1481.

Defontaine, A., J. P. Bouchara, P. Declerk, C. Planchenault, D. Chabasse & J. N. Hallet, (1999) In-vitro resistance to azoles associated with mitochondrial DNA deficiency in *Candida glabrata*. *J Med Microbiol* **48**: 663-670.

Delaveau, T., A. Delahodde, E. Carvajal, J. Subik & C. Jacq, (1994) *PDR3*, a new yeast regulatory gene, is homologous to *PDR1* and controls the multidrug resistance phenomenon. *Mol Gen Genet* **244**: 501-511.

Dempski, R. E., Jr. & B. Imperiali, (2002) Oligosaccharyl transferase: gatekeeper to the secretory pathway. *Curr Opin Chem Biol* **6**: 844-850.

Denning, D. W., (2003) Echinocandin antifungal drugs. *Lancet* **362**: 1142-1151.

Dichtl, B., A. Stevens & D. Tollervey, (1997) Lithium toxicity in yeast is due to the inhibition of RNA processing enzymes. *EMBO J* **16**: 7184-7195.

Dodgson, A. R., C. Pujol, M. A. Pfaller, D. W. Denning & D. R. Soll, (2005) Evidence for recombination in *Candida glabrata*. *Fungal Genet Biol* **42**: 233-243.

Domergue, R., I. Castano, A. De Las Penas, M. Zupancic, V. Lockatell, J. R. Hebel, D. Johnson & B. P. Cormack, (2005) Nicotinic acid limitation regulates silencing of *Candida* adhesins during UTI. *Science* **308**: 866-870.

Donovick, R., W. Gold, J. F. Pagano & H. A. Stout, (1955) Amphotericins A and B, antifungal antibiotics produced by a streptomycete. I. In vitro studies. *Antibiot Annu* **3**: 579-586.

Douglas, L. J., (2003) *Candida* biofilms and their role in infection. *Trends Microbiol* **11**: 30-36.

Dujon, B., D. Sherman, G. Fischer, P. Durrens, S. Casaregola, I. Lafontaine, J. De Montigny, C. Marck, C. Neuveglise, E. Talla, N. Goffard, L. Frangeul, M. Aigle, V. Anthouard, A. Babour, V. Barbe, S. Barnay, S. Blanchin, J. M. Beckerich, E. Beyne, C. Bleykasten, A. Boisrame, J. Boyer, L. Cattolico, F. Confanioleri, A. De Daruvar, L. Despons, E. Fabre, C. Fairhead, H. Ferry-Dumazet, A. Groppi, F. Hantraye, C. Hennequin, N. Jauniaux, P. Joyet, R. Kachouri, A. Kerrest, R. Koszul, M. Lemaire, I. Lesur, L. Ma, H. Muller, J. M. Nicaud, M. Nikolski, S. Oztas, O. Ozier-Kalogeropoulos, S. Pellenz, S. Potier, G. F. Richard, M. L. Straub, A. Suleau, D. Swennen, F. Tekaia, M. Wesolowski-Louvel, E. Westhof, B. Wirth, M. Zeniou-Meyer, I. Zivanovic, M. Bolotin-Fukuhara, A. Thierry, C. Bouchier, B. Caudron, C. Scarpelli, C. Gaillardin, J. Weissenbach, P. Wincker & J. L. Souciet, (2004) Genome evolution in yeasts. *Nature* **430**: 35-44.

Edlind, T. D., K. W. Henry, J. P. Vermitsky, M. P. Edlind, S. Raj & S. K. Katiyar, (2005) Promoter-dependent disruption of genes: simple, rapid, and specific PCR-based method with application to three different yeast. *Curr Genet* **48**: 117-125.

Edmond, M. B., S. E. Wallace, D. K. McClish, M. A. Pfaller, R. N. Jones & R. P. Wenzel, (1999) Nosocomial bloodstream infections in United States hospitals: a three-year analysis. *Clin Infect Dis* **29**: 239-244.

El Barkani, A., K. Haynes, H. Mosch, M. Frosch & F. A. Muhlschlegel, (2000) *Candida glabrata* shuttle vectors suitable for translational fusions to lacZ and use of beta-galactosidase as a reporter of gene expression. *Gene* **246**: 151-155.

Fernandez-Arenas, E., V. Cabezon, C. Bermejo, J. Arroyo, C. Nombela, R. Diez-Orejas & C. Gil, (2007) Integrated proteomics and genomics strategies bring new insight into *Candida albicans* response upon macrophage interaction. *Mol Cell Proteomics* **6**: 460-478.

Ferrari, S., F. Ischer, D. Calabrese, B. Posteraro, M. Sanguinetti, G. Fadda, B. Rohde, C. Bauser, O. Bader & D. Sanglard, (2009) Gain of function mutations in Cg*PDR1* of *Candida glabrata* not only mediate antifungal resistance but also enhance virulence. *PLoS Pathog* **5**: e1000268.

Fitzpatrick, D. A., M. E. Logue, J. E. Stajich & G. Butler, (2006) A fungal phylogeny based on 42 complete genomes derived from supertree and combined gene analysis. *BMC Evol Biol* **6**: 99.

Foury, F. & D. Talibi, (2001) Mitochondrial control of iron homeostasis. A genome wide analysis of gene expression in a yeast frataxin-deficient strain. *J Biol Chem* **276**: 7762-7768.

Fridkin, S. K., (2005) The changing face of fungal infections in health care settings. *Clin Infect Dis* **41**: 1455-1460.

Frieman, M. B., J. M. McCaffery & B. P. Cormack, (2002) Modular domain structure in the *Candida glabrata* adhesin Epa1p, a beta1,6 glucan-cross-linked cell wall protein. *Mol Microbiol* **46**: 479-492.

Frohner, I. E., C. Bourgeois, K. Yatsyk, O. Majer & K. Kuchler, (2009) *Candida albicans* cell surface superoxide dismutases degrade host-derived reactive oxygen species to escape innate immune surveillance. *Mol Microbiol* **71**: 240-252.

Gantner, B. N., R. M. Simmons, S. J. Canavera, S. Akira & D. M. Underhill, (2003) Collaborative induction of inflammatory responses by dectin-1 and Toll-like receptor 2. *J Exp Med* **197**: 1107-1117.

Gantner, B. N., R. M. Simmons & D. M. Underhill, (2005) Dectin-1 mediates macrophage recognition of *Candida albicans* yeast but not filaments. *EMBO J* **24**: 1277-1286.

Garcia-Effron, G., S. Lee, S. Park, J. D. Cleary & D. S. Perlin, (2009) Effect of *Candida glabrata FKS1* and *FKS2* mutations on echinocandin sensitivity and kinetics of 1,3-β-D-glucan synthase: implication for the existing susceptibility breakpoint. *Antimicrob Agents Chemother*.

George-Chandy, A., I. Nordstrom, E. Nygren, I. M. Jonsson, J. Postigo, L. V. Collins & K. Eriksson, (2008) Th17 development and autoimmune arthritis in the absence of reactive oxygen species. *Eur J Immunol* **38**: 1118-1126.

George, D., P. Miniter & V. T. Andriole, (1996) Efficacy of UK-109496, a new azole antifungal agent, in an experimental model of invasive aspergillosis. *Antimicrob Agents Chemother* **40**: 86-91.

Gerber, J., U. Muhlenhoff & R. Lill, (2003) An interaction between frataxin and Isu1/Nfs1 that is crucial for Fe/S cluster synthesis on Isu1. *EMBO Rep* **4**: 906-911.

Ghannoum, M. A. & L. B. Rice, (1999) Antifungal agents: mode of action, mechanisms of resistance, and correlation of these mechanisms with bacterial resistance. *Clin Microbiol Rev* **12**: 501-517.

Giaever, G., A. M. Chu, L. Ni, C. Connelly, L. Riles, S. Veronneau, S. Dow, A. Lucau-Danila, K. Anderson, B. Andre, A. P. Arkin, A. Astromoff, M. El-Bakkoury, R. Bangham, R. Benito, S. Brachat, S. Campanaro, M. Curtiss, K. Davis, A. Deutschbauer, K. D. Entian, P. Flaherty, F. Foury, D. J. Garfinkel, M. Gerstein, D. Gotte, U. Guldener, J. H. Hegemann, S. Hempel, Z. Herman, D. F. Jaramillo, D. E. Kelly, S. L. Kelly, P. Kotter, D. LaBonte, D. C. Lamb, N. Lan, H. Liang, H. Liao, L. Liu, C. Luo, M. Lussier, R. Mao, P. Menard, S. L. Ooi, J. L. Revuelta, C. J. Roberts, M. Rose, P. Ross-Macdonald, B. Scherens, G. Schimmack, B. Shafer, D. D. Shoemaker, S. Sookhai-Mahadeo, R. K. Storms, J. N. Strathern, G. Valle, M. Voet, G. Volckaert, C. Y. Wang, T. R. Ward, J. Wilhelmy, E. A. Winzeler, Y. Yang, G. Yen, E. Youngman, K. Yu, H. Bussey, J. D. Boeke, M. Snyder, P. Philippsen, R. W. Davis & M. Johnston, (2002) Functional profiling of the *Saccharomyces cerevisiae* genome. *Nature* **418**: 387-391.

Gietz, D., A. St Jean, R. A. Woods & R. H. Schiestl, (1992) Improved method for high efficiency transformation of intact yeast cells. *Nucleic Acids Res* **20**: 1425.

Girrbach, V. & S. Strahl, (2003) Members of the evolutionarily conserved PMT family of protein O-mannosyltransferases form distinct protein complexes among themselves. *J Biol Chem* **278**: 12554-12562.

Gladfelter, A. S., J. R. Pringle & D. J. Lew, (2001) The septin cortex at the yeast mother-bud neck. *Curr Opin Microbiol* **4**: 681-689.

Grant, P. A., D. Schieltz, M. G. Pray-Grant, J. R. Yates, 3rd & J. L. Workman, (1998) The ATM-related cofactor Tra1 is a component of the purified SAGA complex. *Mol Cell* **2**: 863-867.

Gregori, C., C. Schuller, A. Roetzer, T. Schwarzmuller, G. Ammerer & K. Kuchler, (2007) The high-osmolarity glycerol response pathway in the human fungal pathogen *Candida glabrata* strain ATCC 2001 lacks a signaling branch that operates in baker's yeast. *Eukaryot Cell* **6**: 1635-1645.

Gudlaugsson, O., S. Gillespie, K. Lee, J. Vande Berg, J. Hu, S. Messer, L. Herwaldt, M. Pfaller & D. Diekema, (2003) Attributable mortality of nosocomial candidemia, revisited. *Clin Infect Dis* **37**: 1172-1177.

Gustin, M. C., J. Albertyn, M. Alexander & K. Davenport, (1998) MAP kinase pathways in the yeast *Saccharomyces cerevisiae*. *Microbiol Mol Biol Rev* **62**: 1264-1300.

Hallstrom, T. C. & W. S. Moye-Rowley, (2000) Multiple signals from dysfunctional mitochondria activate the pleiotropic drug resistance pathway in *Saccharomyces cerevisiae*. *J Biol Chem* **275**: 37347-37356.

Hamada, K., S. Fukuchi, M. Arisawa, M. Baba & K. Kitada, (1998) Screening for glycosylphosphatidylinositol (GPI)-dependent cell wall proteins in *Saccharomyces cerevisiae*. *Mol Gen Genet* **258**: 53-59.

Hampton, M. B., A. J. Kettle & C. C. Winterbourn, (1998) Inside the neutrophil phagosome: oxidants, myeloperoxidase, and bacterial killing. *Blood* **92**: 3007-3017.

Hanahan, D., (1983) Studies on transformation of *Escherichia coli* with plasmids. *J Mol Biol* **166**: 557-580.

Hashimoto, H., A. Sakakibara, M. Yamasaki & K. Yoda, (1997) *Saccharomyces cerevisiae VIG9* encodes GDP-mannose pyrophosphorylase, which is essential for protein glycosylation. *J Biol Chem* **272**: 16308-16314.

Heeres, J., L. J. Backx, J. H. Mostmans & J. Van Cutsem, (1979) Antimycotic imidazoles. part 4. Synthesis and antifungal activity of ketoconazole, a new potent orally active broad-spectrum antifungal agent. *J Med Chem* **22**: 1003-1005.

Heeres, J., L. J. Backx & J. Van Cutsem, (1984) Antimycotic azoles. 7. Synthesis and antifungal properties of a series of novel triazol-3-ones. *J Med Chem* **27**: 894-900.

Heidelberger, C., N. K. Chaudhuri, P. Danneberg, D. Mooren, L. Griesbach, R. Duschinsky, R. J. Schnitzer, E. Pleven & J. Scheiner, (1957) Fluorinated pyrimidines, a new class of tumour-inhibitory compounds. *Nature* **179**: 663-666.

Henry, K. W., J. T. Nickels & T. D. Edlind, (2000) Upregulation of *ERG* genes in *Candida* species by azoles and other sterol biosynthesis inhibitors. *Antimicrob Agents Chemother* **44**: 2693-2700.

Hensel, M., J. E. Shea, C. Gleeson, M. D. Jones, E. Dalton & D. W. Holden, (1995) Simultaneous identification of bacterial virulence genes by negative selection. *Science* **269**: 400-403.

Hernanz-Falcon, P., O. Joffre, D. L. Williams & E. S. C. Reis, (2009) Internalization of Dectin-1 terminates induction of inflammatory responses. *Eur J Immunol* **39**: 507-513.

Hibbett, D. S., M. Binder, J. F. Bischoff, M. Blackwell, P. F. Cannon, O. E. Eriksson, S. Huhndorf, T. James, P. M. Kirk, R. Lucking, H. Thorsten Lumbsch, F. Lutzoni, P. B. Matheny, D. J. McLaughlin, M. J. Powell, S. Redhead, C. L. Schoch, J. W. Spatafora, J. A. Stalpers, R. Vilgalys, M. C. Aime, A. Aptroot, R. Bauer, D. Begerow, G. L. Benny, L. A. Castlebury, P. W. Crous, Y. C. Dai, W. Gams, D. M. Geiser, G. W. Griffith,

C. Gueidan, D. L. Hawksworth, G. Hestmark, K. Hosaka, R. A. Humber, K. D. Hyde, J. E. Ironside, U. Koljalg, C. P. Kurtzman, K. H. Larsson, R. Lichtwardt, J. Longcore, J. Miadlikowska, A. Miller, J. M. Moncalvo, S. Mozley-Standridge, F. Oberwinkler, E. Parmasto, V. Reeb, J. D. Rogers, C. Roux, L. Ryvarden, J. P. Sampaio, A. Schussler, J. Sugiyama, R. G. Thorn, L. Tibell, W. A. Untereiner, C. Walker, Z. Wang, A. Weir, M. Weiss, M. M. White, K. Winka, Y. J. Yao & N. Zhang, (2007) A higher-level phylogenetic classification of the fungi. *Mycol Res* **111**: 509-547.

Hohmann, S., (2002) Osmotic stress signaling and osmoadaptation in yeasts. *Microbiol Mol Biol Rev* **66**: 300-372.

Holland, I., S. Cole, K. Kuchler & C. Higgins, (2003) ABC proteins from bacteria to man. *Academic Press–Elsevier Science*.

Holt, R. J. & R. L. Newman, (1973) The antimycotic activity of 5-fluorocytosine. *J Clin Pathol* **26**: 167-174.

Horn, D. L., D. Neofytos, E. J. Anaissie, J. A. Fishman, W. J. Steinbach, A. J. Olyaei, K. A. Marr, M. A. Pfaller, C. H. Chang & K. M. Webster, (2009) Epidemiology and outcomes of candidemia in 2019 patients: data from the prospective antifungal therapy alliance registry. *Clin Infect Dis* **48**: 1695-1703.

Hort, W., S. Lang, S. Brunke, P. Mayser & B. Hube, (2009) Analysis of differentially expressed genes associated with tryptophan-dependent pigment synthesis in *M. furfur* by cDNA subtraction technology. *Med Mycol* **47**: 248-258.

Huerta-Cepas, J., H. Dopazo, J. Dopazo & T. Gabaldon, (2007) The human phylome. *Genome Biol* **8**: R109.

Hume, D. A. & S. Gordon, (1983) Optimal conditions for proliferation of bone marrow-derived mouse macrophages in culture: the roles of CSF-1, serum, Ca2+, and adherence. *J Cell Physiol* **117**: 189-194.

Igual, J. C., A. L. Johnson & L. H. Johnston, (1996) Coordinated regulation of gene expression by the cell cycle transcription factor Swi4 and the protein kinase C MAP kinase pathway for yeast cell integrity. *EMBO J* **15**: 5001-5013.

Ihmels, J., S. Bergmann, M. Gerami-Nejad, I. Yanai, M. McClellan, J. Berman & N. Barkai, (2005) Rewiring of the yeast transcriptional network through the evolution of motif usage. *Science* **309**: 938-940.

Inaba, K., M. Inaba, N. Romani, H. Aya, M. Deguchi, S. Ikehara, S. Muramatsu & R. M. Steinman, (1992) Generation of large numbers of dendritic cells from mouse bone marrow cultures supplemented with granulocyte/macrophage colony-stimulating factor. *J Exp Med* **176**: 1693-1702.

Inagaki, M., T. Schmelzle, K. Yamaguchi, K. Irie, M. N. Hall & K. Matsumoto, (1999) *PDK1* homologs activate the Pkc1-mitogen-activated protein kinase pathway in yeast. *Mol Cell Biol* **19**: 8344-8352.

Iraqui, I., S. Garcia-Sanchez, S. Aubert, F. Dromer, J. M. Ghigo, C. d'Enfert & G. Janbon, (2005) The Yak1p kinase controls expression of adhesins and biofilm formation in *Candida glabrata* in a Sir4p-dependent pathway. *Mol Microbiol* **55**: 1259-1271.

Iwamoto, T., A. Fujie, K. Sakamoto, Y. Tsurumi, N. Shigematsu, M. Yamashita, S. Hashimoto, M. Okuhara & M. Kohsaka, (1994) WF11899A, B and C, novel antifungal lipopeptides. I. Taxonomy, fermentation, isolation and physico-chemical properties. *J Antibiot (Tokyo)* **47**: 1084-1091.

Izumikawa, K., H. Kakeya, H. F. Tsai, B. Grimberg & J. E. Bennett, (2003) Function of *Candida glabrata* ABC transporter gene, *PDH1*. *Yeast* **20**: 249-261.

Jessup, C. J., N. S. Ryder & M. A. Ghannoum, (2000) An evaluation of the in vitro activity of terbinafine. *Med Mycol* **38**: 155-159.

Jiang, B., J. Sheraton, A. F. Ram, G. J. Dijkgraaf, F. M. Klis & H. Bussey, (1996) *CWH41* encodes a novel endoplasmic reticulum membrane N-glycoprotein involved in beta 1,6-glucan assembly. *J Bacteriol* **178**: 1162-1171.

Johnson, D. R., L. J. Knoll, D. E. Levin & J. I. Gordon, (1994) *Saccharomyces cerevisiae* contains four fatty acid activation (*FAA*) genes: an assessment of their role in regulating protein N-myristoylation and cellular lipid metabolism. *J Cell Biol* **127**: 751-762.

Jouault, T., M. El Abed-El Behi, M. Martinez-Esparza, L. Breuilh, P. A. Trinel, M. Chamaillard, F. Trottein & D. Poulain, (2006) Specific recognition of *Candida albicans* by macrophages requires galectin-3 to discriminate *Saccharomyces cerevisiae* and needs association with TLR2 for signaling. *J Immunol* **177**: 4679-4687.

Kaiser, C., S. Michaelis & A. P. Mitchell, (1994) Methods in yeast genetics. A laboratory course manual. *Cold Spring Harbor Laboratory Press, Cold Spring Harbor, NY.*

Kamran, M., A. M. Calcagno, H. Findon, E. Bignell, M. D. Jones, P. Warn, P. Hopkins, D. W. Denning, G. Butler, T. Rogers, F. A. Muhlschlegel & K. Haynes, (2004) Inactivation of transcription factor gene *ACE2* in the fungal pathogen *Candida glabrata* results in hypervirulence. *Eukaryot Cell* **3**: 546-552.

Karababa, M., E. Valentino, G. Pardini, A. T. Coste, J. Bille & D. Sanglard, (2006) *CRZ1*, a target of the calcineurin pathway in *Candida albicans*. *Mol Microbiol* **59**: 1429-1451.

Katiyar, S., M. Pfaller & T. Edlind, (2006) *Candida albicans* and *Candida glabrata* clinical isolates exhibiting reduced echinocandin susceptibility. *Antimicrob Agents Chemother* **50**: 2892-2894.

Kaur, R., I. Castano & B. P. Cormack, (2004) Functional genomic analysis of fluconazole susceptibility in the pathogenic yeast *Candida glabrata*: roles of calcium signaling and mitochondria. *Antimicrob Agents Chemother* **48**: 1600-1613.

Kaur, R., R. Domergue, M. L. Zupancic & B. P. Cormack, (2005) A yeast by any other name: *Candida glabrata* and its interaction with the host. *Curr Opin Microbiol* **8**: 378-384.

Kaur, R., B. Ma & B. P. Cormack, (2007) A family of glycosylphosphatidylinositol-linked aspartyl proteases is required for virulence of *Candida glabrata*. *Proc Natl Acad Sci U S A* **104**: 7628-7633.

Khatib, R., K. M. Riederer, J. Ramanathan & J. Baran, Jr., (2001) Faecal fungal flora in healthy volunteers and inpatients. *Mycoses* **44**: 151-156.

Kim, S., A. Benguria, C. Y. Lai & S. M. Jazwinski, (1999) Modulation of life-span by histone deacetylase genes in *Saccharomyces cerevisiae*. *Mol Biol Cell* **10**: 3125-3136.

King, L. & G. Butler, (1998) Ace2p, a regulator of *CTS1* (chitinase) expression, affects pseudohyphal production in *Saccharomyces cerevisiae*. *Curr Genet* **34**: 183-191.
Kitada, K., E. Yamaguchi & M. Arisawa, (1995) Cloning of the *Candida glabrata TRP1* and *HIS3* genes, and construction of their disruptant strains by sequential integrative transformation. *Gene* **165**: 203-206.
Kitada, K., E. Yamaguchi, K. Hamada & M. Arisawa, (1997) Structural analysis of a *Candida glabrata* centromere and its functional homology to the *Saccharomyces cerevisiae* centromere. *Curr Genet* **31**: 122-127.
Kliewer, S. A., B. Goodwin & T. M. Willson, (2002) The nuclear pregnane X receptor: a key regulator of xenobiotic metabolism. *Endocr Rev* **23**: 687-702.
Klis, F. M., A. Boorsma & P. W. De Groot, (2006) Cell wall construction in *Saccharomyces cerevisiae*. *Yeast* **23**: 185-202.
Klobucnikova, V., P. Kohut, R. Leber, S. Fuchsbichler, N. Schweighofer, F. Turnowsky & I. Hapala, (2003) Terbinafine resistance in a pleiotropic yeast mutant is caused by a single point mutation in the *ERG1* gene. *Biochem Biophys Res Commun* **309**: 666-671.
Kopp, E. & R. Medzhitov, (2003) Recognition of microbial infection by Toll-like receptors. *Curr Opin Immunol* **15**: 396-401.
Kraus, P. R. & J. Heitman, (2003) Coping with stress: calmodulin and calcineurin in model and pathogenic fungi. *Biochem Biophys Res Commun* **311**: 1151-1157.
Kuchler, K., H. G. Dohlman & J. Thorner, (1993) The a-factor transporter (*STE6* gene product) and cell polarity in the yeast *Saccharomyces cerevisiae*. *J Cell Biol* **120**: 1203-1215.
Kvaal, C., S. A. Lachke, T. Srikantha, K. Daniels, J. McCoy & D. R. Soll, (1999) Misexpression of the opaque-phase-specific gene *PEP1* (*SAP1*) in the white phase of *Candida albicans* confers increased virulence in a mouse model of cutaneous infection. *Infect Immun* **67**: 6652-6662.
Kwast, K. E., P. V. Burke & R. O. Poyton, (1998) Oxygen sensing and the transcriptional regulation of oxygen-responsive genes in yeast. *J Exp Biol* **201**: 1177-1195.
Lachke, S. A., S. Joly, K. Daniels & D. R. Soll, (2002) Phenotypic switching and filamentation in *Candida glabrata*. *Microbiology* **148**: 2661-2674.
Lachke, S. A., T. Srikantha, L. K. Tsai, K. Daniels & D. R. Soll, (2000) Phenotypic switching in *Candida glabrata* involves phase-specific regulation of the metallothionein gene MT-II and the newly discovered hemolysin gene HLP. *Infect Immun* **68**: 884-895.
Lamb, T. M., W. Xu, A. Diamond & A. P. Mitchell, (2001) Alkaline response genes of *Saccharomyces cerevisiae* and their relationship to the *RIM101* pathway. *J Biol Chem* **276**: 1850-1856.
Land, G., J. Burke, C. Shelby, J. Rhodes, J. Collett, I. Bennett & J. Johnson, (1996) Screening protocol for *Torulopsis* (*Candida*) *glabrata*. *J Clin Microbiol* **34**: 2300-2303.
Langfelder, K., M. Streibel, B. Jahn, G. Haase & A. A. Brakhage, (2003) Biosynthesis of fungal melanins and their importance for human pathogenic fungi. *Fungal Genet Biol* **38**: 143-158.
Lapinskas, P. J., S. J. Lin & V. C. Culotta, (1996) The role of the *Saccharomyces cerevisiae CCC1* gene in the homeostasis of manganese ions. *Mol Microbiol* **21**: 519-528.
Lay, J., L. K. Henry, J. Clifford, Y. Koltin, C. E. Bulawa & J. M. Becker, (1998) Altered expression of selectable marker *URA3* in gene-disrupted *Candida albicans* strains complicates interpretation of virulence studies. *Infect Immun* **66**: 5301-5306.
Lesage, G. & H. Bussey, (2006) Cell wall assembly in *Saccharomyces cerevisiae*. *Microbiol Mol Biol Rev* **70**: 317-343.
Lesage, G., A. M. Sdicu, P. Menard, J. Shapiro, S. Hussein & H. Bussey, (2004) Analysis of beta-1,3-glucan assembly in *Saccharomyces cerevisiae* using a synthetic interaction network and altered sensitivity to caspofungin. *Genetics* **167**: 35-49.
Levin, D. E., (2005) Cell wall integrity signaling in *Saccharomyces cerevisiae*. *Microbiol Mol Biol Rev* **69**: 262-291.
Lew, D. J., (2002) Formin' actin filament bundles. *Nat Cell Biol* **4**: E29-30.
Liu, O. W., C. D. Chun, E. D. Chow, C. Chen, H. D. Madhani & S. M. Noble, (2008) Systematic genetic analysis of virulence in the human fungal pathogen *Cryptococcus neoformans*. *Cell* **135**: 174-188.
Liu, T. T., R. E. Lee, K. S. Barker, L. Wei, R. Homayouni & P. D. Rogers, (2005) Genome-wide expression profiling of the response to azole, polyene, echinocandin, and pyrimidine antifungal agents in *Candida albicans*. *Antimicrob Agents Chemother* **49**: 2226-2236.
Locker, J., A. Lewin & M. Rabinowitz, (1979) The structure and organization of mitochondrial DNA from petite yeast. *Plasmid* **2**: 155-181.
Loewith, R., E. Jacinto, S. Wullschleger, A. Lorberg, J. L. Crespo, D. Bonenfant, W. Oppliger, P. Jenoe & M. N. Hall, (2002) Two TOR complexes, only one of which is rapamycin sensitive, have distinct roles in cell growth control. *Mol Cell* **10**: 457-468.
Lorenz, M. C., J. A. Bender & G. R. Fink, (2004) Transcriptional response of *Candida albicans* upon internalization by macrophages. *Eukaryot Cell* **3**: 1076-1087.
Lundqvist, H. & C. Dahlgren, (1996) Isoluminol-enhanced chemiluminescence: a sensitive method to study the release of superoxide anion from human neutrophils. *Free Radic Biol Med* **20**: 785-792.
Lupetti, A., R. Danesi, M. Campa, M. Del Tacca & S. Kelly, (2002) Molecular basis of resistance to azole antifungals. *Trends Mol Med* **8**: 76-81.
Lussier, M., A. M. Sdicu, A. Camirand & H. Bussey, (1996) Functional characterization of the *YUR1*, *KTR1*, *and KTR2* genes as members of the yeast *KRE2*/*MNT1* mannosyltransferase gene family. *J Biol Chem* **271**: 11001-11008.
Ma, B., S. J. Pan, R. Domergue, T. Rigby, M. Whiteway, D. Johnson & B. P. Cormack, (2009) High affinity transporters for NAD+ precursors in *Candida glabrata* are regulated by Hst1 and induced in response to niacin limitation. *Mol Cell Biol*.

Ma, B., S. J. Pan, M. L. Zupancic & B. P. Cormack, (2007) Assimilation of NAD(+) precursors in *Candida glabrata*. *Mol Microbiol* **66**: 14-25.
Magill, S. S., C. Shields, C. L. Sears, M. Choti & W. G. Merz, (2006) Triazole cross-resistance among *Candida* spp.: case report, occurrence among bloodstream isolates, and implications for antifungal therapy. *J Clin Microbiol* **44**: 529-535.
Mah, T. F. & G. A. O'Toole, (2001) Mechanisms of biofilm resistance to antimicrobial agents. *Trends Microbiol* **9**: 34-39.
Malani, A., J. Hmoud, L. Chiu, P. L. Carver, A. Bielaczyc & C. A. Kauffman, (2005) *Candida glabrata* fungemia: experience in a tertiary care center. *Clin Infect Dis* **41**: 975-981.
Marcet-Houben, M. & T. Gabaldon, (2009) The tree versus the forest: the fungal tree of life and the topological diversity within the yeast phylome. *PLoS ONE* **4**: e4357.
Mardh, P. A., A. G. Rodrigues, M. Genc, N. Novikova, J. Martinez-de-Oliveira & S. Guaschino, (2002) Facts and myths on recurrent vulvovaginal candidosis--a review on epidemiology, clinical manifestations, diagnosis, pathogenesis and therapy. *Int J STD AIDS* **13**: 522-539.
Marr, K. A., R. A. Carter, F. Crippa, A. Wald & L. Corey, (2002) Epidemiology and outcome of mould infections in hematopoietic stem cell transplant recipients. *Clin Infect Dis* **34**: 909-917.
Martin, H., M. C. Castellanos, R. Cenamor, M. Sanchez, M. Molina & C. Nombela, (1996) Molecular and functional characterization of a mutant allele of the mitogen-activated protein-kinase gene *SLT2*(*MPK1*) rescued from yeast autolytic mutants. *Curr Genet* **29**: 516-522.
Martin, H., J. M. Rodriguez-Pachon, C. Ruiz, C. Nombela & M. Molina, (2000) Regulatory mechanisms for modulation of signaling through the cell integrity Slt2-mediated pathway in *Saccharomyces cerevisiae*. *J Biol Chem* **275**: 1511-1519.
Masurekar, P. S., J. M. Fountoulakis, T. C. Hallada, M. S. Sosa & L. Kaplan, (1992) Pneumocandins from Zalerion arboricola. II. Modification of product spectrum by mutation and medium manipulation. *J Antibiot (Tokyo)* **45**: 1867-1874.
Mattison, C. P. & I. M. Ota, (2000) Two protein tyrosine phosphatases, Ptp2 and Ptp3, modulate the subcellular localization of the Hog1 MAP kinase in yeast. *Genes Dev* **14**: 1229-1235.
Mavor, A. L., S. Thewes & B. Hube, (2005) Systemic fungal infections caused by *Candida* species: epidemiology, infection process and virulence attributes. *Curr Drug Targets* **6**: 863-874.
Mayser, P., A. Tows, H. J. Kramer & R. Weiss, (2004) Further characterization of pigment-producing *Malassezia* strains. *Mycoses* **47**: 34-39.
Mayser, P., M. Wenzel, H. J. Kramer, B. L. Kindler, P. Spiteller & G. Haase, (2007) Production of indole pigments by *Candida glabrata*. *Med Mycol* **45**: 519-524.
Mayser, P., G. Wille, A. Imkampe, W. Thoma, N. Arnold & T. Monsees, (1998) Synthesis of fluorochromes and pigments in *Malassezia furfur* by use of tryptophan as the single nitrogen source. *Mycoses* **41**: 265-271.
Mean, M., O. Marchetti & T. Calandra, (2008) Bench-to-bedside review: *Candida* infections in the intensive care unit. *Crit Care* **12**: 204.
Mendoza-Cozatl, D., H. Loza-Tavera, A. Hernandez-Navarro & R. Moreno-Sanchez, (2005) Sulfur assimilation and glutathione metabolism under cadmium stress in yeast, protists and plants. *FEMS Microbiol Rev* **29**: 653-671.
Miller, M. G. & A. D. Johnson, (2002) White-opaque switching in *Candida albicans* is controlled by mating-type locus homeodomain proteins and allows efficient mating. *Cell* **110**: 293-302.
Missall, T. A., J. K. Lodge & J. E. McEwen, (2004) Mechanisms of resistance to oxidative and nitrosative stress: implications for fungal survival in mammalian hosts. *Eukaryot Cell* **3**: 835-846.
Miyazaki, H., Y. Miyazaki, A. Geber, T. Parkinson, C. Hitchcock, D. J. Falconer, D. J. Ward, K. Marsden & J. E. Bennett, (1998) Fluconazole resistance associated with drug efflux and increased transcription of a drug transporter gene, *PDH1*, in *Candida glabrata*. *Antimicrob Agents Chemother* **42**: 1695-1701.
Morgan, J., M. I. Meltzer, B. D. Plikaytis, A. N. Sofair, S. Huie-White, S. Wilcox, L. H. Harrison, E. C. Seaberg, R. A. Hajjeh & S. M. Teutsch, (2005) Excess mortality, hospital stay, and cost due to candidemia: a case-control study using data from population-based candidemia surveillance. *Infect Control Hosp Epidemiol* **26**: 540-547.
Mrsa, V., T. Seidl, M. Gentzsch & W. Tanner, (1997) Specific labelling of cell wall proteins by biotinylation. Identification of four covalently linked O-mannosylated proteins of *Saccharomyces cerevisiae*. *Yeast* **13**: 1145-1154.
Muller, H., C. Hennequin, J. Gallaud, B. Dujon & C. Fairhead, (2008) The asexual yeast *Candida glabrata* maintains distinct a and alpha haploid mating types. *Eukaryot Cell* **7**: 848-858.
Mundy, R. D. & B. Cormack, (2009) Expression of *Candida glabrata* Adhesins after Exposure to Chemical Preservatives. *J Infect Dis* **199**: 1891-1898.
Munro, C. A., S. Selvaggini, I. de Bruijn, L. Walker, M. D. Lenardon, B. Gerssen, S. Milne, A. J. Brown & N. A. Gow, (2007) The PKC, HOG and Ca2+ signalling pathways co-ordinately regulate chitin synthesis in *Candida albicans*. *Mol Microbiol* **63**: 1399-1413.
Nace, H. L., D. Horn & D. Neofytos, (2009) Epidemiology and outcome of multiple-species candidemia at a tertiary care center between 2004 and 2007. *Diagn Microbiol Infect Dis*.
Nakayama, H., M. Izuta, S. Nagahashi, E. Y. Sihta, Y. Sato, T. Yamazaki, M. Arisawa & K. Kitada, (1998) A controllable gene-expression system for the pathogenic fungus *Candida glabrata*. *Microbiology* **144 (Pt 9)**: 2407-2415.
Nakayama, H., M. Izuta, N. Nakayama, M. Arisawa & Y. Aoki, (2000) Depletion of the squalene synthase (*ERG9*) gene does not impair growth of *Candida glabrata* in mice. *Antimicrob Agents Chemother* **44**: 2411-2418.

Nakayama, H., K. Tanabe, M. Bard, W. Hodgson, S. Wu, D. Takemori, T. Aoyama, N. S. Kumaraswami, L. Metzler, Y. Takano, H. Chibana & M. Niimi, (2007) The *Candida glabrata* putative sterol transporter gene Cg*AUS1* protects cells against azoles in the presence of serum. *J Antimicrob Chemother* **60**: 1264-1272.

Nelson, B., C. Kurischko, J. Horecka, M. Mody, P. Nair, L. Pratt, A. Zougman, L. D. McBroom, T. R. Hughes, C. Boone & F. C. Luca, (2003) RAM: a conserved signaling network that regulates Ace2p transcriptional activity and polarized morphogenesis. *Mol Biol Cell* **14**: 3782-3803.

Neofytos, D., D. Horn, E. Anaissie, W. Steinbach, A. Olyaei, J. Fishman, M. Pfaller, C. Chang, K. Webster & K. Marr, (2009) Epidemiology and outcome of invasive fungal infection in adult hematopoietic stem cell transplant recipients: analysis of Multicenter Prospective Antifungal Therapy (PATH) Alliance registry. *Clin Infect Dis* **48**: 265-273.

Netea, M. G., G. D. Brown, B. J. Kullberg & N. A. Gow, (2008) An integrated model of the recognition of *Candida albicans* by the innate immune system. *Nat Rev Microbiol* **6**: 67-78.

Netea, M. G., C. A. Van Der Graaf, A. G. Vonk, I. Verschueren, J. W. Van Der Meer & B. J. Kullberg, (2002) The role of toll-like receptor TLR2 and TLR4 in the host defense against disseminated candidiasis. *J Infect Dis* **185**: 1483-1489.

Niimi, M., Y. Nagai, K. Niimi, S. Wada, R. D. Cannon, Y. Uehara & B. C. Monk, (2002) Identification of two proteins induced by exposure of the pathogenic fungus *Candida glabrata* to fluconazole. *J Chromatogr B Analyt Technol Biomed Life Sci* **782**: 245-252.

Noble, S. M. & A. D. Johnson, (2005) Strains and strategies for large-scale gene deletion studies of the diploid human fungal pathogen *Candida albicans*. *Eukaryot Cell* **4**: 298-309.

Nucci, M. & K. A. Marr, (2005) Emerging fungal diseases. *Clin Infect Dis* **41**: 521-526.

Nyfeler, R. & W. Keller-Schierlein, (1974) [Metabolites of microorganisms. 143. Echinocandin B, a novel polypeptide-antibiotic from Aspergillus nidulans var. echinulatus: isolation and structural components]. *Helv Chim Acta* **57**: 2459-2477.

O'Conallain, C., M. T. Doolin, C. Taggart, F. Thornton & G. Butler, (1999) Regulated nuclear localisation of the yeast transcription factor Ace2p controls expression of chitinase (*CTS1*) in *Saccharomyces cerevisiae*. *Mol Gen Genet* **262**: 275-282.

Odds, F. C., (1994) Pathogenesis of *Candida* infections. *J Am Acad Dermatol* **31**: S2-5.

Odds, F. C., A. J. Brown & N. A. Gow, (2003) Antifungal agents: mechanisms of action. *Trends Microbiol* **11**: 272-279.

Odds, F. C., M. G. Rinaldi, C. R. Cooper, Jr., A. Fothergill, L. Pasarell & M. R. McGinnis, (1997) *Candida* and *Torulopsis*: a blinded evaluation of use of pseudohypha formation as basis for identification of medically important yeasts. *J Clin Microbiol* **35**: 313-316.

Onishi, J., M. Meinz, J. Thompson, J. Curotto, S. Dreikorn, M. Rosenbach, C. Douglas, G. Abruzzo, A. Flattery, L. Kong, A. Cabello, F. Vicente, F. Pelaez, M. T. Diez, I. Martin, G. Bills, R. Giacobbe, A. Dombrowski, R. Schwartz, S. Morris, G. Harris, A. Tsipouras, K. Wilson & M. B. Kurtz, (2000) Discovery of novel antifungal (1,3)-beta-D-glucan synthase inhibitors. *Antimicrob Agents Chemother* **44**: 368-377.

Onyewu, C., J. R. Blankenship, M. Del Poeta & J. Heitman, (2003) Ergosterol biosynthesis inhibitors become fungicidal when combined with calcineurin inhibitors against *Candida albicans*, *Candida glabrata*, and *Candida krusei*. *Antimicrob Agents Chemother* **47**: 956-964.

Pammer, M., P. Briza, A. Ellinger, T. Schuster, R. Stucka, H. Feldmann & M. Breitenbach, (1992) *DIT101* (*CSD2, CAL1*), a cell cycle-regulated yeast gene required for synthesis of chitin in cell walls and chitosan in spore walls. *Yeast* **8**: 1089-1099.

Panackal, A. A., J. L. Gribskov, J. F. Staab, K. A. Kirby, M. Rinaldi & K. A. Marr, (2006) Clinical significance of azole antifungal drug cross-resistance in *Candida glabrata*. *J Clin Microbiol* **44**: 1740-1743.

Park, S., R. Kelly, J. N. Kahn, J. Robles, M. J. Hsu, E. Register, W. Li, V. Vyas, H. Fan, G. Abruzzo, A. Flattery, C. Gill, G. Chrebet, S. A. Parent, M. Kurtz, H. Teppler, C. M. Douglas & D. S. Perlin, (2005) Specific substitutions in the echinocandin target Fks1p account for reduced susceptibility of rare laboratory and clinical *Candida* spp. isolates. *Antimicrob Agents Chemother* **49**: 3264-3273.

Parlati, F., M. Dominguez, J. J. Bergeron & D. Y. Thomas, (1995) *Saccharomyces cerevisiae CNE1* encodes an endoplasmic reticulum (ER) membrane protein with sequence similarity to calnexin and calreticulin and functions as a constituent of the ER quality control apparatus. *J Biol Chem* **270**: 244-253.

Perlin, D. S., (2007) Resistance to echinocandin-class antifungal drugs. *Drug Resist Updat* **10**: 121-130.

Perlroth, J., B. Choi & B. Spellberg, (2007) Nosocomial fungal infections: epidemiology, diagnosis, and treatment. *Med Mycol* **45**: 321-346.

Petranyi, G., N. S. Ryder & A. Stutz, (1984) Allylamine derivatives: new class of synthetic antifungal agents inhibiting fungal squalene epoxidase. *Science* **224**: 1239-1241.

Pfaller, M. A., L. Boyken, R. J. Hollis, J. Kroeger, S. A. Messer, S. Tendolkar & D. J. Diekema, (2008) In vitro susceptibility of invasive isolates of *Candida* spp. to anidulafungin, caspofungin, and micafungin: six years of global surveillance. *J Clin Microbiol* **46**: 150-156.

Pfaller, M. A. & D. J. Diekema, (2004a) Rare and emerging opportunistic fungal pathogens: concern for resistance beyond *Candida albicans* and *Aspergillus fumigatus*. *J Clin Microbiol* **42**: 4419-4431.

Pfaller, M. A. & D. J. Diekema, (2004b) Twelve years of fluconazole in clinical practice: global trends in species distribution and fluconazole susceptibility of bloodstream isolates of *Candida*. *Clin Microbiol Infect* **10 Suppl 1**: 11-23.

Pfaller, M. A. & D. J. Diekema, (2007) Epidemiology of invasive candidiasis: a persistent public health problem. *Clin Microbiol Rev* **20**: 133-163.

Pfaller, M. A., S. A. Messer, L. Boyken, C. Rice, S. Tendolkar, R. J. Hollis & D. J. Diekema, (2004) Cross-resistance between fluconazole and ravuconazole and the use of fluconazole as a surrogate marker to

predict susceptibility and resistance to ravuconazole among 12,796 clinical isolates of *Candida* spp. *J Clin Microbiol* **42**: 3137-3141.
Plaine, A., L. Walker, G. Da Costa, H. M. Mora-Montes, A. McKinnon, N. A. Gow, C. Gaillardin, C. A. Munro & M. L. Richard, (2008) Functional analysis of *Candida albicans* GPI-anchored proteins: roles in cell wall integrity and caspofungin sensitivity. *Fungal Genet Biol* **45**: 1404-1414.
Polakova, S., C. Blume, J. A. Zarate, M. Mentel, D. Jorck-Ramberg, J. Stenderup & J. Piskur, (2009) Formation of new chromosomes as a virulence mechanism in yeast *Candida glabrata*. *Proc Natl Acad Sci U S A* **106**: 2688-2693.
Posteraro, B., M. Sanguinetti, B. Fiori, M. La Sorda, T. Spanu, D. Sanglard & G. Fadda, (2006) Caspofungin activity against clinical isolates of azole cross-resistant *Candida glabrata* overexpressing efflux pump genes. *J Antimicrob Chemother* **58**: 458-461.
Qi, M. & E. A. Elion, (2005) MAP kinase pathways. *J Cell Sci* **118**: 3569-3572.
Racki, W. J., A. M. Becam, F. Nasr & C. J. Herbert, (2000) Cbk1p, a protein similar to the human myotonic dystrophy kinase, is essential for normal morphogenesis in *Saccharomyces cerevisiae*. *EMBO J* **19**: 4524-4532.
Ram, A. F., A. Wolters, R. Ten Hoopen & F. M. Klis, (1994) A new approach for isolating cell wall mutants in *Saccharomyces cerevisiae* by screening for hypersensitivity to calcofluor white. *Yeast* **10**: 1019-1030.
Redding, S. W., W. R. Kirkpatrick, S. Saville, B. J. Coco, W. White, A. Fothergill, M. Rinaldi, T. Eng, T. F. Patterson & J. Lopez-Ribot, (2003) Multiple patterns of resistance to fluconazole in *Candida glabrata* isolates from a patient with oropharyngeal candidiasis receiving head and neck radiation. *J Clin Microbiol* **41**: 619-622.
Reinke, A., J. C. Chen, S. Aronova & T. Powers, (2006) Caffeine targets TOR complex I and provides evidence for a regulatory link between the FRB and kinase domains of Tor1p. *J Biol Chem* **281**: 31616-31626.
Reinoso-Martin, C., C. Schuller, M. Schuetzer-Muehlbauer & K. Kuchler, (2003) The yeast protein kinase C cell integrity pathway mediates tolerance to the antifungal drug caspofungin through activation of Slt2p mitogen-activated protein kinase signaling. *Eukaryot Cell* **2**: 1200-1210.
Reuss, O., A. Vik, R. Kolter & J. Morschhauser, (2004) The *SAT1* flipper, an optimized tool for gene disruption in *Candida albicans*. *Gene* **341**: 119-127.
Rex, J. H., M. A. Pfaller, J. N. Galgiani, M. S. Bartlett, A. Espinel-Ingroff, M. A. Ghannoum, M. Lancaster, F. C. Odds, M. G. Rinaldi, T. J. Walsh & A. L. Barry, (1997) Development of interpretive breakpoints for antifungal susceptibility testing: conceptual framework and analysis of in vitro-in vivo correlation data for fluconazole, itraconazole, and *Candida* infections. Subcommittee on Antifungal Susceptibility Testing of the National Committee for Clinical Laboratory Standards. *Clin Infect Dis* **24**: 235-247.
Rice, P., I. Longden & A. Bleasby, (2000) EMBOSS: the European Molecular Biology Open Software Suite. *Trends Genet* **16**: 276-277.
Richardson, K., K. W. Brammer, M. S. Marriott & P. F. Troke, (1985) Activity of UK-49,858, a bis-triazole derivative, against experimental infections with *Candida albicans* and *Trichophyton mentagrophytes*. *Antimicrob Agents Chemother* **27**: 832-835.
Richardson, M. & C. Lass-Florl, (2008) Changing epidemiology of systemic fungal infections. *Clin Microbiol Infect* **14 Suppl 4**: 5-24.
Roelants, F. M., P. D. Torrance, N. Bezman & J. Thorner, (2002) Pkh1 and Pkh2 differentially phosphorylate and activate Ypk1 and Ykr2 and define protein kinase modules required for maintenance of cell wall integrity. *Mol Biol Cell* **13**: 3005-3028.
Roemer, T. & H. Bussey, (1991) Yeast beta-glucan synthesis: *KRE6* encodes a predicted type II membrane protein required for glucan synthesis in vivo and for glucan synthase activity in vitro. *Proc Natl Acad Sci U S A* **88**: 11295-11299.
Roetzer, A., C. Gregori, A. M. Jennings, J. Quintin, D. Ferrandon, G. Butler, K. Kuchler, G. Ammerer & C. Schuller, (2008) *Candida glabrata* environmental stress response involves *Saccharomyces cerevisiae* Msn2/4 orthologous transcription factors. *Mol Microbiol* **69**: 603-620.
Romani, L., (2004) Immunity to fungal infections. *Nat Rev Immunol* **4**: 1-23.
Roncero, C. & A. Duran, (1985) Effect of Calcofluor white and Congo red on fungal cell wall morphogenesis: in vivo activation of chitin polymerization. *J Bacteriol* **163**: 1180-1185.
Rosen, B. P., (2002) Transport and detoxification systems for transition metals, heavy metals and metalloids in eukaryotic and prokaryotic microbes. *Comp Biochem Physiol A Mol Integr Physiol* **133**: 689-693.
Rundlett, S. E., A. A. Carmen, R. Kobayashi, S. Bavykin, B. M. Turner & M. Grunstein, (1996) *HDA1* and *RPD3* are members of distinct yeast histone deacetylase complexes that regulate silencing and transcription. *Proc Natl Acad Sci U S A* **93**: 14503-14508.
Ryder, N. S., (1992) Terbinafine: mode of action and properties of the squalene epoxidase inhibition. *Br J Dermatol* **126 Suppl 39**: 2-7.
Ryder, N. S., (1999) Activity of terbinafine against serious fungal pathogens. *Mycoses* **42 Suppl 2**: 115-119.
Saenz, H. L. & C. Dehio, (2005) Signature-tagged mutagenesis: technical advances in a negative selection method for virulence gene identification. *Curr Opin Microbiol* **8**: 612-619.
Safdar, A., F. van Rhee, J. P. Henslee-Downey, S. Singhal & J. Mehta, (2001) *Candida glabrata* and *Candida krusei* fungemia after high-risk allogeneic marrow transplantation: no adverse effect of low-dose fluconazole prophylaxis on incidence and outcome. *Bone Marrow Transplant* **28**: 873-878.
Sambrook, J., E. Fritsch & T. Maniatis, Molecular cloning: A laboratory manual. *3rd edition, Cold Spring Harbor Press, New York*.

Sanglard, D., F. Ischer & J. Bille, (2001) Role of ATP-binding-cassette transporter genes in high-frequency acquisition of resistance to azole antifungals in *Candida glabrata*. *Antimicrob Agents Chemother* **45**: 1174-1183.

Sanglard, D., F. Ischer, D. Calabrese, P. A. Majcherczyk & J. Bille, (1999) The ATP binding cassette transporter gene Cg*CDR1* from *Candida glabrata* is involved in the resistance of clinical isolates to azole antifungal agents. *Antimicrob Agents Chemother* **43**: 2753-2765.

Sanglard, D., F. Ischer, O. Marchetti, J. Entenza & J. Bille, (2003) Calcineurin A of *Candida albicans*: involvement in antifungal tolerance, cell morphogenesis and virulence. *Mol Microbiol* **48**: 959-976.

Sanglard, D., K. Kuchler, F. Ischer, J. L. Pagani, M. Monod & J. Bille, (1995) Mechanisms of resistance to azole antifungal agents in *Candida albicans* isolates from AIDS patients involve specific multidrug transporters. *Antimicrob Agents Chemother* **39**: 2378-2386.

Sanguinetti, M., B. Posteraro, B. Fiori, S. Ranno, R. Torelli & G. Fadda, (2005) Mechanisms of azole resistance in clinical isolates of *Candida glabrata* collected during a hospital survey of antifungal resistance. *Antimicrob Agents Chemother* **49**: 668-679.

Santos, M. A., T. Ueda, K. Watanabe & M. F. Tuite, (1997) The non-standard genetic code of *Candida* spp.: an evolving genetic code or a novel mechanism for adaptation? *Mol Microbiol* **26**: 423-431.

Scannell, D. R., G. Butler & K. H. Wolfe, (2007) Yeast genome evolution--the origin of the species. *Yeast* **24**: 929-942.

Schmidt, P., J. Walker, L. Selway, D. Stead, Z. Yin, B. Enjalbert, M. Weig & A. J. Brown, (2008) Proteomic analysis of the pH response in the fungal pathogen *Candida glabrata*. *Proteomics* **8**: 534-544.

Schuetzer-Muehlbauer, M., B. Willinger, G. Krapf, S. Enzinger, E. Presterl & K. Kuchler, (2003) The *Candida albicans* Cdr2p ATP-binding cassette (ABC) transporter confers resistance to caspofungin. *Mol Microbiol* **48**: 225-235.

Shen, J., W. Guo & J. R. Kohler, (2005) Ca*NAT1*, a heterologous dominant selectable marker for transformation of *Candida albicans* and other pathogenic *Candida* species. *Infect Immun* **73**: 1239-1242.

Shin, J. H., S. J. Kee, M. G. Shin, S. H. Kim, D. H. Shin, S. K. Lee, S. P. Suh & D. W. Ryang, (2002) Biofilm production by isolates of *Candida* species recovered from nonneutropenic patients: comparison of bloodstream isolates with isolates from other sources. *J Clin Microbiol* **40**: 1244-1248.

Sipos, G. & K. Kuchler, (2006) Fungal ATP-binding cassette (ABC) transporters in drug resistance & detoxification. *Curr Drug Targets* **7**: 471-481.

Slonimski, P. P., G. Perrodin & J. H. Croft, (1968) Ethidium bromide induced mutation of yeast mitochondria: complete transformation of cells into respiratory deficient non-chromosomal "petites". *Biochem Biophys Res Commun* **30**: 232-239.

Slutsky, B., M. Staebell, J. Anderson, L. Risen, M. Pfaller & D. R. Soll, (1987) "White-opaque transition": a second high-frequency switching system in *Candida albicans*. *J Bacteriol* **169**: 189-197.

Srikantha, T., K. J. Daniels, W. Wu, S. R. Lockhart, S. Yi, N. Sahni, N. Ma & D. R. Soll, (2008) Dark brown is the more virulent of the switch phenotypes of *Candida glabrata*. *Microbiology* **154**: 3309-3318.

Srikantha, T., S. A. Lachke & D. R. Soll, (2003) Three mating type-like loci in *Candida glabrata*. *Eukaryot Cell* **2**: 328-340.

Srikantha, T., R. Zhao, K. Daniels, J. Radke & D. R. Soll, (2005) Phenotypic switching in *Candida glabrata* accompanied by changes in expression of genes with deduced functions in copper detoxification and stress. *Eukaryot Cell* **4**: 1434-1445.

Stack, J. H., D. B. DeWald, K. Takegawa & S. D. Emr, (1995) Vesicle-mediated protein transport: regulatory interactions between the Vps15 protein kinase and the Vps34 PtdIns 3-kinase essential for protein sorting to the vacuole in yeast. *J Cell Biol* **129**: 321-334.

Stajich, J. E., D. Block, K. Boulez, S. E. Brenner, S. A. Chervitz, C. Dagdigian, G. Fuellen, J. G. Gilbert, I. Korf, H. Lapp, H. Lehvaslaiho, C. Matsalla, C. J. Mungall, B. I. Osborne, M. R. Pocock, P. Schattner, M. Senger, L. D. Stein, E. Stupka, M. D. Wilkinson & E. Birney, (2002) The Bioperl toolkit: Perl modules for the life sciences. *Genome Res* **12**: 1611-1618.

Stead, D., H. Findon, Z. Yin, J. Walker, L. Selway, P. Cash, B. A. Dujon, C. Hennequin, A. J. Brown & K. Haynes, (2005) Proteomic changes associated with inactivation of the *Candida glabrata ACE2* virulence-moderating gene. *Proteomics* **5**: 1838-1848.

Steinbach, W. J., R. A. Cramer, Jr., B. Z. Perfect, C. Henn, K. Nielsen, J. Heitman & J. R. Perfect, (2007) Calcineurin inhibition or mutation enhances cell wall inhibitors against *Aspergillus fumigatus*. *Antimicrob Agents Chemother* **51**: 2979-2981.

Strahl-Bolsinger, S., M. Gentzsch & W. Tanner, (1999) Protein O-mannosylation. *Biochim Biophys Acta* **1426**: 297-307.

Sudbery, P., N. Gow & J. Berman, (2004) The distinct morphogenic states of *Candida albicans*. *Trends Microbiol* **12**: 317-324.

Tanay, A., A. Regev & R. Shamir, (2005) Conservation and evolvability in regulatory networks: the evolution of ribosomal regulation in yeast. *Proc Natl Acad Sci U S A* **102**: 7203-7208.

Taylor, L. H., S. M. Latham & M. E. Woolhouse, (2001) Risk factors for human disease emergence. *Philos Trans R Soc Lond B Biol Sci* **356**: 983-989.

Taylor, P. R., S. V. Tsoni, J. A. Willment, K. M. Dennehy, M. Rosas, H. Findon, K. Haynes, C. Steele, M. Botto, S. Gordon & G. D. Brown, (2007) Dectin-1 is required for beta-glucan recognition and control of fungal infection. *Nat Immunol* **8**: 31-38.

Thakur, J. K., H. Arthanari, F. Yang, S. J. Pan, X. Fan, J. Breger, D. P. Frueh, K. Gulshan, D. K. Li, E. Mylonakis, K. Struhl, W. S. Moye-Rowley, B. P. Cormack, G. Wagner & A. M. Naar, (2008) A nuclear receptor-like pathway regulating multidrug resistance in fungi. *Nature* **452**: 604-609.

Thevelein, J. M. & J. H. de Winde, (1999) Novel sensing mechanisms and targets for the cAMP-protein kinase A pathway in the yeast *Saccharomyces cerevisiae*. *Mol Microbiol* **33**: 904-918.
Thompson, G. R., 3rd, N. P. Wiederhold, A. C. Vallor, N. C. Villareal, J. S. Lewis, 2nd & T. F. Patterson, (2008) Development of caspofungin resistance following prolonged therapy for invasive candidiasis secondary to *Candida glabrata* infection. *Antimicrob Agents Chemother* **52**: 3783-3785.
Torelli, R., B. Posteraro, S. Ferrari, M. La Sorda, G. Fadda, D. Sanglard & M. Sanguinetti, (2008) The ATP-binding cassette transporter-encoding gene Cg*SNQ2* is contributing to the Cg*PDR1*-dependent azole resistance of *Candida glabrata*. *Mol Microbiol* **68**: 186-201.
Troke, P. F., R. J. Andrews, K. W. Brammer, M. S. Marriott & K. Richardson, (1985) Efficacy of UK-49,858 (fluconazole) against *Candida albicans* experimental infections in mice. *Antimicrob Agents Chemother* **28**: 815-818.
Trombetta, E. S., J. F. Simons & A. Helenius, (1996) Endoplasmic reticulum glucosidase II is composed of a catalytic subunit, conserved from yeast to mammals, and a tightly bound noncatalytic HDEL-containing subunit. *J Biol Chem* **271**: 27509-27516.
Tsai, H. F., M. Bard, K. Izumikawa, A. A. Krol, A. M. Sturm, N. T. Culbertson, C. A. Pierson & J. E. Bennett, (2004) *Candida glabrata erg1* mutant with increased sensitivity to azoles and to low oxygen tension. *Antimicrob Agents Chemother* **48**: 2483-2489.
Tsai, H. F., A. A. Krol, K. E. Sarti & J. E. Bennett, (2006) *Candida glabrata PDR1*, a transcriptional regulator of a pleiotropic drug resistance network, mediates azole resistance in clinical isolates and petite mutants. *Antimicrob Agents Chemother* **50**: 1384-1392.
Tsong, A. E., B. B. Tuch, H. Li & A. D. Johnson, (2006) Evolution of alternative transcriptional circuits with identical logic. *Nature* **443**: 415-420.
Ueno, K., J. Uno, H. Nakayama, K. Sasamoto, Y. Mikami & H. Chibana, (2007) Development of a highly efficient gene targeting system induced by transient repression of *YKU80* expression in *Candida glabrata*. *Eukaryot Cell* **6**: 1239-1247.
Uppuluri, P., J. Nett, J. Heitman & D. Andes, (2008) Synergistic effect of calcineurin inhibitors and fluconazole against *Candida albicans* biofilms. *Antimicrob Agents Chemother* **52**: 1127-1132.
Vermitsky, J. P., K. D. Earhart, W. L. Smith, R. Homayouni, T. D. Edlind & P. D. Rogers, (2006) Pdr1 regulates multidrug resistance in *Candida glabrata*: gene disruption and genome-wide expression studies. *Mol Microbiol* **61**: 704-722.
Vermitsky, J. P. & T. D. Edlind, (2004) Azole resistance in *Candida glabrata*: coordinate upregulation of multidrug transporters and evidence for a Pdr1-like transcription factor. *Antimicrob Agents Chemother* **48**: 3773-3781.
Wach, A., (1996) PCR-synthesis of marker cassettes with long flanking homology regions for gene disruptions in *S. cerevisiae*. *Yeast* **12**: 259-265.
Wada, S., M. Niimi, K. Niimi, A. R. Holmes, B. C. Monk, R. D. Cannon & Y. Uehara, (2002) *Candida glabrata* ATP-binding cassette transporters Cdr1p and Pdh1p expressed in a *Saccharomyces cerevisiae* strain deficient in membrane transporters show phosphorylation-dependent pumping properties. *J Biol Chem* **277**: 46809-46821.
Wada, S., K. Tanabe, A. Yamazaki, M. Niimi, Y. Uehara, K. Niimi, E. Lamping, R. D. Cannon & B. C. Monk, (2005) Phosphorylation of *Candida glabrata* ATP-binding cassette transporter Cdr1p regulates drug efflux activity and ATPase stability. *J Biol Chem* **280**: 94-103.
Walker, L. A., C. A. Munro, I. de Bruijn, M. D. Lenardon, A. McKinnon & N. A. Gow, (2008) Stimulation of chitin synthesis rescues *Candida albicans* from echinocandins. *PLoS Pathog* **4**: e1000040.
Wanke, V., E. Cameroni, A. Uotila, M. Piccolis, J. Urban, R. Loewith & C. De Virgilio, (2008) Caffeine extends yeast lifespan by targeting *TORC1*. *Mol Microbiol* **69**: 277-285.
Weig, M., K. Haynes, T. R. Rogers, O. Kurzai, M. Frosch & F. A. Muhlschlegel, (2001) A GAS-like gene family in the pathogenic fungus *Candida glabrata*. *Microbiology* **147**: 2007-2019.
Weig, M., L. Jansch, U. Gross, C. G. De Koster, F. M. Klis & P. W. De Groot, (2004) Systematic identification in silico of covalently bound cell wall proteins and analysis of protein-polysaccharide linkages of the human pathogen *Candida glabrata*. *Microbiology* **150**: 3129-3144.
Wenzel, R. P. & C. Gennings, (2005) Bloodstream infections due to *Candida* species in the intensive care unit: identifying especially high-risk patients to determine prevention strategies. *Clin Infect Dis* **41 Suppl 6**: S389-393.
Wheeler, R. T., M. Kupiec, P. Magnelli, C. Abeijon & G. R. Fink, (2003) A *Saccharomyces cerevisiae* mutant with increased virulence. *Proc Natl Acad Sci U S A* **100**: 2766-2770.
White, T. C., K. A. Marr & R. A. Bowden, (1998) Clinical, cellular, and molecular factors that contribute to antifungal drug resistance. *Clin Microbiol Rev* **11**: 382-402.
Whittaker, R. H., (1969) New concepts of kingdoms or organisms. Evolutionary relations are better represented by new classifications than by the traditional two kingdoms. *Science* **163**: 150-160.
Wiederhold, N. P., D. P. Kontoyiannis, R. A. Prince & R. E. Lewis, (2005) Attenuation of the activity of caspofungin at high concentrations against *Candida albicans*: possible role of cell wall integrity and calcineurin pathways. *Antimicrob Agents Chemother* **49**: 5146-5148.
Willins, D. A., G. H. Shimer, Jr. & G. Cottarel, (2002) A system for deletion and complementation of *Candida glabrata* genes amenable to high-throughput application. *Gene* **292**: 141-149.
Winzeler, E. A., D. D. Shoemaker, A. Astromoff, H. Liang, K. Anderson, B. Andre, R. Bangham, R. Benito, J. D. Boeke, H. Bussey, A. M. Chu, C. Connelly, K. Davis, F. Dietrich, S. W. Dow, M. El Bakkoury, F. Foury, S. H. Friend, E. Gentalen, G. Giaever, J. H. Hegemann, T. Jones, M. Laub, H. Liao, N. Liebundguth, D. J. Lockhart, A. Lucau-Danila, M. Lussier, N. M'Rabet, P. Menard, M. Mittmann, C. Pai, C. Rebischung, J.

L. Revuelta, L. Riles, C. J. Roberts, P. Ross-MacDonald, B. Scherens, M. Snyder, S. Sookhai-Mahadeo, R. K. Storms, S. Veronneau, M. Voet, G. Volckaert, T. R. Ward, R. Wysocki, G. S. Yen, K. Yu, K. Zimmermann, P. Philippsen, M. Johnston & R. W. Davis, (1999) Functional characterization of the *S. cerevisiae* genome by gene deletion and parallel analysis. *Science* **285**: 901-906.

Wisplinghoff, H., T. Bischoff, S. M. Tallent, H. Seifert, R. P. Wenzel & M. B. Edmond, (2004) Nosocomial bloodstream infections in US hospitals: analysis of 24,179 cases from a prospective nationwide surveillance study. *Clin Infect Dis* **39**: 309-317.

Wong, S., M. A. Fares, W. Zimmermann, G. Butler & K. H. Wolfe, (2003) Evidence from comparative genomics for a complete sexual cycle in the 'asexual' pathogenic yeast *Candida glabrata*. *Genome Biol* **4**: R10.

Wurgler-Murphy, S. M., T. Maeda, E. A. Witten & H. Saito, (1997) Regulation of the *Saccharomyces cerevisiae HOG1* mitogen-activated protein kinase by the *PTP2* and *PTP3* protein tyrosine phosphatases. *Mol Cell Biol* **17**: 1289-1297.

Zhang, X. & W. S. Moye-Rowley, (2001) *Saccharomyces cerevisiae* multidrug resistance gene expression inversely correlates with the status of the F(0) component of the mitochondrial ATPase. *J Biol Chem* **276**: 47844-47852.

Zupancic, M. L., M. Frieman, D. Smith, R. A. Alvarez, R. D. Cummings & B. P. Cormack, (2008) Glycan microarray analysis of *Candida glabrata* adhesin ligand specificity. *Mol Microbiol* **68**: 547-559.

Image references

Figure 1. **A)** www.bath.ac.uk/bio-sci/research/profiles/wheals-a.html);
C) (Berman & Sudbery, 2002); **D)** + **E)** www.mycology.adelaide.edu.au

Figure 3. **A)** + **B)** http://www.doctorfungus.org/;
C) www.oralcancerfoundation.org/dental/candida.htm;
D) www.merck.com/mmpe/sec14/ch180/ch180e.html

All other figures and tables are cited in the text and corresponding references are found in the chapter 7 “literature”.

“Ich habe mich bemüht, sämtliche Inhaber der Bildrechte ausfindig zu machen und ihre Zustimmungzur Verwendung der Bilder in dieser Arbeit eingeholt. Sollte dennoch eine Urheberrechtsverletzung bekannt werden, ersuche ich um Meldung bei mir.“

8 Manuscript: Transcriptional rewiring of the *Candida glabrata* cell wall biosynthesis kinase *CBK1*

This section is shown in a manuscript format containing: Title Page, Abstract, Introduction, Materials and Methods, Results, Discussion, Acknowledgement, Figure Legends, Figures and Tables, Supplementary Materials, References

Transcriptional rewiring of the *Candida glabrata* cell wall biosynthesis kinase *CBK1*

Tobias Schwarzmüller[1], Walter Glaser[1], and Karl Kuchler[1,§]

[1] Medical University Vienna, Max F. Perutz Laboratories, Christian Doppler Laboratory for Infection Biology, Department of Medical Biochemistry, A-1030 Vienna, Austria;

Keywords:
Candida glabrata, virulence, *CBK1*, pathogenicity, cell wall, separation defect

§ Corresponding author - to whom correspondence and reprint requests can be addressed:
Karl Kuchler
Medical University Vienna
Max F. Perutz Laboratories
Christian Doppler Laboratory for Infection Biology
Department of Medical Biochemistry
Dr. Bohr-Gasse 9/2, A-1030 Vienna, Austria
Phone: +43-1-4277-61807; FAX: +43-1-4277-9618
E-mail: karl.kuchler@meduniwien.ac.at

Abstract

Candida glabrata is an opportunistic human fungal pathogen. Like *Candida albicans*, it can cause life-threatening systemic infections in immunocompromised individuals. Cellular morphogenesis has to be controlled in all organisms. The RAM (Regulation of Ace2p transcription factor and polarized Morphogenesis) network controls polarized growth, cell separation and the induction of daughter cell-specific genetic programs in yeast. Inactivation of the *C. glabrata* RAM network transcription factor Cg*ACE2* results in a hypervirulent strain defective in cell separation.

We generated a *C. glabrata* mutant, lacking Cg*CBK1*, which results in a similarly severe growth defect as seen in the Cg*ace2*Δ mutant. Cg*cbk1*Δ cells are unable to separate properly, form large cell aggregates, and display very large growing, round cells. Exposure to various cell wall-perturbing compounds results in growth sensitivity of the Cg*cbk1*Δ mutant. Interestingly, transcriptional profiling identified not only genes regulated by CgCbk1 via the transcription factor CgAce2 but also differential expression of a Cg*FLO9* homologue in Cg*cbk1*Δ cells. In addition, CgCbk1 appears to control several amino acid biosynthesis-related and metabolic genes.

The cause for the hypervirulence phenotype of the Cg*ace2*Δ mutant is unknown. Remarkably, cells lacking either Cg*CBK1* or Cg*ACE2* are not phagocytosed by murine bone marrow-derived macrophages (BMDM) *in vitro*. The inability to internalize the large cell aggregates formed by the mutants is reversed when the cell aggregates are separated into single cells prior to infection or by complementation with the endogenous gene. Thus, the hypervirulent phenotype of the Cg*ace2*Δ mutant may be due to a change in the immune response of the macrophages, which are unable to phagocytose these large cells aggregates.

Introduction

Most cells are polarized, including unicellular organisms as well as cells in multicellular organisms. Cell polarity is characterized by an asymmetry in cell shape, protein distributions and cell functions (Nelson, 2003). Establishment and maintenance of cell polarity are crucial for proper development and cell functions. Although different organisms and cell types differ in many aspects, the core mechanisms of cell polarity establishment seem to be similar, including assembly of the cytoskeleton, spindle orientation, vesicle delivery to the membrane and site selection for polarized growth (Nelson, 2003).

In *S. cerevisiae* the RAM (Regulation of Ace2p transcription factor and polarized Morphogenesis) network controls polarized growth and cell separation (Bidlingmaier *et al.*, 2001), as well as the induction of daughter cell-specific genetic programs (Colman-Lerner *et al.*, 2001, Nelson *et al.*, 2003). The transcription factor ScAce2 localizes to the daughter cell nucleus and is required for expression of distinct target genes, such as the chitinase Sc*CTS1* or the putative glucanase Sc*SCW11* (O'Conallain *et al.*, 1999, Colman-Lerner et al., 2001). Deletion of Sc*ACE2* causes cell separation defects, resulting in cell aggregation, pseudohyphal growth and agar invasion (King & Butler, 1998, Racki *et al.*, 2000).

The RAM signaling network consists of several proteins required for regulation of polarized growth and proper budding pattern. ScKic1, ScHym1 and ScSog2 form a complex, which acts upstream of the ScCbk1-ScMob2 complex (Nelson et al., 2003, Bidlingmaier et al., 2001, Colman-Lerner et al., 2001). Tao3 interacts with ScCbk1 and ScKic1 and may serve as a scaffold protein to allow ScCbk1 activation by ScKic1 (Nelson et al., 2003). ScCbk1 is a serine/threonine kinase, which is regulated itself by phosphorylation (Jansen *et al.*, 2006). Microarray analysis of the RAM network mutants revealed a unique cluster of coregulated genes, including Sc*CTS1*, Sc*SCW11* and Sc*DSE1-4* (Nelson et al., 2003, Colman-Lerner et al., 2001).

In the dimorphic human fungal pathogen *C. albicans*, the conserved RAM network controls cell separation and cell polarity as well (Song *et al.*, 2008). Deletion of Ca*CBK1* leads to a similar morphological defect as seen in baker's yeast. Ca*CBK1* is required for hyphae formation and the loss of RAM network genes results in hypersensitivity against cell wall-perturbing agents. Interestingly, the *C. albicans* RAM network is involved in regulation of ergosterol biosynthesis genes in response to azoles as demonstrated by RT-PCR analysis and azole-susceptibility of a homozygous Ca*mob2*Δ deletion strain (Song et al., 2008). In *Cryptococcus neoformans*, the RAM network also regulates cell separation and polarity. However, disruption of the RAM network pathway resulted in hyperpolarised cells (Walton *et al.*, 2006).

The monomorphic yeast *C. glabrata* is the second most frequent opportunistic human fungal pathogen representing up to 24 percent of all *Candida* isolates (Perlroth *et al.*, 2007,

Pfaller *et al.*, 2008, Borg-von Zepelin *et al.*, 2007). Like *C. albicans*, *C. glabrata* can cause a range of infections, ranging from superficial cutaneous and mucosal to life-threatening systemic infections in immunocompromised individuals (Horn *et al.*, 2009, Mean *et al.*, 2008, Pfaller & Diekema, 2007). Virulence factors of *C. glabrata* are less well-defined when compared to *C. albicans*, although both fungal pathogens share common virulence strategies. Importantly, *C. glabrata* exhibits an inherently reduced susceptibility to commonly used antifungal drugs such as azoles (Cross *et al.*, 2000, Pfaller *et al.*, 2004). Further, the regulation of epithelial adhesins (EPA) and biofilm formation by transcriptional silencing, as well as phenotypic switching are considered as virulence traits (Lachke *et al.*, 2002, Srikantha *et al.*, 2008). Other fungal virulence attributes such as filamentation (Kumamoto & Vinces, 2005b) and the secretion of hydrolases and phospholipases as known from *C. albicans* (Dolan *et al.*, 2004, Ghannoum, 2000, Naglik *et al.*, 2004) are absent or less pronounced in *C. glabrata*.

Inactivation of the *C. glabrata* transcription factor Cg*ACE2* results in a strain defective in cell separation, leading to the formation of large cell aggregates (Kamran *et al.*, 2004). Remarkably, the Cg*ace2*Δ mutant is hypervirulent in a neutropenic mice infection model. Vascular occlusion by the clumpy growth phenotype was excluded as a cause of the acute mortality. Mice infected with separated Cg*ace2*Δ mutant cells died as well, showing that the cells remain hypervirulent. The hypervirulence may at least partially be caused by drastically elevated levels of proinflammatory cytokines (Kamran et al., 2004). Analysis of the proteomic changes in the Cg*ace2*Δ mutant revealed 123 genes to be differentially regulated, including genes associated with metabolism, cellular transport and protein synthesis. Interestingly, the expression of several genes involved in morphogenesis and cell wall remodelling was down-regulated in the Cg*ace2*Δ mutant (Stead *et al.*, 2005).

Here, we describe a Cg*cbk1*Δ mutant, which displays a similar morphological defect as the *S. cerevisiae* Sc*cbk1*Δ and the Cg*ace2*Δ strains. Transcriptional profile analysis revealed a set of genes, involved in cell separation, which may be regulated directly or indirectly by the kinase CgCbk1. While CgCbk1 controls expression of Cg*CTS1* via CgAce2, the regulation of target gene Cg*FLO9* appears not to be controlled via CgAce2. Additionally, we show that Cg*cbk1*Δ and Cg*ace2*Δ mutants are not phagocytosed by murine bone marrow-derived macrophages (BMDM) *in vitro*, which may give an explanation for the observed cytokine release in mice infected with Cg*ace2*Δ cells.

Materials and Methods

Strains, gene disruption, plasmids and growth conditions.

All strains used in this study are listed in Supplementary Table 1. All deletion constructs were generated by a fusion PCR method using 500 bp long homology flanking regions and the dominant markers *NAT1* or *HYGB* (Goldstein & McCusker, 1999). *NAT1* was amplified with primers fp_NAT1-U2 and rp_NAT1-D2 from plasmid pJK863 (Shen *et al.*, 2005) to add constant U2 and D2 regions and ligated into pGEM-T vector (Promega). The resulting plasmid pTS50 was used to amplify the marker with primers 5M-marker and 3M-marker to add the barcode and overlap regions needed for fusion PCR (5'-ccgctgctaggcgcgccgtg-3'; 5'-gcagggatgcggccgctgac-3'). For gene disruption using the *HYGB* marker, we amplified the marker from plasmid pAG32 with primers fpHyg-U1 and rpHyg-D1, adding the overlap regions. Fusion PCR was carried out as described elsewhere (Noble & Johnson, 2005). Transformants were verified by colony PCR, using marker-specific primers (heukan2, heukan3) and gene-specific primers (5c, 3c primers) binding about 150 bp upstream and downstream of the homology regions. In addition, deletion strains were checked by loss-of-gene PCR, using a primer pair binding to the coding sequence. All oligonucleotide sequences used for gene disruption are listed in Table 2.

Rich medium (YPD) and synthetic medium (SC) were prepared as described elsewhere (Kaiser *et al.*, 1994). Unless otherwise indicated, all strains were grown routinely at 30°C.

For transformation, we used a modified electroporation protocol (Reuss *et al.*, 2004). 50 ml of a *C. glabrata* culture in YPD at an optical density of 600nm (OD_{600}) of 1.3 were harvested, washed with H_2O, resuspended in 1x TE buffer, 100mM LiAc and incubated at 30°C for 30 min with slow shaking (130rpm). After addition of 250 µl 1M DTT and further incubation at 30°C for 60 min (130rpm), 40 ml of H_2O were added and the cells were harvested at 1000g for 5 min at 4°C. The cells were washed with 25 ml H_2O, subsequently with 5 ml 1 M cold sorbitol, finally resuspended in 550 µl 1 M sorbitol and kept on ice until use. Sterile electroporation cuvettes were precooled on ice and loaded with a mix of 40 - 45 µl electrocompetent cells and 5 - 10 µl linear DNA deletion construct (app. 2 - 3 µg DNA). Cells were left on ice for 10 min and electroporation was carried out with a BioRad GenePulser (200Ω, 1.5kV, 25µF). For recovery, 950 µl YPD was added and cells incubated for 4 h shaking at 30°C, before plating on YPD supplemented with 200 µg/ml Nourseothricin (Werner Bioagents, Jena) or 300 µg/ml Hygromycin (Sigma). The plates were incubated for 48 hours at 30°C. Transformants were patched on YPD/Nourseothricin plates for colony PCR. Strains were transformed with plasmids essentially as described in (Gietz *et al.*, 1992).

For auxotrophic marker constructs, cells were recovered for 1 h at 30°C before plating on selective SC medium.

For complementation of the Cg*dse2*Δ, we used the pGEM-ACT plasmid harbouring Cg*SHO1* (Gregori *et al.*, 2007), replacing Cg*SHO1* with Cg*DSE2*, including endogenous promoter and terminator using EcoRI restriction sites. Cg*DSE2* was ligated into plasmid pBM51 (received from Biao Ma) for constitutive expression under control of the Sc*PGK1* promoter using XbaI and XhoI restriction sites. For constitutive expression of Cg*CBK1*, the coding sequence was ligated into pBM51, using the restriction sites BamHI and EcoRI, and the CDS of Cg*ACE2* was cloned into pBM51, using EcoRI and SalI.

Growth assays. Growth inhibition assays were performed by spotting serial dilutions of exponentially growing cultures adjusted to an optical density at 600nm (OD_{600}) of 0.1 on YPD and SC plates supplemented with various concentrations of SDS, calcofluor white (CW), congo red (CR), fluconazole (FLC), voriconazole (VOR), caspofungin (CF), $CaCl_2$ or on SC plates, lacking lysine, methionine or arginine and on minimal medium plates (YNB supplemented with (histidine,) leucine and tryptophan). Plates were incubated at 30°C for 48 hours and scanned with a HPScanjet G3010, using Adobe Photoshop CS3 software or pictures were taken with a digital Canon EOS Rebel camera using S&P Robotics imaging software (S&P Robotics, Canada).

Sonication. Cell aggregates were separated using a sonication bath. A 2 ml aliquot of cells with an OD_{600} of 1-2 was transferred into a thin-walled glass tube and subjected to three times 30 seconds of sonication interrupted by 30 second breaks on ice. Complete cell separation was checked under a microscope. The cell numbers were determined with a CASY cell counter (Schärfe Systems, Germany).

Microarray analysis. 50 ml cultures of the *C. glabrata* background strain HTL and the Cg*cbk1*Δ deletion strain were grown in YPD to an OD_{600} of 1, harvested, washed and immediately frozen. Total RNA was prepared by hot phenol method (Sambrook *et al.*) and treated with DNaseI. RNA was additionally precipitated with 2 M LiCl and RNA concentration was measured on a Nanodrop (ThermoScientific, USA) and quality checked, using a Bioanalyzer (Agilent Technologies, Austria). Three independent biological RNA replicates were prepared. Samples of 25 µg total RNA were used for cDNA synthesis using 200 U of Superscript II reverse transcriptase (Invitrogen, USA) with either Cy3-dCTP or Cy5-dCTP (GE Healthcare, Austria). Labelled cDNAs were pooled, and the RNA hydrolyzed for 20 minutes in 50 mM NaOH at 65°C, followed by neutralization with acetic acid and probe clean-up with CyScribe GFX purification kit (GE Healthcare, Austria). Microarrays were incubated

for 45 min at 42°C in prehybridization solution (4 x SSC, 0,1% SDS, 10 mg/ml BSA). Hybridization to *C. glabrata* whole-genome cDNA microarrays was done in hybridisation solution (4 x SSC, 0.1% SDS) at 37°C overnight. Microarrays were washed for one minute in 2 x SSC, 0.1% SDS at 42°C, followed by a 5 minutes wash in 2 x SSC, 0.1% SDS at 42°C and a 10 minutes wash in 0,1 x SSC, 0,1% SDS at room temperature. Microarrays were washed then for two minutes in 0.1 x SSC, 0.1% SDS at room temperature and in 0.01 x SSC for 30 seconds. Glass slides were dried for 3 minutes at 500 rpm in a tabletop centrifuge, scanned on an Axon 4000B scanner (Molecular Devices), analyzed and normalized using Gene Pix Pro4.1 software (Axon). All microarray experiments were carried out with three independent RNA preparations (three biological replicates plus one technical) and dye swaps were performed. For preprocessing, the arrays were background corrected with the normexp method and normalized, using the print-tip loess method of the limma bioconductor/R package (Smyth, 2005). To identify differentially expressed genes a linear model was used with cut-off values of 0.01 for the adjusted p-value and a 2-fold expression change. Custom made DNA microarrays and protocols were obtained from the laboratory of Dr. Steffen Rupp, Fraunhofer Institute, Stuttgart. Oligonucleotides were obtained from Dr. Ken Haynes, Imperial College, London.

qPCR. Primers for quantitative real-time PCR were designed, using PerlPrimer software (http://perlprimer.sourceforge.net/) according to recommendations and tested in a gradient PCR. RNA was extracted by the hot phenol method and treated with DNaseI as described above. Three independent biological replicates were prepared. Reverse transcription was performed in triplicates on 2 µg of total RNA each according to the manufacturer's instructions (Fermentas First-strand cDNA synthesis Kit) with 100 pmol oligo$(dT)_{18}$ and 100pmol random hexamer primer. The sample mixes (4 µl 5 x reaction buffer, 0,5 µl RiboLock RNase inhibitor (20U), 2 µl 10 mM dNTP mix, 1 µl M-MuLV Rev. Transcriptase (200U)) were incubated for 10 min at 25°C followed by 60 min at 42°C and final 10 min at 72°C, diluted 1:10 in H_2O and stored at -20°C. All cDNA and RNA samples were tested in a regular PCR for DNA amplification with the specific primers. Quantitative PCR was carried out in triplicates on a Realplex Mastercycler (Eppendorf, Austria) monitoring cDNA amplification quantitatively by SYBR Green incorporation. The conditions for a 20 µl reaction were as follows: 2 µl cDNA template, 7 µl H_2O, 0.75 µl each primer (375 nM), 10 µl 2 x Mastergreen mix (Eurogentec, Belgium); 95°C 5 min, 40 cycles 95°C 10 s, 62°C 10 s, 72°C 20 s; melting curve 95°C 20 s, 62°C – 94°C gradient, 95°C 15 s. For analysis the Realplex data analysis program was used.

Microscopy. Microscopy was done on an Olympus CellR life imaging station microscope (Olympus, Austria). Pictures were captured with a Hamamatsu ORCA-ER camera. Cells were grown to exponential growth phase, harvested and washed twice with water before transferring them onto microscopy slides. For chitin staining, cells in the early exponential growth phase were incubated with calcofluor white (Fluorescent Brightener 28, Sigma-Aldrich) at a final concentration of 50 µg/ml in medium for 1 hour at room temperature in the dark. Cells were washed twice with water and transferred to a microscopy slide and observed with a DAPI filter. Colony pictures were taken with a Zeiss Discovery.V12 Stereomicroscope and a AxioCam MRc5 camera (Zeiss, Germany). Cells were grown in liquid YPD to logarithmic phase, diluted and plated on a fresh YPD plated. After 3 days of growth at 30°C pictures of the colony morphology were taken.

Infection experiments and FACS analysis. Murine bone marrow-derived macrophages (BMDMs) were prepared and cultured as described elsewhere (Frohner et al., 2009). BMDMs (bone marrow-derived macrophages) media contained DMEM, 10% heat-inactivated FCS, 20% L-conditioned medium. BMDMs were routinely grown at 37°C and 5 % CO_2.
BMDMs were seeded into 24 well dishes 24 hours prior to infection. Fungal cells from an exponential culture were prestained with FUN-1 for 20 minutes in PBS buffer at 30°C in the dark, washed twice with PBS and used for infection of BMDMs at an MOI of 5:1 (*C. glabrata* : BMDMs). Fungal cells were added in 100 µl aliquots and cells were co-incubated at 37°C, 5% CO_2 for 90 minutes. During addition of the fungal cells, BMDMs were kept on ice. As a phagocytosis negative control, BMDMs were infected the same way in parallel but kept on ice for 90 minutes. After infection, non-phagocytosed fungal cells were washed away by five extensive washes with PBS. BMDMS were collected with a tissue scraper and resuspended in 1 ml PBS, 0.1 %BSA. To determine the number of macrophages with internalized fungal cells FACS analysis was performed (10,000 counts), using a FACSCalibur flow cytometer (Becton Dickinson, USA), and data were analyzed with FlowJo software (Treestar, USA).
For microscopy, macrophages were seeded onto round glass cover slides and infection was performed essentially as described above. After infection, glass slides were washed in cold PBS and fixed in 2 % paraformaldehyde. After 1 hour of incubation at 4°C in blocking buffer (PBS, 4 % BSA), a *Candida* cell wall-specific primary antibody was added (1:500) in blocking buffer and incubated at 4°C overnight. Secondary Cy5-conjugated anti-rabbit antibody (1:350; Jackson ImmunoResearch, UK) was added after three PBS washes and incubated for 2 hours at RT in the dark. Cover slides were washed in PBS and inverted on a drop of mounting medium (Dako Cytomation, Denmark) containing 1 µg/ml DAPI. Slides were observed, using DIC and fluoresceine, DAPI and Cy5-specific filters on an Olympus CellR life imaging station microscope (Olympus, Austria).

Results

The kinase CgCbk1 is involved in determination of cell morphology.

Screening our *C. glabrata* gene deletion library (Schwarzmüller et al., unpublished) for colony morphology phenotypes, we found a mutant with a pronounced wrinkled colony and cell morphology. This mutant lacked the cell wall biosynthesis kinase gene Cg*CBK1*. ScCbk1 is the major regulator of the RAM network in *S. cerevisiae* and controls the expression of cell separation genes via the transcriptional regulator ScAce2. In addition, the Cg*ace2*Δ deletion strain has been associated with hypervirulence (Kamran et al., 2004). Therefore, we investigated the role of Cg*CBK1* in cell separation in more detail. To compare the phenotypes of Cg*cbk1*Δ and Cg*ace2*Δ deletion strains, we also generated a gene deletion strain lacking Cg*ACE2*. Further, Cg*DSE2* is a possible target gene of CgCbk1. The putative glucanase CgDse2 may be involved in cell separation by septum degradation.

The Cg*cbk1*Δ and Cg*ace2*Δ gene deletion strains displayed similarly wrinkled colony morphologies, while the Cg*dse2*Δ mutant showed smooth colonies, which get slightly wrinkled only after several days of growth (Figure 1A). However, the cellular morphology of the Cg*dse2*Δ strain was clearly affected, with cells displaying a pseudohyphal growth phenotype, which indicated a separation defect. In contrast, the Cg*cbk1*Δ mutant formed large cell aggregates very similar to the appearance of the Cg*ace2*Δ strain (Kamran et al., 2004). Although the morphology of both strains looked similar, differences were visible. Cells of the Cg*ace2*Δ strain were composed of ellipsoid, wild type-sized cells, which were unable to separate properly. Cells of the Cg*cbk1*Δ mutant had a heterogeneous appearance. All Cg*cbk1*Δ cells displayed a pronounced round cell morphology. In addition, we observed that some cells grew very large, forming large vacuoles (Figure 1A, lower panel). When compared to the single cells of the wild type strain or the Cg*dse2*Δ mutant, the large cell aggregates of the Cg*cbk1*Δ and Cg*ace2*Δ settled much faster (Figure 1B). After 30 minutes on the bench, both strains formed a loose pellet. This was not observed for the wild type strains or the complemented strains, carrying the wild type allele on a plasmid.

In *S. cerevisiae*, ScAce2 regulates the expression of the chitinase Sc*CTS1* (Dohrmann *et al.*, 1992). This seems to be true for the *C. glabrata* homologue as well (Kamran et al., 2004). Therefore, the lack of Cg*ACE2* may lead to decreased expression of Cg*CTS1* and in consequence to the accumulation of chitin in the cell wall. Likewise, a Cg*cbk1*Δ mutant may have more chitin embedded in the cell wall. To investigate the cell separation defect more closely, we stained the cells with calcofluor white, which interferes with cell wall chitin. Chitin was mainly localized to the bud neck of the cells in the Cg*ace2*Δ cell aggregate (Figure 2). This localization is similar as the chitin distribution in the parental HTL strain. However, in the middle of the cell aggregate much more chitin appeared to be

accumulated. In contrast, in the Cg*cbk1*Δ cell aggregates, the chitin distribution appeared to be more dislocalized and some large cells were intensively stained by calcofluor white, suggesting a more severe defect in cell wall assembly and maintenance.

Due to its aggregation phenotype, it is difficult to directly compare growth of the Cg*cbk1*Δ mutant to the wild type. To reassure that the Cg*cbk1*Δ cells have a cell separation defect and do not simply flocculate during growth, we separated the cells by sonication in a water bath. Three subsequent 30 seconds sonication steps were used to separate Cg*cbk1*Δ, Cg*ace2*Δ and wild type cells. This treatment did not influence the viability, as tested by CFU counts (data not shown). The separated cells were then grown in YPD and the degree of cell aggregation over time was determined by OD measurement directly after inoculation, and after three and seven hours of growth at 30°C. At these time points, aliquots were diluted in water, mixed and the OD_{600} was measured after 30 minutes to give the cell particles time to settle. At the three hours time point, there was no difference between mutants and wild type cells (Figure 3A). After seven hours, a clear difference was seen between wild type and mutant cells. Cg*cbk1*Δ and Cg*ace2*Δ strains settled almost completely in 30 minutes, indicating that the initially separated cells formed aggregates again. In contrast, the wild type and the complemented strains did not settle so fast and showed high OD_{600} values.

To further confirm the cell separation defect, we filmed the growth of the Cg*cbk1*Δ mutant and compared it to the growth of the wild type strain, using a CellASIC microfluidic platform (CellASIC, USA). The growth of sonication-separated cells was monitored over 12 hours, taking single pictures every 10 minutes. The hourly pictures of the movie demonstrate that the Cg*cbk1*Δ cells formed cell plaques over time due to their inability to separate properly (Figure 3B). Also the round cell morphology of the Cg*cbk1*Δ mutant was very apparent (magnified picture). At the seven hour time point the formation of large cells with large vacuoles is clearly visible (black arrows). In contrast, the wild type parental cells formed ellipsoid cells, displaying a bipolar budding pattern like it is usually seen for diploid *S. cerevisiae* cells (Figure 3B).

A Cg*cbk1*Δ deletion strain is sensitive to cell wall-perturbing agents.

In *S. cerevisiae*, ScCbk1 regulates several genes implicated in cell wall remodelling and maintenance, including the chitinase Sc*CTS1*, the putative daughter-specific genes Sc*DSE1-4* and the glucanase Sc*SCW11* (Colman-Lerner et al., 2001). To analyze the growth phenotype of the Cg*cbk1*Δ strain in more detail, we spotted cells on media containing various cell wall-perturbing agents, such as calcofluor white (CW), congo red (CR), SDS and the antifungal drug fluconazole (FLC). Cg*cbk1*Δ cells were unable to grow on SDS-supplemented media but grew on CW, CR and FLC (Figure 4A). Complementation of Cg*cbk1*Δ cells with the endogenous *C. glabrata* gene resulted in restoration of the wild type phenotype on YPD but only partially restored growth on SDS. Interestingly, Cg*ace2*Δ cells

were only slightly impaired in growth on SDS, indicating that CgCbk1 may have a broader effect on cell wall biogenesis then CgAce2. Deletion of Cg*SCW11* (CAGL0E02915g) did not result in a growth defect. We could not generate a strain lacking the other Cg*SCW11* homologue CAGL0A01474g to test its growth phenotypes.

Due to the formation of the large cell aggregates, it was difficult to prepare comparable inocula of the Cg*cbk1*Δ and Cg*ace2*Δ strains for the spotting assays. Therefore, we also separated the cells by sonication to be able to prepare serial dilutions, starting from the same cell number. The growth assays were repeated, testing for sensitivity to CW, CR, $CaCl_2$ and caffeine (CAF), and susceptibility to the antifungal drugs FLC, voriconazole (VOR) and caspofungin (CF). In this modified growth assay, the Cg*cbk1*Δ strain showed growth sensitivities to all tested compounds as well as a slight susceptibility to azole drugs. Exposure to the glucan synthase inhibitor CF resulted in a very pronounced growth defect (Figure 4B). Interestingly, the Cg*ace2*Δ cells displayed no growth deficiency under any tested condition. The Cg*cbk1*Δ strain also grew slower on SC medium when compared to the other strains. Complementation of Cg*cbk1*Δ cells with the endogenous Cg*CBK1* gene under control of the Sc*PGK1* promoter (pBM51-Cg*CBK1*) resulted in normal growth.

Taken together, the Cg*cbk1*Δ deletion strain showed several growth deficiencies under cell wall-perturbing conditions, indicating that its cell wall composition is severely changed. Interestingly, the lack of Cg*ACE2* did not result in similar phenotypes. Therefore, it seems likely that CgCbk1 controls one set of genes, which may be regulated through the transcriptional regulator CgAce2, and an additional different set of genes, which is CgAce2-independently regulated. Indeed, CgAce2 may only control a small set of target genes subject to CgCbk1.

Transcriptional profiling of the Cg*cbk1*Δ deletion strain revealed regulation of genes implicated in cell wall biogenesis and metabolism.

ScAce2 is a transcription factor required for expression of early G1-specific genes. After cytokinesis it localizes to the daughter cell nucleus. In *S. cerevisiae*, ScCbk1 controls activity of ScAce2 by phosphorylation (Nelson et al., 2003, Bidlingmaier et al., 2001, Colman-Lerner et al., 2001). Since deletion of Cg*CBK1* resulted in a *C. glabrata* mutant displaying growth phenotypes different from the Cg*ace2*Δ strain, we decided to perform microarray analysis, comparing the HTL background strain with the Cg*cbk1*Δ deletion strain under normal growth conditions in YPD at 30°C to identify potential CgCbk1 target genes. Therefore, we used custom-made *C. glabrata* microarray chips (spotting and preparation of arrays were done by Dr. Steffen Rupp, Fraunhofer IGB, Stuttgart; oligonucleotides were kindly provided by Dr. Ken Haynes, Imperial College, London). Three biological replicates of total RNA were prepared, and four microarray experiments (three biological plus one

technical replicate) were performed, including dye swaps. For preprocessing, the arrays were background corrected with the normexp method and normalized using the print-tip loess method of the limma bioconductor/R package (Smyth, 2005). To identify differentially expressed genes a linear model was used with cut-off values of 0.01 for the adjusted p-value and a 2-fold expression change.

In total, 99 genes were found to be differentially regulated at least two-fold. Some 70 genes were upregulated and 29 genes were down-regulated (Figure 5, Table 1 & 2). About one third of the genes represented uncharacterized or unknown ORFs. The largest group of CgCbk1-regulated genes comprised cell wall biogenesis genes. The expression of several transcriptional regulators was also affected in the Cg*cbk1*Δ mutant, as well as genes involved in amino acid and nucleic acid biosynthesis, metabolism, plasma membrane transport and signaling genes. Moreover, expression of a heterogeneous group of genes implicated in cytokinesis, fatty acid biosynthesis, actin organization and chromatin remodelling appeared to be controlled by CgCbk1.

As expected, the expression of Cg*DSE2*, Cg*CTS1*, Cg*SCW11* genes was more than 2.5 fold down-regulated in the microarray experiments (Table 2). Several other cell wall genes, such as Cg*FLO9* and Cg*TIR4* homologues were also among the strongest down-regulated genes, as well as Cg*ROX1* and two ORFs (CAGL0A02277g, CAGL0A02255g) homologous to the uncharacterized baker's yeast ORF YCL049C (Table 2). Notably, other cell wall genes, such as Cg*SED1*, Cg*FLO1*, Cg*EXG1*, Cg*SCW4*, Cg*CRH1* were upregulated most strongly (Table 1). In addition, expression of amino acid biosynthesis (Cg*ARG1*, Cg*ARG4*, Cg*TMT1*), plasma membrane transporters (Cg*PPZ1*, Cg*MCH5*) and metabolism (Cg*GLK1*, Cg*ENO1*) genes was also increased. Many genes with unknown functions displayed elevated transcript levels as well. The microarray analysis also revealed differential regulation of the cell wall integrity pathway genes, such as Cg*SLT2* and Cg*RLM1*, suggesting that the lack of Cg*CBK1* leads to cell wall defects activating the cell wall integrity pathway.

To confirm the microarray results, quantitative RT-PCR was performed on cell wall-associated genes (Figure 6). As expected, the daughter cell-specific gene Cg*DSE2* and the chitinase encoding gene Cg*CTS1* were strongly down-regulated in both deletion strains Cg*cbk1*Δ and Cg*ace2*Δ (Figure 6A). Expression of Cg*CBK1* itself was not changed in a Cg*ace2*Δ strain, Cg*ACE2* expression was also not drastically affected by the lack of Cg*CBK1*. In *S. cerevisiae*, ScCbk1 is thought to regulate ScAce2 activity by phosphorylation (Sbia *et al.*, 2008, Colman-Lerner et al., 2001). Thus, CgCbk1 may also not regulate expression of CgAce2 but control its activation, which would explain that mRNA levels remained mainly unchanged. Expression of Cg*DSE2* and Cg*CTS1* was dependent on CgCbk1 and CgAce2 because Cg*DSE2* and Cg*CTS1* transcriptional levels were drastically

reduced in the Cg*cbk1*Δ and Cg*ace2*Δ deletion strains. The regulation of both genes seems to be controlled by similar factors as in *S. cerevisiae*. A strain lacking Cg*DSE2* had no effect on expression of Cg*CTS*, Cg*ACE2* and Cg*CBK1*. Expression levels in the ATCC2001 and the HTL strain were similar for all tested genes.

The highest upregulated gene in the Cg*cbk1*Δ mutant was Cg*SED1* as confirmed by quantitative RT-PCR. Its *S. cerevisiae* homologue encodes a major stress induced structural GPI-anchored protein, which is required for compensation of cell wall instability in mutants with GPI-anchored protein defects (Hagen *et al.*, 2004). Expression of Cg*KSS1* and Cg*FLO11* was also highly induced (Figure 6B). Cg*KSS1* is the homologue of a baker's yeast MAP-kinase, controlling filamentous growth (Chen & Thorner, 2007). ScKss1 is the MAPK, which regulates expression of flocculins in *S. cerevisiae*. Cg*FLO11* is the closest homologue of a GPI-anchored glycoprotein of the flocculin family (*FLO* genes) in *S. cerevisiae*, which is required for pseudohyphal and invasive growth, flocculation, and biofilm formation (Lambrechts *et al.*, 1996, Guo *et al.*, 2000). Remarkably, the *FLO* gene family of *S. cerevisiae* is homologous to the *C. glabrata*-specific *EPA* family. The *EPA* genes comprise a family of some 23 genes encoding for GPI-anchored adhesins, which are implicated in *C. glabrata* virulence (Cormack *et al.*, 1999, De Las Penas *et al.*, 2003, Domergue *et al.*, 2005).

Sc*SCW11* encodes a cell wall protein with similarity to glucanases and is coregulated with other RAM network targets, such Sc*CTS1* and Sc*DSE1-4* (Nelson et al., 2003, Colman-Lerner et al., 2001). *C. glabrata* harbors two homologous Cg*SCW11* genes (CAGL0E02915g and CAGL0A01474g), both of which showed decreased transcript levels in Cg*ace2*Δ and Cg*cbk1*Δ cells.

Interestingly, transcript levels of Cg*FLO9*, another *FLO* homologue, were unchanged in Cg*ace2*Δ cells, while in the Cg*cbk1*Δ deletion strain its expression was strongly decreased (Figure 6C). When compared to the expression of Cg*DSE2*, Cg*CTS1*, Cg*SCW11*, Cg*KSS1*, Cg*SED1*, and Cg*FLO11*, it gets apparent that Cg*FLO9* expression levels are only affected in Cg*cbk1*Δ, supporting the hypothesis that CgCbk1 may control a specific subset of cell wall genes independently of CgAce2.

Taken together, the microarray data and the spotting assays show that Cg*CBK1* may control or influence the transcription and/or activity of genes with various functions, including genes implicated in cell separation and morphology

The Cg*cbk1*Δ deletion strain has a growth defect on amino acid-depleted medium.

Remarkably, the expression of many genes involved in metabolism, amino acid biosynthesis and several plasma membrane transporters was also increased (Figure 5, Table 1). Upregulation of Cg*ARG1*, Cg*ARG4*, Cg*ARG8*, Cg*TMT1*, Cg*MCH5*, Cg*CAN1*, and Cg*PUT1* suggested that CgCbk1 has an influence on amino acid biosynthesis and

metabolism genes. In addition, the big vacuoles observed in the Cg*cbk1*Δ cells (Figure 1 & 2) may also be due to metabolic defects indicated by the transcriptional changes of these genes.

To test growth deficiencies of the Cg*cbk1*Δ mutant on amino acid-depleted medium, we spotted the strain on minimal medium and on medium lacking arginine, lysine or methionine (Figure 7). In contrast to the Cg*ace2*Δ and Cg*dse2*Δ, the Cg*cbk1*Δ strains displayed a strong growth defect on minimal medium and medium depleted of both lysine and methionine. On medium lacking only one of the amino acids the Cg*cbk1*Δ mutant showed a slight growth deficiency. This effect was seen much stronger for the cells separated by sonication before spotting, although even visible for not sonicated cells (Figure 7).

Taken together, the microarray data and the spotting assays show that the lack of Cg*CBK1* causes transcriptional changes, leading to metabolic defects and dependence on the supply of exogenous amino acids.

Cg*cbk1*Δ and Cg*ace2*Δ deletion strains are not phagocytosed by murine bone marrow-derived macrophages.

Inactivation of the *C. glabrata* transcription factor Cg*ACE2* results in a strain defective in cell separation, leading to the formation of large cell aggregates (Kamran *et al.*, 2004). Moreover, the Cg*ace2*Δ mutant is hypervirulent in a neutropenic mice infection model. Although the cause for this hypervirulence is not clear, drastically elevated levels of proinflammatory cytokines, such as TNFα and IL-6, may explain the acute mortality of the mice (Kamran et al., 2004).

Phagocytic cells such as macrophages and dendritic cells represent the first defence line of the mammalian immune system. *In vitro*, small particles are readily internalized by macrophages, while phagocytosis of large particles (>100µm) is hindered (Hernanz-Falcon *et al.*, 2009). Therefore, it may be possible that macrophages are unable to phagocytose the large cell aggregates, which are formed by cells lacking Cg*CBK1* or Cg*ACE2*.

To test the hypothesis, we infected murine bone marrow-derived macrophages (BMDM) with *C. glabrata* wild type, Cg*ace2*Δ and Cg*cbk1*Δ cells and additionally compared the effect of cells separated by sonication and unseparated cell aggregates. Fungal cells were prestained with the FUN-1 dye (Millard *et al.*, 1997) before infection and incubated with BMDMs for 90 minutes to allow phagocytosis. For microscopic analysis, non-phagocytosed cells were detected with an anti-*Candida* antibody and nuclei of BMDMs were DAPI stained.

After 90 minutes of infection most of the wild type cells were phagocytosed as seen by the low number of undetected non-phagocytosed cells and the large number of FUN-1 stained cells inside the macrophages (Figure 8). In contrast, the large cell aggregates

detected by the anti-*Candida* antibody suggests that these cell aggregates of the Cg*cbk1*Δ and Cg*ace2*Δ mutants were attached to the macrophages but not phagocytosed. However, separation of these cell aggregates into single cells reversed that phenotype and resulted in internalization of the majority of cells (Figure 8).

This observation was also confirmed by FACS analysis (Figure 9). About 80 % of wild type cells were phagocytosed, while only a very low number of macrophages carried labelled fungal cells when infected with the Cg*cbk1*Δ (4 %) and Cg*ace2*Δ (1 %) mutants. Some 68 % of BMDMs carried Cg*cbk1*Δ cells separated by sonication and 67 % internalized complemented Cg*cbk1*Δ cells, carrying a plasmid with the endogenous Cg*CBK1* gene. This indicated that the BMDMs were unable to internalize the large cell aggregates formed by the mutants.

In summary, murine BMDMs appeared to be unable to phagocytose the large cell aggregates formed by the Cg*cbk1*Δ and Cg*ace2*Δ mutants. This effect was not due to putative changes in the cell wall but rather due to the size of the cell particles, since uptake of separated cells was almost at wild type levels.

Discussion

This study shows that the deletion of the cell wall biosynthesis kinase Cg*CBK1* in *C. glabrata* results in a severe cell separation defect, which is similar to the phenotype of the Cg*ace2*Δ mutant. In addition to the known phenotype, we could show that the Cg*cbk1*Δ deletion strain is sensitive to a variety of compounds, affecting the cell wall. Moreover, transcriptional profiling led to the identification of differentially expressed genes and to the hypothesis that CgCbk1 controls at least two different sets of genes. Expression of one set is CgAce2-dependent, the other one may be regulated by CgCbk1 directly. Finally, the large cell aggregates of the Cg*cbk1*Δ and Cg*ace2*Δ deletion strains are not well phagocytosed by BMDMs *in vitro*, suggesting an explanation for the hypervirulent phenotype observed for the Cg*ace2*Δ mutant.

The particular morphology of the Cg*cbk1*Δ deletion strain, its growth phenotypes and the results of the transcriptional profiling strongly indicate that its cell wall composition is severely altered. To be sure that the cells do not separate properly instead of exhibiting regular flocculation, we developed a sonication protocol to separate the cells. As expected from the *S. cerevisiae* mutant, the separated cells regrew from single cells to large cell aggregates and did not simply flocculate after some time of growth. Interestingly, we observed that the wild type cells showed a bipolar budding pattern, which is usually seen for diploid *S. cerevisiae* cells. The cell wall defects of the Cg*cbk1*Δ strain are further confirmed by several other facts. First, the expression of the chitinase Cg*CTS1* and the daughter-specific putative glucanase Cg*DSE2* is abandoned in the Cg*cbk1*Δ mutant. Second, the chitin distribution appears to be affected in the Cg*cbk1*Δ strain. This would be expected in a strain, which is unable to express Cg*CTS1* and consequently, is impaired in chitin degradation. Third, cells lacking Cg*CBK1* are sensitive to various cell wall-perturbing agents. Finally, many cell wall genes are differentially regulated in the Cg*cbk1*Δ strain, with Cg*SED1* most strongly upregulated. In *S. cerevisiae*, ScSed1 is a major stress-induced structural GPI-anchored protein. In cell wall mutants, ScSed1 is highly abundant and required for compensation of cell wall instability (Hagen *et al.*, 2004).

Transcriptional profiling of the Sc*cbk1*Δ and other components of the RAM signaling network in *S. cerevisiae* demonstrated the differential regulation of a specific gene cluster, including Sc*CTS1*, Sc*SCW11* and Sc*DSE1-4* (Colman-Lerner et al., 2001, Nelson et al., 2003). We found *C. glabrata* homologues of these genes differentially regulated, suggesting that the control of cell separation is a conserved function in both organisms. A series of other cell wall-related genes implicated in glucan assembly, is additionally up- or down-regulated, indicating that the cell wall of the Cg*cbk1*Δ strain is severely affected.

Most interestingly, expression of Cg*FLO9* (CAGL0L13332g) is down-regulated in the Cg*cbk1*Δ mutant but not affected in the Cg*ace2*Δ strain, which displays Cg*FLO9* expression

levels similar to the wild type. In contrast, Cg*FLO1* expression is induced in both, Cg*cbk1*Δ and Cg*ace2*Δ strains. The baker's yeast homologues Sc*FLO1* and Sc*FLO9* belong to the flocculin gene family (Verstrepen & Klis, 2006). Several of these flocculins (Sc*FLO1*, Sc*FLO5*, Sc*FLO9*, Sc*FLO10*) are implicated in cell-cell adhesion, while Sc*FLO11* is necessary for adhesion to substrates (Guo et al., 2000, Verstrepen & Klis, 2006). The down-regulation of Cg*FLO9* solely in the Cg*cbk1*Δ mutant suggests that CgCbk1 may control a set of genes independently of the transcription factor CgAce2. In addition, there are also differences between the *C. glabrata* and the baker's yeast RAM network for other target genes. For instance, *C. glabrata* harbors two homologues of the glucanase Sc*SCW11*. *S. cerevisiae* encodes four daughter-specific genes Sc*DSE1-4*, while no Sc*DSE4* homologue can be found in *C. glabrata*. The flocculin family is also related to the *C. glabrata EPA1* gene family, encoding adhesins responsible for adherence to human epithelial cells (Cormack et al., 1999, De Las Penas et al., 2003), and to the *ALS* genes of *C. albicans* (Hoyer, 2001, Kumamoto & Vinces, 2005a). In general, *C. glabrata* harbors a large number of adhesin-like GPI-anchored proteins, including the EPA gene family and the recently identified putative adhesins Awp1-4 (de Groot *et al.*, 2008). Interestingly, the abundance of these proteins in the cell wall of *C. glabrata* partly depends on the growth stage. All these proteins may contribute to *C. glabrata* virulence through modification of the cell wall properties and therefore its adaptability to changing environmental conditions. Taken together, while the main functions of the RAM network seem to be conserved in of *C. glabrata*, differences can be found in the set of target genes and the transcriptional regulators, putatively affecting the composition of the cell wall.

Beside several cell wall genes, CgCbk1 also seems to regulate genes involved in amino acid biosynthesis and other metabolic functions. This hypothesis is supported by a number of genes, which are found upregulated in the microarray analysis and the growth defect displayed by Cg*cbk1*Δ cells on medium lacking methionine, lysine or arginine. The defects in the amino acid biosynthesis pathway may cause depletion of some metabolites. This starvation may explain the formation of the large vacuoles, which become visible in the sporadic very large cells of the Cg*cbk1*Δ cell aggregates. Large vacuoles often indicate starving cells, which use autophagy to survive nutrient starvation conditions (Levine & Klionsky, 2004). However, the deletions were made in a triple-auxotrophic background, which influence the amino acid biosynthesis. Thus, it is not unlikely that the observed growth defects and changes in gene expression are due to synergistic effects.

The hypervirulent phenotype of the Cg*ace2*Δ mutant raises two questions. First, does a Cg*cbk1*Δ strain cause a similar strong phenotype in infected mice? Second, do the differences in the cell aggregates and the cell wall composition result in a different immune response? Drastically elevated levels of proinflammatory cytokines, such as TNFα and IL-6,

in mice infected with Cg*ace2*Δ cells, may give an explanation for the acute mortality of the mice (Kamran et al., 2004). Fungal pathogens are recognized by pattern-recognition receptors (PRR) of macrophages and dendritic cells. Dectin-1 is a PRR and can function as phagocytic receptor, mediating internalization of fungal cells and expression of cytokine response genes (Gantner *et al.*, 2003, Gantner *et al.*, 2005, Goodridge *et al.*, 2007, Rogers *et al.*, 2005). Inhibition of dectin-1 ligand-dependent internalization by large β-glucan particles or by inhibition of actin polymerization and dynamin results in constant activation of the downstream signaling pathways and increased cytokine production (Hernanz-Falcon et al., 2009). Mice infected with Cg*ace2*Δ cells showed high levels of cytokine, such as TNF-α and IL-6 (Kamran et al., 2004). Therefore, the cytokine release may be explained by our observation that Cg*ace2*Δ and also Cg*cbk1*Δ cells are not phagocytosed at least *in vitro*. Interestingly, it is the size of the cell aggregates, which prevents internalization. Separated mutant cells are phagocytosed similar to wild type cells. If dectin-1 elicits a strong cytokine response because dectin-1 signaling is not attenuated through internalization of the receptor (Hernanz-Falcon et al., 2009) due to the inability to phagocytose the large cell aggregates, the constant signaling may explain the observed septicemia, which causes the acute mortality of Cg*ace2*Δ infected mice. It has to be tested if Cg*cbk1*Δ cells cause the same dramatic effect in mice.

Future studies on phagocytosis and the cytokine response due to interaction between BMDMs and Cg*cbk1*Δ cells may help to determine the profile of cytokine release and also give an idea about the involvement of immune cell receptors.

Acknowledgement

We thank all laboratory members for helpful discussions and critical comments on the manuscript. We are indebted to Julia Köhler for providing plasmid pJK863. We also thank Steffen Rupp for providing the *C. glabrata* microarrays; and Ken Haynes for providing the microarray oligonucleotides. This work was supported by a grant from the Christian Doppler Society to K.K. T.S. was supported in part by the EraNet Pathogenomics project FunPath (FWF-API-0125).

Figure legends

Figure 1. Cell and colony morphologies of Cg*dse2*Δ, Cg*cbk1*Δ, and Cg*ace2*Δ mutants. (A) Dilutions of cells were plated on YPD plates and incubated at 30°C for 3 days, before taking pictures (Zeiss Discovery.V12 Stereomicroscope, AxioCam MRc5, Germany). Cells were grown in YPD to an OD_{600} of 1 and pictures were taken on an Olympus CellR (Olympus, Austria) microscope at 400 x magnification. The arrow points to the large cells seen in the Cg*cbk1*Δ mutant (bar = 10 µm). (B) Cells from an overnight culture were grown to an OD_{600} of 5 on a shaker at 30°C, vortexed and pictures were taken before and after 30 minutes on the bench.

Figure 2. Chitin staining of Cg*cbk1*Δ, and Cg*ace2*Δ mutants. Cells were grown in YPD to an OD_{600} of 1 and stained with 50 µg/ml calcofluor white for one hour in the dark to visualize chitin. Pictures were taken on an Olympus CellR (Olympus, Austria) microscope at 400 x magnification after washing of cells with water. The arrow points to the large cells seen in the Cg*cbk1*Δ mutant (bar = 10 µm).

Figure 3. Growth of Cg*cbk1*Δ strain from separated cells. (A) Cells were separated by sonication (three times for 30 seconds in a sonication water bath), the cell number determined and cells were inoculated to an OD_{600} of 0.3 in YPD and grown at 30°C on a shaker for 0, 3 and 7 hours. Then 100 µl aliquots were diluted in water and the OD_{600} was measured after 30 minutes sitting on the bench to let cells settle. OD measurement was done in triplicates and the experiment repeated two times; shown is one representative experiment. (B) Cells from an exponential culture were separated by sonication as described above and 50 µl of an inoculum (10^7 cells/ml) in YPD were transferred into the Y2 microfluidic plate (Cellasic, USA). Cells were grown in YPD at a constant medium flow of 6 psi. Microscopy was done with the Olympus CellR life imaging station microscope (Olympus, Austria). Pictures were taken every 10 minutes over 12 hours. The upper panel shows the Cg*cbk1*Δ mutant, the lower panels shows the parental strain HTL. 200 x magnification. Black arrows indicate very large cells.

Figure 4. Growth sensitivities of Cg*dse2*Δ, Cg*cbk1*Δ, and Cg*ace2*Δ mutants. (A) Cells from an exponential culture were diluted to an OD_{600} of 0.1 and 10 fold serial dilutions were spotted on YPD and YPD supplemented with the indicated amounts of compounds. (B) Cells from an exponential culture were separated by sonication (three times for 30 seconds in a sonication water bath). OD_{600} was determined, cells were diluted to an OD_{600} of 0.1 and serial 10 fold dilutions were spotted on SC plates without histidine supplemented with the indicated

amounts of compounds. All plates were incubated at 30°C for 48 hours. * cells form cell aggregates.

Figure 5. Distribution of genes found differentially regulated in a Cg*cbk1*Δ deletion strain. Genes were assigned to functional categories using gene ontology (GO) terms of the *Saccharomyces* genome data base (SGD; http://www.yeastgenome.org/): cell wall biogenesis, transcriptional regulators, amino acid biosynthesis, metabolism, plasma membrane transporters, signalling components, fatty acid metabolism, chromatin modifications, miscellaneous and unknowns. An annotated list of all genes up- and down-regulated can be found in Table 1 and Table 2. Percent refers to the percentage of genes assigned to a functional category from the total number of genes differentially regulated.

Figure 6. Confirmation of CgCbk1-regulated genes by qRT-PCR analysis. The most strongly regulated genes found in the microarray analysis were confirmed by individual qRT-PCR analysis. All transcript levels were related to the transcript level of Cg*PGK1* and normalized to the HTL parental strain. cDNA was isolated from three independent cultures and qRT-PCR reactions were performed in triplicates. Data are shown as mean +/- SD of one representative experiment. (A) Regulation of Cg*CBK1*, Cg*ACE2*, Cg*DSE2* and Cg*CTS1* in the ATCC2001, HTL, Cg*cbk1*Δ, Cg*ace2*Δ and Cg*dse2*Δ strains. (B) Upregulation of Cg*SED1*, Cg*FLO11* and Cg*KSS1* in HTL, Cg*cbk1*Δ, Cg*ace2*Δ strains. (C) Down-regulation of both *SCW11* homologues and Cg*FLO9* in HTL, Cg*cbk1*Δ, Cg*ace2*Δ strains.

Figure 7. Growth of Cg*cbk1*Δ cells on amino acid-depleted and minimal medium. Cells from an exponential culture were separated by sonication (three times for 30 seconds in a sonication water bath) and serial 1:10 dilutions of ATCC2001, HTL Cg*cbk1*Δ, Cg*ace2*Δ and Cg*dse2*Δ cells, carrying an empty or complementing vector, were spotted on SC plates, lacking the indicated amino acids and incubated for 48 hours at 30°C. * cells form cell aggregates.

Figure 8. Microscopic analysis of BMDMs infected with Cg*cbk1*Δ and Cg*ace2*Δ cells. Cells from an exponential culture were prestained with FUN-1 and used for infection of BMDMs at an MOI of 5:1 (*C. glabrata* : BMDMs) after extensive washing in PBS. BMDMs were pregrown on round microscopy cover slides in cell culture medium. Fungal cells were added in 100 µl aliquots and cells were co-incubated at 37°C, 5 % CO_2 for 90 minutes. After infection, slides were washed, blocked and incubated with anti-*Candida* antibody. Macrophage nuclei were stained with DAPI.

Figure 9. FACS analysis of BMDMs infected with Cg*cbk1*Δ and Cg*ace2*Δ cells. Cells from an exponential culture were prestained with FUN-1 and used for infection of BMDMs at an MOI of 5:1 (*C. glabrata* : BMDMs) after extensive washing with PBS. Fungal cells were added in 100 µl aliquots and co-incubated with BMDMs at 37°C, 5 % CO_2 for 90 minutes. After infection, non-phagocytosed fungal cells were washed away by five extensive washes with PBS, the BMDMS were collected with a tissue scraper and resuspended in FACS buffer.

Table 1. List of genes upregulated in the Cg*cbk1*Δ mutant. For each *C. glabrata* ORF the homologous *S. cerevisiae* ORF and gene are annotated. Fold corresponds to fold upregulation of a given gene in the Cg*cbk1*Δ mutant compared to the parental HTL strain. To identify differentially expressed genes a linear model was used with cut-off values of 0.01 for the adjusted p-value and a 2-fold expression change. Descriptions of homologous genes are taken from SGD (http://www.yeastgenome.org/). References relate to *S. cerevisiae* data.

Table 2. List of genes down-regulated in the Cg*cbk1*Δ mutant. For each *C. glabrata* ORF the homologous *S. cerevisiae* ORF and gene are annotated. Fold corresponds to fold down-regulation of a given gene in the Cg*cbk1*Δ mutant compared to the parental HTL strain. To identify differentially expressed genes a linear model was used with cut-off values of 0.01 for the adjusted p-value and a 2-fold expression change. Descriptions are taken from SGD (http://www.yeastgenome.org/). * p-value refers to the adjusted p-value. # refers to references relate to *S. cerevisiae* data.

Supplementary Table 1. Strains used in this study. All gene deletion strains are isogenic to strain HTL, which is derived from ATCC2001

Supplementary Table 2. Primers used in this study. Bold and italic sequences were used for adding the barcode sequences to the marker, bold sequences in lower case were used for fusion of two DNA sequences in a PCR reaction to generate the deletion cassettes. Bold capital sequences mark restriction sites used for cloning.

Figure 1. Cell and colony morphologies of Cg*dse2*Δ, Cg*cbk1*Δ, and Cg*ace2*Δ mutants.

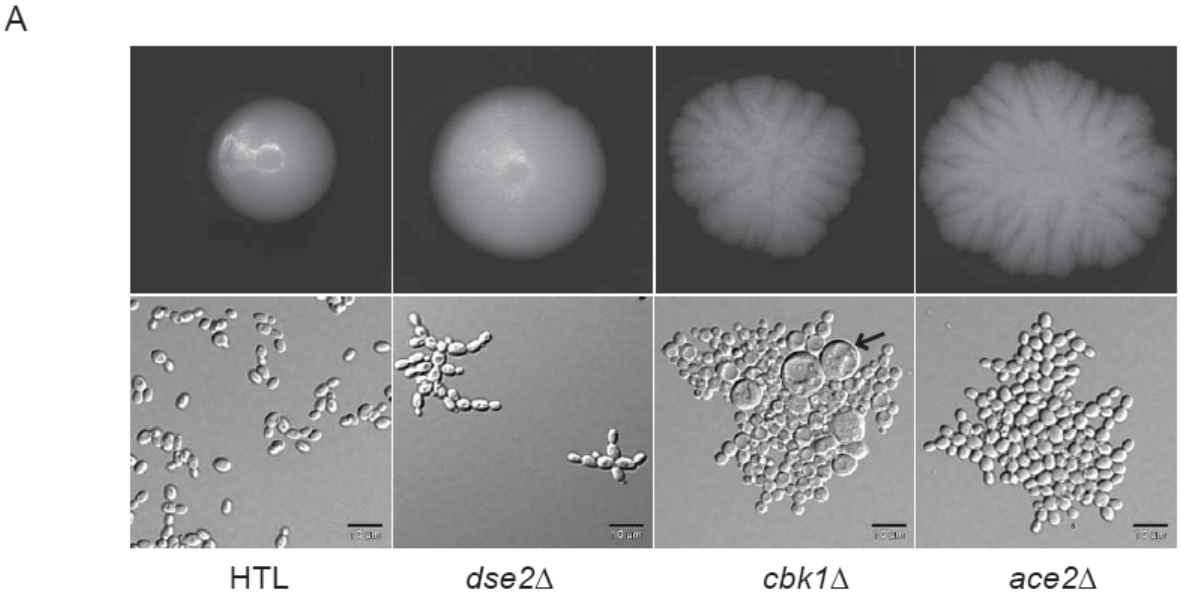

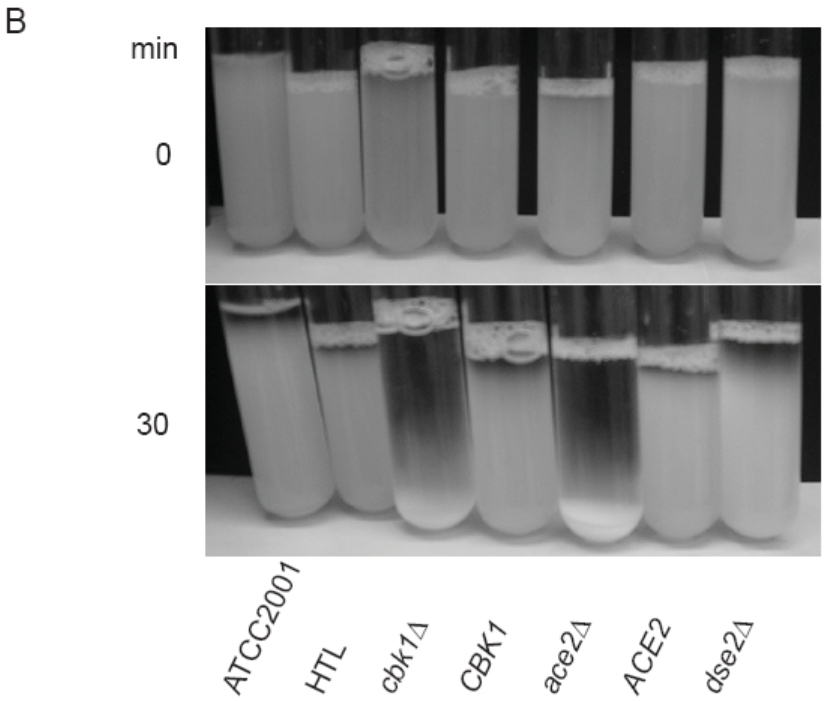

Figure 2. Chitin staining of Cg*cbk1*Δ, and Cg*ace2*Δ mutants.

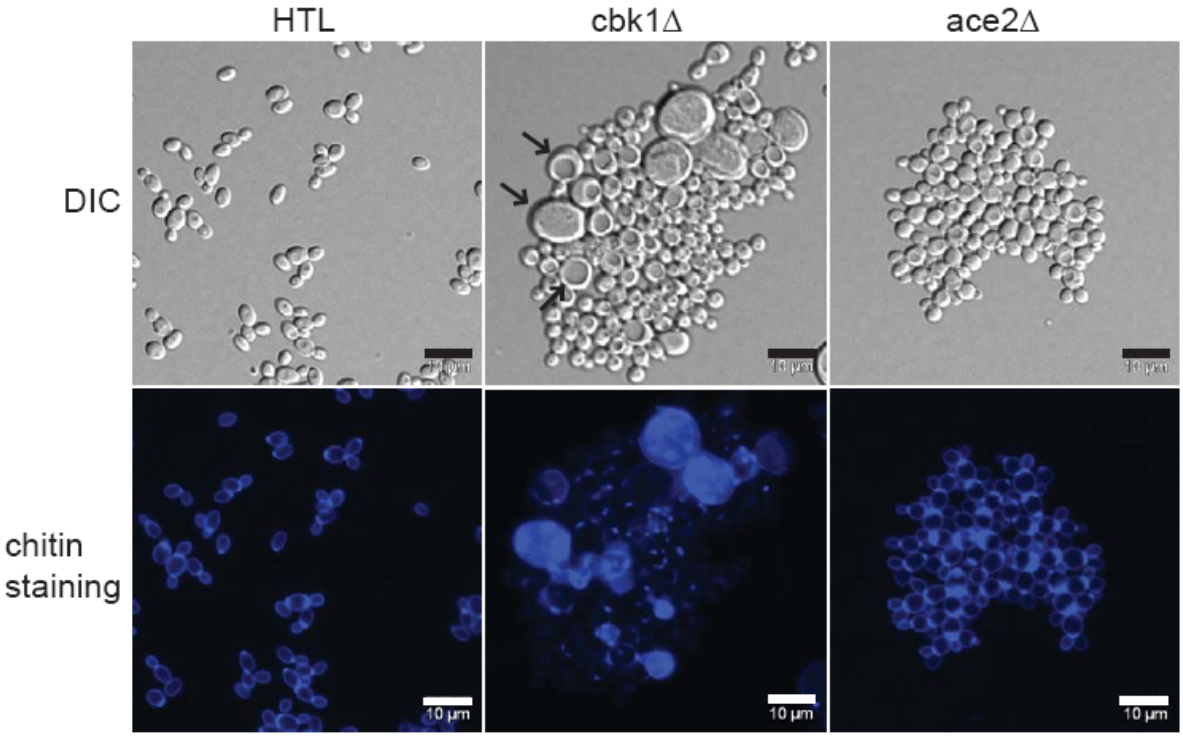

Figure 3. Growth of Cg*cbk1*Δ strain from separated cells.

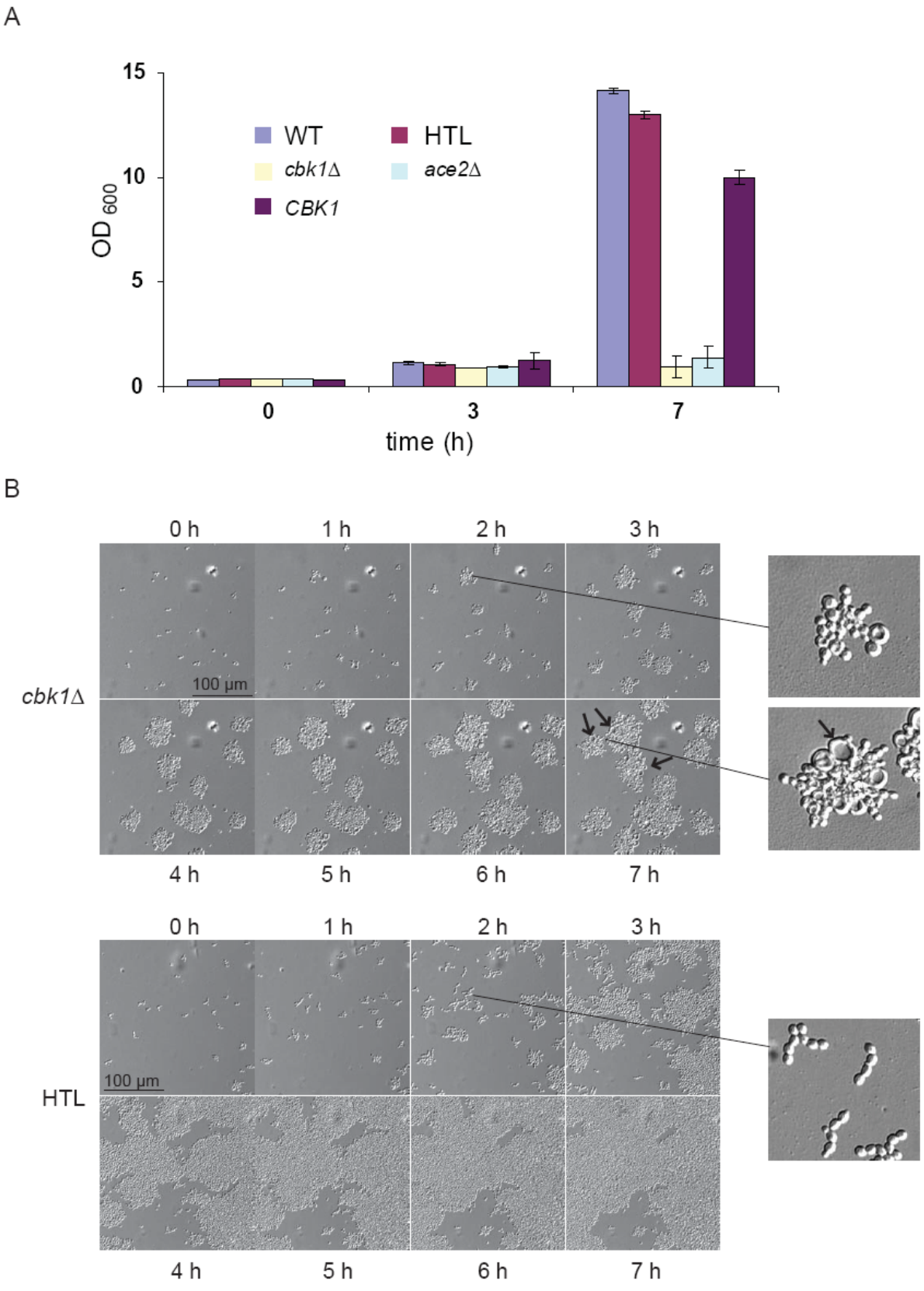

Figure 4. Growth sensitivities of Cg*dse2*Δ, Cg*cbk1*Δ, and Cg*ace2*Δ mutants.

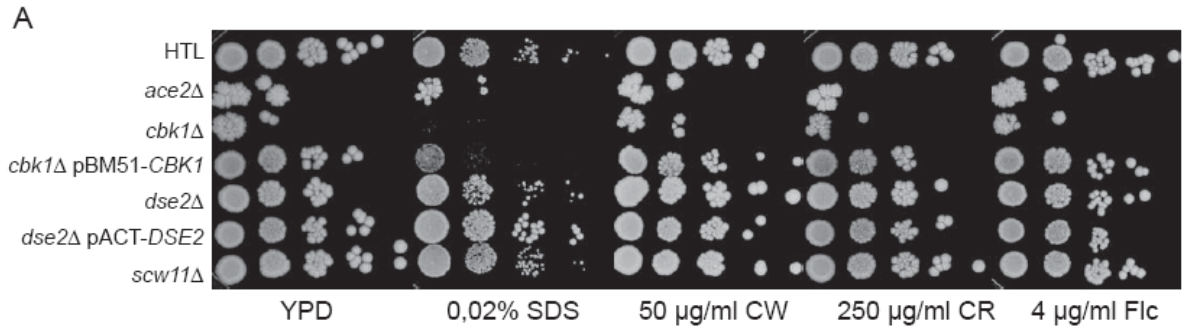

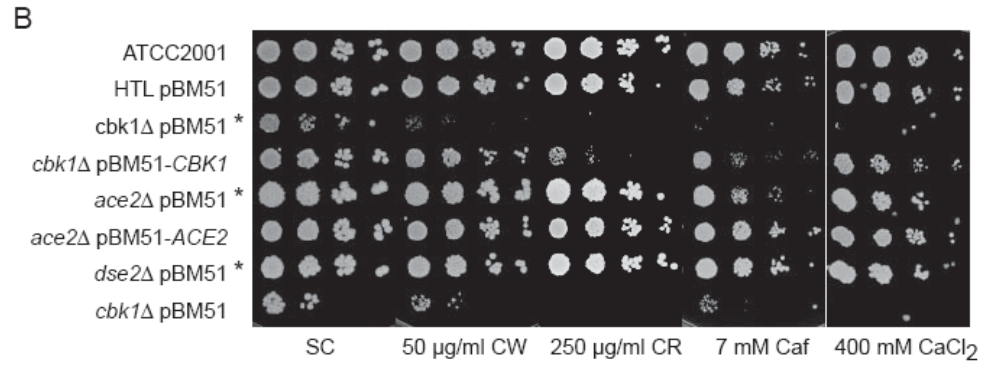

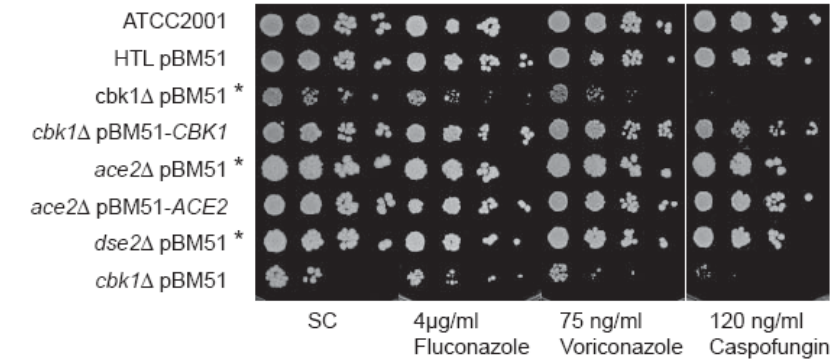

Figure 5. Distribution of genes found differentially regulated in a Cg*cbk1*Δ deletion strain.

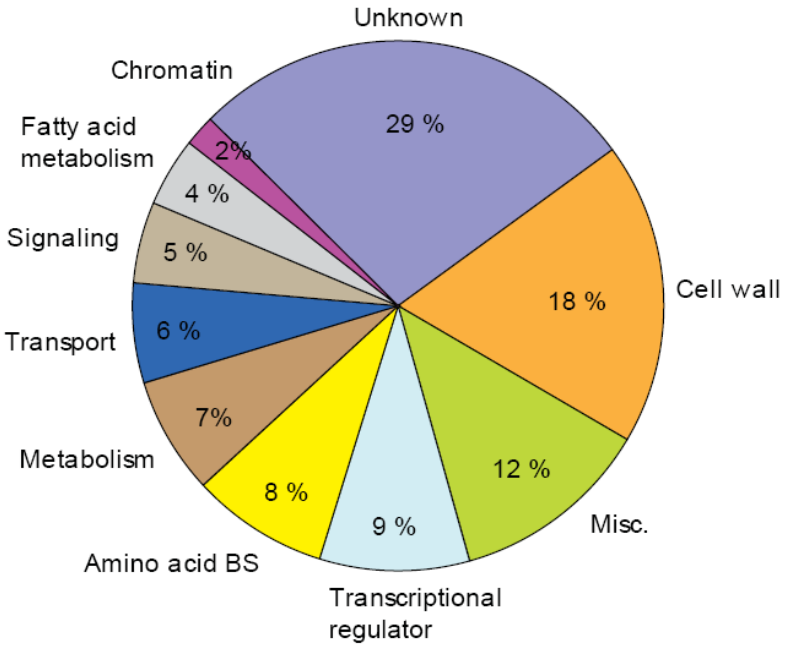

Figure 6. Confirmation of CgCbk1-regulated genes by qRT-PCR analysis.

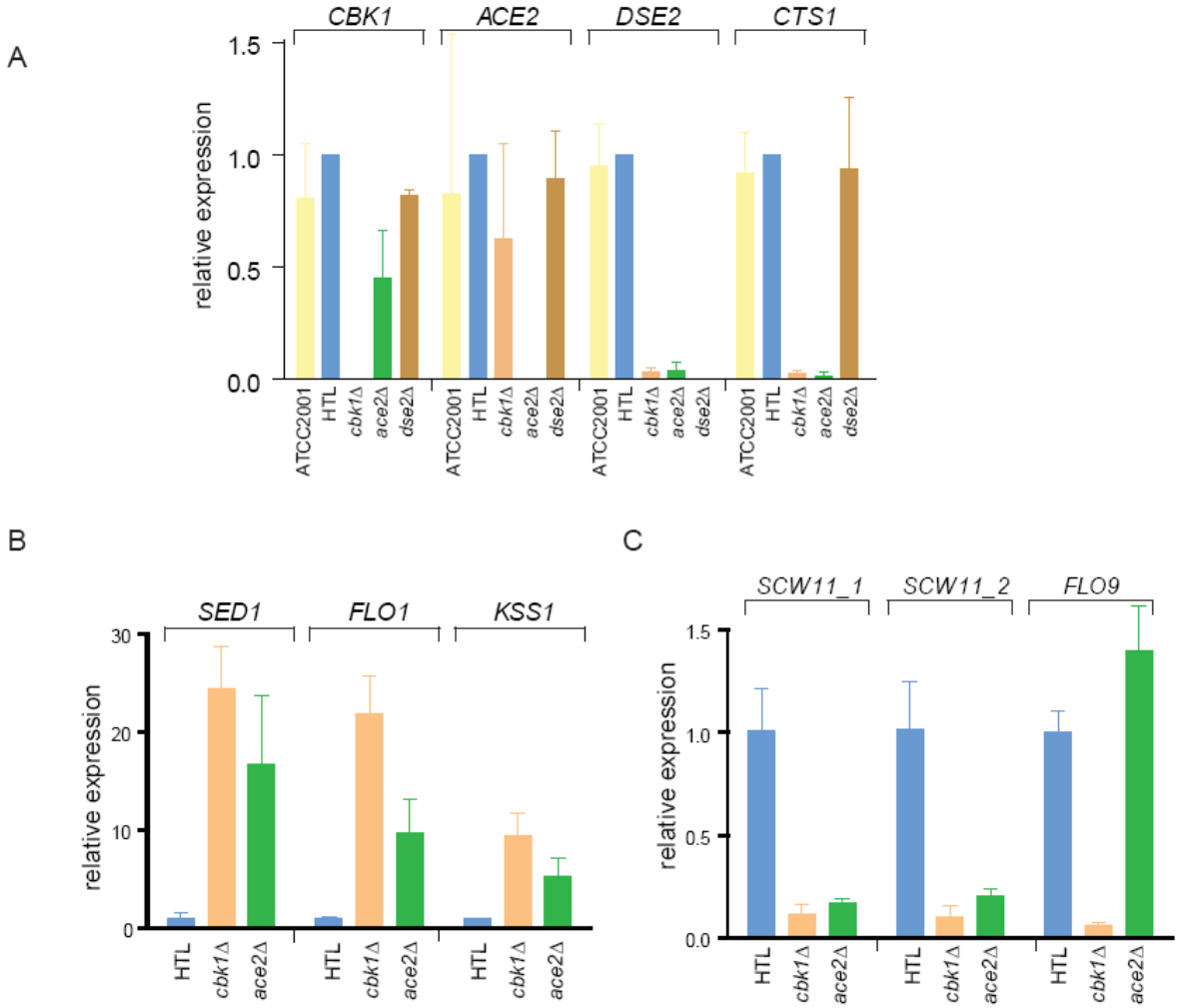

Figure 7. Growth of Cg*cbk1*Δ cells on amino acid-depleted and minimal medium.

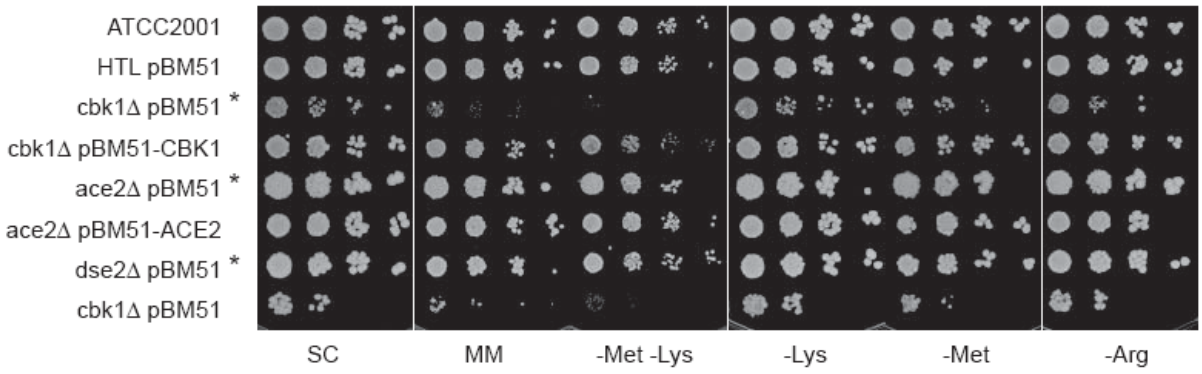

Figure 8. Microscopic analysis of BMDMs infected with Cg*cbk1*Δ and Cg*ace2*Δ cells.

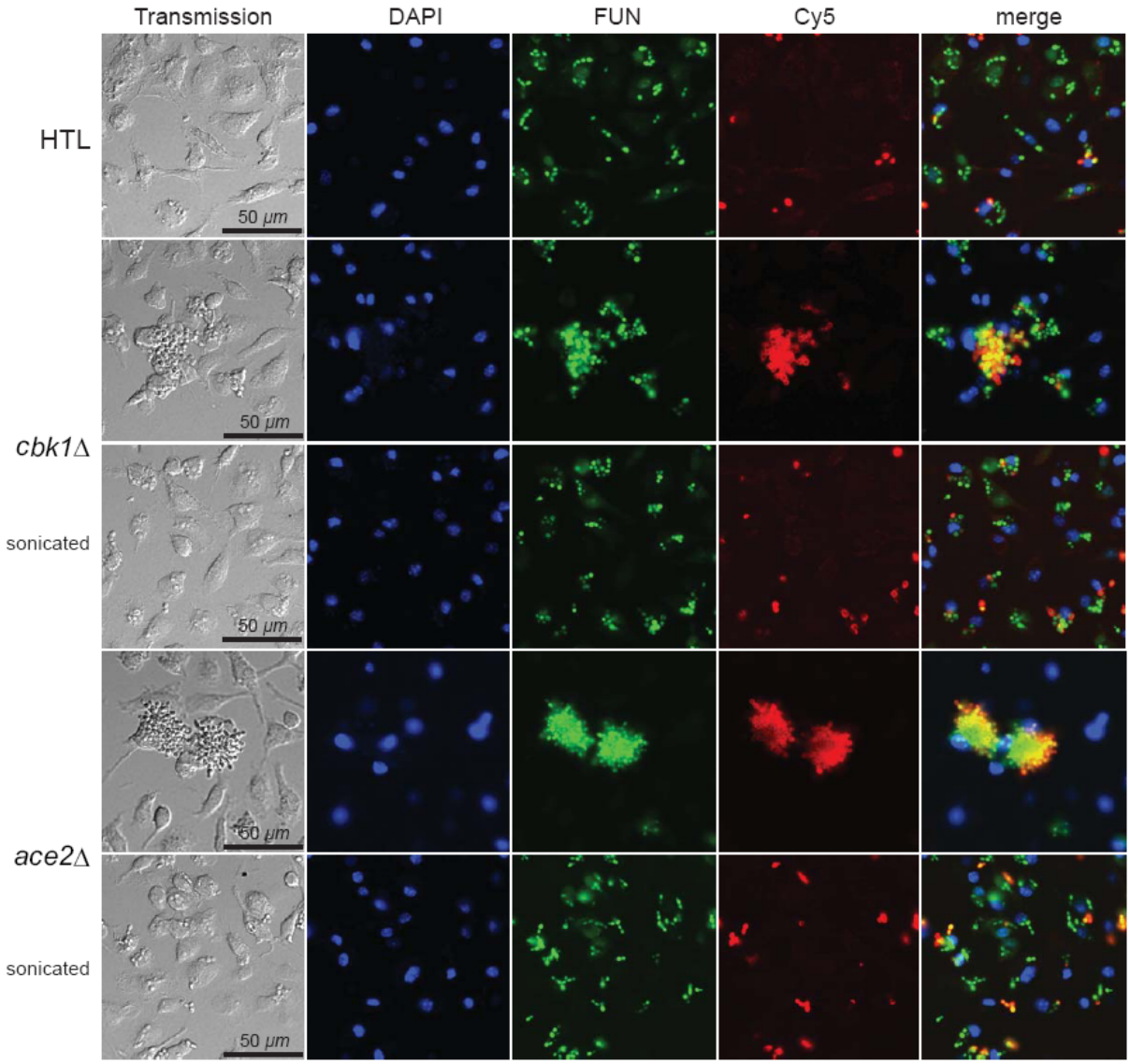

Figure 9. FACS analysis of BMDMs infected with Cg*cbk1*Δ and Cg*ace2*Δ cells.

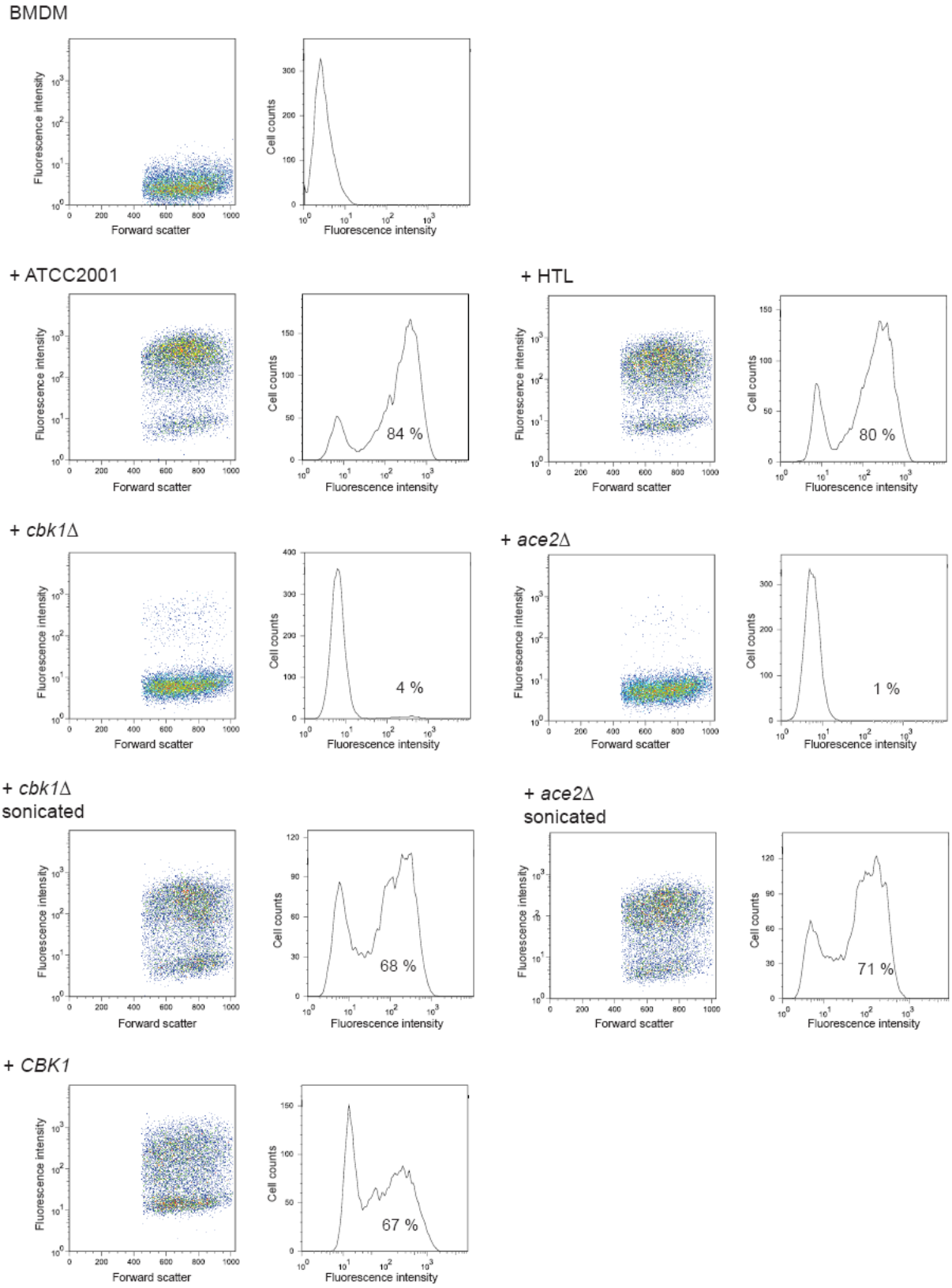

Table 1.

Table 1. Genes upregulated in Cg*cbk1*Δ mutant

Cg ORF	Sc ORF	Gene	fold	p-value	Description	Reference
CAGL0K10164g	YDR077W	*SED1*	16,2	1,00E-05	Major stress-induced structural GPI-cell wall glycoprotein in stationary-phase cells, possible role in mitochondrial genome maintenance	(Hagen et al., 2004)
CAGL0I00220g	YAR050W	*FLO1*	8,3	3,60E-04	Lectin-like protein involved in flocculation, cell wall protein that binds to mannose chains on the surface of other cells, confers floc-forming ability	(Lambrechts *et al.*, 1996)
CAGL0H04851g	YML016C	*PPZ1*	6,9	2,00E-05	Serine/threonine protein phosphatase Z; involved in regulation of K^+ -transport, which affects osmotic stability, cell cycle progression, and halotolerance	(Posas *et al.*, 1995)
CAGL0G09515g	YLR300W	*EXG1*	6,1	2,00E-05	Major exo-1,3-beta-glucanase of the cell wall, involved in cell wall beta-glucan assembly; exists as three differentially glycosylated isoenzymes	(Vazquez de Aldana *et al.*, 1991)
CAGL0C05115g	YOL058W	*ARG1*	4,6	3,00E-05	Arginosuccinate synthetase, catalyzes the formation of L-argininosuccinate from citrulline and L-aspartate in the arginine biosynthesis pathway	
CAGL0K04169g	YGR040W	*KSS1*	4,6	2,00E-05	Mitogen-activated protein kinase (MAPK) involved in signal transduction pathways that control filamentous growth and pheromone response	
CAGL0H00418g	YER175C	*TMT1*	4,3	2,00E-05	Trans-aconitate methyltransferase, cytosolic enzyme that catalyzes methyl esterification of 3-isopropylmalate, intermediate of leucine BS pathway	
CAGL0H03619g	YNL011C	-	3,7	3,00E-05	Putative protein of unknown function; YNL011C is not an essential gene	
CAGL0I09724g	YOR306C	*MCH5*	3,6	1,00E-05	Plasma membrane riboflavin transporter; facilitates the uptake of vitamin B2; required for FAD-dependent processes	
CAGL0F00154g	YHR185C	*PFS1*	3,5	3,00E-05	Sporulation protein required for prospore membrane formation at selected spindle poles, ensures functionality of spindle pole bodies during meiosis	
CAGL0M13805g	YGR279C	*SCW4*	3,4	6,00E-05	Cell wall protein with similarity to glucanases; scw4 scw10 double mutants exhibit defects in mating	(Cappellaro *et al.*, 1998)
CAGL0H08844g	YMR173W	*DDR48*	3,3	2,30E-04	DNA damage-responsive protein, expression is increased in response to heat-shock stress or treatments that produce DNA lesion	
CAGL0E02145g	YNL298W	*CLA4*	3,2	6,00E-05	Cdc42p activated signal transducing kinase; involved in septin ring assembly and cytokinesis; directly phosphorylates septins Cdc3 and Cdc10	
CAGL0G09449g	YGR189C	*CRH1*	3,1	2,00E-05	Putative chitin transglycosidase, transfer of chitin to β(1-6) glucan; localizes to polarized growth sites; induced under cell wall stress conditions	
CAGL0L10186g	YOR052C	-	3,0	4,70E-04	Nuclear protein of unknown function; expression induced by nitrogen limitation in a GLN3, GAT1-independent manner and by weak acid	
CAGL0F00165g	YPR062W	*FCY1*	2,9	4,53E-03	Cytosine deaminase, zinc metalloenzyme that catalyzes the deamination of cytosine to uracil; deamination of 5-fluorocytosine to form 5-fluorouracil	
CAGL0L07480g	YBR066C	*NRG2*	2,9	1,20E-04	Transcriptional repressor that mediates glucose repression and negatively regulates filamentous growth; has similarity to Nrg1p	
CAGL0M12551g	YIL057C	-	2,9	8,60E-04	Putative protein of unknown function; expression induced under carbon limitation and repressed under high glucose	
CAGL0J11176g	YNL176C	-	2,9	1,00E-04	Cell cycle-regulated gene of unknown function, promoter bound by Fkh2	
CAGL0D00198g	YAL060W	*BDH1*	2,9	2,00E-05	NAD-dependent (R,R)-butanediol dehydrogenase, catalyzes oxidation of (R,R)-2,3-butanediol to (3R)-acetoin	
CAGL0F00605g	YCL040W	*GLK1*	2,9	7,00E-05	Glucokinase, catalyzes the phosphorylation of glucose at C6 in the first irreversible step of glucose metabolism	
CAGL0I08987g	YHR018C	*ARG4*	2,9	2,30E-04	Argininosuccinate lyase, catalyzes the final step in the arginine biosynthesis pathway	
CAGL0I06644g	YDR077W	*SED1*	2,8	7,70E-04	Major stress-induced structural GPI-cell wall glycoprotein in stationary-phase cells, possible role in mitochondrial genome maintenance	
CAGL0A01221g	YPR192W	*AQY1*	2,8	5,20E-04	Spore-specific water channel that mediates transport of water across cell membranes; may play a role in spore maturation	
CAGL0H04037g	YOR178C	*GAC1*	2,7	6,60E-04	Regulatory subunit for Glc7 type-1 protein phosphatase, tethers Glc7 to Gsy2 glycogen synthase, binds heat shock TF Hsf1	
CAGL0F08261g	YGR254W	*ENO1*	2,6	1,72E-03	Enolase I, a phosphopyruvate hydratase, catalyzes conversion of 2-phosphoglycerate to phosphoenolpyruvate	
CAGL0H00572g	YJR116W	-	2,6	7,87E-03	Putative protein of unknown function	
CAGL0E02409g	YOL007C	-	2,5	2,00E-04	Protein of unknown function; green fluorescent protein (GFP)- fusion protein localizes to the mother side of the bud neck and the vacuole	

Table 1. continued

Cg ORF	Sc ORF	Gene	fold	p-value	Description	Ref.
CAGL0J04554g	YLR027C	*AAT2*	2,5	3,00E-05	Cytosolic aspartate aminotransferase, involved in nitrogen metabolism; localizes to peroxisomes in oleate-grown cells	
CAGL0J08184g	YEL063C	*CAN1*	2,5	3,00E-05	Plasma membrane arginine permease, exclusively associated with lipid rafts; mutation confers canavanine resistance	
CAGL0K04719g	YNL208W	-	2,5	6,00E-04	Protein of unknown function; may interact with ribosomes; authentic, non-tagged protein is detected in purified mitochondria	
CAGL0I00484g	YLR300W	*EXG1*	2,5	2,00E-04	Major exo-1,3-beta-glucanase of the cell wall, involved in cell wall beta-glucan assembly; exists as three differentially glycosylated isoenzymes	
CAGL0J03960g	YOR230W	*WTM2*	2,5	2,10E-04	Transcriptional modulator, regulation of meiosis, silencing, and expression of RNR genes; required for localization of Rnr2 and Rnr4	
CAGL0G05632g	YDL218W	-	2,5	5,30E-04	Putative protein of unknown function; YDL218W transcription is regulated by Azf1p and induced by starvation and aerobic conditions	
CAGL0F08085g	YGR243W	*FMP43*	2,4	6,80E-04	Putative protein of unknown function; the authentic, non-tagged protein is detected in highly purified mitochondria in high-throughput studies	
CAGL0G06006g	YHR138C	-	2,4	1,90E-04	Putative protein of unknown function; has similarity to Pbi2p; double null mutant lacking Pbi2p and Yhr138p exhibits highly fragmented vacuoles	
CAGL0K05687g	YHR179W	*OYE2*	2,4	4,60E-04	NADPH oxidoreductase containing flavin mononucleotide, homologue to Oye3 with differences in ligand binding; may be involved in sterol metabolism	
CAGL0J04048g	YOR226C	*ISU2*	2,4	2,00E-05	Conserved protein of mito. matrix, required for synthesis of mito. and cytosolic iron-sulfur proteins, scaffolding function in mito. during Fe/S cluster assembly	
CAGL0L00605g	YKL190W	*CNB1*	2,3	1,07E-03	Calcineurin B; the regulatory subunit of calcineurin, a Ca++/calmodulin-regulated type 2B protein phosphatase which regulates Crz1p	
CAGL0M04499g	YLR142W	*PUT1*	2,3	3,60E-04	Proline oxidase, nuclear-encoded mito. protein involved in utilization of proline as nitrogen source; PUT1 induced in presence of proline, absence of nitrogen	
CAGL0J08437g	YDR503C	*LPP1*	2,3	3,60E-04	Lipid phosphate phosphatase, catalyzes Mg^{2+}-independent dephosphorylation of phosphatidic and lysophosphatidic acid, and diacylglycerol pyrophosphate	
CAGL0M11902g	YAL034C	*FUN19*	2,3	8,90E-04	Non-essential protein of unknown function; expression induced in response to heat stress	
CAGL0J00253g	YGR023W	*MTL1*	2,3	7,00E-05	Protein with structural & functional similarity to Mid2, a PM sensor required for cell integrity signaling during pheromone-induced morphogenesis	
CAGL0K12892g	YFL047W	*RGD2*	2,3	3,60E-04	GTPase-activating protein (RhoGAP) for Cdc42 and Rho5	
CAGL0K05665g	YHR112C	-	2,3	1,84E-03	Putative protein of unknown function	
CAGL0L11902g	YER170W	*ADK2*	2,3	3,70E-04	Mitochondrial adenylate kinase, catalyzes the reversible synthesis of GTP and AMP from GDP and ADP	
CAGL0M07381g	YPL053C	*KTR6*	2,3	3,00E-05	Probable mannosylphosphate transferase involved in the synthesis of core oligosaccharides in protein glycosylation pathway	
CAGL0B00946g	YCL028W	*RNQ1*	2,3	1,00E-04	[PIN(+)] prion, an infectious protein conformation that is generally an ordered protein aggregate	
CAGL0L08338g	YIL138C	*TPM2*	2,3	1,89E-03	Minor isoform of tropomyosin, binds to and stabilizes actin cables and filaments, which direct polarized cell growth and the distribution of several organelles	
CAGL0H05621g	YPL089C	*RLM1*	2,2	1,40E-04	MADS-box transcription factor, component of the PKC-mediated MAP kinase pathway involved in the maintenance of cell integrity;activated by Slt2p	
CAGL0K02519g	YKL093W	*MBR1*	2,2	4,64E-03	Protein involved in mitochondrial functions and stress response; overexpression suppresses growth defects of hap2, hap3, and hap4 mutants	
CAGL0J03806g	YOR230W	*WTM1*	2,2	4,10E-04	Transcriptional modulator, regulation of meiosis, silencing, and expression of RNR genes; required for nuclear localization of Rnr2 and Rnr4	
CAGL0E01793g	YLR120C	*YPS1*	2,2	8,04E-03	Aspartic protease, attached to the plasma membrane via a GPI anchor	
CAGL0G00858g	YLR332W	*MID2*	2,2	4,00E-05	O-glycosylated plasma membrane protein that acts as sensor for cell wall integrity signaling and activates pathway; interacts with Rom2 and Zeo1	
CAGL0E02123g	YOL114C	-	2,1	3,60E-04	Putative protein of unknown function with similarity to human ICT1 and prokaryotic factors that may function in translation termination	
CAGL0H06787g	YIL160C	*POT1*	2,1	9,90E-04	3-ketoacyl-CoA thiolase with broad chain length specificity, cleaves 3-ketoacyl-CoA into acyl-CoA and acetyl-CoA during beta-oxidation of fatty acids	
CAGL0F04895g	YPR160W	*GPH1*	2,1	7,40E-04	Non-essential glycogen phosphorylase required for mobilization of glycogen, regulated by cAMP-mediated phosphorylation, regulated by HOG pathway	

Table 1. continued

Cg ORF	Sc ORF	Gene	fold	p-value	Description	Ref.
CAGL0G02849g	YPL186C	*UIP4*	2,1	4,70E-04	Interacts with Ulp1, a Ubl-specific protease for Smt3 protein conjugates; detected in phosphorylated state in the mito. outer memb., ER & nuclear envelope	
CAGL0G09064g	YPL201C	*YIG1*	2,1	4,89E-03	Protein that interacts with glycerol 3-phosphatase and plays a role in anaerobic glycerol production; localizes to the nucleus and cytosol	
CAGL0K06105g	YLR267W	*BOP2*	2,1	8,70E-04	Protein of unknown function	
CAGL0B01507g	YOL140W	*ARG8*	2,1	9,27E-03	Acetylornithine aminotransferase, catalyzes the fourth step in the biosynthesis of the arginine precursor ornithine	
CAGL0I01100g	YOR120W	*GCY1*	2,1	6,60E-04	Putative NADP(+) coupled glycerol dehydrogenase, proposed to be involved in an alternative pathway for glycerol catabolism	
CAGL0M06325g	YPL089C	*RLM1*	2,1	6,60E-04	MADS-box transcription factor, component of the PKC-mediated MAP kinase pathway involved in the maintenance of cell integrity; activated by Slt2p	
CAGL0A04829g	YGL253W	*HXK2*	2,0	1,37E-03	Hexokinase isoenzyme 2, catalyzes phosphorylation of glucose; predominant hexokinase during growth on glucose; represses expression of HXK1 + GLK1	
CAGL0D05082g	YLL039C	*UBI4*	2,0	2,70E-04	Ubiquitin, becomes conjugated to proteins, marking them for selective degradation via the ubiquitin-26S proteasome system; essential for stress response	
CAGL0J09240g	YDL131W	*LYS21*	2,0	4,00E-05	Homocitrate synthase isozyme, catalyzes the condensation of acetyl-CoA and alpha-ketoglutarate to form homocitrate; first step in lysine biosynthesis	
CAGL0M09108g	YPR042C	*PUF2*	2,0	9,00E-04	Member of PUF family, which is defined by presence of Pumilio homology domains; binds mRNAs encoding membrane-associated proteins	
CAGL0H10362g	YDL110C	-	2,0	7,64E-03	Protein of unknown function, associates with ribosomes; heterozygous deletion demonstrated increases in chromosome instability in a *rad9*Δ background	
CAGL0J00539g	YHR030C	*SLT2*	2,0	4,00E-05	Serine/threonine MAP kinase involved in regulating maintenance of cell wall integrity; regulated by the PKC1-mediated signaling pathway	

Table 2.

Table 2. Genes downregulated in Cg*cbk1*Δ mutant

Cg ORF	Sc ORF	Gene	fold	p-value	Description	Ref.
CAGL0G05896g	YHR143W	*DSE2*	8,9	8,82E-03	Daughter cell-specific secreted protein with similarity to glucanases, degrades cell wall of daughter cell causing separation from mother; repressed by cAMP	(Colman-Lerner *et al.*, 2001)
CAGL0M09779g	YLR286C	*CTS1*	5,1	6,60E-04	Endochitinase, required for cell separation after mitosis; transcriptional activation during the G1 phase of the cell cycle mediated by transcription factor Ace2	(O'Conallain *et al.*, 1999)
CAGL0L13332g	YAL063C	*FLO9*	3,6	5,00E-05	Lectin-like protein with similarity to Flo1, thought to be expressed and involved in flocculation	(Teunissen & Steensma, 1995)
CAGL0A02277g	YCL049C	-	3,4	1,40E-03	Protein of unknown function; localizes to membrane fraction	
CAGL0A02255g	YCL049C	-	3,4	6,60E-04	Protein of unknown function; localizes to membrane fraction	
CAGL0E02915g	YGL028C	*SCW11*	2,9	2,72E-03	Cell wall protein with similarity to glucanases; may play a role in conjugation during mating based on its regulation by Ste12p	(Cappellaro *et al.*, 1998)
CAGL0D05434g	YPR065W	*ROX1*	2,8	5,23E-03	Heme-dependent repressor of hypoxic genes; contains an HMG domain that is responsible for DNA bending activity	
CAGL0A01474g	YGL028C	*SCW11*	2,7	3,60E-04	Cell wall protein with similarity to glucanases; may play a role in conjugation during mating based on its regulation by Ste12p	(Cappellaro et al., 1998)
CAGL0J02508g	YOR009W	*TIR4*	2,7	3,00E-05	Cell wall mannoprotein of the Srp1p/Tip1p family of serine-alanine-rich proteins; expressed under anaerobic conditions and required for anaerobic growth	
CAGL0H07051g	YDR321W	*ASP1*	2,6	2,00E-05	Cytosolic L-asparaginase, involved in asparagine catabolism	
CAGL0G02409g	YKR092C	*SRP40*	2,3	8,80E-03	Nucleolar, serine-rich protein with a role in preribosome assembly or transport; may function as a chaperone of small nucleolar ribonucleoprotein particles	
CAGL0A03102g	YDR380W	*ARO10*	2,3	1,11E-03	Phenylpyruvate decarboxylase, catalyzes decarboxylation of phenylpyruvate to phenylacetaldehyde, which is the first specific step in the Ehrlich pathway	
CAGL0F00407g	YJR070C	*LIA1*	2,3	7,10E-04	Deoxyhypusine hydroxylase, a HEAT-repeat containing metalloenzyme that catalyses hypusine formation; binds to & is required for the modification of Hyp2	
CAGL0B00792g	YCL037C	*SRO9*	2,2	6,70E-04	Cytoplasmic RNA-binding protein that associates with translating ribosomes; involved in heme regulation of Hap1p as a component of the HMC complex	
CAGL0M09801g	YLR285W	*NNT1*	2,2	2,10E-04	Putative nicotinamide N-methyltransferase, has a role in rDNA silencing and in lifespan determination	
CAGL0G05764g	YLR229C	*CDC42*	2,2	5,91E-03	Small rho-like GTPase, essential for establishment and maintenance of cell polarity; mutants have defects in the organization of actin and septins	
CAGL0M02783g	YPL127C	*HHO1*	2,2	4,12E-03	Histone H1, linker histone required for nucleosome packaging at restricted sites; suppresses DNA repair involving homologous recombination	
CAGL0A01804g	YDR345C	*HXT3*	2,2	3,10E-04	Low affinity glucose transporter of the major facilitator superfamily, expression is induced in low or high glucose conditions	
CAGL0D01716g	YBR088C	*POL30*	2,2	1,66E-03	Putative protein of unknown function with similarity to human ICT1 and prokaryotic factors, may function in translation termination;	
CAGL0M05599g	YBR162C	*TOS1*	2,1	5,50E-04	PCNA, functions as sliding clamp for DNA polymerase delta; docking site for proteins required for mitotic & meiotic chromosomal DNA replication & repair	
CAGL0L00495g	YMR186W	*HSC82*	2,1	2,20E-03	Suppressor of sphingoid long chain base sensitivity of an LCB-lyase mutation; putative integral membrane transporter that may transport LCBs	
CAGL0L10142g	YOR049C	*RSB1*	2,1	9,90E-04	Constituent of 66S pre-ribosomal particles, required for maturation of the large ribosomal subunit	
CAGL0L10890g	YOR272W	*YTM1*	2,1	3,60E-04	Covalently-bound cell wall protein, unknown function; identified as cell cycle regulated SBF target gene; mutants are resistant to β-1,3-glucanase treatment	
CAGL0I05764g	YNR009W	-	2,1	6,90E-04	Cytoplasmic chaperone of the Hsp90 family, redundant in function & identical with Hsp82; expressed constitutively at 10-fold higher basal levels	
CAGL0L07678g	YPL266W	*DIM1*	2,1	2,29E-03	Transcriptional co-repressor of MBF-regulated gene expression; Nrm1p associates stably with promoters via MBF to repress transcription upon exit from G1	
CAGL0I04290g	YGL169W	*SUA5*	2,0	1,33E-03	Ceramide synthase component, involved in synthesis of ceramide from C26(acyl)-coenzyme A or phytosphingosine, func. equi. to Lac1	
CAGL0K02739g	YHL003C	*LAG1*	2,0	1,20E-03	Essential 18S rRNA dimethylase, responsible for conserved m6(2)Am6(2)A dimethylation in 3'-terminal loop of 18S rRNA	
CAGL0E06138g	YPL231W	*FAS2*	2,0	2,00E-04	Protein required for respiratory growth; null mutation suppresses Cyc1 translation defect caused by aberrant ATG codon upstream of correct start	

Supplementary Table 1. Strains used in this study

Strain	Genotype	Reference or source
ATCC2001	Wild type	ATCC collection
HTL	Isogenic to ATCC2001	Jungwirth/Schwarzmüller, unpub.
*cbk1*Δ	Isogenic to HTL; *cbk1*Δ::*NAT1*	This study
*dse2*Δ	Isogenic to HTL; *dse2*Δ:: *NAT1*	This study
*ace2*Δ	Isogenic to HTL; *ace2*Δ::*HygB*	This study
*scw11*Δ	Isogenic to HTL; *scw11*Δ:: *NAT1*	This study

Supplementary Table 2. Oligonucleotides used in this study

Name	Sequence
fp_NAT1-U2	5'-***CGTACGCTGCAGGTCGAC***agcttgcctcgtccccgccg-3'
rp_NAT1-D2	5'-***CTACGAGACCGACACCG***ctggatggcggcgttagtatcg-3'
fpHyg-U1	5'-**ccgctgctaggcgcgccgtg**CCCATAAAGCACGTGGCCTC-3'
rpHyg-D1	5'-**gcagggatgcggccgctgac**CCTGCAGCCCCTTTACCTC-3'
Heukan2	5'-CGTCAAGACTGTCAAGGAGGG-3'
Heukan3	5'-CATCATCTGCCCAGATGCGAAG-3'
5M-marker	5'-**ccgctgctaggcgcgccgtg**BARCODE-UP***cgtacgctgcaggtcgac***-3'
3M-marker	5'-**gcagggatgcggccgctgac**BARCODE-DOWN***ctacgagaccgacaccg***-3'
55_CBK1	5'-AGGGTCAGAACTACTGGAAG-3'
53_CBK1	5'-**cacggcgcgcctagcagcgg**CATACTGGTTTTTGCTCTAC-3'
35_CBK1	5'-**gtcagcggccgcatccctgc**TAAGTTTTTTCCTTAGTTTC-3'
33_CBK1	5'-TTTGATTTCAATATCTTTGC-3'
5c_CBK1	5'-GGTCAGAGAGTAAGGATGGATG-3'
3c_CBK1	5'-TGAGTCTGGGTGTACAGGTG-3'
5i_CBK1	5'-ATGCAATCGAGAGGAACGAG-3'
3i_CBK1	5'-TCACCACCCGGTAGAAACTC-3'
55_DSE2	5'-TGTTGAACAACTGTTTTAATG-3'
53_DSE2	5'-**cacggcgcgcctagcagcgg**CATTATAAAAATCTTTGATGG-3'
35_DSE2	5'-**gtcagcggccgcatccctgc**TAAATGATTTCAAACAGTTTTC-3'
33_DSE2	5'-AGTGCTGTGATCAGTTGAAG-3'
5c_DSE2	5'-CTATGCAGATACTGCCTCACC-3'
3c_DSE2	5'-CTCAAACTGCACCATTCTTC-3'
5i_DSE2	5'-AGTACATTGGCTCCAGCATC-3'
3i_DSE2	5'-TCGACAGAGGATGGCATAAAG-3'
55_ACE2	5'-GTCCCTTAGGAGGGTATAAG-3'
53_ACE2	5'-**cacggcgcgcctagcagcgg**CATTATTTTAGAACGACGAG-3'
35_ACE2	5'-**gtcagcggccgcatccctgc**TAGTATATAGTACAAACTTCACATGC-3'
33_ACE2	5'-TGTAATCACACAACTAAATTCC-3'
5c_ACE2	5'-CAAGTGTTAGGGTTGTTACGC-3'

3c_ACE2	5’-GCTGTGCTTGGTACACTTTG-3’
55_SCW11	5’-GCTTTGTATAATAGGTAAATC-3’
53_SCW11	5’-**cacggcgcgcctagcagcgg**CATCTTATATTTTAATAGAAC-3’
35_SCW11	5’-**gtcagcggccgcatccctgc**TGAACCTAGAAGATCCAAAC-3’
33_SCW11	5’-ATATTAGACGTTAGCAACAG-3’
5c_SCW11	5’-CAGCATTTTGTACACTGTAGCC-3’
3c_SCW11	5’-CTAAGAGGCAGCAAATTGAG-3’
fCBK1_BamHI	5’-agt**GGATCC**atgtttggtggcgagtatgatcac-3’
rCBK1_EcoRI	5’-atc**GAATTC**ttataatgcattctttctcgtcaagtag-3’
fCBK1_EP_EcoRI	5’-tca**GAATTC**gcattggcggctatgactgtg-3’
rCBK1_EP_EcoRI	5’-tga**GAATTC**acacacatgcataggcacacag-3’
fDSE2_Xba	5’-agtc**TCTAGA**atgcaattccgtgccgctacac-3’
rDSE2_Xho	5’-gact**CTCGAG**ttaattagcagaaacagttttgtataccg-3’
fDSE2_EcoRI	5’-agtc**GAATTC**aacccctatgaaatcaggggc-3’
rDSE2_EcoRI	5’-gact**GAATTC**ggacagtgaatagaatgctggc-3’
fACE2_EcoRI	5’-agtc**GAATTC**atgaatactttccaggcggattgg-3’
rACE2_SalI	5’-agtc**GTCGAC**tatactactcctcaatcgtccc-3’
fp-CBK1	5’-TGATATACCTCAGTTACACCCTTCC-3’
rp-CBK1	5’-GTTGTTCATGTTACTTGTGCTCGG-3’
fp-ACE2	5’-GACAGGAGAGCATCAACATCGT-3’
rp-ACE2	5’-GACAGGAGAGCATCAACATCGT-3’
fp-DSE2	5’-ATCTGCTTCCTCTAGTAGTGTTTCC-3’
rp-DSE2	5’-TACACTTGAGCTATCGTTGTCTAGG-3’
fp-CTS1	5’-AATGTCCATACCCAGATGCCTC-3’
rp-CTS1	5’-GAAATTCTTCCAGTCGTCCCAG-3’
fp-PGK1	5’-TCATTGCTGACGCTTTCTCC-3’
rp-PGK1	5’-CGAACAACTTTCTGGACTCTGG-3’
fp_cgFLO9	5’-GTGAGTAAGACTATTTCCAGCGG-3’
rp_cgFLO9	5’-GGTCCCACCATCACTTACAG-3’
fp_cgSED1	5’-ACTACCACTGTCTCTTCTACTACC-3’
rp_cgSED1	5’-GTAAGCAGTAACAACTTCGATCTC-3’
fp_cgMUC1	5’-GCTAACAAATCCGTCATCTACTG-3’
rp_cgMUC1	5’-ATTGTCAGGTCCCGTAATATAGG-3’
fp_cgKSS1	5’-CATCCTTTCTTAGCAACATACCAC-3’
rp_cgKSS1	5’-CTGTCGTCTGTCCCATATCC-3’
fp-cgSCW4	5’-ATGCTCATGCTTACTTTGACCA-3’
rp-cgSCW4	5’-CTTTCTTACCGTCACAAGCAGTC-3’
fp-EPA1	5’-GCGTAATCAAGGAAACCAAAGAC-3’
rp-EPA1	5’-GTTCCACCTAAAGACTCATAACTG-3’
fp-EPA7	5’-AGATCCGAACCCTGTAATAGAC-3’
rp-EPA7	5’-TCAACACCGATGATTGTAGATGAG-3’

fp-EXG1	5’-CCGCTTTAACCGATTGTACCA-3’
rp-EXG1	5’-TGAACCTATGTAAGAAGAGCCC-3’

References

Bidlingmaier, S., E. L. Weiss, C. Seidel, D. G. Drubin & M. Snyder, (2001) The Cbk1p pathway is important for polarized cell growth and cell separation in *Saccharomyces cerevisiae*. *Mol Cell Biol* **21**: 2449-2462.

Borg-von Zepelin, M., L. Kunz, R. Ruchel, U. Reichard, M. Weig & U. Gross, (2007) Epidemiology and antifungal susceptibilities of *Candida* spp. to six antifungal agents: results from a surveillance study on fungaemia in Germany from July 2004 to August 2005. *J Antimicrob Chemother* **60**: 424-428.

Cappellaro, C., V. Mrsa & W. Tanner, (1998) New potential cell wall glucanases of *Saccharomyces cerevisiae* and their involvement in mating. *J Bacteriol* **180**: 5030-5037.

Chen, R. E. & J. Thorner, (2007) Function and regulation in MAPK signaling pathways: lessons learned from the yeast *Saccharomyces cerevisiae*. *Biochim Biophys Acta* **1773**: 1311-1340.

Colman-Lerner, A., T. E. Chin & R. Brent, (2001) Yeast Cbk1 and Mob2 activate daughter-specific genetic programs to induce asymmetric cell fates. *Cell* **107**: 739-750.

Cormack, B. P., N. Ghori & S. Falkow, (1999) An adhesin of the yeast pathogen *Candida glabrata* mediating adherence to human epithelial cells. *Science* **285**: 578-582.

Cross, E. W., S. Park & D. S. Perlin, (2000) Cross-Resistance of clinical isolates of *Candida albicans* and *Candida glabrata* to over-the-counter azoles used in the treatment of vaginitis. *Microb Drug Resist* **6**: 155-161.

de Groot, P. W., E. A. Kraneveld, Q. Y. Yin, H. L. Dekker, U. Gross, W. Crielaard, C. G. de Koster, O. Bader, F. M. Klis & M. Weig, (2008) The cell wall of the human pathogen *Candida glabrata*: differential incorporation of novel adhesin-like wall proteins. *Eukaryot Cell* **7**: 1951-1964.

De Las Penas, A., S. J. Pan, I. Castano, J. Alder, R. Cregg & B. P. Cormack, (2003) Virulence-related surface glycoproteins in the yeast pathogen *Candida glabrata* are encoded in subtelomeric clusters and subject to *RAP1*- and *SIR*-dependent transcriptional silencing. *Genes Dev* **17**: 2245-2258.

Dohrmann, P. R., G. Butler, K. Tamai, S. Dorland, J. R. Greene, D. J. Thiele & D. J. Stillman, (1992) Parallel pathways of gene regulation: homologous regulators *SWI5* and *ACE2* differentially control transcription of *HO* and chitinase. *Genes Dev* **6**: 93-104.

Dolan, J. W., A. C. Bell, B. Hube, M. Schaller, T. F. Warner & E. Balish, (2004) *Candida albicans PLD I* activity is required for full virulence. *Med Mycol* **42**: 439-447.

Domergue, R., I. Castano, A. De Las Penas, M. Zupancic, V. Lockatell, J. R. Hebel, D. Johnson & B. P. Cormack, (2005) Nicotinic acid limitation regulates silencing of *Candida* adhesins during UTI. *Science* **308**: 866-870.

Frohner, I. E., C. Bourgeois, K. Yatsyk, O. Majer & K. Kuchler, (2009) *Candida albicans* cell surface superoxide dismutases degrade host-derived reactive oxygen species to escape innate immune surveillance. *Mol Microbiol* **71**: 240-252.

Gantner, B. N., R. M. Simmons, S. J. Canavera, S. Akira & D. M. Underhill, (2003) Collaborative induction of inflammatory responses by dectin-1 and Toll-like receptor 2. *J Exp Med* **197**: 1107-1117.

Gantner, B. N., R. M. Simmons & D. M. Underhill, (2005) Dectin-1 mediates macrophage recognition of *Candida albicans* yeast but not filaments. *EMBO J* **24**: 1277-1286.

Ghannoum, M. A., (2000) Potential role of phospholipases in virulence and fungal pathogenesis. *Clin Microbiol Rev* **13**: 122-143, table of contents.

Gietz, D., A. St Jean, R. A. Woods & R. H. Schiestl, (1992) Improved method for high efficiency transformation of intact yeast cells. *Nucleic Acids Res* **20**: 1425.

Goldstein, A. L. & J. H. McCusker, (1999) Three new dominant drug resistance cassettes for gene disruption in *Saccharomyces cerevisiae*. *Yeast* **15**: 1541-1553.

Goodridge, H. S., R. M. Simmons & D. M. Underhill, (2007) Dectin-1 stimulation by *Candida albicans* yeast or zymosan triggers NFAT activation in macrophages and dendritic cells. *J Immunol* **178**: 3107-3115.

Gregori, C., C. Schuller, A. Roetzer, T. Schwarzmuller, G. Ammerer & K. Kuchler, (2007) The high-osmolarity glycerol response pathway in the human fungal pathogen *Candida glabrata* strain ATCC 2001 lacks a signaling branch that operates in baker's yeast. *Eukaryot Cell* **6**: 1635-1645.

Guo, B., C. A. Styles, Q. Feng & G. R. Fink, (2000) A *Saccharomyces* gene family involved in invasive growth, cell-cell adhesion, and mating. *Proc Natl Acad Sci U S A* **97**: 12158-12163.

Hagen, I., M. Ecker, A. Lagorce, J. M. Francois, S. Sestak, R. Rachel, G. Grossmann, N. C. Hauser, J. D. Hoheisel, W. Tanner & S. Strahl, (2004) Sed1p and Srl1p are required to compensate for cell wall instability in *Saccharomyces cerevisiae* mutants defective in multiple GPI-anchored mannoproteins. *Mol Microbiol* **52**: 1413-1425.

Hernanz-Falcon, P., O. Joffre, D. L. Williams & E. S. C. Reis, (2009) Internalization of Dectin-1 terminates induction of inflammatory responses. *Eur J Immunol* **39**: 507-513.

Horn, D. L., D. Neofytos, E. J. Anaissie, J. A. Fishman, W. J. Steinbach, A. J. Olyaei, K. A. Marr, M. A. Pfaller, C. H. Chang & K. M. Webster, (2009) Epidemiology and outcomes of candidemia in 2019 patients: data from the prospective antifungal therapy alliance registry. *Clin Infect Dis* **48**: 1695-1703.

Hoyer, L. L., (2001) The *ALS* gene family of *Candida albicans*. *Trends Microbiol* **9**: 176-180.

Jansen, J. M., M. F. Barry, C. K. Yoo & E. L. Weiss, (2006) Phosphoregulation of Cbk1 is critical for RAM network control of transcription and morphogenesis. *J Cell Biol* **175**: 755-766.

Kaiser, C., S. Michaelis & A. P. Mitchell, (1994) Methods in yeast genetics. A laboratory course manual. *Cold Spring Harbor Laboratory Press, Cold Spring Harbor, NY.*

Kamran, M., A. M. Calcagno, H. Findon, E. Bignell, M. D. Jones, P. Warn, P. Hopkins, D. W. Denning, G. Butler, T. Rogers, F. A. Muhlschlegel & K. Haynes, (2004) Inactivation of transcription factor gene *ACE2* in the fungal pathogen *Candida glabrata* results in hypervirulence. *Eukaryot Cell* **3**: 546-552.

King, L. & G. Butler, (1998) Ace2p, a regulator of *CTS1* (chitinase) expression, affects pseudohyphal production in *Saccharomyces cerevisiae*. *Curr Genet* **34**: 183-191.

Kumamoto, C. A. & M. D. Vinces, (2005a) Alternative *Candida albicans* lifestyles: growth on surfaces. *Annu Rev Microbiol* **59**: 113-133.

Kumamoto, C. A. & M. D. Vinces, (2005b) Contributions of hyphae and hypha-co-regulated genes to *Candida albicans* virulence. *Cell Microbiol* **7**: 1546-1554.

Lachke, S. A., S. Joly, K. Daniels & D. R. Soll, (2002) Phenotypic switching and filamentation in *Candida glabrata*. *Microbiology* **148**: 2661-2674.

Lambrechts, M. G., F. F. Bauer, J. Marmur & I. S. Pretorius, (1996) Muc1, a mucin-like protein that is regulated by Mss10, is critical for pseudohyphal differentiation in yeast. *Proc Natl Acad Sci U S A* **93**: 8419-8424.

Levine, B. & D. J. Klionsky, (2004) Development by self-digestion: molecular mechanisms and biological functions of autophagy. *Dev Cell* **6**: 463-477.

Mean, M., O. Marchetti & T. Calandra, (2008) Bench-to-bedside review: *Candida* infections in the intensive care unit. *Crit Care* **12**: 204.

Millard, P. J., B. L. Roth, H. P. Thi, S. T. Yue & R. P. Haugland, (1997) Development of the FUN-1 family of fluorescent probes for vacuole labeling and viability testing of yeasts. *Appl Environ Microbiol* **63**: 2897-2905.

Naglik, J., A. Albrecht, O. Bader & B. Hube, (2004) *Candida albicans* proteinases and host/pathogen interactions. *Cell Microbiol* **6**: 915-926.

Nelson, B., C. Kurischko, J. Horecka, M. Mody, P. Nair, L. Pratt, A. Zougman, L. D. McBroom, T. R. Hughes, C. Boone & F. C. Luca, (2003) RAM: a conserved signaling network that regulates Ace2p transcriptional activity and polarized morphogenesis. *Mol Biol Cell* **14**: 3782-3803.

Nelson, W. J., (2003) Adaptation of core mechanisms to generate cell polarity. *Nature* **422**: 766-774.

Noble, S. M. & A. D. Johnson, (2005) Strains and strategies for large-scale gene deletion studies of the diploid human fungal pathogen *Candida albicans*. *Eukaryot Cell* **4**: 298-309.

O'Conallain, C., M. T. Doolin, C. Taggart, F. Thornton & G. Butler, (1999) Regulated nuclear localisation of the yeast transcription factor Ace2p controls expression of chitinase (*CTS1*) in *Saccharomyces cerevisiae*. *Mol Gen Genet* **262**: 275-282.

Perlroth, J., B. Choi & B. Spellberg, (2007) Nosocomial fungal infections: epidemiology, diagnosis, and treatment. *Med Mycol* **45**: 321-346.

Pfaller, M. A., L. Boyken, R. J. Hollis, J. Kroeger, S. A. Messer, S. Tendolkar & D. J. Diekema, (2008) In vitro susceptibility of invasive isolates of *Candida* spp. to anidulafungin, caspofungin, and micafungin: six years of global surveillance. *J Clin Microbiol* **46**: 150-156.

Pfaller, M. A. & D. J. Diekema, (2007) Epidemiology of invasive candidiasis: a persistent public health problem. *Clin Microbiol Rev* **20**: 133-163.

Pfaller, M. A., S. A. Messer, L. Boyken, C. Rice, S. Tendolkar, R. J. Hollis & D. J. Diekema, (2004) Cross-resistance between fluconazole and ravuconazole and the use of fluconazole as a surrogate marker to predict susceptibility and resistance to ravuconazole among 12,796 clinical isolates of *Candida* spp. *J Clin Microbiol* **42**: 3137-3141.

Posas, F., M. Bollen, W. Stalmans & J. Arino, (1995) Biochemical characterization of recombinant yeast *PPZ1*, a protein phosphatase involved in salt tolerance. *FEBS Lett* **368**: 39-44.

Racki, W. J., A. M. Becam, F. Nasr & C. J. Herbert, (2000) Cbk1p, a protein similar to the human myotonic dystrophy kinase, is essential for normal morphogenesis in *Saccharomyces cerevisiae*. *EMBO J* **19**: 4524-4532.

Reuss, O., A. Vik, R. Kolter & J. Morschhauser, (2004) The *SAT1* flipper, an optimized tool for gene disruption in *Candida albicans*. *Gene* **341**: 119-127.

Rogers, N. C., E. C. Slack, A. D. Edwards, M. A. Nolte, O. Schulz, E. Schweighoffer, D. L. Williams, S. Gordon, V. L. Tybulewicz, G. D. Brown & C. Reis e Sousa, (2005) Syk-dependent cytokine induction by Dectin-1 reveals a novel pattern recognition pathway for C type lectins. *Immunity* **22**: 507-517.

Sambrook, J., E. Fritsch & T. Maniatis, Molecular cloning: A laboratory manual. *3rd edition, Cold Spring Harbor Press, New York*.

Sbia, M., E. J. Parnell, Y. Yu, A. E. Olsen, K. L. Kretschmann, W. P. Voth & D. J. Stillman, (2008) Regulation of the yeast Ace2 transcription factor during the cell cycle. *J Biol Chem* **283**: 11135-11145.

Shen, J., W. Guo & J. R. Kohler, (2005) Ca*NAT1*, a heterologous dominant selectable marker for transformation of *Candida albicans* and other pathogenic *Candida* species. *Infect Immun* **73**: 1239-1242.

Smyth, G. K., (2005) Limma: linear modesl for microarray data. In: Bioinformatics and Computational Biology Solutions using R and Bioconductor. V. C. R. Gentleman, S. Dudoit, R. Irizarry, W. Huber (ed). Springer pp. 397-420.

Song, Y., S. A. Cheon, K. E. Lee, S. Y. Lee, B. K. Lee, D. B. Oh, H. A. Kang & J. Y. Kim, (2008) Role of the RAM network in cell polarity and hyphal morphogenesis in *Candida albicans*. *Mol Biol Cell* **19**: 5456-5477.

Srikantha, T., K. J. Daniels, W. Wu, S. R. Lockhart, S. Yi, N. Sahni, N. Ma & D. R. Soll, (2008) Dark brown is the more virulent of the switch phenotypes of *Candida glabrata*. *Microbiology* **154**: 3309-3318.

Stead, D., H. Findon, Z. Yin, J. Walker, L. Selway, P. Cash, B. A. Dujon, C. Hennequin, A. J. Brown & K. Haynes, (2005) Proteomic changes associated with inactivation of the *Candida glabrata ACE2* virulence-moderating gene. *Proteomics* **5**: 1838-1848.

Teunissen, A. W. & H. Y. Steensma, (1995) Review: the dominant flocculation genes of *Saccharomyces cerevisiae* constitute a new subtelomeric gene family. *Yeast* **11**: 1001-1013.

Vazquez de Aldana, C. R., J. Correa, P. San Segundo, A. Bueno, A. R. Nebreda, E. Mendez & F. del Rey, (1991) Nucleotide sequence of the exo-1,3-beta-glucanase-encoding gene, *EXG1*, of the yeast *Saccharomyces cerevisiae*. *Gene* **97**: 173-182.

Verstrepen, K. J. & F. M. Klis, (2006) Flocculation, adhesion and biofilm formation in yeasts. *Mol Microbiol* **60**: 5-15.

Walton, F. J., J. Heitman & A. Idnurm, (2006) Conserved elements of the RAM signaling pathway establish cell polarity in the basidiomycete *Cryptococcus neoformans* in a divergent fashion from other fungi. *Mol Biol Cell* **17**: 3768-3780.

9 Publications

Transcriptional loops meet chromatin: a dual-layer network controls white-opaque switching in *C. albicans*

Denes Hnisz, Tobias Schwarzmüller, Karl Kuchler

Molecular Microbiology, 2009

Long homology flanking regions increase the recombination efficiency needed for target gene deletion in several *Candida* spp, including *C. albicans* (Noble & Johnson, 2005). After setting up and optimizing the generation of gene deletion constructs using fusion PCR for *C. glabrata*, we adopted this method also for the generation of *C. albicans* deletion strains. The deletion constructs carry auxotrophic markers (Cd*HIS1*, Cm*LEU2*, Cd*ARG4*) based on the pSN plasmids (Noble & Johnson, 2005). This technique is also used for generation of deletion constructs based on the dominant marker *SAT1* (Reuss *et al.*, 2004).
My contribution to the following work published in Molecular Microbiology comprises the generation of all auxotrophic marker-based gene deletion cassettes used for the generation of the single gene deletion strains and their preparation for transformation by electroporation.

Transcriptional loops meet chromatin: a dual-layer network controls white–opaque switching in *Candida albicans*

Denes Hnisz, Tobias Schwarzmüller and Karl Kuchler*
Medical University Vienna, Christian Doppler Laboratory for Infection Biology, Max F. Perutz Laboratories, Campus Vienna Biocenter, A-1030 Vienna, Austria.

Summary

The human pathogen *Candida albicans* is able to undergo a reversible switch between two distinct cell types called white and opaque, which are considered different transcriptional states of cells harbouring identical genomes. The present model of switching regulation includes the bistable expression of a master switch gene that is controlled by multiple transcriptional feedback loops. Here, we show that chromatin-modifying enzymes constitute an additional important regulatory layer of morphogenetic switching. We identify eight chromatin modifiers as switching modulators. Extensive epistasis analysis maps them into at least two independent signalling pathways overlaying the known transcriptional network. Interestingly, we identify the conserved Set3/Hos2 histone deacetylase complex as a key regulator relying on the methylation status of histone H3 lysine 4 for switching modulation. Furthermore, we demonstrate that opaque to white switching is facilitated by the presence of adenine *in vitro*, but adenine has no effect on switching once the Set/Hos2 complex is disrupted. Our observations postulate that chromatin modifications may serve as a means to integrate environmental or host stimuli through the underlying transcriptional circuits to determine cell fate in *C. albicans*.

Introduction

Individual cells in a genetically homogenous microbial culture may display different phenotypic characteristics. Such cell-to-cell variability is suggested to enhance the ability of microbial populations to adapt to a wide range of environmental stimuli, which, in the case of pathogens, may represent a strategy to evade host defences (Avery, 2006). The fungal pathogen *Candida albicans* displays a remarkable spectrum of heritable morphogenetic variations which is considered a major factor in the transition from a harmless commensal to a systemic pathogen of its human host (Whiteway and Bachewich, 2007). An intriguing and unique ability of *C. albicans* is to form two distinct cell types: the so-called white and opaque phases. White and opaque cells contain the same genome, yet they differ in cellular morphology, colony shape, gene expression profile and virulence properties. In addition, white cells are unable to mate, whereas opaque cells are mating-competent (Bennett and Johnson, 2005).

White–opaque switching is an epigenetic phenomenon that was already described some 20 years ago (Slutsky *et al.*, 1987), but the underlying molecular mechanisms have been only recently investigated. The white and opaque phases are heritable for many generations and switching between both phases is reversible, occurring at a frequency of one per ~10^3–10^4 cell divisions (Rikkerink *et al.*, 1988). The regulation of switching is believed to be transcriptional, and several transcription factors involved have been identified. *C. albicans* is diploid and harbours a mating type-like locus (*MTL*) holding two alleles, '**a**' and 'α'. Hence, the possible *MTL* configurations include *MTL***a**/**a**, *MTL*α/α and *MTL***a**/α (Hull and Johnson, 1999). A heterodimeric a/α repressor encoded by the a and α alleles respectively, locks *MTL* heterozygous cells in the white phase (Miller and Johnson, 2002) by repressing *WOR1*, the master opaque-promoting factor (Zordan *et al.*, 2006). *MTL* homozygous cells lack the a/α repressor, and are thus permissive to switching. In *MTL***a**/**a** or *MTL*α/α white cells, *WOR1* is expressed at a very low level, and high-level expression of *WOR1* is required for the conversion to the opaque phase (Huang *et al.*, 2006; Srikantha *et al.*, 2006; Zordan *et al.*, 2006). By contrast, the transcription factor Efg1 is enriched in white cells and is required for maintenance of the white phase (Sonneborn *et al.*, 1999; Srikantha *et al.*, 2000). According to the current model, stochastic increase in Wor1 levels drive the transition from the white to the opaque phase. Furthermore, Wor1 autoregulates its own expression, facilitates expression of its cofactor *WOR2*; and represses *EFG1* both directly and indirectly through promoting the expression of *CZF1*, a repressor of *EFG1*. As *EFG1* is a

Accepted 9 June, 2009. *For correspondence. E-mail karl.kuchler@meduniwien.ac.at; Tel. (+43) 1 4277 61807; Fax (+43) 1 4277 9618.

putative repressor of *WOR2*, *WOR1* thus co-ordinates three positive feedback loops to ensure high Wor1 levels, explaining the heritability of the opaque phase (Zordan *et al*., 2007). In addition, the histone deacetylases Hda1 and Rpd3 have been implicated in the regulation of white–opaque switching (Klar *et al*., 2001; Srikantha *et al*., 2001) but their precise role remains to be clarified.

In this work, we show that a complex dual-layer network, comprising of transcriptional regulators and chromatin-modifying enzymes, determines cellular identity in *C. albicans*. Our results experimentally confirm previous suggestions that cellular shape and phase-specific genes are regulated at different branching points of the transcriptional circuit, and that the genetic information affecting phase commitment converges at the *WOR1* locus. Importantly, we identify eight genes encoding putative histone-modifying enzymes as novel modulators of white–opaque switching in *C. albicans*. An extensive epistasis analysis maps various histone-modifiers into the transcriptional circuit. Strikingly, we show that the Set3/Hos2 histone deacetylase complex is a key regulator of *WOR1* expression, thus conversion to the opaque phase. Furthermore, we provide genetic evidence that the newly identified Set3/Hos2 defines a pathway depending on histone H3 lysine 4 (H3K4) methylation for switching regulation. Finally, we identify adenine as novel environmental factor facilitating opaque to white conversion, and demonstrate that the regulatory effect of adenine on switching requires *SET3*. We propose a comprehensive model whereby chromatin modifiers constitute a layer of regulation modulating the transcriptional circuits to trigger switching. Chromatin modification offers a possible mechanism to integrate environmental stimuli, contrary to the current models that explain morphogenetic switching as a stochastic process. Moreover, we postulate that the dependence of the Set3/Hos2 complex on H3K4 methylation at certain loci may be an evolutionary conserved mechanism among other eukaryotic taxa.

Results

WOR1 *acts downstream of* EFG1 *in phase commitment, while* EFG1 *acts downstream of* WOR1 *in morphology determination*

The white and opaque cell types of *C. albicans* are distinguished based on four criteria. (i) Cellular morphology: white cells have a round shape; opaque cells are larger and elongated (Slutsky *et al*., 1987). (ii) Colony appearance: white cells form white, dome-shaped colonies on solid agar, while opaque cells form larger, flattened colonies that are stained pink on media containing Phloxin B (Slutsky *et al*., 1987). (iii) Gene expression profile: about 400 genes are regulated differentially in the two phases (Lan *et al*., 2002). For diagnostic purposes, the white-specific genes *WH11* (Srikantha and Soll, 1993) and *EFG1* (Sonneborn *et al*., 1999), as well as opaque-specific genes *OP4* (Morrow *et al*., 1993) and *SAP1* (Morrow *et al*., 1992) are commonly used. (iv) Mating competence: white cells are mating incompetent, whereas opaque cells can mate with opaque cells of the opposite mating type (Miller and Johnson, 2002).

Previous studies established *WOR1* as the master regulator of the opaque phase. Deletion of *WOR1* locks *MTL***a**/**a** or *MTL*α/α cells in the white phase, whereas ectopic overexpression of *WOR1* results in the conversion to the opaque phase (Huang *et al*., 2006; Zordan *et al*., 2006). On the other hand, *MTL* homozygous *efg1*Δ/Δ cells predominantly exist in the opaque phase, while ectopic *EFG1* expression drives opaque to white conversion (Sonneborn *et al*., 1999). Recently, *EFG1* was suggested to promote the white phase by repressing *WOR2*, a cofactor of *WOR1* (Zordan *et al*., 2007). In addition, *EFG1* was proposed to act downstream of the switching event to regulate cellular morphology (Srikantha *et al*., 2000).

In order to experimentally verify the latter two suggestions, we created an *efg1*Δ/Δ *wor1*Δ/Δ double mutant in an *MTL***a**/**a** background. The *MTL***a**/**a** *efg1*Δ/Δ *wor1*Δ/Δ mutant displayed an elongated cell shape, albeit shorter than wild-type opaque cells, similar to the rare *MTL***a**/**a** *efg1*Δ/Δ white cells as well as *MTL***a**/α *efg1*Δ/Δ cells. In addition, the *MTL***a**/**a** *efg1*Δ/Δ *wor1*Δ/Δ mutant formed large, flattened colonies appearing light pink on Phloxin B agar, intermediate to the white and pink colour of wild-type white and opaque cells respectively. Conversely, *MTL***a**/**a** *efg1*Δ/Δ white isolates and *MTL***a**/α *efg1*Δ/Δ cells were white on Phloxin B plates (Fig. 1A). We inspected over 2000 colonies and all of them displayed the described morphology.

Next, we found that the *efg1*Δ/Δ *wor1*Δ/Δ double mutant expressed the white-specific transcript *WH11* similar to wild-type white and *wor1*Δ/Δ cells (the latter being locked in the white phase). Conversely, the opaque-specific transcripts *OP4* and *SAP1* were virtually undetectable. *MTL***a**/α *efg1*Δ/Δ cells also showed a white-phase expression profile (Fig. 1B). This datum in accordance with previous publications (see *Introduction*) suggests that in switching-permissive cells, loss of *EFG1* results in the formation of true opaque cells due to the upregulation of *WOR1*, which we directly confirmed by immunoblotting (Fig. 1C). As expected, the **a**/α repressor still inhibits *WOR1* expression in *MTL***a**/α *efg1*Δ/Δ cells, thus locking cells in a white-like phase (Fig. 1A–C). Therefore, *EFG1* indeed promotes the white phase by repressing *WOR1* either directly or indirectly.

We also tested the mating ability of the *MTL***a**/**a** *efg1*Δ/Δ *wor1*Δ/Δ double mutant, and found that its mating competence was as negligible as that of wild-type white cells

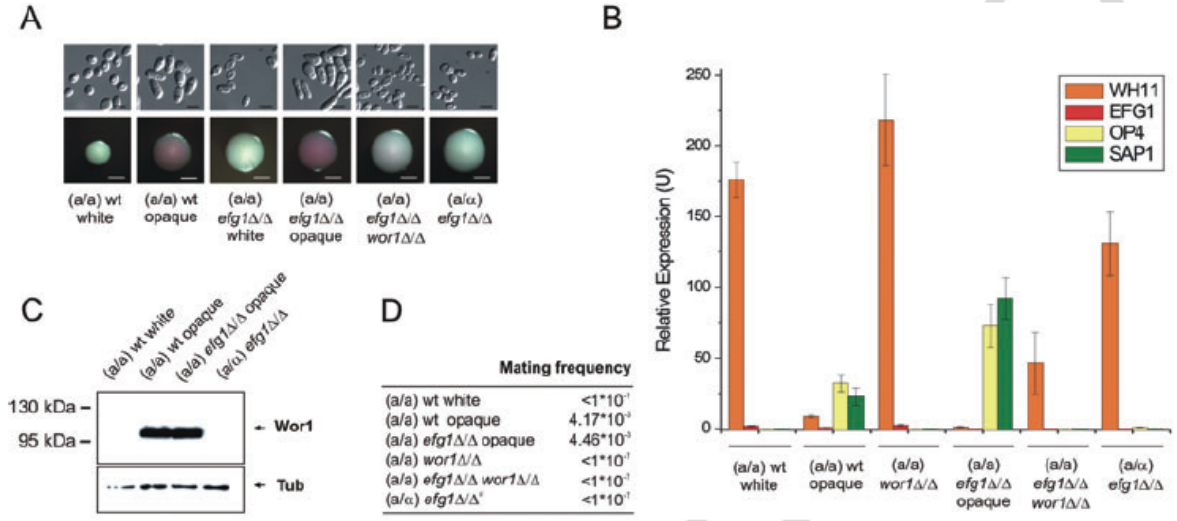

Fig. 1. *WOR1* acts downstream of *EFG1* in phase commitment, while *EFG1* acts downstream of *WOR1* in morphology determination.
A. Colony and cellular morphologies on modified Lee's medium containing 5 μg ml^{-1} Phloxin B. Scale bars correspond to 5 μm (upper panel) and 2 mm (lower panel).
B. qRT-PCR analysis of phase-specific mRNA transcripts. *WH11*, *EFG1* (white-specific) and *OP4*, *SAP1* (opaque-specific) transcript levels were normalized to the transcript level of *PAT1* (Zordan *et al.*, 2006). qRT-PCR reactions were performed in triplicates and cDNA isolated from two independent cultures were analysed. Data are shown as mean ± SD.
C. Immunoblot analysis confirms that *WOR1* is repressed by *EFG1* and the a/α repressor. Tubulin indicates equivalent loading.
D. *WOR1* is required for mating. Quantitative mating assays were performed with an opaque phase *MTL*α/α tester strain. At least two independent experiments per genotype were performed yielding qualitatively similar results. Values are shown of one representative experiment. #: tested with both an *MTL***a**/**a** and an *MTL*α/α tester strain.

(Fig. 1D). Therefore, *MTL***a**/**a** *efg1*Δ/Δ *wor1*Δ/Δ cells are functionally white and express white-specific genes. Nevertheless, they show an elongated morphology distinguishable from wild-type white cells. These data demonstrate that *WOR1* acts downstream of *EFG1* in phase commitment, while *EFG1* acts downstream of *WOR1* in morphology determination.

Several histone-modifying genes modulate white–opaque switching

Although transcription factors are known to regulate white–opaque conversion, neither a rearrangement in DNA sequences nor any modification of chromatin has been associated with switching. Notably, lack of the histone deacetylase genes *HDA1* and *RPD3* modify frequencies of switching (Klar *et al.*, 2001; Srikantha *et al.*, 2001). Therefore, we decided to analyse the contribution of histone-modifying enzymes to phase transitions in a comprehensive way. We analysed the genome of related fungal species *Saccharomyces cerevisiae* (http://www.yeastgenome.org) to identify open reading frames (ORFs) encoding putative histone modifiers (acetyltransferases, deacetylases, methyltransferases and dephosphorylases) either as regulatory or catalytic subunits of larger protein complexes. Out of some 90 genes, we selected only those encoding catalytic subunits, yielding a total of 23 genes (including one additional ORF: *SET3*). BLAST searches (http://www.ncbi.nlm.nih.gov/blast) against the *C. albicans* genome identified all potential orthologues, revealing that *S. cerevisiae* histone modifiers are highly conserved in *C. albicans*. Subsequently, we constructed homozygous deletion mutants of the listed ORFs in an *MTL***a**/**a** *C. albicans* strain. Out of 23 candidates, we successfully created homozygous deletion strains of 18 genes. The identified ORFs, their predicted functions, the BLAST*E*-values and whether a deletion mutant was created are listed in Table S1.

Next, we analysed the effect of gene deletions on the frequency of white to opaque conversion using quantitative switching assays. Briefly, pure white cultures were plated on Phloxin B plates, and the frequency of opaque colonies or colonies containing at least one opaque sector was scored (as monitored by colony morphology and microscopy). Knock-out mutants showing significant alterations compared with the background strain are listed in Table 1. *C. albicans* genes whose deletion facilitated the formation of opaque colonies or sectors included *SET1*, a H3K4 methyltransferase (Roguev *et al.*, 2001; Raman *et al.*, 2006) required for gene silencing at telomeres and rDNA sequences in *S. cerevisiae* (Nislow *et al.*, 1997); *HDA1*, a histone deacetylase (Carmen *et al.*, 1996) acting

Table 1. Histone-modifier genes are modulators of white–opaque switching.

	White → opaque		Opaque → white	
Strain	Switch (%)	*n*	Switch (%)	*n*
wt (**a**/α)	0 ± 0	1808	–	–
wt (**a**/**a**)	11.3 ± 1.9	1113	10.2 ± 1.1	1089
*set1*Δ/Δ	19.5 ± 4.5*	863	10.0 ± 4.5	1886
*hda1*Δ/Δ	30.8 ± 13.2*	2328	10.8 ± 5.4	1320
*rpd31*Δ/Δ	32.2 ± 0.7**	1289	12.5 ± 1.4	800
*set3*Δ/Δ	1.8 ± 0.3**	1352	27.6 ± 2.4**[a]	743
*hos2*Δ/Δ	1.5 ± 0.2**	1539	23.4 ± 2.2**[a]	1495
*hst2*Δ/Δ	0.4 ± 0.4**	1994	19.0 ± 14.0	1272
*nat4*Δ/Δ	1.4 ± 0.6**	2006	34.9 ± 13.7*	1171
*hst1*Δ/Δ	14.6 ± 4.8	2038	3.8 ± 0.4**	1270
*pho13*Δ/Δ	10.5 ± 1.1	807	51.1 ± 7.9**	1033

a. Informative value (see text).
*$P < 0.05$ and **$P < 0.005$ relative to wild type (Student's *t*-test).
Quantitative white to opaque (left panel) and opaque to white (right panel) switching assays were performed with multiple homozygous deletion mutants. The percentages represent the fraction of colonies that showed an alteration of the original phenotype. The gene deletions were constructed in the wild-type *MTL***a**/**a** background strain (second row). As expected, wild-type *MTL***a**/α strains are locked in the white phase. Data are displayed as a mean ± SD as well as the total number of colonies scored in three independent experiments carried out with the same strain.

as a global repressor of transcription in *S. cerevisiae* (Rundlett *et al.*, 1996); *HDA1* served as a control in our gene set, because its loss was previously shown to increase the frequency of opaque formation (Klar *et al.*, 2001); and *RPD31*, one of the two orthologues of yeast *RPD3*, a histone deacetylase involved in transcriptional repression in *S. cerevisiae* (Rundlett *et al.* (1996). The genome of *C. albicans* harbours two potential orthologues of *RPD3* designated *RPD3* and *RPD31* (Table S1). Interestingly, a deletion of *RPD3* has similar effects on the white to opaque switching frequency (Srikantha *et al.*, 2001). Genes whose deletion significantly decreased opaque conversion relative to wild-type included: *SET3*, an essential component of the Set3 histone deacetylase complex involved in the suppression of meiotic genes in *S. cerevisiae* (Pijnappel *et al.*, 2001); *HOS2*, a histone deacetylase and subunit of the Set3 complex (Pijnappel *et al.*, 2001) required for gene activity in *S. cerevisiae* (Wang *et al.*, 2002); *HST2*, a histone deacetylase similar to *SIR2* (Landry *et al.*, 2000) required for centromeric and rDNA silencing in *S. cerevisiae* (Durand-Dubief *et al.*, 2007); and *NAT4*, an acetyltransferase mediating histone H4 and H2A acetylation (Song *et al.*, 2003).

Furthermore, we analysed the impact of the deletions on the heritability of the opaque phase using quantitative switching assays. In these assays, opaque phase cultures were plated on Phloxin B agar, and the arising frequency of pure white colonies and colonies containing at least one white sector was scored (Table 1). Genes whose deletion increased the heritability of the opaque phase (i.e. displaying a lower frequency of conversion to white than wild type) included *HST1*, a histone deacetylase, a nonessential subunit of the Set3 complex (Pijnappel *et al.*, 2001), as well as an essential subunit of the Sum1/Rfm1/Hst1 complex, which functions as a repressor of sporulation-specific genes in *S. cerevisiae* (Xie *et al.*, 1999). Genes whose deletion destabilized the opaque phase (i.e. the deletion mutant showed a higher frequency of conversion to white than wild type) included *PHO13*, a phosphatase dephosporylating H2A *in vitro* (Tuleva *et al.*, 1998) and implicated in carbohydrate metabolism in *S. cerevisiae* (Van Vleet *et al.*, 2007); and *NAT4* (see above).

Surprisingly, the loss of either *SET3* or *HOS2* led to an unexpected phenotype: the opaque colonies of the *set3*Δ/Δ and *hos2*Δ/Δ mutants displayed filamentous growth (D. Hnisz and K. Kuchler, in preparation). We assayed the opaque to white switching frequencies of these filamenting mutants, and found an increase in the conversion to the white phase when compared with wild-type cultures (Table 1); however, this datum should be interpreted with caution, because the filaments could not be reliably fragmented into individual colony forming units with our method (see *Experimental procedures*). Moreover, a lack of *SET3* or *HOS2* is likely to exert pleiotropic effects on both white–opaque switching and filamentation, i.e. by affecting two distinct transcriptional programmes, whose putative cross-talk would inherently impact the scoring method.

To confirm the switching data, we created a second independent set of deletion mutants of all genes showing an effect on switching and repeated the quantitative switching assays in both directions. In all cases, the independent deletion strains qualitatively reproduced all relevant phenotypes of the first deletion strains (data not shown). Furthermore, we complemented the deletions of *SET3*, *HOS2*, *NAT4* and *HST2* which were the key genes of our further analyses. The complemented strains displayed switching frequencies comparable to wild type (Table S8). As summarized in Fig. 2A, these results show that histone-modifying enzymes of various classes can modulate white–opaque switching in multiple ways. However, where and how histone modifiers modulate phase conversion is not yet clear.

Histone modifiers act upstream of WOR1

Previous work established that the formation of mating-competent opaque cells requires Wor1 (see above). Indeed, we were unable to detect Wor1 by immunoblotting in any of the investigated white phase single mutant cultures. By contrast, opaque phase mutant cells expressed Wor1 at levels comparable to those present in wild-type opaque strains (Fig. 2B). Furthermore, white

A

opaque ⇨ white	⇧	⇩	Ø
⇧		*hos2Δ/Δ* *set3Δ/Δ* *nat4Δ/Δ*	*pho13Δ/Δ*
⇩			*hst1Δ/Δ*
Ø	*set1Δ/Δ* *rpd31Δ/Δ* *hda1Δ/Δ*	*hst2Δ/Δ*	

white ⇨ opaque

B

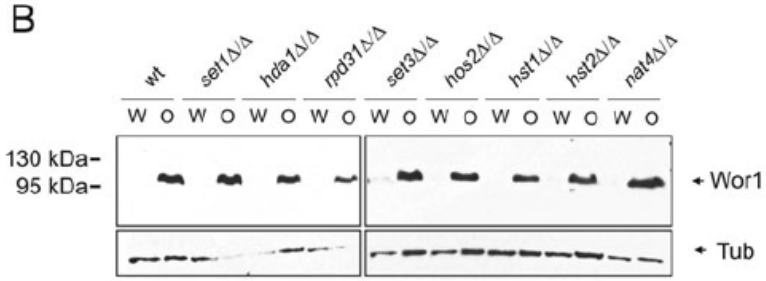

C

Strain	Mating frequency White	Opaque
wt	$<1*10^{-7}$	$3.92*10^{-3}$
set1Δ/Δ	$<1*10^{-7}$	$1.89*10^{-3}$
hda1Δ/Δ	$<1*10^{-7}$	$1.04*10^{-3}$
rpd31Δ/Δ	$<1*10^{-7}$	$1.29*10^{-3}$
set3Δ/Δ	$<1*10^{-7}$	$3.88*10^{-3}$
hos2Δ/Δ	$<1*10^{-7}$	$1.41*10^{-3}$
hst1Δ/Δ	$<1*10^{-7}$	$2.55*10^{-3}$
hst2Δ/Δ	$<1*10^{-7}$	$2.76*10^{-3}$
pho13Δ/Δ	$<1*10^{-7}$	$2.86*10^{-3}$
nat4Δ/Δ	$<1*10^{-7}$	$2.59*10^{-3}$

D

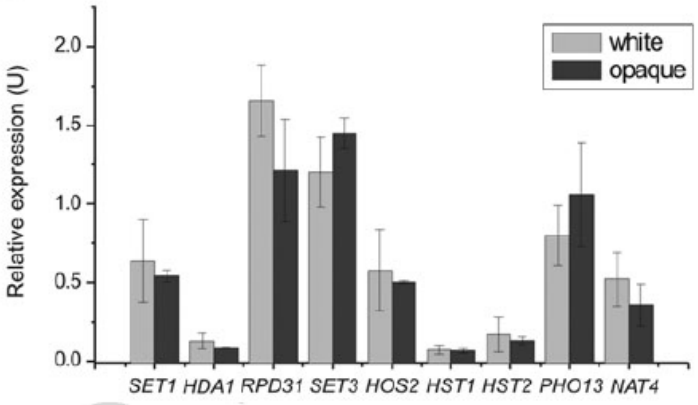

Fig. 2. Histone modifiers act upstream of *WOR1*.
A. Functional categories of single gene deletions on white–opaque switching.
B. Immunoblot analysis demonstrates that Wor1 is expressed in a similar pattern in wild type and mutant white (W) and opaque (O) cultures. Tubulin indicates equivalent loading.
C. Mating competence is differentially regulated in single mutant cells similar to wild type. Quantitative mating assays were performed with an opaque phase *MTLα/α* tester strain. At least two independent experiments per genotype were performed giving qualitatively similar results. Values are shown of one representative experiment.
D. Transcript levels of histone modifiers are phase-independent. qRT-PCR was performed in triplicates and cDNA isolated from two independent cultures were analysed. Transcript levels are normalized to *PAT1*. Data are shown as mean ± SD.

and opaque phase single deletion mutants exhibited mating competence comparable to wild-type white and opaque strains respectively (Fig. 2C). These results suggest that histone modifiers act either upstream or at the level of *WOR1* expression.

To address whether phase-specific expression of genes is responsible for phase changes, we performed quantitative RT-PCR to compare expression levels of the switching modulators in the white and opaque phases (Fig. 2D). We failed to detect any significant differences of transcript levels between the two phases, neither in our *MTL***a**/**a** background strain (Fig. 2D) nor in the independent *MTL***a**/**a** clinical isolate L26 (data not shown). These results demonstrate that the activities rather then expression levels of histone modifiers modulate the outcome of the transcriptional regulatory circuit(s), which converge(s) at the master switch locus *WOR1*.

Epistasis of SET3, HOS2, HST2, NAT4 and EFG1 reveals multiple pathways

Interestingly, although the genes have different molecular functions, deletion of *SET3*, *HOS2*, *HST2* and *NAT4* all reduced the switching frequency about 5–10-fold from white to opaque (see above). Altered chromatin state can influence DNA accessibility to non-histone proteins such as the transcriptional machinery or transcription factors can recruit chromatin-modifying enzymes to facilitate their activities (Kouzarides, 2007). For instance, the *C. albicans* transcription factor Efg1 is a basic helix–loop–helix protein displaying DNA-binding activity *in vitro* has also been implicated in phase switching (Stoldt *et al.*, 1997). To elucidate whether *SET3*, *HOS2*, *HST2* or *NAT4* modulate white to opaque switching in concert with *EFG1*, we constructed *efg1Δ/Δ hos2Δ/Δ*, *efg1Δ/Δ set3Δ/Δ*,

Table 2. Epistasis analysis of *SET3*, *HOS2*, *NAT4*, *HST2* and *EFG1*.

	White → opaque		Opaque → white	
Strain	Switch (%)	*n*	Switch (%)	*n*
wt	11.3 ± 1.9	1113	10.2 ± 1.1	1089
efg1Δ/Δ	97.7 ± 1.0	1110	0.6 ± 0.8	1576
efg1Δ/Δ hst2Δ/Δ	87.9 ± 20.1	940	1.9 ± 2.6	1969
efg1Δ/Δ nat4Δ/Δ	89.2 ± 10.7	812	0.3 ± 0.6	1568
efg1Δ/Δ set3Δ/Δ	3.0 ± 1.6	2685	12.9 ± 6.7	1299
efg1Δ/Δ hos2Δ/Δ	3.6 ± 1.3	1148	5.2 ± 6.3	1061
efg1Δ/Δ hst2Δ/Δ hos2Δ/Δ	5.6 ± 3.6	1117	5.5 ± 3.7	599
efg1Δ/Δ nat4Δ/Δ set3Δ/Δ	2.7 ± 1.3	1322	10.4 ± 6.9	906

Quantitative white to opaque (left panel) and opaque to white (right panel) switching assays were performed with multiple homozygous deletion mutants. The percentages represent the fraction of colonies that showed an alteration of the original phenotype. All strains are *MTLa/a* strains. Data are displayed as a mean ± SD as well as the total number of colonies scored in three independent experiments carried out with the same strain.

efg1Δ/Δ hst2Δ/Δ and *efg1Δ/Δ nat4Δ/Δ* double mutants, and performed epistasis analysis by comparing their switching frequencies with those of the corresponding single mutants (Tables 1 and 2). The phases were verified by colony morphology, microscopy (data not shown) and quantitative mating assays (Table S5). The results were as follows: *efg1Δ/Δ*: 97.7%, *set3Δ/Δ*: 1.8%, *hos2Δ/Δ*: 1.5%, *hst2Δ/Δ*: 0.4% and *nat4Δ/Δ*: 1.4%, whereas for the double mutants: *efg1Δ/Δ set3Δ/Δ*: 3.0%, *efg1Δ/Δ hos2Δ/Δ*: 3.6%, *efg1Δ/Δ hst2Δ/Δ*: 87.9% and *efg1Δ/Δ nat4Δ/Δ*: 89.2% (Tables 1 and 2). Hence, loss of *EFG1* is epistatic to the deletion of either *HST2* or *NAT4*, whereas *HOS2* or *SET3* deletion qualitatively suppresses the loss of *EFG1*. In other words, although the repression of *EFG1* on *WOR1* is relieved, stable high-level expression of *WOR1* still requires both *SET3* and *HOS2*. On the other hand, *HST2* and *NAT4* are likely to exert their effect in a transcriptional loop converging at the *WOR1* locus either at the level of *EFG1* or upstream of it. Notably, the opposite switching frequencies from opaque to white showed a similar epistasis (right panel, Table 2). As a further control, we restored the *SET3* and *HOS2* ORFs in the *efg1Δ/Δ set3Δ/Δ* and *efg1Δ/Δ hos2Δ/Δ* respectively, and found that the complemented mutants showed switching frequencies comparable to the *efg1Δ/Δ* mutant (Table S8).

To verify that *HOS2* and *SET3* indeed act in an independent pathway of either *NAT4* or *HST2*, we tested the switching frequencies of *efg1Δ/Δ hst2Δ/Δ hos2Δ/Δ* and *efg1Δ/Δ nat4Δ/Δ set3Δ/Δ* triple mutants in both switching directions. As predicted, deletion of *NAT4* in an *efg1Δ/Δ set3Δ/Δ* mutant, and deletion of *HST2* in an *efg1Δ/Δ hos2Δ/Δ* mutant had no significant effect on switching frequencies when compared with the respective double deletion strains (Table 2). In summary, the epistasis analysis revealed at least two independent regulatory pathways affecting the transcriptional loops controlling morphogenetic switching.

Loss of SET3 or HOS2 suppresses deletion of RPD31 or HDA1

The *S. cerevisiae* orthologues of Hos2, Hda1 and Rpd31 are histone deacetylases catalytically active on multiple acetylated lysine residues of core histones (Pijnappel *et al.*, 2001; Suka *et al.*, 2001; Wu *et al.*, 2001). Set3 is an integral subunit of the Set3/Hos2 deacetylase complex (Pijnappel *et al.*, 2001). To address whether there is a division of labour between deacetylase complexes in the regulation of *C. albicans* white–opaque switching, we created a series of double deletion strains and compared their switching frequencies with those of single deletion mutants. As shown in Tables 1 and 3, deletion of *SET3* is epistatic to the loss of *HDA1* and *RPD31*, and deletion of *HOS2* is epistatic to the deletion of *RPD31*. Phases were verified by colony morphology, microscopy (data not shown) and quantitative mating assays (Table S6). These results support the notion that Set3 and Hos2 act in a

Table 3. Loss of *SET3* or *HOS2* is epistatic to the deletion of *HDA1* or *RPD31*.

	White → opaque		Opaque → white	
Strain	Switch (%)	*n*	Switch (%)	*n*
wt	11.6 ± 4.5	560	21.8 ± 9.5	609
hda1Δ/Δ set3Δ/Δ	1.4 ± 0.8	1295	NA	–
rpd31Δ/Δ set3Δ/Δ	2.1 ± 0.9	1409	NA	–
rpd31Δ/Δ hos2Δ/Δ	0.7 ± 0.3	1479	NA	–

Quantitative white to opaque (left panel) and opaque to white (right panel) switching assays were performed with multiple homozygous deletion mutants. The percentages represent the fraction of colonies that showed an alteration of the original phenotype. All strains are *MTLa/a* strains. The opaque to white switching frequencies were not scored because of the opaque-specific filamentation phenotype caused by the loss of *SET3* or *HOS2* (see text). Data are displayed as a mean ± SD as well as the total number of colonies scored in three independent experiments carried out with the same strain.
NA, not assayed.

complex in *C. albicans* functioning as a downstream regulator of white–opaque switching.

Loss of H3K4 methylation suppresses the effect of the deletion of SET3 or HOS2

Where and how is the Set3/Hos2 complex recruited? Inspection of the CaSet3 primary sequence revealed two characteristic domains: a SET and a PHD (Plant HomeoDomain) domain (Fig. 3A). This domain architecture is conserved among many genes implicated in epigenetic regulation, including *ASH1* and *Thrithorax* in *Drosophila* (Stassen *et al.*, 1995; Tripoulas *et al.*, 1996). The SET domains have two functions: methyltransferase activity acting on histones (Rea *et al.*, 2000) or other non-histone substrates, and they may serve as protein–protein interaction surfaces (Rozenblatt-Rosen *et al.*, 1998). The PHD finger is a specialized methyl-lysine binding domain found in various proteins 'reading' histone marks (Shi *et al.*, 2006). Recently, the purified PHD finger of ScSet3 was shown to preferentially bind trimethylated H3K4 (Allis *et al.*, 2007). Notably, *CaSET1* appears as the only *C. albicans* methyltransferase modifying H3K4, and its deletion results in a complete loss of H3K4 methylation (Raman *et al.*, 2006).

To address whether the Set3/Hos2 complex requires H3K4 methylation for the regulation of white–opaque switching in *C. albicans*, we compared the switching frequencies of *set1*Δ/Δ *set3*Δ/Δ and *set1*Δ/Δ *hos2*Δ/Δ double mutants to those of the respective single deletion strains (Tables 1 and 4). Strikingly, the absence of *SET1* almost completely suppressed the loss of *SET3* or *HOS2* (white to opaque switching frequencies: *set1*Δ/Δ: 19.5%, *hos2*Δ/Δ: 1.5%, *set3*Δ/Δ: 1.8%, *set1*Δ/Δ *set3*Δ/Δ 10.5%, *set1*Δ/Δ *hos2*Δ/Δ 12.8%). To verify the rescue effect, we performed an epistasis analysis of *SET1* and *HOS2* in a genetic background where the transcriptional feedback from *EFG1* towards *WOR1* is disrupted. Therefore, we compared the white to opaque switching frequencies of *efg1*Δ/Δ, *efg1*Δ/Δ *set1*Δ/Δ, *efg1*Δ/Δ *hos2*Δ/Δ and *efg1*Δ/Δ *set1*Δ/Δ *hos2*Δ/Δ mutants (Tables 1, 2 and 4). White *efg1*Δ/Δ cells converted at high frequencies to opaque

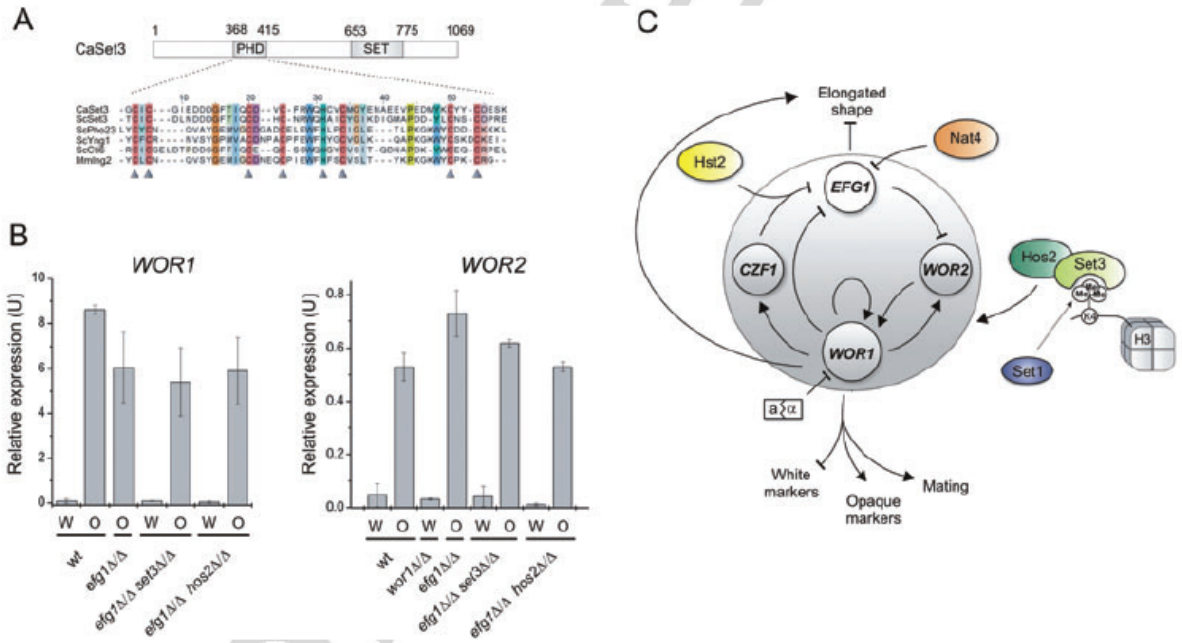

Fig. 3. The Set3/Hos2 complex is a key regulator of white–opaque switching.
A. The PHD finger of CaSET3. The amino acid sequence was aligned to the PHD fingers of ScSet3, ScPho23, ScYng1, ScCti6 and MmIng2 that were shown to bind H3K4me3 specifically *in vitro* (Shi *et al.*, 2006; Allis *et al.*, 2007). Colours indicate homologous residues. Arrowheads highlight the residues of the characteristic Cys_4-His-Cys_3 Zn^{2+} co-ordination motif.
B. qRT-PCR analysis of *WOR1* and *WOR2* expression in Set3/Hos2-pathway mutants. Deletion of either *SET3* or *HOS2* in an *efg1*Δ/Δ background does not cause significant changes in the steady-state transcription level of either *WOR1* or *WOR2*. The mRNA levels are normalized to *PAT1*. qRT-PCR reactions were performed in triplicates and cDNA isolated from two independent cultures were analysed. Data are shown as mean ± SD.
C. Dual-layer model of the regulation of white–opaque switching in *C. albicans*. The dotted grey circle denotes the transcriptional circuit as described (Zordan *et al.*, 2007). White and opaque enriched regulators are shown in white and grey respectively. Coloured elements represent histone-modifying pathways modulating the output of the transcriptional circuit.

Table 4. Loss of H3K4 methylation suppresses the effects of *SET3* or *HOS2* deletions.

	White → opaque		Opaque → white	
Strain	Switch (%)	*n*	Switch (%)	*n*
wt	11.6 ± 4.5	560	21.8 ± 9.5	609
set1Δ/Δ hos2Δ/Δ	12.8 ± 2.7	1303	NA	–
set1Δ/Δ set3Δ/Δ	10.5 ± 4.4	1108	NA	–
efg1Δ/Δ set1Δ/Δ	NA	–	0.2 ± 0.3	1636
efg1Δ/Δ set1Δ/Δ hos2Δ/Δ	80.6 ± 7.5	1318	1.4 ± 1.5	1730
wor1Δ/Δ	0 ± 0	1661	NA	–
wor1Δ/Δ set1Δ/Δ	0 ± 0	1458	NA	–
wor1Δ/Δ set3Δ/Δ	0 ± 0	1734	NA	–
wor1Δ/Δ hos2Δ/Δ	0 ± 0	1079	NA	–
wor1Δ/Δ set1Δ/Δ hos2Δ/Δ	0 ± 0	1662	NA	–

Quantitative white to opaque (left panel) and opaque to white (right panel) switching assays were performed with multiple homozygous deletion mutants. The percentages represent the fraction of colonies that showed an alteration of the original phenotype. All strains are *MTL***a**/**a** strains. Data are displayed as a mean ± SD as well as the total number of colonies scored in three independent experiments carried out with the same strain. NA, not assayed.

(97.7%, Table 2). *efg1Δ/Δ set1Δ/Δ* cells almost exclusively existed in the opaque phase, as we failed to isolate single white phase colonies of this mutant. *efg1Δ/Δ hos2Δ/Δ* white cells converted at low frequencies to opaque cells (3.6%, Table 2). As expected, *efg1Δ/Δ set1Δ/Δ hos2Δ/Δ* white cells also readily convert to the opaque phase (80.6%, Table 4), while the opaque phase appears as stable as in *efg1Δ/Δ* and *efg1Δ/Δ set1Δ/Δ* opaque isolates (Tables 2 and 4). The phases were verified by colony morphology, microscopy (data not shown) and quantitative mating assays (Table S7).

As deletion of either *SET3* or *HOS2* was epistatic to the deletion of *EFG1* in switching modulation (Table 3), we sought evidence that the newly identified Set3/Hos2 pathway indeed regulates *WOR1* expression to drive phenotypic switching. As shown in Table 4, deletion of *WOR1* in *set1Δ/Δ*, *set3Δ/Δ*, *hos2Δ/Δ* and *set1Δ/Δ hos2Δ/Δ* mutants locks cells in the white phase, supporting that the Set3/Hos2 pathway mediates regulatory input upstream or at the level of *WOR1* expression. To test whether the disruption of the pathway is reflected in the steady state transcript levels of *WOR1*, we performed quantitative real-time PCR analysis, but found no difference in *WOR1* mRNA levels between wild-type, *efg1Δ/Δ*, *efg1Δ/Δ set3Δ/Δ* and *efg1Δ/Δ hos2Δ/Δ* cultures neither in the white nor in the opaque phase. It is to note that we analysed the double deletion strains, because we repeatedly failed to maintain the *set3Δ/Δ* and *hos2Δ/Δ* single deletion mutants in relatively pure opaque phase cultures, most likely because they show an elevated opaque to white switching frequency (Table 1). However, because of the epistatic relationship of *SET3*, *HOS2* and *EFG1*, the input of the Set3/Hos2 pathway can be measured in an *EFG1*-deletion background, and the *efg1Δ/Δ set3Δ/Δ* as well as the *efg1Δ/Δ hos2Δ/Δ* mutants are marginally more stable in the opaque phase than the *set3Δ/Δ* and *hos2Δ/Δ* mutants (compare Tables 1 and 2). To address whether the Set3/Hos2 complex acts at other possible loci, we analysed the transcript levels of *WOR2*, the cofactor of *WOR1*, in wild type, *efg1Δ/Δ*, *efg1Δ/Δ set3Δ/Δ* and *efg1Δ/Δ hos2Δ/Δ* mutants, but again found no significant differences between wild type and the deletion mutants in either of the phases. Taken together, these results demonstrate that deletion of *SET1* and loss of H3K4 methylation suppresses the deletion of *SET3* or *HOS2*, suggesting that the Set3/Hos2 complex acts through Set1 and thus requires H3K4 methylation for switching regulation.

Adenine facilitates opaque to white switching depending on SET3

Environmental factors can modulate morphogenetic switching of *C. albicans*. For instance, opaque cells convert to the white phase at elevated temperatures (Rikkerink *et al.*, 1988), whereas white cells of certain strains readily convert to the opaque phase under anaerobic conditions (Ramirez-Zavala *et al.*, 2008). To address whether our newly identified modulators link environmental signals to white–opaque switching, we analysed switching frequencies of wild-type and several single deletion strains under different conditions, including changes in temperature, CO_2 and nutrient concentrations. Strikingly, we found that supplementation of the routinely used Lee's medium with 100 μg ml^{-1} adenine increased the conversion frequency from the opaque to the white phase. In these experiments, cells were grown on source plates for 5 days at 25°C, resuspended in water, spread onto destination plates at a low density and cultivated for another 5 days at 25°C. The effect was most pronounced if both plates contained

Table 5. Adenine stimulates opaque-white switching in wild type but not in *set3*Δ/Δ cells.

Strain	Source plate (adenine)	Destination plate (adenine)	Switch %	Switch *n*
wt opaque	–	–	2.2 ± 0.9	376
		+	5.8 ± 1.9	286
	+	–	7.7 ± 3.7	290
	+	+	14.1 ± 6.6	260
*set3*Δ/Δ opaque	–	–	30.2 ± 2.7	180
		+	31.7 ± 2.5	202
	+	–	31.7 ± 4.8	250
	+	+	32.3 ± 1.0	228

Quantitative opaque to white switching assays were performed with multiple homozygous deletion mutants. Cells were incubated for 5 days on the source plates containing either none (–) or 100 μg ml^{-1} adenine (+) and were spread onto the destination plates containing none (–) or 100 μg ml^{-1} adenine (+). The percentages represent the fraction of white phase colonies scored after 5 days' incubation period. All strains are *MTL***a**/**a** strains. Data are displayed as a mean ± SD as well as the total number of colonies scored in three independent experiments carried out with the same strain.

adenine (Table 5). This regulatory effect is also supported by the observation that our wild-type background strain showed elevated opaque to white switching frequencies on SD plates when compared with Lee's medium (Tables 1 and 3). Furthermore, the *set3*Δ/Δ deletion mutant displayed no alteration in opaque to white switching frequency in the presence of adenine in the medium (Table 5). These results identify adenine as a novel environmental factor regulating morphogenetic switching of *C. albicans*, and demonstrate that a functional Set3/Hos2 pathway is required to transmit the relevant input signal in the transcriptional circuit underlying switching.

Discussion

A model of white–opaque switching in C. albicans *including two regulatory layers*

In this study, we used the phenomenon of white–opaque switching in *C. albicans* to analyse the mechanisms of heritable phenotypic variation in a eukaryotic unicellular pathogen. The white and opaque cell types of *C. albicans* represent different transcriptional states of cells containing otherwise identical genomes. Morphogenetic switching is thought to generate distinct cell variants with different capabilities to adapt to various host niches and/or host defences *in vivo*. Current models explain the regulation of switching by a transcription circuitry amplifying stochastic changes of the expression of one master transcription factor gene, *WOR1*. We used a reverse genetic approach to decipher the role of chromatin-modifying enzymes in white–opaque switching. Based on our data, we propose a novel dual-layer network model for the regulation of morphogenetic switching in *C. albicans* (Fig. 3C).

Transcriptional layer of regulation

The architecture of the transcriptional circuit has been described earlier (Zordan *et al.*, 2007). In *MTL* heterozygous cells, *WOR1* is repressed by the *MTL***a**/α repressor. In *MTL* homozygous white cells, Wor1 levels are low because *EFG1* represses *WOR2*, a putative cofactor of *WOR1*. Once the level or activity of Wor1 reaches a threshold, cells convert to the opaque phase. Conversely, opaque cells maintain Wor1 at high levels requiring multiple positive feedback loops mediated by Wor1, including (i) autoregulation of the *WOR1* locus; (ii) through the activation of *WOR2*; (iii) through repressing *EFG1* directly and also indirectly by activating *CZF1*, a repressor of Efg1. In this model, *EFG1* and *WOR1* promote the white and opaque phases respectively (Zordan *et al.*, 2007). However, our data demonstrate that cells lacking both *EFG1* and *WOR1* not only fail to express opaque-specific genes such as *OP4* and *SAP1*, but also express the white-specific *WH11* transcript like wild-type white cells (Fig. 1B). Wor1 in wild-type opaque cells therefore must repress certain white-specific genes such as *WH11*, irrespective of its function to repress *EFG1*. This argues that wild-type white cells are in the white phase, primarily because they lack Wor1 and not because they express Efg1. Furthermore, we demonstrate that *EFG1* regulates cellular morphology downstream of *WOR1* (Fig. 1A), arguing that wild-type opaque cells display an elongated cell morphology mainly because of Efg1 expression occurs at lower levels than in round-shaped wild-type white cells (Fig. 1B), confirming a previously proposed idea (Srikantha *et al.*, 2000).

Chromatin-level layer of regulation

In addition to transcriptional regulation, we found that several chromatin-modifying enzymes strongly modulate white–opaque switching. Notably, deletions of genes in the transcriptional circuit appear to have a more severe effect on white–opaque switching (Zordan *et al.*, 2007). We argue that even an apparently subtle twofold change in switching frequencies must require substantial changes in transcription, because the circuitry inherently 'buffers' small fluctuations by multiple feedback loops. The newly identified genes fall into distinct functional categories based on the direction(s) of switching they modulate. This strongly suggests that chromatin modifications modulate the activity of the underlying transcriptional network at multiple branching points. Interestingly, the phenotype of chromatin-modifier deletions in some cases correlates with phenotypes of transcription factor deletions, suggest-

ing that they function at the same branch of the transcriptional circuit. For example, lack of *HST2* specifically results in a 10-fold decrease in the white to opaque switching, but fails to impact the opaque to white switching. Moreover, loss of *HST2* is suppressed by the loss of *EFG1* (Tables 1 and 2), while all of these effects are phenocopied by the deletion of *CZF1* (Zordan *et al.*, 2007), indicating that *HST2* impacts transcriptional regulation at the *CZF1*-branch. This input could be, for instance, exerted either at the *CZF1* locus or through the *CZF1*-dependent repression of *EFG1*. In addition, loss of *NAT4* promotes the white phase, which is suppressed by the deletion of *EFG1* (Tables 1 and 2), suggesting that *NAT4* influences transcriptional activity at the *EFG1* locus, independent of *CZF1* (Fig. 3B). The formal possibility that *NAT4* modulates binding of Wor1 at the *EFG1* promoter seems plausible but requires further experimental confirmation.

Likewise, as loss of either *HOS2* or *SET3* promotes the white phase and their deletions suppress the loss of *EFG1*, both *HOS2* and *SET3* map to a pathway operating downstream of *EFG1* and upstream of *WOR1*, possibly at the *WOR1* or *WOR2* loci. Nevertheless, it may not be surprising that we did not observe differences in mRNA levels of either *WOR1* or *WOR2* in deletion mutants of the Set3/Hos2 pathway, because in *S. cerevisiae* loss of Hos2 was shown to change the transcription kinetics rather than the steady state transcript level of its target genes (Wang *et al.*, 2002). Therefore, more direct experiments are needed to prove at which loci the Set3/Hos2 complex exerts its function to regulate white–opaque switching in *C. albicans*. Theoretically, the possibility that *SET3* or *HOS2* effects are exerted at the *WOR2* locus seems more unlikely, because overexpression of *WOR2* has no influence on switching rates (Zordan *et al.*, 2007). Hence, the genetic circuitry appears relatively well buffered against fluctuations of *WOR2* levels.

Set3 and Hos2 function as a complex in C. albicans

In this study, we provide four lines of genetic evidence that Set3 and Hos2 act as a complex in *C. albicans*. First, the phenotype of single deletions is identical; second, a loss of either *HOS2* or *SET3* is epistatic to the loss of *EFG1*; third, the loss of either *HOS2* or *SET3* is epistatic to the loss of *RPD31*; and fourth, deletion of *SET1* suppresses the loss of either *HOS2* or *SET3*. Hence, the situation in *C. albicans* appears similar to the Set3/Hos2 complex in *S. cerevisiae*, where deletion of either *SET3* or *HOS2* prevents assembly of a functional histone deacetylase complex *in vivo* (Pijnappel *et al.*, 2001). Notably, a similar architecture is present in the mammalian HDAC3/SMRT complex, indicating a strong evolutionary conservation (Guenther *et al.*, 2000).

Interestingly, loss of H3K4 methylation suppresses the disruption of the complex, suggesting that proper localization of Set3/Hos2 requires an interaction of the Set3 PHD finger with a methylated H3K4 residue. This notion is further supported by the finding that the purified PHD domain of ScSet3 specifically binds trimethylated H3K4 *in vitro* (Allis *et al.*, 2007). In the context of our work, it is important to note that loss of *SET1* failed to revert the opaque filamentation phenotype of the *hos2*Δ/Δ and *set3*Δ/Δ mutants. This strongly suggests that Set3/Hos2 localization requires H3K4 methylation only at specific loci. An alternative way to interpret the epistasis relationships of *SET1*, *SET3* and *HOS2* is that *SET1* and methylation of H3K4 represses white-to-opaque switching. The Set3/Hos2 complex counteracts this repressive effect. Consequently, in *set1*Δ/Δ mutant cells lacking methylation of H3K4, Set3/Hos2 seems dispensable for establishing a normal white-to-opaque switching rate. Further biochemical assays with appropriate tools which are currently being developed will be necessary to establish detailed mechanistic relationships and the interplay of these gene products. However, we provide compelling genetic evidence that *SET1*, *SET3* and *HOS2* define a novel pathway regulating *WOR1* expression and white–opaque switching in *C. albicans*.

Environmental control of phenotypic switching

Although white–opaque switching is a unique characteristic of *C. albicans*, reversible switching between distinct phenotypes has been described in a vast number of microbes, including the non-pathogenic yeast *S. cerevisiae*, the pathogen *Cryptococcus neoformans*, the protozoan parasites *Trypanosoma brucei* and *Plasmodium falciparum*, as well as many prokaryotic microbes such as *Escherichia coli* and *Bacillus subtilis* (Avery, 2006). Typically, two extreme cases of switching are considered: responsive switching occurs as a direct consequence of a change in environmental conditions, which is sensed by a dedicated apparatus; alternatively, stochastic switching occurs without an outside input mostly as a result of intrinsic transcriptional fluctuations of one or more regulatory genes (Kaern *et al.*, 2005; Kussell and Leibler, 2005). Theoretical models support that stochastic switching of phenotypes is favourable when the environment only seldom changes. By contrast, the more fluctuating the environment is, the more beneficial it is to have a sensing apparatus enabling the cells to actively respond to changes (Kussell and Leibler, 2005).

Recent models explain white–opaque switching as a stochastic process, whereby the fluctuations of one central factor (*WOR1*), along with at least three other regulators (*WOR2*, *CZF1*, *EFG1*), are buffered by multiple feedback loops (Huang *et al.*, 2006; Zordan *et al.*, 2006; 2007). On

the other hand, several lines of evidence in the literature and data presented here argue that white–opaque switching is likely to respond to environmental or even host stimuli. For instance, high temperature causes opaque cells to convert *en masse* to the white phase (Rikkerink *et al.*, 1988). Conversely, anaerobic conditions in some strains promote the formation of opaque cells both *in vitro* and more significantly, in the murine gastrointestinal tract (Ramirez-Zavala *et al.*, 2008). Most notably, the latter study also revealed that the *CZF1* gene is required for the anaerobiosis-induced white-to-opaque conversion in the strain WO-1, which interlinks environmental sensing and the genetic circuit driving white–opaque switching. The notion that the regulation of white–opaque switching is likely to have a responsive nature is further supported by numerous studies that report differences of white and opaque cells in their abilities to adapt to various host niches. It is fair to state that infectious microbes encounter many distinct local environments of varying parameters during an infection of the human host. Opaque phase *C. albicans* cells, for instance, are better colonizers of the skin, whereas white phase cells are more prevalent in bloodstream infections (Kvaal *et al.*, 1999). Furthermore, opaque cells are more susceptible to killing by neutrophils than white cells (Kolotila and Diamond, 1990), whereas macrophages preferentially phagocytose white cells over opaque cells (Lohse and Johnson, 2008).

The cell-fate decision machinery may encounter many different sometimes conflicting signals, which need proper processing in order to adapt in a favourable fashion. We propose that changing the chromatin status at adequate regulatory loci is a plausible mechanism to integrate multiple environmental stimuli. Notably, although an elevated temperature and anaerobiosis favour the white and the opaque phenotype respectively, anaerobic conditions stabilize opaque cells even at elevated temperatures *in vitro* (Dumitru *et al.*, 2007). Furthermore, white cells of some strains convert to the opaque phase in the murine gastrointestinal tract, whose 37°C temperature is much higher than 25°C, the normal laboratory condition used to stably propagate opaque cells (Ramirez-Zavala *et al.*, 2008). Such a proposed relay function of chromatin is further supported by the finding that Wor1 in opaque cells can be immunoprecipitated from promoters of many genes whose expression does not change during the white–opaque switch under laboratory conditions (Zordan *et al.*, 2007).

In this study, we identify another novel external stimulus, showing that the presence of adenine facilitates opaque to white switching *in vitro*, and, importantly, that *SET3* is required for this regulatory effect. This finding is in very good agreement with the proposed functional consequence of the dual layer model, whereby the chromatin modifiers are involved in the integration of environmental stimuli to shape cell fate. Notably, it was recently shown that the nicotinic acid (a precursor for NAD) concentration of urine regulates the adherence properties of the related species *Candida glabrata* in a urinary tract infection model, and that chromatin-mediated gene silencing is linked to the process (Domergue *et al.*, 2005). Therefore, it will be interesting in the future to test whether nucleotide or nucleotide precursor concentrations and chromatin-based regulatory mechanisms also play a role in *C. albicans* infection models *in vivo*.

The mechanism(s) driving morphogenetic switching thus may be quite simple. For instance, changes in the chromatin modification status could directly or indirectly fine-tune promoter occupancy of transcription factors by changing their affinities or modulate the assembly of the mediator complex. Alternatively, it is tantalizing to speculate that histone modifiers may even cause changes in post-translational modifications of transcription factors by modulating complex assembly.

Finally, *C. albicans* during its commensalistic co-evolution with the human host must have developed elaborate systems of specific and rapidly acting sensing mechanisms to allow for environmental and host signal integration. This machinery consists of two layers: a transcriptional level which co-ordinates the downstream response at the gene expression level, and a chromatin-level layer that may have a relay function at key loci integrating the stimuli affecting cellular identity. Moreover, the architecture combining specific transcription factors with chromatin modifiers is reminiscent of the cell-fate and developmental decision machineries in higher eukaryotic systems. Indeed, a differential chromatin status at key loci has been linked to lineage-committed stem cell differentiation (Mikkelsen *et al.*, 2007). Strikingly, a selective H3K4 methylation pattern has been recently linked to lineage commitment during hematopoesis (Orford *et al.*, 2008). These and other similarities make *C. albicans* an attractive alternative model system to dissect the molecular mechanisms of chromatin dynamics and enzyme recruitment to delineate developmental processes controlling cell-fate decision and developmental changes.

Experimental procedures

Media and growth conditions

Rich medium (YPD) and complete synthetic medium (SD) was prepared as previously described (Kaiser *et al.*, 1994). Modified Lee's medium was prepared as described (Bedell and Soll, 1979). Cultures were routinely grown at 25°C unless indicated otherwise.

Strain construction

The complete list of *C. albicans* strains, primers and plasmids used in this study are listed in Tables S2, S3 and S4

respectively. All strains were derived from SN152 (Noble and Johnson, 2005), a leucine, histidine, arginine auxotrophic derivative of the clinical isolate SC5314 (Gillum *et al.*, 1984). The *MTL***a**/α SN152 was cultured on sorbose medium (Janbon *et al.*, 1998) to construct the *MTL***a**/**a** strain DHCA202. *MTL* homozygosis was verified by PCR and Southern blot analyses (data not shown). Single gene deletions (*SET1*, *SET2*, *HDA1*, *SAS2*, *RPD31*, *SET3*, *HOS2*, *HST1*, *SIR2*, *HST2*, *ELP3*, *PHO13*, *PHO8*, *DOT1*, *HOS1*, *HPA2*, *HOS3* and *WOR1*) were created by using the *C.m.LEU2* and *C.d.HIS1* marker cassettes as described in Noble and Johnson (2005). In addition, the same strategy utilizing the *C.d.ARG4* and a *SAT1* cassette (amplified from the plasmid pSFS2A) was used to delete *WOR1* in the *set1*Δ/Δ, *hos2*Δ/Δ, *set3*Δ/Δ and *set1*Δ/Δ *hos2*Δ/Δ backgrounds.

Other multiple gene deletion mutants, as well as the *efg1*Δ/Δ in the DHCA202 and SC5314 backgrounds were created using the '*SAT1*-flipping' method (Reuss *et al.*, 2004). *EFG1* was deleted in the *wor1*Δ/Δ, *hos2*Δ/Δ, *set3*Δ/Δ, *hst2*Δ/Δ, *nat4*Δ/Δ and *set1*Δ/Δ single deletion strains to create all possible double deletions. Likewise, *SET3* and *HOS2* were deleted in the single deletion strains *hda1*Δ/Δ, *rpd31*Δ/Δ, *hst2*Δ/Δ, *nat4*Δ/Δ or *set1*Δ/Δ to obtain all double mutants. Moreover, *EFG1* was deleted in the *hst2*Δ/Δ *hos2*Δ/Δ, *nat4*Δ/Δ *set3*Δ/Δ and *set1*Δ/Δ *hos2*Δ/Δ double deletion backgrounds to construct the corresponding triple deletion strains. Except for single gene deletions that did not display any phenotypes (Table S2), at least two independent homozygous deletion strains were created derived from independent heterozygote isolates. Transformation was performed via electroporation as described (Reuss *et al.*, 2004). Genomic integration events were verified with PCR and Southern blot analyses (data not shown). The mating tester strains DHCA210 (*MTL*α/α) and DHCA209 (*MTL***a**/**a**) were created in the SC5314 background using the sorbose selection method. Subsequent disruption of the *ADE2* gene used the 'SAT1-flipping' strategy (see Tables S2 and S3).

Gene complementation constructs for the *HOS2*, *HST2* and *NAT4* ORFs were created using the *SAT1* marker cassette of the plasmid pSFS2A and the fusion PCR strategy (Noble and Johnson, 2005). For the restoration of the *SET3* gene, the SAT1-flipping strategy was used with the modification that the in pSFS2A plasmid the upstream homology region was replaced by the same upstream region and the coding sequence (Tables S3 and S4). Transformation was performed via electroporation as described (Reuss *et al.*, 2004). Genomic integration events were verified with PCR analysis.

Microscopy

Colony morphology was analysed using a Discovery V12 Stereoscope (Zeiss) equipped with an Axiocam MR5 camera (Zeiss). Microscopic analysis was performed with using an Axioplan 2 microscope (Zeiss) equipped with a Spot Pursuit camera (Sony). Images were analysed with the Axiovision 4.1 software (Zeiss).

White–opaque switching assays

Quantitative switching assays were performed as previously described (Miller and Johnson, 2002) with modifications. Briefly, white strains were streaked from frozen stocks on YPD plates and grown at 30°C for 2 days. Single colonies were then restreaked onto modified Lee's medium (Tables 1 and 2) or SD medium (Tables 3 and 4) and grown at 25°C for 5 days. Single colonies were picked and resuspended in sterile H_2O, checked by microscopy and spread onto modified Lee's plates (Tables 1 and 2) or SD plates (Tables 3 and 4) containing 5 μg ml^{-1} Phloxin B. Formation of opaque colonies or sectors was scored after 7 days. The opaque to white switching assays were performed using pure opaque colonies obtained in the white to opaque switching assays. The frequency of white colonies or colonies containing at least one white sector was scored after 7 days. For each strain, at least three independent experiments were carried out. The data listed in Tables 1–5 were obtained using one deletion strain of the genotype. For each genotype except for the *set1*Δ/Δ *set3*Δ/Δ, *wor1*Δ/Δ *hos2*Δ/Δ and *wor1*Δ/Δ *set1*Δ/Δ *hos2*Δ/Δ mutants at least two independent homozygous deletion strains were created derived from independent heterozygous deletion strains. The analysis of independent deletion mutants showed qualitatively similar results (data not shown).

Quantitative mating assays

Quantitative mating assays were performed essentially as described (Miller and Johnson, 2002) with modifications. Pure white and opaque cultures were isolated on plates as described above. Strains were grown in liquid medium at 25°C until an OD_{600} 1–3. A total of 3×10^7 cells of each mating partner were mixed, and deposited on sterile Whatman filter paper placed onto a YPD plate supplemented with 100 μg ml^{-1} adenine, and incubated at 25°C for 18 h. Cells were washed off the filter, resuspended in 10 ml sterile H_2O and were dispersed by vortex-mixing. Serial dilutions were plated on double-selective (–arginine –adenine) SD plates to select for the prototrophic conjugants, and on single selective (–arginine or –adenine) SD plates to score the single parent population plus conjugants. The mating frequencies were calculated as the ratio of conjugants and the limiting parent plus conjugants.

RNA isolation and quantitative RT-PCR

Cultures were grown in modified Lee's medium until OD_{600} 1–3 and harvested by centrifugation. Pellets were washed with sterile H_2O, frozen in liquid nitrogen and mechanically pulverized in a sterile porcelain mortar in the frozen state. RNA was extracted using TRI reagent (Molecular Research Center). About 1–5 μg of total RNA was reverse-transcribed with the First Strand cDNA synthesis kit (Fermentas). cDNA amplification was monitored quantitatively by SYBR Green incorporation in a Realplex Mastercycler (Eppendorf).

Immunoblotting

Cultures were grown in liquid medium until OD 1–3 and cells were harvested by centrifugation. Cell pellets were resuspended in 0.25 M NaOH and 1% β-mercaptoethanol, and incubated on ice for 10 min. Proteins were precipitated by the addition of 5.8 V/V% trichloroacetic acid for 10 min on ice,

centrifuged and resuspended in SDS sample buffer. Total protein extracts derived from 0.5 OD of the starting cultures were separated by SDS/PAGE and analysed by Western blotting. The C-terminal anti-Wor1 antibody has been previously described (Zordan *et al.*, 2006). Loading controls were visualized using a monoclonal anti-tubulin antibody (Sigma).

Acknowledgements

We thank all laboratory members for helpful discussions; W. Glaser for assistance with the bioinformatics and statistical analyses; N. Landstetter for helpful and critical comments on the manuscript. We are indebted to Alexander Johnson for providing fungal strains, plasmids, anti-Wor1 antibodies, helpful discussions as well as encouragement. We also thank J. Morschhäuser for critical reading of the manuscript and for the pSFS2A plasmid; S. Rupp for the strain HLC67; D.R. Soll for the strain L26. This work was supported by a grant from the Christian Doppler Society to K.K. D.H. was supported through the Vienna Biocenter PhD Programme WK001, and T.S. in part by the EraNet Pathogenomics project FunPath (FWF-API-0125).

References

Allis, C.D., Berger, S.L., Cote, J., Dent, S., Jenuwien, T., Kouzarides, T., *et al.* (2007) New nomenclature for chromatin-modifying enzymes. *Cell* **131:** 633–636.

Avery, S.V. (2006) Microbial cell individuality and the underlying sources of heterogeneity. *Nat Rev Microbiol* **4:** 577–587.

Bedell, G.W., and Soll, D.R. (1979) Effects of low concentrations of zinc on the growth and dimorphism of *Candida albicans*: evidence for zinc-resistant and – sensitive pathways for mycelium formation. *Infect Immun* **26:** 348–354.

Bennett, R.J., and Johnson, A.D. (2005) Mating in *Candida albicans* and the search for a sexual cycle. *Annu Rev Microbiol* **59:** 233–255.

Carmen, A.A., Rundlett, S.E., and Grunstein, M. (1996) *HDA1* and *HDA3* are components of a yeast histone deacetylase (HDA) complex. *J Biol Chem* **271:** 15837–15844.

Domergue, R., Castano, I., De Las Penas, A., Zupancic, M., Lockatell, V., Hebel, J.R., *et al.* (2005) Nicotinic acid limitation regulates silencing of *Candida* adhesins during UTI. *Science* **308:** 866–870.

Dumitru, R., Navarathna, D.H., Semighini, C.P., Elowsky, C.G., Dumitru, R.V., Dignard, D., *et al.* (2007) *In vivo* and *in vitro* anaerobic mating in *Candida albicans*. *Eukaryot Cell* **6:** 465–472.

Durand-Dubief, M., Sinha, I., Fagerstrom-Billai, F., Bonilla, C., Wright, A., Grunstein, M., and Ekwall, K. (2007) Specific functions for the fission yeast Sirtuins Hst2 and Hst4 in gene regulation and retrotransposon silencing. *EMBO J* **26:** 2477–2488.

Gillum, A.M., Tsay, E.Y., and Kirsch, D.R. (1984) Isolation of the *Candida albicans* gene for orotidine-5′-phosphate decarboxylase by complementation of *S. cerevisiae ura3* and *E. coli* pyrF mutations. *Mol Gen Genet* **198:** 179–182.

Guenther, M.G., Lane, W.S., Fischle, W., Verdin, E., Lazar, M.A., and Shiekhattar, R. (2000) A core SMRT corepressor complex containing HDAC3 and TBL1, a WD40-repeat protein linked to deafness. *Genes Dev* **14:** 1048–1057.

Huang, G., Wang, H., Chou, S., Nie, X., Chen, J., and Liu, H. (2006) Bistable expression of *WOR1*, a master regulator of white-opaque switching in *Candida albicans*. *Proc Natl Acad Sci USA* **103:** 12813–12818.

Hull, C.M., and Johnson, A.D. (1999) Identification of a mating type-like locus in the asexual pathogenic yeast *Candida albicans*. *Science* **285:** 1271–1275.

Janbon, G., Sherman, F., and Rustchenko, E. (1998) Monosomy of a specific chromosome determines 1-sorbose utilization: a novel regulatory mechanism in *Candida albicans*. *Proc Natl Acad Sci USA* **95:** 5150–5155.

Kaern, M., Elston, T.C., Blake, W.J., and Collins, J.J. (2005) Stochasticity in gene expression: from theories to phenotypes. *Nat Rev Genet* **6:** 451–464.

Kaiser, C., Michaelis, S., and Mitchell, A. (1994) *Methods in Yeast Genetics. A Laboratory Course Manual.* New York: ••.

Klar, A.J., Srikantha, T., and Soll, D.R. (2001) A histone deacetylation inhibitor and mutant promote colony-type switching of the human pathogen *Candida albicans*. *Genetics* **158:** 919–924.

Kolotila, M.P., and Diamond, R.D. (1990) Effects of neutrophils and in vitro oxidants on survival and phenotypic switching of *Candida albicans* WO-1. *Infect Immun* **58:** 1174–1179.

Kouzarides, T. (2007) Chromatin modifications and their function. *Cell* **128:** 693–705.

Kussell, E., and Leibler, S. (2005) Phenotypic diversity, population growth, and information in fluctuating environments. *Science* **309:** 2075–2078.

Kvaal, C., Lachke, S.A., Srikantha, T., Daniels, K., McCoy, J., and Soll, D.R. (1999) Misexpression of the opaque-phase-specific gene *PEP1* (*SAP1*) in the white phase of *Candida albicans* confers increased virulence in a mouse model of cutaneous infection. *Infect Immun* **67:** 6652–6662.

Lan, C.Y., Newport, G., Murillo, L.A., Jones, T., Scherer, S., Davis, R.W., and Agabian, N. (2002) Metabolic specialization associated with phenotypic switching in *Candida albicans*. *Proc Natl Acad Sci USA* **99:** 14907–14912.

Landry, J., Sutton, A., Tafrov, S.T., Heller, R.C., Stebbins, J., Pillus, L., and Sternglanz, R. (2000) The silencing protein Sir2 and its homologs are NAD-dependent protein deacetylases. *Proc Natl Acad Sci USA* **97:** 5807–5811.

Lohse, M.B., and Johnson, A.D. (2008) Differential phagocytosis of white versus opaque *Candida albicans* by *Drosophila* and mouse phagocytes. *PLoS ONE* **3:** e1473.

Mikkelsen, T.S., Ku, M., Jaffe, D.B., Issac, B., Lieberman, E., Giannoukos, G., *et al.* (2007) Genome-wide maps of chromatin state in pluripotent and lineage-committed cells. *Nature* **448:** 553–560.

Miller, M.G., and Johnson, A.D. (2002) White-opaque switching in *Candida albicans* is controlled by mating-type locus homeodomain proteins and allows efficient mating. *Cell* **110:** 293–302.

Morrow, B., Srikantha, T., and Soll, D.R. (1992) Transcription of the gene for a pepsinogen, *PEP1*, is regulated by white-opaque switching in *Candida albicans*. *Mol Cell Biol* **12:** 2997–3005.

Morrow, B., Srikantha, T., Anderson, J., and Soll, D.R. (1993) Coordinate regulation of two opaque-phase-specific genes during white-opaque switching in *Candida albicans*. *Infect Immun* **61:** 1823–1828.

Nislow, C., Ray, E., and Pillus, L. (1997) SET1, a yeast member of the trithorax family, functions in transcriptional silencing and diverse cellular processes. *Mol Biol Cell* **8:** 2421–2436.

Noble, S.M., and Johnson, A.D. (2005) Strains and strategies for large-scale gene deletion studies of the diploid human fungal pathogen *Candida albicans*. *Eukaryot Cell* **4:** 298–309.

Orford, K., Kharchenko, P., Lai, W., Dao, M.C., Worhunsky, D.J., Ferro, A., *et al.* (2008) Differential H3K4 methylation identifies developmentally poised hematopoietic genes. *Dev Cell* **14:** 798–809.

Pijnappel, W.W., Schaft, D., Roguev, A., Shevchenko, A., Tekotte, H., Wilm, M., *et al.* (2001) The *S. cerevisiae SET3* complex includes two histone deacetylases, Hos2 and Hst1, and is a meiotic-specific repressor of the sporulation gene program. *Genes Dev* **15:** 2991–3004.

Raman, S.B., Nguyen, M.H., Zhang, Z., Cheng, S., Jia, H.Y., Weisner, N., *et al.* (2006) *Candida albicans SET1* encodes a histone 3 lysine 4 methyltransferase that contributes to the pathogenesis of invasive candidiasis. *Mol Microbiol* **60:** 697–709.

Ramirez-Zavala, B., Reuss, O., Park, Y.N., Ohlsen, K., and Morschhauser, J. (2008) Environmental induction of white-opaque switching in *Candida albicans*. *PLoS Pathog* **4:** e1000089.

Rea, S., Eisenhaber, F., O'Carroll, D., Strahl, B.D., Sun, Z.W., Schmid, M., *et al.* (2000) Regulation of chromatin structure by site-specific histone H3 methyltransferases. *Nature* **406:** 593–599.

Reuss, O., Vik, A., Kolter, R., and Morschhauser, J. (2004) The SAT1 flipper, an optimized tool for gene disruption in *Candida albicans*. *Gene* **341:** 119–127.

Rikkerink, E.H., Magee, B.B., and Magee, P.T. (1988) Opaque-white phenotype transition: a programmed morphological transition in *Candida albicans*. *J Bacteriol* **170:** 895–899.

Roguev, A., Schaft, D., Shevchenko, A., Pijnappel, W.W., Wilm, M., Aasland, R., and Stewart, A.F. (2001) The *Saccharomyces cerevisiae* Set1 complex includes an Ash2 homologue and methylates histone 3 lysine 4. *EMBO J* **20:** 7137–7148.

Rozenblatt-Rosen, O., Rozovskaia, T., Burakov, D., Sedkov, Y., Tillib, S., Blechman, J., *et al.* (1998) The C-terminal SET domains of ALL-1 and TRITHORAX interact with the INI1 and SNR1 proteins, components of the SWI/SNF complex. *Proc Natl Acad Sci USA* **95:** 4152–4157.

Rundlett, S.E., Carmen, A.A., Kobayashi, R., Bavykin, S., Turner, B.M., and Grunstein, M. (1996) *HDA1* and *RPD3* are members of distinct yeast histone deacetylase complexes that regulate silencing and transcription. *Proc Natl Acad Sci USA* **93:** 14503–14508.

Shi, X., Hong, T., Walter, K.L., Ewalt, M., Michishita, E., Hung, T., *et al.* (2006) ING2 PHD domain links histone H3 lysine 4 methylation to active gene repression. *Nature* **442:** 96–99.

Slutsky, B., Staebell, M., Anderson, J., Risen, L., Pfaller, M., and Soll, D.R. (1987) 'White-opaque transition': a second high-frequency switching system in *Candida albicans*. *J Bacteriol* **169:** 189–197.

Song, O.K., Wang, X., Waterborg, J.H., and Sternglanz, R. (2003) An Nalpha-acetyltransferase responsible for acetylation of the N-terminal residues of histones H4 and H2A. *J Biol Chem* **278:** 38109–38112.

Sonneborn, A., Tebarth, B., and Ernst, J.F. (1999) Control of white-opaque phenotypic switching in *Candida albicans* by the Efg1p morphogenetic regulator. *Infect Immun* **67:** 4655–4660.

Srikantha, T., and Soll, D.R. (1993) A white-specific gene in the white-opaque switching system of *Candida albicans*. *Gene* **131:** 53–60.

Srikantha, T., Tsai, L.K., Daniels, K., and Soll, D.R. (2000) *EFG1* null mutants of *Candida albicans* switch but cannot express the complete phenotype of white-phase budding cells. *J Bacteriol* **182:** 1580–1591.

Srikantha, T., Tsai, L., Daniels, K., Klar, A.J., and Soll, D.R. (2001) The histone deacetylase genes *HDA1* and *RPD3* play distinct roles in regulation of high-frequency phenotypic switching in *Candida albicans*. *J Bacteriol* **183:** 4614–4625.

Srikantha, T., Borneman, A.R., Daniels, K.J., Pujol, C., Wu, W., Seringhaus, M.R., *et al.* (2006) TOS9 *regulates white-opaque switching in* Candida albicans. *Eukaryot Cell* **5:** 1674–1687.

Stassen, M.J., Bailey, D., Nelson, S., Chinwalla, V., and Harte, P.J. (1995) The *Drosophila* trithorax proteins contain a novel variant of the nuclear receptor type DNA binding domain and an ancient conserved motif found in other chromosomal proteins. *Mech Dev* **52:** 209–223.

Stoldt, V.R., Sonneborn, A., Leuker, C.E., and Ernst, J.F. (1997) Efg1p, an essential regulator of morphogenesis of the human pathogen *Candida albicans*, is a member of a conserved class of bHLH proteins regulating morphogenetic processes in fungi. *EMBO J* **16:** 1982–1991.

Suka, N., Suka, Y., Carmen, A.A., Wu, J., and Grunstein, M. (2001) Highly specific antibodies determine histone acetylation site usage in yeast heterochromatin and euchromatin. *Mol Cell* **8:** 473–479.

Tripoulas, N., LaJeunesse, D., Gildea, J., and Shearn, A. (1996) The *Drosophila* Ash1 gene product, which is localized at specific sites on polytene chromosomes, contains a SET domain and a PHD finger. *Genetics* **143:** 913–928.

Tuleva, B., Vasileva-Tonkova, E., and Galabova, D. (1998) A specific alkaline phosphatase from *Saccharomyces cerevisiae* with protein phosphatase activity. *FEMS Microbiol Lett* **161:** 139–144.

Van Vleet, J.H., Jeffries, T.W., and Olsson, L. (2007) Deleting the para-nitrophenyl phosphatase (pNPPase), *PHO13*, in recombinant *Saccharomyces cerevisiae* improves growth and ethanol production on d-xylose. *Metab Eng* **••:** ••–••.

Wang, A., Kurdistani, S.K., and Grunstein, M. (2002) Requirement of Hos2 histone deacetylase for gene activity in yeast. *Science* **298:** 1412–1414.

Whiteway, M., and Bachewich, C. (2007) Morphogenesis in *Candida albicans*. *Annu Rev Microbiol* **61:** 529–553.

Wu, J., Suka, N., Carlson, M., and Grunstein, M. (2001) Tup1 utilizes histone H3/H2B-specific Hda1 deacetylase to repress gene activity in yeast. *Mol Cell* **7:** 117–126.

Xie, J., Pierce, M., Gailus-Durner, V., Wagner, M., Winter, E., and Vershon, A.K. (1999) Sum1 and Hst1 repress middle sporulation-specific gene expression during mitosis in *Saccharomyces cerevisiae*. *EMBO J* **18:** 6448–6454.

Zordan, R.E., Galgoczy, D.J., and Johnson, A.D. (2006) Epigenetic properties of white-opaque switching in *Candida albicans* are based on a self-sustaining transcriptional feedback loop. *Proc Natl Acad Sci USA* **103:** 12807–12812.

Zordan, R.E., Miller, M.G., Galgoczy, D.J., Tuch, B.B., and Johnson, A.D. (2007) Interlocking transcriptional feedback loops control white-opaque switching in *Candida albicans*. *PLoS Biol* **5:** e256.

Supporting information

Additional supporting information may be found in the online version of this article.

Please note: Wiley-Blackwell are not responsible for the content or functionality of any supporting materials supplied by the authors. Any queries (other than missing material) should be directed to the corresponding author for the article.

The High-Osmolarity Glycerol Response Pathway in the Human Fungal Pathogen *Candida glabrata* Strain ATCC2001 Lacks a Signaling Branch That Operates in Baker's Yeast

Christa Gregori, Christoph Schüller, Andreas Rötzer, Tobias Schwarzmüller, Gustav Ammerer, Karl Kuchler

Eukaryotic Cell, 2007

The work presented in this publication comprises the characterization of the *C. glabrata* high osmolarity glycerol (HOG) pathway. This work describes also the identification of the *ssk2-1* mutation of the ATCC2001 strain, which disables the Sln1 branch of the HOG pathway. The strain is used as the parental strain for the triple-auxotrophic strain, which serves as the background strain for the *C. glabrata* gene deletion project presented in this thesis. This means, every gene deletion strain effectively represents a double deletion with *ssk2-1*.
My contribution to this work comprises the generation of the *NAT1* marker-based gene deletion construct for the Cg*SSK2* gene.

EUKARYOTIC CELL, Sept. 2007, p. 1635–1645 Vol. 6, No. 9
1535-9778/07/$08.00+0 doi:10.1128/EC.00106-07

The High-Osmolarity Glycerol Response Pathway in the Human Fungal Pathogen *Candida glabrata* Strain ATCC 2001 Lacks a Signaling Branch That Operates in Baker's Yeast[▽]

Christa Gregori,[1] Christoph Schüller,[2] Andreas Roetzer,[2] Tobias Schwarzmüller,[1] Gustav Ammerer,[2] and Karl Kuchler[1]*

Department of Medical Biochemistry, Max F. Perutz Laboratories, Medical University Vienna,[1] and Department of Biochemistry and Molecular Cell Biology, Max F. Perutz Laboratories, University of Vienna,[2] A-1030 Vienna, Austria

Received 4 April 2007/Accepted 26 June 2007

The high-osmolarity glycerol (HOG) mitogen-activated protein (MAP) kinase pathway mediates adaptation to high-osmolarity stress in the yeast *Saccharomyces cerevisiae*. Here we investigate the function of HOG in the human opportunistic fungal pathogen *Candida glabrata*. *C. glabrata sho1*Δ (Cg*sho1*Δ) deletion strains from the sequenced ATCC 2001 strain display severe growth defects under hyperosmotic conditions, a phenotype not observed for yeast *sho1*Δ mutants. However, deletion of Cg*SHO1* in other genetic backgrounds fails to cause osmostress hypersensitivity, whereas cells lacking the downstream MAP kinase Pbs2 remain osmosensitive. Notably, ATCC 2001 Cg*sho1*Δ cells also display methylglyoxal hypersensitivity, implying the inactivity of the Sln1 branch in ATCC 2001. Genomic sequencing of Cg*SSK2* in different *C. glabrata* backgrounds demonstrates that ATCC 2001 harbors a truncated and mutated Cg*ssk2-1* allele, the only orthologue of yeast *SSK2*/*SSK22* genes. Thus, the osmophenotype of ATCC 2001 is caused by a point mutation in Cg*ssk2-1*, which debilitates the second HOG pathway branch. Functional complementation experiments unequivocally demonstrate that HOG signaling in yeast and *C. glabrata* share similar functions in osmostress adaptation. In contrast to yeast, however, Cg*sho1*Δ mutants display hypersensitivity to weak organic acids such as sorbate and benzoate. Hence, CgSho1 is also implicated in modulating weak acid tolerance, suggesting that HOG signaling in *C. glabrata* mediates the response to multiple stress conditions.

Yeast cells have developed the ability to counteract changing osmolarity conditions by inducing appropriate physiological responses and adaptive adjustments (4). Osmoadaptation pathways have been studied primarily in *Saccharomyces cerevisiae* but lately also in pathogenic fungi with clinical relevance, such as *Candida albicans* (2, 37, 42). The haploid *Candida glabrata* is the second most prevalent fungal pathogen in humans after *C. albicans* (15, 35), accounting for about 20% of all systemic diseases caused by *Candida* spp. *C. glabrata* populates mucosal surfaces and the guts of healthy individuals, but it also causes life-threatening systemic infections in immunocompromised patients (29).

Candida spp. must be able to adapt to osmotic changes in the microenvironment during host invasion and systemic spreading, as well as to evade host defense strategies (2). However, the underlying mechanisms are not well understood. In yeast, mitogen-activated protein kinase (MAPK) cascades drive important signaling pathways, thus allowing cells to adapt to changing environmental conditions. *S. cerevisiae* harbors at least five MAPK signaling pathways mediating stress response, including the protein kinase C (PKC) cell integrity pathway (22), the protein kinase A growth control pathway (36), the mating pheromone response pathway (30, 40), and the spore wall assembly pathway (19, 39). Finally, the well-characterized high-osmolarity glycerol (HOG) pathway is essential for yeast survival under-high osmolarity conditions, since it triggers adaptation through intracellular accumulation of glycerol as the adaptive osmolyte (4, 10). Two cell surface membrane sensors, Sho1 and Sln1, constitute two functionally redundant signaling branches that sense and transduce signals through the downstream HOG MAPK pathway (23, 44). Sho1 and Sln1 have been termed osmosensors, but recent studies indicate that Sho1 transduces the stress signal rather than sensing changes in osmolarity (33, 43). Experiments based on systems biology analysis have demonstrated that Sho1 is phosphorylated in a Hog1-dependent manner, indicating a negative-feedback loop acting on the transmembrane protein (11). The key MAPK, Hog1, is activated by phosphorylation through the upstream MAPK kinase (MAPKK) Pbs2. Whereas *pbs2*Δ and *hog1*Δ deletion strains are osmosensitive (4), mutations affecting only one of two upstream branches do not cause osmophenotypes, since Sln1 and Sho1 can each independently trigger Hog1 activation (27, 44).

Orthologues of Hog1 are present in other fungi as well as in animals (27). In *S. cerevisiae*, the HOG pathway responds to a limited range of stress conditions, mainly high osmolarity, heat stress (46), intracellular methylglyoxal accumulation (1, 24), citric and acetic acid stresses (21, 25), and oxidative stress (3). Interestingly, Hog1 orthologues play a more general role in regulating a core stress response in *C. albicans* and *Schizosaccharomyces pombe* (7, 42). Furthermore, a lack of *C. albicans* Hog1 (CaHog1) leads to impaired virulence (2). Recent studies demonstrated that CaSho1 plays only a minor role in osmostress adaptation. Nevertheless, CaSho1 is important for

* Corresponding author. Mailing address: Medical University Vienna, Max F. Perutz Laboratories, Department of Medical Biochemistry, Dr. Bohr-Gasse 9/2, A-1030 Vienna, Austria. Phone: 43-1-4277-61807. Fax: 43-1-4277-9618. E-mail: karl.kuchler@meduniwien.ac.at.

▽ Published ahead of print on 6 July 2007.

TABLE 1. Fungal strains used in this study

Strain	Genotype	Reference or source
C. glabrata		
ATCC 2001 (CBS138)	Wild type	ATCC collection[a]
ΔHT6	Isogenic to ATCC 2001; *his3*::*URA3 ura3*Δ *trp1*Δ	45
ΔHTU (ATCC 200989)	Isogenic to ATCC 2001; *his3*Δ *ura3*Δ *trp1*Δ	16
Cg2633	Clinical isolate	Helena Bujdakova
BG2	Clinical isolate	6
ATCC 2001 *sho1*Δ	Isogenic to ATCC 2001; *sho1*Δ::*SAT1*	This study
ATCC 2001 *pbs2*Δ	Isogenic to ATCC 2001; *pbs2*Δ::*SAT1*	This study
ATCC 2001 *sho1*Δ *SSK2* C1	Isogenic to ATCC 2001; *sho1*Δ::*SAT1 SSK2*	This study
ATCC 2001 *sho1*Δ *SSK2* C2	Isogenic to ATCC 2001; *sho1*Δ::*SAT1 SSK2*	This study
ATCC 2001 *sho1*Δ *SSK2* C3	Isogenic to ATCC 2001; *sho1*Δ::*SAT1 SSK2*	This study
BG2 *sho1*Δ	Isogenic to BG2; *sho1*Δ::*SAT1*	This study
BG2 *pbs2*Δ	Isogenic to BG2; *pbs2*Δ::*SAT1*	This study
BG2 *ssk2*Δ	Isogenic to BG2; *ssk2*Δ::*NAT1*	This study
Cg2633 *sho1*Δ	Isogenic to Cg2633; *sho1*Δ::*SAT1*	This study
Cg2633 *pbs2*Δ	Isogenic to Cg2633; *pbs2*Δ::*SAT1*	This study
ΔHTU *sho1*Δ	Isogenic to ΔHTU; *sho1*Δ::*HIS3*	This study
ΔHT6 *sho1*Δ	Isogenic to ΔHT6; *sho1*Δ::*HIS3*	This study
S. cerevisiae		
W303-1B	*MAT*α *ura3-1 leu2-3,112 his3-11,15 trp1-1 ade2-1 can1-100*	38
YCG9A	Isogenic to W303-1B; *sho1*Δ::*TRP1 ssk2*Δ::*KanMX ssk22*Δ::*KanMX*	This study
BY4741	*MAT*a *ura3-*Δ*0 leu2-*Δ*0 his3-*Δ*1 met1-*Δ*0*	EUROSCARF
BY4741 *sho1*Δ	Isogenic to BY4741; *sho1*Δ::*KanMX*	EUROSCARF
BY4741 *pbs2*Δ	Isogenic to BY4741; *pbs2*Δ::*KanMX*	EUROSCARF
BY4741 *ssk1*Δ	Isogenic to BY4741; *ssk1*Δ::*KanMX*	EUROSCARF
BY4741 *sho1*Δ *ssk1*Δ	Isogenic to BY4741; *sho1*Δ::*KanMX ssk1*Δ::*KanMX*	This study

[a] Available at www.atcc.org.

growth under oxidative stress conditions, and it mediates phosphorylation of the Cek1 MAPK in exponentially growing cells (37).

Because all components of the yeast HOG pathway are present in *C. glabrata*, we constructed strains lacking *C. glabrata SHO1* (Cg*SHO1*) and Cg*PBS2* from strain ATCC 2001, which was sequenced by the Génolevures Consortium (8). Unexpectedly, a Cg*sho1*Δ strain displays severe osmosensitivity, a phenotype not observed for the corresponding *S. cerevisiae sho1* (Sc*sho1*) mutant. However, the Cg*sho1*Δ phenotype is restricted to ATCC 2001. Genomic sequencing demonstrates the inactivity of the Sln1 branch in ATCC 2001, since this strain harbors a truncated nonfunctional Cg*ssk2-1* allele, causing the removal of the CgSsk2 kinase domain. Importantly, analysis of ATCC 2001 and other strain backgrounds revealed that the physiology of the *C. glabrata* HOG pathway is closely related to that of *S. cerevisiae*. Interestingly, it also seems distinct from the yeast HOG pathway, since it performs additional functions, such as involvement in modulating resistance to certain weak organic acids in *C. glabrata*.

MATERIALS AND METHODS

Strains, plasmids, and growth conditions. All strains used in this study are listed in Table 1. *S. cerevisiae* strain YCG9A was obtained by crossing W303-1A *ssk2*Δ *ssk22*Δ with W303-1B *sho1*Δ. BY4741 *sho1*Δ *ssk1*Δ was obtained by crossing strains BY4741 *sho1*Δ and BY4742 *ssk1*Δ. For gene disruption in the ATCC 2001, BG2, and Cg2633 backgrounds, we used the dominant *SAT1* marker cassette amplified from plasmid pSFS2 (34) with primers SAT1-P2 and SAT1-P5 (Table 2). For construction of the Cg*SSK2* genomic deletion cassette, the nourseothricin marker gene *NAT1* was amplified from plasmid pJK863 (41) using primers NAT1-P2 and NAT1-P5. Disruption cassettes were generated by fusion PCRs as described previously (26) and transformed into *C. glabrata* strains via electroporation as described elsewhere (34). For gene disruption using the *HIS3* marker, we amplified the marker gene from plasmid pTW23 (14) using primers HIS3-P2 and HIS3-P5. Sequences of all primers used for PCR amplification of disruption cassettes are listed in Table 2.

For genomic integration of *SSK2*, a 6,970-bp PCR fragment containing the entire *SSK2* open reading frame (ORF) including flanking 5′ and 3′ untranslated regions was amplified from genomic DNA of strain BG2 and transformed into strain ATCC 2001 *sho1*Δ. Transformants were selected on yeast extract-peptone-dextrose (YPD) supplemented with 1.2 M NaCl. Correct genomic replacement of *ssk2-1* by *SSK2* was verified by sequence analysis of the relevant genomic region. Of 10 transformants tested, all encoded the wild-type Cys1668, demonstrating restoration of the mutated *ssk2-1* allele. Clones C1, C2, and C3 were selected for further experiments to test for pathway activation.

Rich medium (YPD) and synthetic medium (SC) for yeast cultures were prepared essentially as described elsewhere (13). Unless otherwise indicated, all strains were grown routinely at 30°C. For the selection of nourseothricin-resistant transformants, 200 μg/ml of nourseothricin (Werner Bioagents, Jena, Germany) was added to YPD agar plates. For reintroducing Cg*SHO1* into the deletion strain, a 2,330-bp fragment containing the entire *SHO1* ORF, including the 600-bp 5′ promoter and the 700-bp 3′ untranslated region, was PCR amplified from ATCC 2001 genomic DNA und ligated into the pGEM-T easy vector (Promega). Primers used for PCR were 5-ExSHO1 (5′-GCAATTGTGGGAGC CACAGGATC-3′) and 3-ExSHO1 (5′-GAGAAAGAAGGTTATGCCAGC-3′). The ARS-*CEN-TRP* cassette was isolated from plasmid pCgACT14 (17) via partial digestion with AatII and ligated into the corresponding restriction site of pGEM-T Easy harboring Cg*SHO1*. For the empty-vector control, the *SHO1* insert was removed from the vector with EcoRI restriction sites, followed by religation. The same EcoRI-digested fragment was used for cloning into EcoRI-digested pRS316 and YEp352, yielding two *S. cerevisiae* plasmids named pRS-CgSHO1 and YEp-CgSHO1, respectively.

Growth inhibition assays. To determine susceptibilities to osmostress, methylglyoxal or high temperatures, exponentially growing cultures were adjusted to an optical density at 600 nm (OD_{600}) of 0.1 and diluted 1:10, 1:100, and 1:1,000. Equal volumes of serial dilutions were spotted onto YPD plates containing various concentrations of NaCl, sorbitol, KCl, or methylglyoxal. Plates were incubated at 30°C or 42°C for 24 h to 48 h. For acetate plates, YPD (pH 4.5) (adjusted with HCl) was supplemented with acetate from an 8.7 M acetic acid stock solution adjusted to pH 4.5 with NaOH. Plates containing other weak acids were prepared exactly as previously described (18).

TABLE 2. Oligonucleotides used in this study

Name	Sequence[a]
SHO1-SAT1-P1	5′-AACCAGAGGTGATAGATTGC-3′
SHO1-SAT1-P3	5′-***CACGGCGCGCCTAGCAGCGG***AACTAAATTCTATATCGTTACTG-3′
SHO1-SAT1-P4	5′-***GTCAGCGGCCGCATCCCTGC***ACAATAGCAATTGCATCACA-3′
SHO1-SAT1-P6	5′-CCAAGAGTTGCCTCCAACTCC-3′
PBS2-SAT1-P1	5′-GATAATCAACCTAGGCAAGTGC-3′
PBS2-SAT1-P3	5′-***CACGGCGCGCCTAGCAGCGG***TGCCTCATTAACACTCGCTAC-3′
PBS2-SAT1-P4	5′-***GTCAGCGGCCGCATCCTGC***TAAACTGTAAGTTATCGAACGAC-3′
PBS2-SAT1-P6	5′-CAACTTCCATCAGTGGAAATC-3′
SAT1-P2	5′-***CCGCTGCTAGGCGCGCCGTG***CGTCAAAACTAGAGAATAATAAAGAAAACG-3′
SAT1-P5	5′-***GCAGGGATGCGGCCGCTGAC***AGGACCACCTTTGATTGTAAATAG-3′
SHO1-HIS3-P1	Identical to *SHO1-SAT1*-P1
SHO1-HIS3-P3	5′-GTCATAGCTGTTTCCTGAACTAAATTCTATATCGTTA-3′
SHO1-HIS3-P4	5′-TACAACGTCGTGACTGGGACAATAGCAATTGCATCACA-3′
SHO1-HIS3-P6	Identical to *SHO1-SAT1*-P6
HIS3-P2	5′-TAACGATATAGAATTTAGTTCAGGAAACAGCTATGAC-3′
HIS3-P5	5′-TGTGATGCAATTGCTATTGTCCCAGTCACGACGTTGTA-3′
SSK2-P1	5′-CAACTAATAACTCAGCAGACG-3′
SSK2-P3	5′-***CACGGCGCGCCTAGCAGCGG***TTTTCATGTTACTCCATAGTTTTATC-3′
SSK2-P4	5′-***GTCAGCGGCCGCATCCCTGC***TGAGTTGTTTTAGAGATGATTAC-3′
SSK2-P6	5′-AGGTGTGTGAGAAACGATAG-3′
NAT1-P2	5′-***CCGCTGCTAGGCGCGCCGTG***AGCTTGCCTCGTCCCCGCCG-3′
NAT1-P5	5′-***GCAGGGATGCGGCCGCTGAC***CTGGATGGCGGCGTTAGTATCG-3′

[a] Overlapping sequences required for the fusion PCR are italicized and boldfaced.

Preparation of cell extracts and immunoblotting. To investigate phosphorylation of Hog1 using self-made antibodies, cultures of the Cg*sho1*Δ strain transformed either with a plasmid expressing Cg*SHO1* or with the empty-vector control were grown to the exponential-growth phase before addition of 0.5 M NaCl. Cells were harvested from 40-ml samples taken at different time points and were washed with H_2O. Cells were then lysed with glass beads in 300 μl of buffer A [50 mM HEPES (pH 8.0), 0.4 M $(NH_4)_2SO_4$, 2 mM EDTA, 5% (vol/vol) glycerol, 50 mM sodium fluoride, 20 mM tetra-natrium-diphosphate, 1 mM sodium orthovanadate, 10 mM beta-glycerophosphate, protease inhibitor] using the Fast Prep machine (Qbiogene). Extracts were cleared by centrifugation steps at 3,000 × *g* and 20,000 × *g*. Aliquots corresponding to 50 μg of total extract per lane were fractionated by 10% sodium dodecyl sulfate-polyacrylamide gel electrophoresis (10% SDS-PAGE) and transferred to nitrocellulose membranes. Immunoblotting was carried out using phosphospecific polyclonal antibodies recognizing activated Hog1 isoforms. For detection of phosphorylated Hog1 isoforms using anti-phospho-p38 MAPK antibodies (Cell Signaling Technologies), trichloroacetic acid extracts were prepared as described elsewhere (9), and cell lysates equivalent to 0.4 OD_{600} unit were resolved by SDS-PAGE. Anti-ScPgk1 antibodies recognizing CgPgk1 were used to detect the loading control (20).

Preparation of antibodies. Polyclonal anti-phospho-Hog1 antibodies were raised in rabbits against a 16-residue Hog1-specific peptide conjugated to the keyhole limpet hemocyanin carrier protein. The crude Hog1 phosphopeptide NH_2-CARIQDPQM**T**G**Y**VSTR-COOH (phosphorylated residues are boldfaced) was purified by high-performance liquid chromatography through a Phenomix Jupiter column with a linear acetonitrile gradient, and fractions were analyzed by mass spectrometry. Fractions containing peptides with the predicted mass of the Hog1 phosphopeptide were lyophilized and reconstituted in Tris-buffered saline. About 1 mg of purified keyhole limpet hemocyanin-coupled peptide antigen was used for immunization of rabbits, carried out by Gramsch Laboratories (Schwabhausen, Germany). The specificity of the antiserum obtained was tested using appropriate cell extracts of wild-type *S. cerevisiae* and mutants lacking Hog1.

Southern blotting and DNA sequencing. For identification of mutations and for filling the unsequenced genomic gap, Cg*SSK2* fragments up to 4 kb were amplified from genomic DNA and directly subjected to DNA sequencing using the BigDye Terminator cycle sequencing kit (version 3.0) and ABI PRISM sequencing system 310 (Applied Biosystems, Germany) according to the manufacturer's instructions.

Southern blotting was performed as described elsewhere (2a). Genomic DNA was isolated by phenol-chloroform-isoamyl alcohol (PCI) extraction and digested with HindIII for 3 h, followed by overnight digestion with NotI (5 U/μg). Probes were obtained by PCR amplification using primers SHO1-SAT1-P1 and SHO1-SAT1-P2 (probe A) as well as SHO1-SAT1-P4 and SHO1-SAT1-P6 (probe B). [α-^{32}P]CTP radiolabeling was carried out with the Megaprime DNA labeling system (Amersham) according to the manufacturer's protocol.

Microscopy. Microscopy was done on an Axioplan 2 (Zeiss) microscope. Pictures were captured with a Spot Pursuit (Sony) camera. Time lapse microscopy was controlled by MetaFluor software. Cells were grown to the early-exponential-growth phase in synthetic medium, made to adhere to a coverslip by using concanavalin A, mounted, and fixed on microscopy slides with silicon vacuum grease.

Nucleotide sequence accession numbers. The genomic sequences for the Cg*SSK2* genes in various *C. glabrata* strain backgrounds have been deposited in GenBank under accession numbers EF193044 and EF193045.

RESULTS

***C. glabrata* strains display different osmostress sensitivities.** To investigate the role of the HOG pathway in the pathogenic fungus *C. glabrata*, we generated deletion mutants lacking crucial genes of the HOG pathway. In *S. cerevisiae*, the HOG pathway bifurcates upstream of the MAPKK Pbs2 into two branches, the Sho1 and the Sln1 branch. Each of these branches can independently mediate the osmostress response (30). In strain ATCC 2001, for which a genomic sequence has been determined (8), the Sln1 branch seems to be truncated at the level of the MAPKK kinase (MAPKKK) gene *SSK2*. The database entry indicates that the genomic Cg*SSK2* region is disrupted by an unresolved sequence gap. More importantly, the kinase domain of the Cg*SSK2* gene is disrupted by a stop codon, suggesting a pseudogene, or at least a nonfunctional Ssk2 protein encoded by this locus. These facts suggested to us a possible difference between the *C. glabrata* and *S. cerevisiae* HOG pathways.

Therefore, we chose the Cg*SHO1* gene to inactivate the remaining branch in ATCC 2001, as well as the downstream Cg*PBS2* gene to achieve complete inactivation of the HOG pathway. Furthermore, we generated disruptions of *SHO1* and *PBS2* in two other *C. glabrata* strains, BG2 (6) and the clinical isolate Cg2633 (kindly provided by Helena Bujdakova). We took advantage of the dominant nourseothricin resistance

marker *SAT1*, since no auxotrophic marker is available in these clinical strains. *SHO1* and *PBS2* were disrupted using the three-way PCR method in BG2, Cg2633, and ATCC 2001. Correct deletion of the *SHO1* locus was tested by Southern blot analysis (Fig. 1B). The Cg*sho1*Δ deletion strains obtained were then tested for growth under high-osmolarity conditions (Fig. 1A). Only the ATCC 2001 Cg*sho1*Δ strain showed severely impaired growth on high salt concentrations, whereas a lack of *SHO1* in BG2 and Cg2633 did not result in increased osmosensitivity (Fig. 1A). As expected, however, deletion of *PBS2* led to osmostress hypersensitivity in all three strains (Fig. 1A). Thus, deletion of the MAPKK Pbs2 causes a severe phenotype on high NaCl concentrations that is independent of the genetic background. The observed salt stress sensitivity of a *C. glabrata* Cg*sho1*Δ strain is hence restricted to ATCC 2001, supporting the idea of an inactive Sln1 branch in strain ATCC 2001. Disruption of *SHO1* in this strain could therefore lead to complete inactivation of the HOG pathway.

Deletion of Cg*SHO1* in ATCC 2001 causes general osmostress sensitivity and thermosensitivity. To investigates the role of Sho1 and the HOG pathway in the ATCC 2001 background, we constructed further *SHO1* deletion strains. We chose strains ΔHT6 and ΔHTU (16, 45), since auxotrophic markers are available in these strains. Genomic disruption cassettes were generated by three-way PCR using the Cg*HIS3* gene as a selectable marker and were used for transformation. Several independent transformants were obtained, and homologous recombination leading to gene disruption was confirmed by PCR and Southern blot analysis (data not shown).

Transformants of ΔHT6 and ΔHTU derivatives in which *SHO1* was correctly replaced were then tested for growth under high-osmolarity conditions. Strain ΔHTU Cg*sho1*Δ showed impaired growth on plates containing 0.7 M NaCl and completely failed to grow on 1 M NaCl, whereas the wild-type strain tolerated concentrations as high as 1.2 M NaCl (Fig. 2). Deletion of Cg*SHO1* also led to reduced growth on plates supplemented with other types of osmolytes, namely, sorbitol and KCl. Interestingly, we observed an increased temperature sensitivity of ΔHTU Cg*sho1*Δ at 42°C, although at 37°C no altered sensitivity was observed (data not shown). Reintroducing *SHO1* on a plasmid could restore growth at high osmolarity and elevated temperatures (Fig. 2). Similar phenotypes were also observed for ΔHT6 Cg*sho1*Δ strains (data not shown). In *S. cerevisiae*, the HOG pathway is also involved in the response to increasing concentrations of methylglyoxal (1, 24), a toxic intermediate of carbon metabolism. Similarly, the ΔHTU Cg*sho1*Δ strain displayed slightly increased sensitivity to 40 mM and 50 mM methylglyoxal relative to that of wild-type strains (Fig. 2).

Lack of Cg*SHO1* in the ATCC 2001 genetic background inactivates the HOG pathway. In *S. cerevisiae*, HOG pathway activation leads to dual phosphorylation of Hog1 to ultimately activate the MAPK cascade. We therefore investigated the phosphorylation status of Hog1 in *C. glabrata* in response to osmostress. Cultures of the Cg*sho1*Δ strain transformed either with a plasmid expressing Cg*SHO1* or with the empty vector were grown to the exponential-growth phase before addition of 0.5 M NaCl. Samples were taken at several time points and extracts separated by SDS-PAGE. Activated Hog1 isoforms were detected using phosphospecific polyclonal antibodies rec-

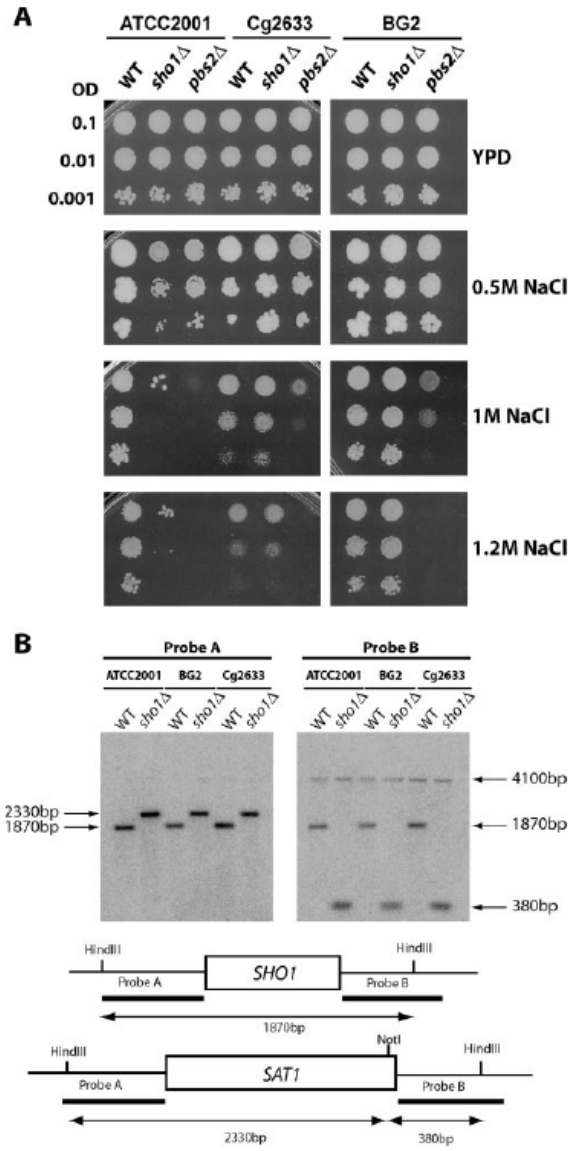

FIG. 1. Osmostress sensitivities of *C. glabrata pbs2*Δ and *sho1*Δ strains. (A) Cultures of the *C. glabrata* strains ATCC 2001, Cg2633, and BG2, as well as their isogenic Cg*pbs2*Δ and Cg*sho1*Δ deletion strains, were grown to an OD_{600} of 1, diluted to an OD_{600} of 0.1, 0.01, or 0.001, and spotted onto YPD and YPD agar plates containing the indicated amounts of NaCl. Plates were incubated at 30°C for 2 days. WT, wild type. (B) Genomic DNA was isolated from ATCC 2001, BG2, Cg2633, and their isogenic Cg*sho1* deletion strains, followed by digestion with HindIII and NotI. After agarose separation of DNA fragments and transfer to nitrocellulose membranes, radiolabeled probes A and B were used for detection of the *SHO1* WT gene and the disrupted allele. Restriction sites and expected fragment sizes for the WT and Cg*sho1* disruption strains are illustrated schematically (not drawn to scale).

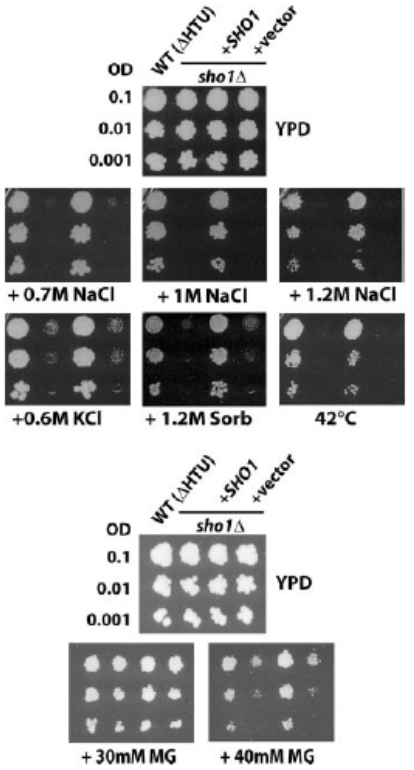

FIG. 2. Sensitivity of the ΔHTU Cg*sho1*Δ strain to osmostress, high temperatures, and methylglyoxal. Cultures of the wild-type (WT) strain (ΔHTU), ΔHTU Cg*sho1*Δ, and ΔHTU Cg*sho1*Δ transformed either with a vector expressing Cg*SHO1* or with the empty vector were diluted to an OD_{600} of 0.1, 0.01, or 0.001 and spotted onto YPD and YPD agar plates containing the indicated amounts of NaCl, KCl, sorbitol (Sorb), or methylglyoxal (MG). Plates were incubated at 30°C for 2 days or at 42°C for 1 day.

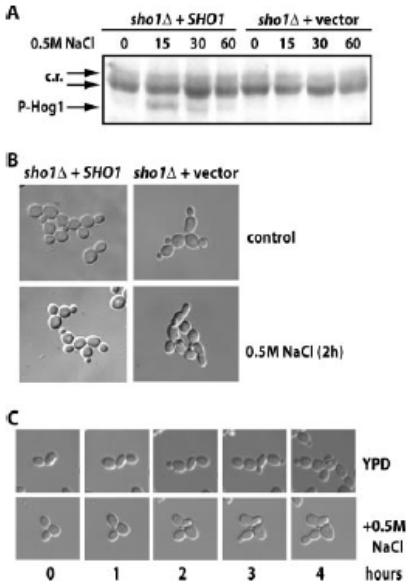

FIG. 3. Loss of Hog1 phosphorylation and altered morphology of ΔHTU Cg*sho1*Δ under salt stress. (A) Cultures of ΔHTU Cg*sho1*Δ transformed either with a plasmid expressing Cg*SHO1* or with the empty vector were grown to an OD_{600} of 1 before addition of 0.5 M NaCl. Samples were taken at the indicated time points (minutes). Glass bead extracts were prepared from these samples, and 50 μg of total-cell extract per lane was separated on a 10% SDS-PAGE gel. Immunoblotting was carried out using phosphospecific polyclonal antibodies detecting activated Hog1 isoforms. c.r., cross-reactions. (B) Cultures of ΔHTU Cg*sho1*Δ transformed either with a vector expressing Cg*SHO1* or with the empty vector were grown to an OD_{600} of 0.6 and then either treated with 0.5 M NaCl or left unstressed for 2 h before pictures were taken. (C) ΔHTU Cg*sho1*Δ was grown to an OD_{600} of 0.6 before cells were immobilized onto a slide with concanavalin A. Growth was then inspected under the microscope under stress and nonstress conditions for 4 h, and pictures were taken at the indicated time points.

ognizing phosphorylated Hog1 (P-Hog1). Whereas in the strain harboring wild-type Cg*SHO1* a transient phosphorylation signal in response to osmostress was detectable, this signal was absent in the Cg*sho1*Δ strain (Fig. 3A). This finding supports a functional block of the signaling cascade upstream of CgHog1. Even increasing the NaCl concentration to 1 M failed to trigger phosphorylation and activation of CgHog1 in the absence of Sho1 (data not shown).

In *C. albicans*, deletion of components of the HOG pathway influences cell morphology and filamentation (37). Likewise, in *S. cerevisiae*, cells lacking *HOG1* exhibit a cell morphology phenotype (5). Therefore, we microscopically inspected Cg*sho1*Δ cells with respect to their morphology under osmostress. We took pictures of exponentially growing cells 2 h after incubation with or without 0.5 M NaCl (Fig. 3B). Cells containing wild-type *SHO1* looked normal under both conditions, whereas growth of the Cg*sho1*Δ strain caused abnormal cell morphology under high-osmolarity conditions (Fig. 3B). About 50 to 80% of the cells were elongated or swollen. We then immobilized cells on a microscope slide and inspected the growth patterns of the same cells under stress and nonstress conditions for as long as 4 h, covering several cell divisions. In response to osmotic stress, the Cg*sho1*Δ strain seemed to display severe budding defects (Fig. 3C). Therefore, Sho1 must play a major role in mediating the osmostress response and Hog1 phosphorylation in *C. glabrata* strains ΔHT6 and ΔHTU, demonstrating an inactive Sln1 branch in the ATCC 2001 background.

***C. glabrata* Sho1 can functionally complement the lack of *S. cerevisiae* Sho1.** Next, we investigated whether the function of Sho1 within the signaling cascade of the HOG pathway is conserved between *C. glabrata* and *S. cerevisiae*. To check the functionality of the Cg*SHO1* gene in *S. cerevisiae*, we cloned the Cg*SHO1* ORF, including the 600-bp promoter and 700-bp 3′ untranslated regions, into the *CEN*-based yeast vector pRS316 and the multicopy vector YEp352. Plasmids pRS-CgSHO1 and YEp-CgSHO1 were used for transformation of the *S. cerevisiae* recipient strain YCG9A (*sho1*Δ *ssk2*Δ *ssk22*Δ). Positive transformants were then analyzed for growth on plates containing 1 M or 1.2 M NaCl, concentrations that severely impaired the growth of the control strain YCG9A (Fig. 4A). Introducing Cg*SHO1* either on a multicopy plasmid or on a *CEN*-based plasmid fully restored growth of the *S. cerevisiae*

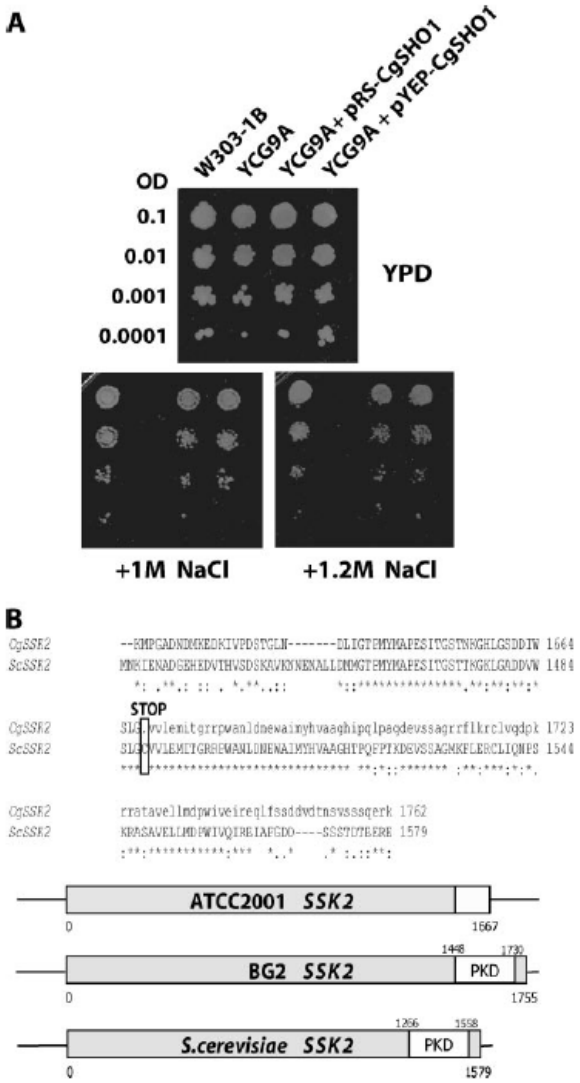

FIG. 4. Expression of CgSho1 in yeast can complement the loss of ScSho1. (A) *S. cerevisiae* strains W303-1B, YCG9A (*sho1*Δ *ssk2*Δ *ssk22*Δ), and YCG9A transformed with either pRS-CgSHO1 or pYEp-CgSHO1 were diluted to an OD_{600} of 0.1, 0.01, 0.001, or 0.0001 and spotted onto YPD and YPD agar plates containing NaCl. Plates were incubated at 30°C for 2 days. (B) Alignment of the protein kinase domains of *C. glabrata* (ATCC 2001) and *S. cerevisiae* Ssk2. Cg*SSK2* encodes a translational stop within a region highly conserved between *S. cerevisiae* and *C. glabrata* (indicated). Below the alignment are diagrams of the proteins encoded by the *SSK2* ORFs in the two distinct *C. glabrata* strains, ATCC 2001 and BG2, as well as *S. cerevisiae* Ssk2. PKD, protein kinase domain.

*sho1*Δ *ssk2*Δ *ssk22*Δ strain YCG9A (Fig. 4A). These data suggest that we have indeed identified CgSho1 as the orthologue of Sho1 from *S. cerevisiae*.

Cg*SSK2* carries a point mutation in ATCC 2001 but not in other *C. glabrata* strains. We initially found that only ATCC 2001 *sho1*Δ is hypersensitive to osmostress. In other backgrounds, the same deletion did not influence resistance to high concentrations of NaCl. Hence, we assumed that the Sln1 branch in ATCC 2001 either is not functional or is absent, perhaps due to inactivity of one of the proteins of this branch. The annotated genome sequence of ATCC 2001 published by the Génolevures Consortium contains two ORFs highly similar to the 5′ and 3′ halves of the *S. cerevisiae SSK2* gene. These are separated by an unsequenced gap, implying the possibility of a pseudogene. To fill this sequence gap completely, we sequenced this region by standard primer walking, covering a sequence of 1,680 bp. The deduced amino acid sequence is identical for all three strains, ATCC 2001, BG2, and Cg2633. This newly sequenced region combines both previously identified ORFs into a single ORF encoding a 1,667-residue protein. However, the genome sequence of the ATCC 2001 Cg*SSK2* locus carries a translational stop codon within the predicted protein kinase domain, which is otherwise highly conserved between *S. cerevisiae* and *C. glabrata* (Fig. 4B). Sequencing of the equivalent genomic region showed that BG2 and Cg2633 did encode the conserved Cys1668 at the identical position. Furthermore, we sequenced the relevant genomic region in the *SSK2* genes of seven *C. glabrata* clinical isolates (kindly provided by Helena Budjakova). However, none of the clinical isolates carried this stop mutation present in the ATCC 2001 strain (data not shown). Moreover, we sequenced the entire *SSK2* gene in the BG2 wild-type strain, potentially encoding a 1,755-residue CgSsk2 protein containing the entire protein kinase domain (Fig. 4B).

Because methylglyoxal sensitivity and acetic acid hypersensitivity in *S. cerevisiae* are caused mainly by an inactive Sln1 branch (24, 25), we performed additional spot tests using these compounds. These experiments revealed that wild-type ATCC 2001 was also significantly more sensitive to methylglyoxal and acetate than other strains investigated (Fig. 5A). On methylglyoxal, ATCC 2001 showed growth defects similar to those of a BG2 Cg*pbs2*Δ deletion strain (Fig. 5A); disruption of Cg*SHO1* further increased sensitivities, as described above. The Cg*sho1*Δ and Cg*pbs2*Δ deletions in ATCC 2001 did not further increase acetate sensitivity. For complementation analysis, we introduced a functional *SSK2* allele into the genome of the ATCC 2001 *sho1*Δ strain. Since all attempts to clone Cg*SSK2* into a *C. glabrata* vector failed, we integrated the Cg*SSK2* allele encoded in the BG2 genome into the corresponding genomic locus of ATCC 2001 *sho1*Δ. Cells carrying the replaced *SSK2* gene were selected on plates containing 1.2 M NaCl and verified by genomic sequencing. Growth inhibition analysis with three independent transformants (C1 to C3) revealed that introduction of the gene encoding full-length Cg*SSK2* into ATCC 2001 *sho1*Δ restored growth at high osmolarity and elevated temperatures. Moreover, all clones grew on higher acetate and methylglyoxal concentrations than the corresponding wild-type strain (Fig. 5B).

Furthermore, we deleted parts of the Cg*SSK2* ORF (bp 2063 to 5005) in wild-type BG2. As expected, the mutant strain obtained, BG2 Cg*ssk2*Δ, displayed higher sensitivity on acetate and, to a lesser extent, on methylglyoxal than wild-type BG2 but growth similar to that of wild-type ATCC 2001 (Fig. 5C). Furthermore, we performed immunoblot analysis to determine the phosphorylation status of CgHog1 in strains lacking *SSK2* or cells expressing restored CgSsk2. In strain BG2 with

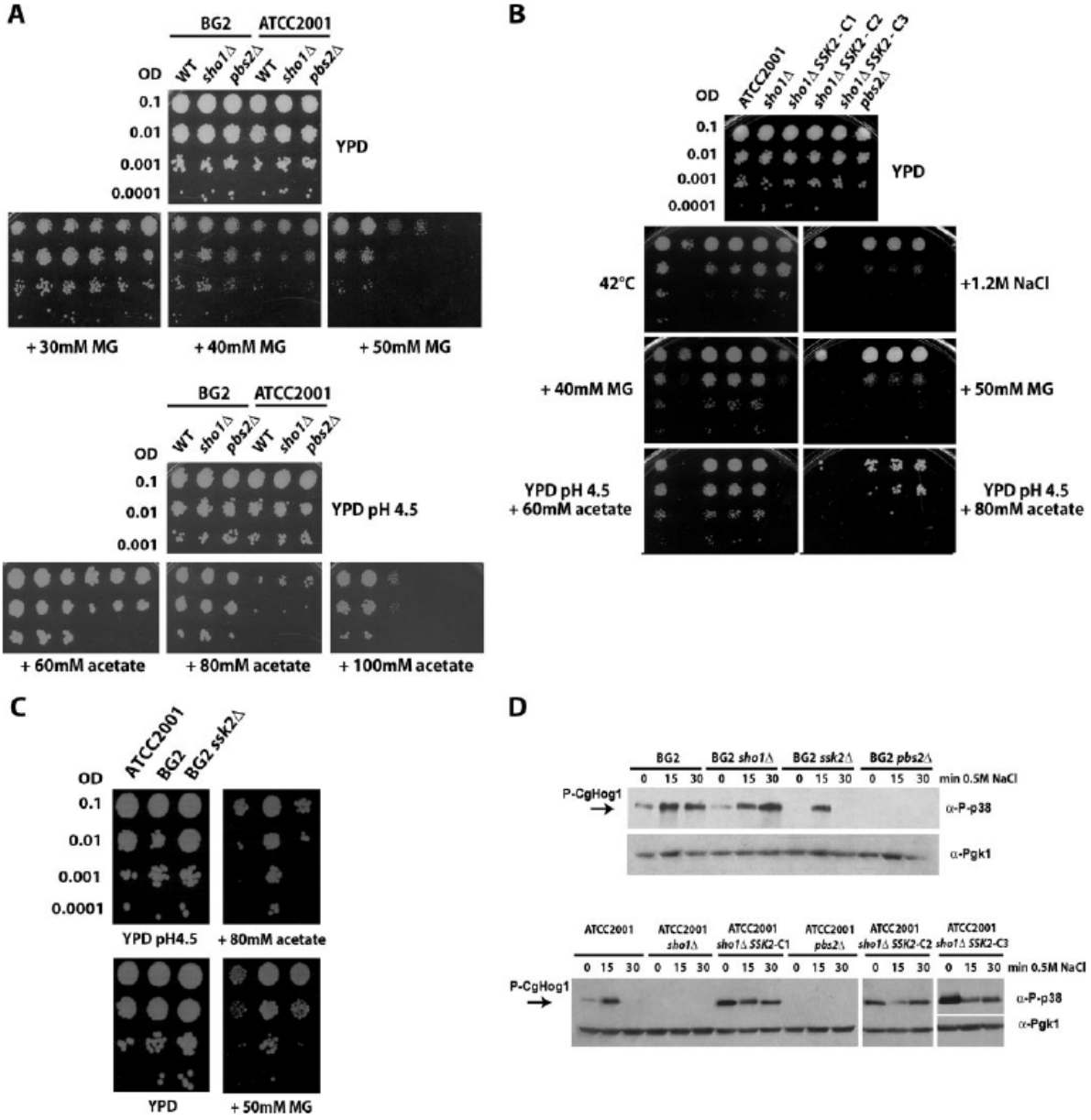

FIG. 5. The ATCC 2001 genome carries a nonfunctional truncated *ssk2-1* allele. (A) Cultures of the *C. glabrata* strains ATCC 2001 and BG2 as well as their isogenic C*gpbs2*Δ and C*gsho1*Δ deletion strains were diluted to an OD_{600} of 0.1, 0.01, or 0.001 and spotted onto YPD and YPD agar plates containing the indicated amounts of methylglyoxal (MG) or onto YPD (pH 4.5) and YPD (pH 4.5) agar plates containing the indicated amounts of acetate. Plates were incubated at 30°C for 2 days. (B) Cultures of the *C. glabrata* strain ATCC 2001 and the isogenic C*gpbs2*Δ and C*gsho1*Δ deletion strains, as well as three independent clones of ATCC 2001 *sho1*Δ *SSK2* (C1 to C3), were grown to the exponential-growth phase, diluted to an OD_{600} of 0.1, and spotted along with serial 1:10 dilutions onto plates containing the indicated amounts of NaCl, MG, or acetate. Plates were incubated at 30°C for 2 days or at 42°C for 1 day. (C) Cultures of ATCC 2001, BG2, and BG2 C*gssk2*Δ were diluted to an OD_{600} of 0.1, 0.01, or 0.001; serial dilutions were spotted onto YPD and YPD agar plates containing 50 mM MG or onto YPD (pH 4.5) and YPD (pH 4.5) agar plates containing 80 mM acetate. Plates were incubated at 30°C for 2 days. (D) Cultures of BG2 and ATCC 2001 and the indicated isogenic deletion strains, as well as three clones of ATCC 2001 *sho1*Δ complemented for *SSK2* (C1 to C3), were grown to the early-exponential-growth phase before 0.5 M NaCl was added. Samples were taken at the indicated time points and crude trichloroacetic acid extracts prepared. Aliquots corresponding to 0.4 OD_{600} equivalent per lane were fractionated through a 10% SDS-PAGE gel. Immunoblotting was carried out using polyclonal anti-phospho-p38 MAPK or anti-Pgk1 antibodies. Extracts of ATCC 2001 *sho1*Δ *SSK2* C2 and C3 were detected on different immunoblots, as indicated by the separation of these gels.

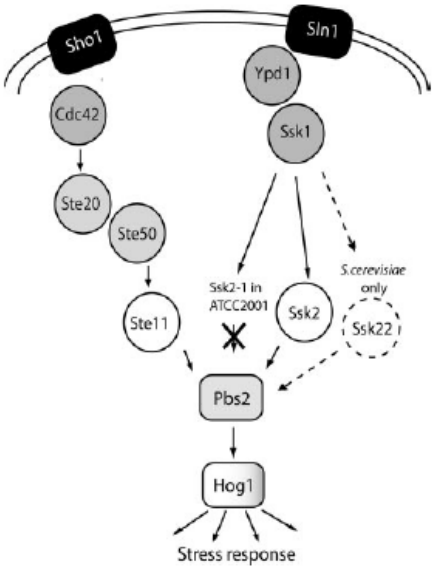

FIG. 6. HOG pathways operating in *S. cerevisiae* and *C. glabrata*. Activation of the MAPKK Pbs2 can occur through at least two distinct upstream osmosensing mechanisms. One branch links the osmosensing protein Sln1 via Ypd1, Ssk1, and the MAPKKKs Ssk2 and Ssk22 to Pbs2. In the other branch, Sho1 functions to link an as yet unidentified osmosensor to the downstream components Cdc42, Ste20, Ste50, and the MAPKKK Ste11. Activated Pbs2 phosphorylates the MAPK Hog1, which in turn activates a variety of transcription factors. As indicated, Ssk22 does not exist in *C. glabrata*, and ATCC 2001 contains the *ssk2-1* allele, encoding a truncated and nonfunctional Ssk2 version.

Cg*SSK2* deleted, the Hog1 phosphorylation signal decreased more rapidly after osmostress than that in the wild type. Strikingly, reintegration of the functional Cg*SSK2* allele in the ATCC 2001 background with Cg*SHO1* deleted led to a phosphorylation signal in the unstressed situation, indicating constitutive Hog1 phosphorylation. This hyperphosphorylation phenotype was observed for all three independent clones tested (Fig. 5D). Taken together, our results show that the truncated allele of Cg*SSK2* in ATCC 2001 (Cg*ssk2-1*) completely debilitates the Sln1 branch. Moreover, our data also demonstrate that the HOG pathway plays similar physiological roles in the osmostress response in baker's yeast and the human fungal pathogen *C. glabrata* (Fig. 6).

Mutants of the *C. glabrata* HOG pathway display sensitivity to weak organic acids. Recent studies in yeast revealed that Hog1 plays a role in resistance to acetic acid and that the response to acetic acid stress is mediated through the Sln1 branch of the HOG pathway (25). Our results indicate similar roles of the HOG pathway in *C. glabrata* and baker's yeast. A Cg*pbs2*Δ mutant in the BG2 background showed defects in growth on plates containing 100 mM acetate relative to the wild type, whereas the Cg*sho1*Δ mutant in the same background did not show altered sensitivities (Fig. 5A). However, as already observed for methylglyoxal, ATCC 2001 is clearly more sensitive to acetic acid than BG2. The Cg*sho1*Δ and Cg*pbs2*Δ deletions did not further increase sensitivities in ATCC 2001. Since we observed acetate hypersensitivity in HOG pathway mutants, we tested the growth of the same set of *C. glabrata* strains on plates containing the weak organic acids sorbate, propionate, and benzoate. Surprisingly, we also observed increased sensitivities of mutant strains under these conditions, a phenotype that was not observed in *S. cerevisiae*. Disruption of Cg*PBS2* in BG2 led to slightly impaired growth on 5 mM benzoate and 2.5 mM sorbate, whereas deletion of Cg*SHO1* did not cause hypersensitivity in a strain background with a functional Sln1 branch (Fig. 7A). Similar sorbate and benzoate hypersensitivities were observed for Cg*pbs2*Δ in ATCC 2001. Notably, a Cg*sho1*Δ mutant was even more sensitive to sorbate, benzoate, and propionate in this genetic background. In contrast, neither blockage of one or both upstream branches nor a lack of the downstream MAPKK Pbs2 caused any detectable weak-acid sensitivities in *S. cerevisiae* (Fig. 7B). In summary, our data suggest an additional role of the *C. glabrata* HOG pathway in weak-acid response, which is quite distinct from its osmosensing function in *S. cerevisiae*. However, blockage of the signaling of both upstream branches caused a more severe phenotype than disruption of the downstream MAPKK Pbs2, perhaps implying yet another signal transfer bypassing Pbs2 or involvement in another parallel and yet undisclosed pathway in stress sensing.

DISCUSSION

Adaptation to changes in the microenvironment during disease progression is an essential mechanism for the survival of fungal pathogens. MAPK cascades are important components in such cellular adaptation programs. This work aimed to define the role of orthologues of the *S. cerevisiae* HOG MAPK pathway in the pathogenic yeast *C. glabrata*. The analysis of physiological roles for the HOG pathway in the well-studied human fungal pathogen *C. albicans* revealed a strong phenotype, quite distinct from corresponding single mutations in *S. cerevisiae*. For example, Hog1 appears to be implicated in more-diverse stress conditions than its *S. cerevisiae* orthologue (42). Likewise, the role of Sho1 in *C. albicans* seems different from its osmosensing function in baker's yeast (37).

C. glabrata is a close relative of *S. cerevisiae*, considering genome evolution (8). Therefore, most adaptive functions of the HOG pathway are most likely also conserved. However, we show here that the genome of *C. glabrata* ATCC 2001 carries a putative orthologue of yeast *SSK2* in a mutated form. Moreover, the *SSK2* homologue *SSK22* is absent from the *C. glabrata* genome. This fact hinted at possibly distinct functions of the MAPK pathways in these fungi, since one of the two major upstream signaling branches is debilitated. Here we show that (i) the overall functions of HOG signaling in *C. glabrata* are closely related to its functional counterpart in baker's yeast; (ii) CgSho1 can complement the corresponding *S. cerevisiae* mutant; and (iii) the Sln1 branch is inactive in the ATCC 2001 strain background due to a point mutation in the Cg*SSK2* gene but active in all other *C. glabrata* strain backgrounds tested.

Our analysis of HOG pathway mutants revealed a spectrum of phenotypes very similar to the respective mutants in baker's yeast. In *S. cerevisiae*, two HOG branches drive Hog1 activation; one branch uses Sln1, Ypd1, Ssk1, and the MAPKKKs Ssk2 and Ssk22, which then activate downstream Pbs2 (4, 32). The second branch senses through Sho1 and transduces via

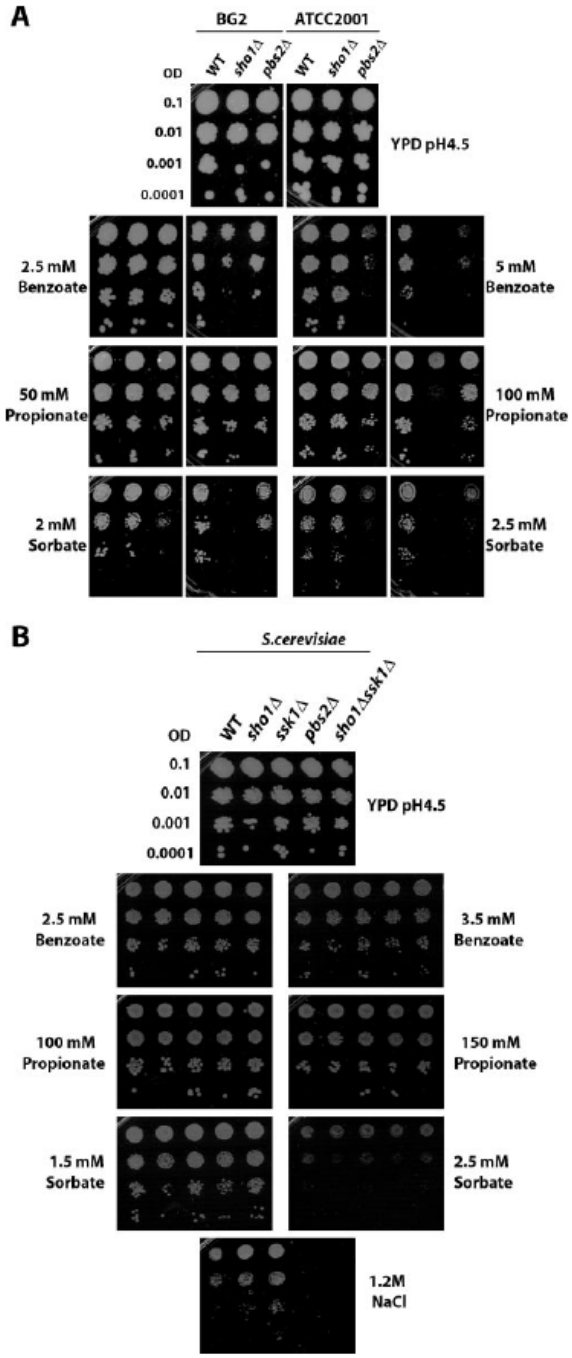

FIG. 7. *C. glabrata* HOG pathway mutants display sensitivity to weak acids. (A) Cultures of the *C. glabrata* strains ATCC 2001 and BG2, as well as their isogenic Cg*pbs2*Δ and Cg*sho1*Δ deletion strains, were diluted to an OD_{600} of 0.1, 0.01, or 0.001 and spotted onto YPD (pH 4.5) and YPD (pH 4.5) agar plates containing the indicated amounts of sorbate, propionate, or benzoate. Plates were incubated at 30°C for 2 days. WT, wild type. (B) Cultures of WT *S. cerevisiae* W303-1A and its isogenic *sho1*Δ, *ssk1*Δ, *pbs2*Δ, and *ssk1*Δ *sho1*Δ deletion strains were grown to the exponential-growth phase, and serial dilutions were spotted onto YPD (pH 4.5) and YPD (pH 4.5) agar plates containing the indicated amounts of sorbate, propionate, or benzoate or onto YPD containing 1.2 M NaCl.

Cdc42 and Ste20, Ste50, and Ste11 to converge with the Sln1 branch in the activation of Pbs2 and the key kinase Hog1 further downstream (31). It is known that *S. cerevisiae* Sln1 carries an intrinsic histidine kinase activity and is able to control Ssk1 activity using a phosphorelay system involving Ypd1. Ssk1 then interacts with the MAPKKKs Ssk2 and Ssk22, which in turn activate Pbs2. Even though the two upstream branches of the HOG pathway seem highly specialized in detecting slightly different concentrations of salt (28), only mutations that block both branches cause severe osmosensitivities.

Our deletion analysis demonstrates that loss of *C. glabrata SHO1* alone can cause osmostress hypersensitivity as a function of the genetic background. Experiments with different *C. glabrata* strains demonstrated that osmosensitivity of Cg*sho1* mutants is restricted to ATCC 2001-derived "wild-type" strains. Our results are in line with the conclusion that the Sln1 branch is inactivated in the ATCC 2001 background. This was not observed for other clinical isolates and is therefore not a general peculiarity of *C. glabrata*. Although we did not detect an enhanced sensitivity of this strain to osmotic stress, methylglyoxal and acetate were markedly less well tolerated.

Sho1, the transmembrane protein of one branch of the HOG pathway, was previously thought to be a sensor of osmostress. However, recent studies also reveal an important role of Sho1 downstream of Ste11 by binding to both the activated Ste11–Ste50 complex and Pbs2, perhaps tethering a "signaling complex" at the cell surface (43). Bringing together Ste11 and Pbs2 is required for activation of Pbs2 and therefore of Hog1. The *C. glabrata* orthologue of yeast *SHO1* can functionally complement *S. cerevisiae sho1* mutants. Studies of *C. albicans* report that Ca*SHO1* plays only a negligible role in osmostress resistance, whereas Ca*sho1* mutants are sensitive to oxidative stress (37). In our work, we failed to detect hypersensitivity of the *C. glabrata* Cg*sho1* mutant on H_2O_2 or menadione (data not shown). Furthermore, CgHog1 phosphorylation was undetectable in response to oxidative stress (data not shown), indicating a negligible role of the *C. glabrata* HOG pathway in the oxidative-stress response.

It is unclear when during evolution the Cg*SSK2* mutation was acquired by the ATCC 2001 strain. Since inactivity of the Sln1 branch might decrease fitness in the host environment, and because other isolates do not carry the Cg*ssk2-1* allele, it appears likely that the Cg*ssk2-1* mutation was acquired during or after the isolation of the strain from its human source. Interestingly, ATCC 2001 strains carrying restored *SSK2* showed increased levels of phosphorylated Hog1. Hence, acquisition of the mutated *ssk2-1* allele might be a natural suppressor mutation of constitutively active Hog1 in order to bypass associated toxicities, a mechanism similar to dominant-negative activities observed for a constitutive Pbs2 kinase in baker's yeast (12). Nevertheless, this work provides highly relevant information for the fungal pathogen community, since one should keep in mind that all mutations or deletions gen-

erated in the ATCC 2001-derived genetic backgrounds are in fact double mutants also carrying a Cg*ssk2-1* allele. Thus, any stress-related phenotypes and molecular cross talk between different signaling pathways may be caused by synthetic genetic interactions due to the presence of the mutated Cg*ssk2-1* allele and the lack of the second gene. This is particularly relevant and should be considered for genome-wide knockout approaches on *C. glabrata* or studies addressing the molecular cross talk between several MAPK pathways in stress response and adaptation. Determining possible differences in the virulence of HOG pathway mutants would indeed be interesting, since this may relate to the in vivo host situation. However, available mouse models for *Candida glabrata* are suboptimal and difficult to establish. Therefore, we are in the process of establishing a novel *Drosophila melanogaster* insect model with mutations in the *toll* pathway to be employed for *Candida glabrata* virulence studies (D. Ferrandon et al., unpublished data).

Response to weak organic acids, apart from acetic acid, fails to trigger Hog1 signaling in yeast. By contrast, we show that *C. glabrata* double mutants in the Ssk2 and Sho1 branch are highly sensitive against weak acids of medium chain length such as sorbic acid. No similar phenotype is observed for yeast. The observation that Cg*pbs2* mutants are less sensitive than the Cg*ssk2* Cg*sho1* double mutant perhaps points to a bypass to compensate for the lack of CgPbs2, although indirect genetic effects cannot be ruled out. However, the hypersensitivity of the Cg*ssk2* Cg*sho1* double mutant implies a compensatory mechanism that is operative in *S. cerevisiae* but missing or nonfunctional in *C. glabrata*. In conclusion, our data demonstrate that several characteristics of HOG signaling are conserved between baker's yeast and the human pathogen *C. glabrata*, although fundamental differences exist with regard to the activating cues. Exploring these differences will also shed further light on networks and cross talk between MAPK pathways in yeast.

ACKNOWLEDGMENTS

We thank our colleagues Ken Haynes, Janet Quinn, Helena Budjakova, and Steffen Rupp for the gifts of reagents, strains, and materials as well as for stimulating discussions. We thank Wolfgang Reiter for providing the phosphospecific antibodies and Walter Glaser for help with designing oligonucleotides and with DNA sequence deposition. We thank Dominique Ferrandon for fruitful suggestions about the use of the fly model to study the virulence of *C. glabrata*.

This work was supported in part by the EC project "EURESFUN" (STREP-2004-CT-PL518199), the EC Marie Curie Training Network "CanTrain" (CT-2004-512481), and a project of the "Wiener Wissenschafts & Technologie Fonds" WWTF (HOPI-LS133) (to K.K. and G.A.). Additional funds came from the Herzfelder Foundation (to C.S.).

REFERENCES

1. **Aguilera, J., S. Rodriguez-Vargas, and J. A. Prieto.** 2005. The HOG MAP kinase pathway is required for the induction of methylglyoxal-responsive genes and determines methylglyoxal resistance in *Saccharomyces cerevisiae*. Mol. Microbiol. **56:**228–239.
2. **Alonso-Monge, R., F. Navarro-Garcia, G. Molero, R. Diez-Orejas, M. Gustin, J. Pla, M. Sanchez, and C. Nombela.** 1999. Role of the mitogen-activated protein kinase Hog1p in morphogenesis and virulence of *Candida albicans*. J. Bacteriol. **181:**3058–3068.

2a. **Ausubel, F. M., R. Brent, R. E. Kingston, D. D. Moore, J. G. Seidman, J. A. Smith, and K. Struhl.** 1998. Current protocols in molecular biology. John Wiley & Sons, Inc., New York, NY.

3. **Bilsland, E., C. Molin, S. Swaminathan, A. Ramne, and P. Sunnerhagen.** 2004. Rck1 and Rck2 MAPKAP kinases and the HOG pathway are required for oxidative stress resistance. Mol. Microbiol. **53:**1743–1756.
4. **Brewster, J. L., T. de Valoir, N. D. Dwyer, E. Winter, and M. C. Gustin.** 1993. An osmosensing signal transduction pathway in yeast. Science **259:**1760–1763.
5. **Brewster, J. L., and M. C. Gustin.** 1994. Positioning of cell growth and division after osmotic stress requires a MAP kinase pathway. Yeast **10:**425–439.
6. **Castano, I., S. J. Pan, M. Zupancic, C. Hennequin, B. Dujon, and B. P. Cormack.** 2005. Telomere length control and transcriptional regulation of subtelomeric adhesins in *Candida glabrata*. Mol. Microbiol. **55:**1246–1258.
7. **Chen, D., W. M. Toone, J. Mata, R. Lyne, G. Burns, K. Kivinen, A. Brazma, N. Jones, and J. Bahler.** 2003. Global transcriptional responses of fission yeast to environmental stress. Mol. Biol. Cell **14:**214–229.
8. **Dujon, B., D. Sherman, G. Fischer, P. Durrens, S. Casaregola, I. Lafontaine, J. De Montigny, C. Marck, C. Neuveglise, E. Talla, N. Goffard, L. Frangeul, M. Aigle, V. Anthouard, A. Babour, V. Barbe, S. Barnay, S. Blanchin, J. M. Beckerich, E. Beyne, C. Bleykasten, A. Boisrame, J. Boyer, L. Cattolico, F. Confanioleri, A. De Daruvar, L. Despons, E. Fabre, C. Fairhead, H. Ferry-Dumazet, A. Groppi, F. Hantraye, C. Hennequin, N. Jauniaux, P. Joyet, R. Kachouri, A. Kerrest, R. Koszul, M. Lemaire, I. Lesur, L. Ma, H. Muller, J. M. Nicaud, M. Nikolski, S. Oztas, O. Ozier-Kalogeropoulos, S. Pellenz, S. Potier, G. F. Richard, M. L. Straub, A. Suleau, D. Swennen, F. Tekaia, M. Wesolowski-Louvel, E. Westhof, B. Wirth, M. Zeniou-Meyer, I. Zivanovic, M. Bolotin-Fukuhara, A. Thierry, C. Bouchier, B. Caudron, C. Scarpelli, C. Gaillardin, J. Weissenbach, P. Wincker, and J. L. Souciet.** 2004. Genome evolution in yeasts. Nature **430:**35–44.
9. **Egner, R., and K. Kuchler.** 1996. The yeast multidrug transporter Pdr5 of the plasma membrane is ubiquitinated prior to endocytosis and degradation in the vacuole. FEBS Lett. **378:**177–181.
10. **Gustin, M. C., J. Albertyn, M. Alexander, and K. Davenport.** 1998. MAP kinase pathways in the yeast *Saccharomyces cerevisiae*. Microbiol. Mol. Biol Rev. **62:**1264–1300.
11. **Hao, N., M. Behar, S. C. Parnell, M. P. Torres, C. H. Borchers, T. C. Elston, and H. G. Dohlman.** 2007. A systems-biology analysis of feedback inhibition in the Sho1 osmotic-stress-response pathway. Curr. Biol. **17:**659–667.
12. **Jiang, L., S. Niu, K. L. Clines, D. J. Burke, and T. W. Sturgill.** 2004. Analyses of the effects of Rck2p mutants on Pbs2pDD-induced toxicity in *Saccharomyces cerevisiae* identify a MAP kinase docking motif, and unexpected functional inactivation due to acidic substitution of T379. Mol. Genet. Genomics **271:**208–219.
13. **Kaiser, C., S. Michaelis, and A. Mitchell.** 1994. Methods in yeast genetics. A laboratory course manual. Cold Spring Harbor Laboratory Press, Cold Spring Harbor, NY.
14. **Kamran, M., A. M. Calcagno, H. Findon, E. Bignell, M. D. Jones, P. Warn, P. Hopkins, D. W. Denning, G. Butler, T. Rogers, F. A. Muhlschlegel, and K. Haynes.** 2004. Inactivation of transcription factor gene *ACE2* in the fungal pathogen *Candida glabrata* results in hypervirulence. Eukaryot. Cell **3:**546–552.
15. **Kaur, R., R. Domergue, M. L. Zupancic, and B. P. Cormack.** 2005. A yeast by any other name: *Candida glabrata* and its interaction with the host. Curr. Opin. Microbiol. **8:**378–384.
16. **Kitada, K., E. Yamaguchi, and M. Arisawa.** 1995. Cloning of the *Candida glabrata TRP1* and *HIS3* genes, and construction of their disruptant strains by sequential integrative transformation. Gene **165:**203–206.
17. **Kitada, K., E. Yamaguchi, and M. Arisawa.** 1996. Isolation of a *Candida glabrata* centromere and its use in construction of plasmid vectors. Gene **175:**105–108.
18. **Kren, A., Y. M. Mamnun, B. E. Bauer, C. Schuller, H. Wolfger, K. Hatzixanthis, M. Mollapour, C. Gregori, P. Piper, and K. Kuchler.** 2003. War1p, a novel transcription factor controlling weak acid stress response in yeast. Mol. Cell. Biol. **23:**1775–1785.
19. **Krisak, L., R. Strich, R. S. Winters, J. P. Hall, M. J. Mallory, D. Kreitzer, R. S. Tuan, and E. Winter.** 1994. *SMK1*, a developmentally regulated MAP kinase, is required for spore wall assembly in *Saccharomyces cerevisiae*. Genes Dev. **8:**2151–2161.
20. **Kuchler, K., H. G. Dohlman, and J. Thorner.** 1993. The *a*-factor transporter (*STE6* gene product) and cell polarity in the yeast *Saccharomyces cerevisiae*. J. Cell Biol. **120:**1203–1215.
21. **Lawrence, C. L., C. H. Botting, R. Antrobus, and P. J. Coote.** 2004. Evidence of a new role for the high-osmolarity glycerol mitogen-activated protein kinase pathway in yeast: regulating adaptation to citric acid stress. Mol. Cell. Biol. **24:**3307–3323.
22. **Levin, D. E.** 2005. Cell wall integrity signaling in *Saccharomyces cerevisiae*. Microbiol. Mol. Biol. Rev. **69:**262–291.
23. **Maeda, T., S. M. Wurgler-Murphy, and H. Saito.** 1994. A two-component system that regulates an osmosensing MAP kinase cascade in yeast. Nature **369:**242–245.
24. **Maeta, K., S. Izawa, and Y. Inoue.** 2005. Methylglyoxal, a metabolite derived from glycolysis, functions as a signal initiator of the high osmolarity glycerol-mitogen-activated protein kinase cascade and calcineurin/Crz1-mediated pathway in *Saccharomyces cerevisiae*. J. Biol. Chem. **280:**253–260.

25. **Mollapour, M., and P. W. Piper.** 2006. Hog1p mitogen-activated protein kinase determines acetic acid resistance in *Saccharomyces cerevisiae*. FEMS Yeast Res. **6:**1274–1280.
26. **Noble, S. M., and A. D. Johnson.** 2005. Strains and strategies for large-scale gene deletion studies of the diploid human fungal pathogen *Candida albicans*. Eukaryot. Cell **4:**298–309.
27. **O'Rourke, S. M., and I. Herskowitz.** 2002. A third osmosensing branch in *Saccharomyces cerevisiae* requires the Msb2 protein and functions in parallel with the Sho1 branch. Mol. Cell. Biol. **22:**4739–4749.
28. **O'Rourke, S. M., and I. Herskowitz.** 2004. Unique and redundant roles for HOG MAPK pathway components as revealed by whole-genome expression analysis. Mol. Biol. Cell **15:**532–542.
29. **Pfaller, M. A., D. J. Diekema, R. N. Jones, H. S. Sader, A. C. Fluit, R. J. Hollis, and S. A. Messer.** 2001. International surveillance of bloodstream infections due to *Candida* species: frequency of occurrence and in vitro susceptibilities to fluconazole, ravuconazole, and voriconazole of isolates collected from 1997 through 1999 in the SENTRY antimicrobial surveillance program. J. Clin. Microbiol. **39:**3254–3259.
30. **Posas, F., M. Takekawa, and H. Saito.** 1998. Signal transduction by MAP kinase cascades in budding yeast. Curr. Opin. Microbiol. **1:**175–182.
31. **Posas, F., E. A. Witten, and H. Saito.** 1998. Requirement of *STE50* for osmostress-induced activation of the *STE11* mitogen-activated protein kinase kinase kinase in the high-osmolarity glycerol response pathway. Mol. Cell. Biol. **18:**5788–5796.
32. **Posas, F., S. M. Wurgler-Murphy, T. Maeda, E. A. Witten, T. C. Thai, and H. Saito.** 1996. Yeast *HOG1* MAP kinase cascade is regulated by a multistep phosphorelay mechanism in the *SLN1-YPD1-SSK1* "two-component" osmosensor. Cell **86:**865–875.
33. **Raitt, D. C., F. Posas, and H. Saito.** 2000. Yeast Cdc42 GTPase and Ste20 PAK-like kinase regulate Sho1-dependent activation of the Hog1 MAPK pathway. EMBO J. **19:**4623–4631.
34. **Reuss, O., A. Vik, R. Kolter, and J. Morschhäuser.** 2004. The *SAT1* flipper, an optimized tool for gene disruption in *Candida albicans*. Gene **341:**119–127.
35. **Richardson, M. D.** 2005. Changing patterns and trends in systemic fungal infections. J. Antimicrob. Chemother. **56**(Suppl. 1)**:**i5–i11.
36. **Rohde, J. R., and M. E. Cardenas.** 2004. Nutrient signaling through TOR kinases controls gene expression and cellular differentiation in fungi. Curr. Top. Microbiol. Immunol. **279:**53–72.
37. **Roman, E., C. Nombela, and J. Pla.** 2005. The Sho1 adaptor protein links oxidative stress to morphogenesis and cell wall biosynthesis in the fungal pathogen *Candida albicans*. Mol. Cell. Biol. **25:**10611–10627.
38. **Rothstein, R. J.** 1983. One-step gene disruption in yeast. Methods Enzymol. **101:**202–211.
39. **Schaber, M., A. Lindgren, K. Schindler, D. Bungard, P. Kaldis, and E. Winter.** 2002. *CAK1* promotes meiosis and spore formation in *Saccharomyces cerevisiae* in a *CDC28*-independent fashion. Mol. Cell. Biol. **22:**57–68.
40. **Schwartz, M. A., and H. D. Madhani.** 2004. Principles of MAP kinase signaling specificity in *Saccharomyces cerevisiae*. Annu. Rev. Genet. **38:**725–748.
41. **Shen, J., W. Guo, and J. R. Kohler.** 2005. *CaNAT1*, a heterologous dominant selectable marker for transformation of *Candida albicans* and other pathogenic *Candida* species. Infect. Immun. **73:**1239–1242.
42. **Smith, D. A., S. Nicholls, B. A. Morgan, A. J. Brown, and J. Quinn.** 2004. A conserved stress-activated protein kinase regulates a core stress response in the human pathogen *Candida albicans*. Mol. Biol. Cell **15:**4179–4190.
43. **Tatebayashi, K., K. Yamamoto, K. Tanaka, T. Tomida, T. Maruoka, E. Kasukawa, and H. Saito.** 2006. Adaptor functions of Cdc42, Ste50, and Sho1 in the yeast osmoregulatory HOG MAPK pathway. EMBO J. **25:**3033–3044.
44. **van Drogen, F., and M. Peter.** 2002. MAP kinase cascades: scaffolding signal specificity. Curr. Biol. **12:**R53–R55.
45. **Weig, M., K. Haynes, T. R. Rogers, O. Kurzai, M. Frosch, and F. A. Mühlschlegel.** 2001. A GAS-like gene family in the pathogenic fungus *Candida glabrata*. Microbiology **147:**2007–2019.
46. **Winkler, A., C. Arkind, C. P. Mattison, A. Burkholder, K. Knoche, and I. Ota.** 2002. Heat stress activates the yeast high-osmolarity glycerol mitogen-activated protein kinase pathway, and protein tyrosine phosphatases are essential under heat stress. Eukaryot. Cell **1:**163–173.

A mutation of the H-loop selectively affects rhodamine transport by the yeast multidrug ABC transporter Pdr5

Robert Ernst, Petra Kueppers, Cornelia Klein, Tobias Schwarzmüller, Karl Kuchler, Lutz Schmitt

PNAS, 2008

ABC transporters of *S. cerevisiae* are a well-studied family of membrane proteins. Many ABC pumps contribute to pleitotropic drug resistance PDR, transporting a huge variety of structurally and functionally diverse compounds. However, the mechanism of action of these pumps is poorly understood. Mutational studies and structural analysis of this protein class can give valuable information about the mode of action.
My contribution to this work included the drug resistance assays of the different *pdr5* mutants testing for sensitivity to azoles, cycloheximide and rhodamine 123 and rhodamine G6 transport assays.

A mutation of the H-loop selectively affects rhodamine transport by the yeast multidrug ABC transporter Pdr5

Robert Ernst*, Petra Kueppers*, Cornelia M. Klein†, Tobias Schwarzmueller†, Karl Kuchler†, and Lutz Schmitt*‡

*Institute of Biochemistry, Heinrich Heine University Duesseldorf, Universitaetsstrasse 1, 40225 Duesseldorf, Germany; and †Max F. Perutz Laboratories, Medical University Vienna, Campus Vienna Biocenter, Dr. Bohr-Gasse 9/2, A-1030 Vienna, Austria

Edited by H. Ronald Kaback, University of California, Los Angeles, CA, and approved February 7, 2008 (received for review January 9, 2008)

The yeast ABC transporter Pdr5 plays a major role in drug resistance against a large number of structurally unrelated compounds. Although Pdr5 has been extensively studied, many important aspects regarding its molecular mechanisms remain unresolved. For example, a striking degeneration of conserved amino acid residues exists in the nucleotide binding domains (NBDs), but their functional relevance is unknown. Here, we performed *in vivo* and *in vitro* experiments to address the functional asymmetry of NBDs. It became evident by ATPase activity and drug transport studies that catalysis at only one of the two NBD composite sites is crucial for protein function. Furthermore, mutations of the proposed "catalytic carboxylate" (E1036) and the "catalytic dyad histidine" (H1068) were characterized. Although a mutation of the glutamate abolished ATPase activity and substrate transport, mutation of H1068 had no influence on ATP consumption. However, the H1068A mutation abolished rhodamine transport *in vivo* and *in vitro*, while leaving the transport of other substrates unaffected. By contrast to mammalian P-glycoprotein (P-gp), the ATPase activity of yeast Pdr5 is not stimulated by the addition of substrates, indicating that Pdr5 is an uncoupled ABC transporter that constantly hydrolyses ATP to ensure active substrate transport. Taken together, our data provide important insights into the molecular mechanism of Pdr5 and suggest that not solely the transmembrane domains dictate substrate selection.

ATPase activity | multidrug resistance | substrate recognition

The plasma membrane ABC transporter Pdr5 is a central element of the pleiotropic drug resistance (PDR) network in the yeast *Saccharomyces cerevisiae* (1). The phenomenon of PDR has received special attention as the Cdr1 orthologue overexpressed in azole-resistant *Candida spp.* hampers therapy of infections with opportunistic fungal pathogens affecting patients with impaired immune systems (2).

Numerous studies unraveled the complex nature of the yeast PDR network (3), which is composed of several stress response factors and transcriptional regulators, ultimately controlling expression of *PDR5* and related drug pumps (4). Pdr5 is the most abundant ABC transporter in *S. cerevisiae*, capable of extruding hundreds of structurally unrelated hydrophobic compounds across the plasma membrane in an ATP-dependent manner (5–7). The discovery that mutations in the transcription factor Pdr1 lead to a dramatic overexpression of *PDR5* has opened the possibility to study the function of this ABC transporter *in vivo* and *in vitro* (5–8). Characterization in a cellular context and/or the native membrane environment provide an excellent tool to assay the substrate specificity and the ATPase and transport activities without interference from solubilization and purification in detergents, which have also been proposed to be substrates of Pdr5 (9).

Like all functional ABC transporters, Pdr5 carries two transmembrane domains (TMDs) and two nucleotide binding domains (NBDs). The NBDs contain all characteristic sequence motifs of ABC proteins, such as the Walker A and B motifs; the C-loop, the hallmark of the ABC family; and the H- and D-loop sequences (10). However, the primary structure of Pdr5 reveals a profound asymmetry between the two NBDs (Fig. 1*A*). The highly conserved lysine of the Walker A motif and the histidine of the H-loop are missing in the N-terminal NBD (NBD1), whereas the C-loop sequence in the C-terminal NBD (NBD2) deviates from the canonical amino acids (LNVEQ instead of LSGGQ). The crystal structures of isolated NBDs (for a recent review, see ref. 11) and of fully assembled ABC transporters (for example, ref. 12), demonstrated a "head-to-tail" arrangement of NBDs that suggests a functional asymmetry in Pdr5 with one corrupted and one intact catalytic site. Here, the intact site, sandwiched between the Walker A motif of NBD2 and the C-loop of NBD1, will be referred to as the "NBD2 composite" site. The corrupted site, the NBD1 composite site, includes the nonconsensus residues from the Walker A motif of NBD1 and the C-loop of NBD2.

Furthermore, two opposing models of ATP hydrolysis in ABC transporters have been proposed, the "catalytic carboxylate" (13) and the "catalytic dyad" models (14). According to the first model, the glutamate C-terminal to the Walker B motif is essential for ATP hydrolysis. Interestingly, in Pdr5, this glutamate (E1036) is present only in NBD2 but not in NBD1 (Fig. 1*A*). The second, the catalytic dyad model, proposed an interaction between the glutamate and the histidine of the H-loop as a prerequisite for ATP hydrolysis. Again, the histidine is only found in NBD2 of Pdr5 (H1068) (Fig. 1*A*). Remarkably, both models are supported by experimental data (15, 16), and, currently, it is not even clear whether ATP hydrolysis occurs by a single universal mechanism in ABC transporters or whether certain subfamilies use different mechanisms.

A fascinating feature of ABC transporters is the cross-talk between substrate binding and ATP hydrolysis. Many ABC systems display a so-called "basal" ATPase activity in the absence of transport substrates, which, however, is stimulated in the presence of substrates. In the case of P-gp, basal and stimulated ATPase activity are thought to reflect two different modes of operation and are a prerequisite to ensure the proper function of this human drug efflux pump (17). In contrast, the substrate transport and ATP hydrolysis appear strictly coupled in the bacterial uptake systems for histidine and maltose (18, 19), because ATPase activity is only observed in presence of transport substrates in reconstituted systems. The existence of cou-

Author contributions: R.E., K.K., and L.S. designed research; R.E., P.K., C.M.K., and T.S. performed research; R.E., P.K., K.K., and L.S. analyzed data; and R.E., K.K., and L.S. wrote the paper.

The authors declare no conflict of interest.

This article is a PNAS Direct Submission.

‡To whom correspondence should be addressed. E-mail: lutz.schmitt@uni-duesseldorf.de.

This article contains supporting information online at www.pnas.org/cgi/content/full/0800191105/DCSupplemental.

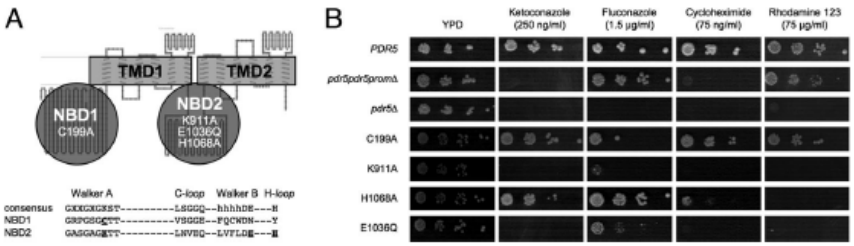

Fig. 1. Mutational analysis of Pdr5. (*A*) Schematic representation based on a membrane topology prediction of Pdr5 [supporting information (SI) Fig. S1]. Mutants within NBD1 or NBD2 used in this study are indicated. (*B*) Drug resistance assays with *PDR5* variants. Serial dilutions of WT cells, isogenic *pdr5pdr5prom*Δ and *pdr5*Δ null mutant cells, and cells expressing mutants of *PDR5* were spotted on drug agar plates.

pled and partially uncoupled systems raises the question of the evolutionarily benefit from an energy-wasting uncoupled mode.

Here, we report functional and mutational studies of Pdr5 in yeast cells and in highly enriched plasma membrane preparations. The results shed new light on the functional asymmetry of both NBDs and suggest that substrate selection in this eukaryotic multidrug transporter might be dictated not only by the TMDs, but presumably also by nucleotide-protein interactions.

Results

Functional Characterization of Pdr5. We performed site-directed mutagenesis of the *S. cerevisiae* multidrug transporter Pdr5 to study its mechanism of ATP hydrolysis. The constructed mutants were characterized *in vivo* by analyzing their substrate specificities, and *in vitro* via ATPase and transport assays, using preparations of highly enriched plasma membranes.

Drug Resistance Phenotypes of *PDR5* Mutants. The most straightforward methods to analyze the functionality of Pdr5 are drug susceptibility assays either on drug agar plates (Fig. 1*B*) or in liquid culture (Fig. S2) (1). As expected, cells overexpressing *PDR5* are highly resistant to ketoconazole (KA), fluconazole (FA), cycloheximide (CHX), and rhodamine 123 (R123) (Fig. 1*B*, *PDR5*) (5, 20, 21), whereas cells deleted of *PDR5* were highly susceptible to all tested drugs (Fig. 1*B*, *pdr5*Δ). Because the presence of a removable N-terminal histidine-tag did not affect Pdr5-dependent drug resistance phenotypes or its expression levels (data not shown), we used only the tagged Pdr5 version in all subsequent experiments.

The disruption of the *PDR5* promotor and *PDR5* (for details, see *SI Text*) resulted in cells being more resistant against FA and R123 when compared with cells lacking only *PDR5* (Fig. 1*B*; *pdr5pdr5prom*Δ). Immuno-detection of Pdr5 in a crude cell extract confirmed the complete absence of Pdr5 (data not shown). Therefore, the observed drug resistance can depend only on the *PDR5* promotor, not *PDR5*. Interestingly, the *PDR5* promotor acts bidirectionally, also controlling expression of *YOR152C*, which may be involved in the phenomenon of drug resistance as well (4, 9).

We constructed mutant variants of Pdr5 and used cell-based resistance assays to address (*i*) the function of NBD1 and NBD2 and (*ii*) the mechanism of ATP hydrolysis. The asymmetry of NBD1 and NBD2, already evident from the primary structure, was assessed by mutation of highly conserved residues within the Walker A sequence motifs (Fig. 1*A*, C199A and K911A). Both residues may be essential for ATP hydrolysis and transport activity in related (22–24) and more distant ABC transporters (25, 26). In the case of Pdr5, mutation of the Walker A cysteine in NBD1 resulted in cells with a drug resistance phenotype undistinguishable from WT cells (Fig. 1*B*, C199A). The corresponding mutation in NBD2 (K911A) resulted in hypersensitive cells against all tested drugs with the only exception (Fig. 1*B*, K911A) of a very modest resistance to FA. This result was confirmed in an alternative drug susceptibility assay in liquid culture (Fig. S2), and may be due to alternative drug resistance mechanisms controlled by the expression of the *YOR152C* gene neighbouring *PDR5* (see above).

Taken together, these data clearly demonstrate a functional nonequivalence of NBD1 and NBD2 in Pdr5. Consistent with previous studies, a catalytically active NBD1 composite site appears to be dispensable for protein function, whereas the NBD2 composite site is essential for drug transport.

To test, whether Pdr5 hydrolyzes ATP according to the catalytic carboxylate or the catalytic dyad model, the glutamate adjacent to the Walker B motif and the histidine of the H-loop in NBD2, individually proposed to be essential for catalytic activity, were mutated to glutamine and alanine, respectively (Fig. 1*A*, E1036Q and H1068A). Cells expressing the E1036Q mutant were highly sensitive against all tested drugs, with only residual resistance against FA (Fig. 1*B*, E1036Q). However, cells expressing the H1068A mutant are highly resistant to KA, FA, and CHX but exhibit a dramatic loss of resistance to R123 (Fig. 1*B*, H1068A). This was confirmed by liquid culture assays (Fig. S2). Therefore, this histidine is not essential for Pdr5 function, and ATP is most likely hydrolyzed by the catalytic carboxylate mechanism. However, the loss of resistance against R123 in the H1068A mutant raises the question for the role of the H-loop in the selection of substrates.

Isolation of *S. cerevisiae* Plasma Membranes. For a more detailed analysis of the constructed *PDR5* mutants, we isolated plasma membranes from mutant cells according to a protocol pioneered by Goffeau and coworkers (7, 27). A specific band could be assigned to Pdr5 (asterisk in Fig. 2 *Upper*) but was missing in control membranes from *pdr5*Δ cells. This was further confirmed by immunodetection of Pdr5 (Fig. 2 *Lower*). No immunoreactivity was observed for plasma membranes isolated from *pdr5*Δ cells. The identity of the second prominent band in the Coomassie-stained SDS/PAGE (double asterisks in Fig. 2 *Upper*) was analyzed by mass spectrometry and identified as the plasma membrane ATPase Pma1 (data not shown).

ATPase Activity of Pdr5. Isolated plasma membranes were subsequently used to characterize the Pdr5-specific ATPase activity. The ATPase activity of Pdr5 peaks over a relatively broad pH range (Fig. 3*A*, Pdr5 WT) and was reduced severely by the addition of 20 μg/ml oligomycin (OM). The maximal OM-sensitive ATPase activity of 2.2 ± 0.3 $\mu mol \cdot (mg \cdot min)^{-1}$ was determined at pH 9.5. Control membranes lacking Pdr5 exhibited only background activity of 0.20 ± 0.02 $\mu mol \cdot (mg \cdot min)^{-1}$ (Fig. 3*A*, no Pdr5).

How do the results from the drug susceptibility assays relate to ATPase activities observed for mutants of NBD1 and NBD2? As depicted in Fig. 3*B*, the C199A mutant (Walker A motif of

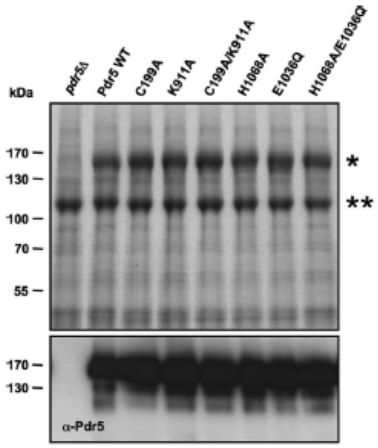

Fig. 2. Expression of Pdr5 variants. (*Upper*) Isolated plasma membrane fractions (15 μg/lane) were fractionated through a 7% SDS/PAGE and stained with Coomassie blue. The two major bands correspond to Pdr5 (*) and to the plasma membrane ATPase Pma1 (**). The positions of molecular mass markers are indicated at *Left*. (*Lower*) The identity of Pdr5 was verified by immunoblotting with Pdr5-specific antibodies.

NBD1) exhibited an ATPase activity identical to WT Pdr5 [1.9 ± 0.2 μmol·(mg·min)$^{-1}$]. In contrast, the equivalent mutation K911A in NBD2 strongly impaired the ATPase activity [0.4 ± 0.1 μmol·(mg·min)$^{-1}$]. These results mirror the observations of the drug susceptibility assays, which identified a crucial role of the NBD2 composite site for protein function.

Further insights into the mechanism of ATP hydrolysis were obtained from the analysis of the H1068A and E1036Q mutants. If the proposed catalytic carboxylate is mutated (E1036Q), no significant Pdr5-specific ATPase activity was detectable [0.3 ± 0.1 μmol·(mg·min)$^{-1}$]. The H1068A mutant should exhibit, according to the catalytic dyad model, no Pdr5-specific ATPase activity. However, the steady-state ATPase activity of the H1068A mutant was identical to WT Pdr5 [2.0 ± 0.3 μmol·(mg·min)$^{-1}$].

Transport Activity of Pdr5 and Its Mutant Variants. In parallel to the ATPase activity, we analyzed the capability of Pdr5 and its mutant variants to transport rhodamine 6G (R6G) *in vitro*. Active transport of this fluorescent dye is monitored by an ATP-, Mg^{2+}-, and Pdr5-dependent fluorescence quenching reaction, which reflects the concentration-dependent formation of non-fluorescent R6G excimers upon its redistribution between the leaflets of the plasma membrane bilayer (7). Full reversibility of R6G quenching was confirmed with several inhibitors, such as OM, vanadate, beryllium fluoride, FK506, or EDTA (Fig. S3).

Only membranes containing Pdr5 mediated dye transport (Fig. 3*D*, Pdr5 WT and no Pdr5). Mutants with abolished ATPase activity exhibited no active transport, demonstrating that ATPase activity is a prerequisite for transport. Analysis of the transport activities of Walker A variants (Fig. 3*E*, C199A and K911A) provided further proof for the functional asymmetry of NBD1 and NBD2. The K911A mutant in NBD2 abolished Pdr5-mediated dye transport, whereas the equivalent mutation in NBD1 (C199A) exhibited similar dye transport as WT Pdr5. Taken together, the presented *in vivo* and *in vitro* data provide compelling evidence that ATP hydrolysis and active drug transport are catalyzed exclusively by the NBD2 composite site.

The central role of a functional NBD2 for drug transport becomes even more evident, when the transport assay was performed with additional mutants. Significantly, the H1068A and E1036Q mutations (both located in NBD2) abolished active dye transport (Fig. 3*F*, H1068A and E1036Q). Numerous independent studies on different ABC transporters proposed a crucial role for these residues in ATP hydrolysis. However, the H1068A mutation impaired solely R6G transport and had no impact on the observed steady-state ATPase activity (Fig. 3*C*, H1068A). According to available crystal structures, this residue is most likely in close proximity to the γ-phosphate of ATP (14, 25, 28). If this holds true for Pdr5 as well, it implies that the absence of the histidine in the H1068A mutant directly or

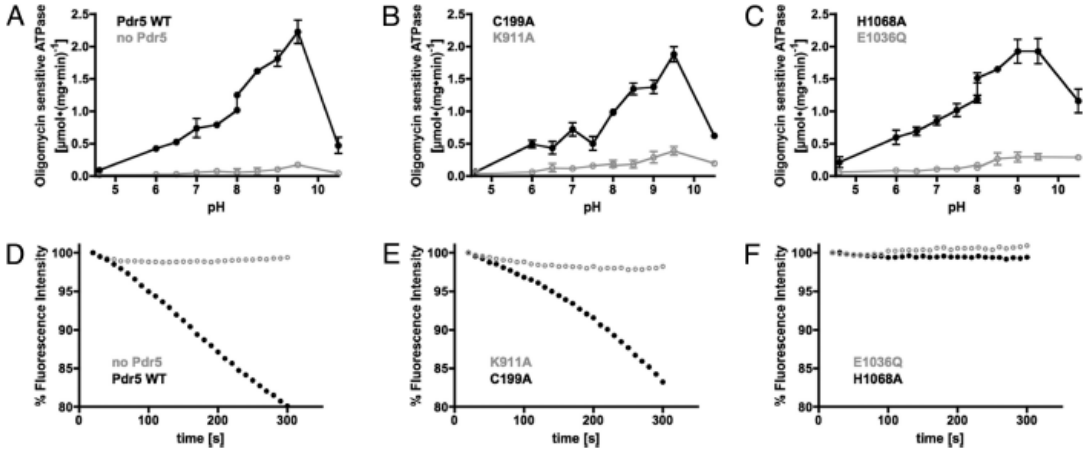

Fig. 3. Pdr5-specific ATPase activity and R6G transport. (*A–C*) OM-sensitive ATPase activities of plasma membrane preparations derived from cells overexpressing N-terminally 14-His-tagged Pdr5 (Pdr5 WT) and of control membranes derived from isogenic *pdr5*Δ cells (no Pdr5) (*A*) was assayed and plotted against pH values. The asymmetry of the NBDs was analyzed by using two mutants (C199A and K911A) (*B*). Furthermore, the role of the glutamate adjacent to the Walker B motif (E1036Q) and the histidine of the H-loop (H1068A) were assayed (*C*). (*D–F*) Isolated plasma membranes were incubated with R6G, and the fluorescence signal was recorded after the addition of Mg^{2+}/ATP (t = 0 s). (*D*) A decrease in R6G fluorescence represents active transport and is only observed in plasma membranes containing N-terminally 14-His-tagged Pdr5 (Pdr5 WT) but not in control membranes derived from isogenic *pdr5*Δ cells (no Pdr5). (*E*) The asymmetric role of the NBDs for R6G transport was analyzed by the C199A and the K911A mutant (C199A and K911A). (*F*) The influence of the H1068A and the E1036Q mutation on ATPase activity was also analyzed.

Table 1. Drug mediated inhibition of Pdr5-specifc ATPase activity

Drug	$K_{i,\ WT}$, μM	$K_{i,\ H1068A}$, μM	$K_{i,\ H1068A}/K_{i,\ WT}$	*F* test	*n*
R123	13.7 ± 3.6	50.3 ± 11.0	3.7	$P < 0.05$	2
R6G	0.6 ± 0.1	1.8 ± 0.2	2.8	$P < 0.0001$	5
KA	5.4 ± 0.8	4.2 ± 0.7	equal	$P > 0.05$	2
FK506	0.05 ± 0.01	0.12 ± 0.04	2.4	$P < 0.05$	2

indirectly affects the R6G selection at the substrate binding site. To learn more about this intimate cross-talk, we determined the impact of several drugs on the Pdr5-specific ATPase activities.

ATPase Activity of Pdr5 Is Uncoupled from Drug Transport. Many ABC transporters exhibit a severalfold stimulated ATPase activity in the presence of their transport substrate. However, many ABC transporters display also a so-called basal or "substrate-uncoupled" ATPase activity that was observed even in the absence of substrates (29). In the case of P-gp, the ATPase activity exhibits a biphasic response to transport substrates. At low concentrations of added drugs, the basal ATPase activity is stimulated severalfold (30), whereas it is inhibited at higher concentrations. Hence, we determined ATPase activities of Pdr5 in the presence or absence of well known substrates (FA, KA, CHX, and R6G) and an inhibitor of Pdr5-mediated drug resistance (FK506) at different concentrations ranging from picomolars to millimolars (see Fig. S4). Remarkably, no significant stimulation of ATPase activity above the basal level could be observed for all tested drugs. However, some of the tested substances, including R6G, inhibited the Pdr5-specific ATPase activity at high concentrations (Fig. S4). The data were fitted by using a model for ATPase inhibition by inhibitory drug concentrations (Eq. **1**). The K_i values for this inactivation are summarized in Table 1. *n* represents the number of independent experiments. The *F* test was used to test the assumption that the K_i value of the H1068A mutant and the WT version were distinct. The assumption was only rejected for KA ($P > 0.05$). Thus, significantly higher concentrations of R6G, R123, and FK506 were required to inhibit the H1068A mutant compared with WT Pdr5. Smaller molecules like FA and CHX did not inhibit the ATPase activity of both Pdr5 versions (data not shown). Thus, consistent with data from systematic studies by Golin *et al.*, it became evident that a strong size dependence determines the interaction between Pdr5 and its substrates (6, 31).

Discussion

Functional Asymmetry in Pdr5. Our parallel *in vitro* and *in vivo* analysis of Pdr5 revealed nonequivalent functions of NBD1 and NBD2 (Figs. 1 and 3). ATP-hydrolysis at the NBD1 composite site is negligible, whereas ATP-hydrolysis at the NBD2 composite site is essential for drug transport. Consistent with our data, similar observations have been made in earlier studies of Pdr5 and the closely related multidrug transporter Cdr1 from *Candida glabrata* (5, 24). In sharp contrast, other studies indicated a critical role of the Walker A motif in the NBD1 of Cdr1 from *C. albicans* for ATPase activity and transport (22, 23). However, swapping experiments between NBD1 and NBD2 in Cdr1 support our interpretation that ATP hydrolysis at the NBD2 composite site is more critical for protein function (32). Such functional asymmetry has also been described for other related ABC transporters (25, 33, 34). Thus, the role of the NBD1 composite site could be architectural, by providing in its nucleotide bound form a platform for the interaction with the opposing NBD, or regulatory, as proposed for the N-terminal NBD of the cystic fibrosis transmembrane conductance regulator (33).

Residues involved in ATP hydrolysis. Numerous studies in the field of ABC transporters were dedicated to the mechanism of ATP hydrolysis. Because of the complex and to some extent contradicting data, this issue remains under dispute (13–16, 25, 34). As already stated above, two mutually exclusive models have been proposed. Our simplistic approach in this study was to mutagenize two key residues, each of them individually proposed to be essential (Figs. 1*B* and 3*C*). The functional characterization of these mutant variants resulted in several major observations: First, the proposed catalytic carboxylate E1036 adjacent to the Walker B motif is essential for ATP hydrolysis. Second, the mutation of H1068, according to the catalytic dyad essential for ATP hydrolysis, did not have any impact on the observed steady-state ATPase activity. Third, the basal ATPase activity was not stimulated by any substrate tested, implying that ATPase and transport are uncoupled in Pdr5 (Fig. S4). Fourth, and most important, the mutation of H1068 selectively abolished transport of R6G by Pdr5 (Fig. 1*B*).

Not surprisingly, because the proposed catalytic carboxylate E1036 is crucial for ATP hydrolysis, it is essential for R6G transport and mediating drug resistance in living cells as well. Notably, and in contrast to other ABC systems (14, 35, 36), Pdr5 is the first ABC transporter for which a mutation of the H-loop histidine to alanine did not affect the steady-state ATPase activity. Strikingly, the observation that the H1068A mutation abolishes R6G transport without any impact on the observed ATPase activity clearly represents a novelty in the field of ABC transporters (Fig. 3).

Uncoupled ATPase activity of Pdr5. We determined the steady-state ATPase activity of Pdr5 in the presence of different substrates (Table 1 and Fig. S4) to further investigate the communication between substrate binding and ATP hydrolysis. Because none of the substrates stimulated the steady-state ATPase activity of Pdr5 we concluded that Pdr5 is a strictly uncoupled transport system exhibiting only basal ATPase activity. Several substrates, however, even inhibited the ATPase activity of Pdr5, implying that substrate release from the transporter may be rate-limiting. Most likely, this inhibition is due to a substrate-mediated lock of the outward facing conformation. Taking into account the observations by Golin *et al.*, this substrate-mediated inhibition appears to require a certain substrate size (6, 31).

Many ABC transporters have been shown to exhibit basal ATPase activity, which is stimulated in the presence of transport substrates. P-gp, for example, switches between these two modes: a basal uncoupled mode and a substrate-dependent coupled mode (17). Prerequisite for such behavior is an intense cross-talk between substrate binding and ATP hydrolysis. However, in the case of the bacterial importers for histidine and maltose, it has been demonstrated that substrate transport and ATP hydrolysis are strictly coupled (18, 19). Interestingly, the ATPase activity is strictly dependent on the H-loop histidine in these systems. In marked contrast, the uncoupled system Pdr5 exhibits only basal ATPase activity (Fig. S4), which is not influenced by mutation of the histidine of the H-loop (Fig. 3). Whether or not this is only coincidence remains to be established.

Does the basal, uncoupled ATPase activity of Pdr5 mean a great waste of energy and an evolutionarily drawback? Interestingly, also in the case of the closely related multidrug transporter Cdr1 from *C. albicans*, if at all, only a very minor stimulation (<50%) of the basal ATPase activity is observed in the presence of drugs (23). Obviously, the waste of energy by futile, basal ATP hydrolysis is evolutionarily conserved. First of all, this is no surprise because a strictly coupled multidrug transporter is extremely hard to envision. How can thousands of different inputs (binding of highly diverse substrates) give rise to a single specific answer (stimulated ATP hydrolysis and coupled transport)? As proposed for P-gp, the constant turnover of ATP may

be necessary in Pdr5 and related fungal ABC transporters to induce conformational changes that always keep the cytosolic substrate binding sites accessible (17, 30). Thus, instead of being a waste of energy, the basal ATPase activity might represent a concept indispensable to life by keeping the protein in a transport-competent conformation, representing an open "guarding mode conformation" for rapid detoxification events.

Mutation of H-Loop Selectively Abolishes Transport of R6G. Even though Pdr5 is a highly uncoupled transport system, some cross-talk between substrate binding and ATP hydrolysis appears to be conserved. Surprisingly, the H1068A mutation selectively abolished the transport of R6G despite of its expendability for steady-state ATPase activity. Mutant cells showed normal resistance against FA and KA, but were highly susceptible to R123 (Fig. 1). A complete loss of R6G transport activity was confirmed *in vitro* (Fig. 3). Because R6G is still capable to inhibit the activity of the H1068A mutant (Table 1), presumably by locking the outward facing conformation, we assume that this mutation rather affects the duration of the initial drug binding during nucleotide exchange, when Pdr5 is in the inward facing conformation.

Previously, the histidine of the H-loop has been designated a "linchpin" because of its intense interactions within a catalytic dyad with the γ-phosphate of bound ATP and the conserved D-loop to the opposing NBD (14). Mutation of this residue may have structural effects on the substrate binding site via this network of interactions and explains the changed substrate specificity. However, a much more likely interpretation is that substrate selection by Pdr5 is not only determined by static structural features but also by kinetics. Crucial to an understanding is that, even though it does not affect the steady-state ATPase activity, the H1068A mutant might have changed the kinetics of certain substeps of the catalytic cycle, such as nucleotide binding, hydrolysis, or release, which appear not to be rate-limiting. Manipulating the kinetics of nucleotide binding and release either by mutation (presumably H1068A) or by the use of different nucleotides (e.g., UTP instead of ATP) will change the equilibration time of transport substrates with the inward facing drug binding site. Because also each drug exhibits specific on- and off-rates upon binding and release, an altered duration of equilibration (and competition) between substrates and the drug binding site would result in an altered selection of substrates as well. Such kinetic substrate selection can also explain the somewhat mysterious observation that, even though it is efficiently hydrolyzed by Pdr5, UTP does not mediate R6G transport (7).

Remarkably, also the ATPase inhibition characteristics were altered by the H1068A mutation. In contrast to WT Pdr5, R6G is not efficiently transported to the outward facing drug binding site in the H1068A mutant. Therefore, this binding site is less populated in the H1068A mutant and higher drug concentrations are required for saturation, which then results in the inhibition of ATPase activity by a conformational lock. Consistent with this model, the K_i value for KA, which is efficiently transported by WT Pdr5 and the H1068A mutant, is identical for both variants. Thus, differences in inhibition are only a consequence of the altered substrate selection (Table 1).

The idea of a kinetic substrate selection is strongly supported by other mutations identified in the NBDs of Pdr5 (5, 37) and is consistent with the different inhibition of the Pdr5-specific ATPase and UTPase activities by diverse drugs (8). Very recently, it was proposed that GTP and ATP might be used as an energy source for substrate transport. Fully consistent with our proposed model, the Pdr5-specific ATPase and GTPase activities were differently inhibited by clotrimazole (38), implying that protein-nucleotide interactions dictate substrate selection and presumably as a consequence ATPase activity inhibition.

In summary, the lack of any observable substrate stimulation implies that Pdr5 is functioning as an uncoupled ABC transporter, i.e., that ATP is constantly hydrolyzed even in the absence of a transport substrate. The new observation that a H1068A mutation abolished R6G transport without affecting the steady-state ATPase activity contributes to the molecular understanding of the communication between substrate binding and ATP hydrolysis and will pave the way for future investigations related to the dynamics of substrate selection, using purified Pdr5 in reconstituted systems.

Materials and Methods

Materials. All chemicals were reagent-grade and obtained from commercial sources. OM represents a mixture of components A, B, and C. Stock solutions of KA, FA, CHX, OM, and FK506 were prepared in dimethyl sulfoxide, and R6G and R123 were dissolved in ethanol.

Yeast Strains and Plasmid Mutagenesis. Yeast strains were cultured either in rich medium (YPD) and synthetic medium supplemented with appropriate auxotrophic components. The following *S. cerevisiae* strains were used in this study: YALF-A1 (*MATa; ura3-52 trp1-1 leu2-3,112 his3-11,15 ade2-1 PDR1-3*), YHW-A5 (*MATa ura3-52 trp1-1 leu2-3,112 his3-11,15 ade2-1 PDR1-3 pdr5Δ::TRP1*) from the K.K. laboratory strain collection, and YRE1001 (*MATa ura3-52 trp1-1 leu2-3,112 his3-11,15 ade2-1 pdr1-3 pdr5pdr5promΔ::TRP1*). A detailed description of plasmid and strain construction can be found in *SI Text*. Site-directed mutagenesis of *PDR5* was performed on plasmid pRE5 with the QuikChange II XL site-directed mutagenesis kit (Stratagene).

Drug Resistance Assays. Drug resistance assays were performed essentially as described, by spotting serial dilutions of exponentially growing cell cultures from a fresh liquid YPD culture onto appropriate drug containing plates (5, 39).

Isolation of Plasma Membranes. Cells were grown in YPD at 30°C. At an OD_{600} of 1.5, the nitrogen source was refreshed by addition of a 10th volume of 5× YP (50 g/liter yeast extract; 100 g/liter tryptone/peptone). Cells were harvested at OD_{600} = 3.5. The isolation of plasma membranes was performed essentially as described in ref. 7. Further information is provided in *SI Text*.

Rhodamine 6G Transport Assay. Active R6G transport was recorded according to the protocol developed by Kolaczkowski *et al.*, using a Fluorolog II fluorescence spectrometer (Horiba) (7). Isolated plasma membranes (30 μg of protein) were resuspended in 1 ml of transport buffer [50 mM Hepes (pH 7.0), 5 mM $MgCl_2$, 150 nM R6G, and 10 mM azide] and incubated at 35°C. Transport was initiated by addition of 4 mM ATP. To stop transport reactions, 20 μg/ml OM was added to the solution.

ATPase Activity Assays. OM-sensitive ATPase activity of plasma membrane fractions was measured by a colorimetric assay and performed in 96-well microtiter plates (27, 40, 41). Further information is provided in *SI Text*.

Drug Titrations. Drug titrations of ATPase activities were fitted to a steady-state kinetic model (30). This model describes the observed inhibition of the basal Pdr5-specific ATPase activity by increased drug concentrations. The equation represents a simplification of the nonpartitioning model described for human P-glycoprotein (ABCB1) (30) and is given by

$$v = 100 \times \frac{1 - [\text{drug}]}{K_i + [\text{drug}]}, \qquad [1]$$

where v is the percentage of residual ATPase activity, [drug] is the drug concentration in mol/liter, and K_i is the inhibition constant.

ACKNOWLEDGMENTS. We thank Robin Klemm, Gergely Szakacs, Joost Holthuis, Gerrit van Meer, and Sander Smits for stimulating discussions and constant support. This work was supported by European Molecular Biology Organization Short-Term Fellowship ASFT 193-2004 (to R.E.), Deutsche Forschungsgemeinschaft Grant Sch1279/5-3 (to L.S.), Austrian Science Foundation Project FWF-SFB35-04 (to K.K.), a grant from the transnational SysMO program (Project MOSES) (to K.K.), and European Commission FP6 Marie Curie Training Network "Flippases" Grant MCRTN-CT-2004-005330 (to K.K.). C.M.K. was supported by a Marie-Curie Early Stage Training Fellowship through Flippases.

1. Ernst R, Klemm R, Schmitt L, Kuchler K (2005) Yeast ATP-binding cassette transporters: Cellular cleaning pumps. *Methods Enzymol* 400:460–484.
2. Sanglard D (2002) Resistance of human fungal pathogens to antifungal drugs. *Curr Opin Microbiol* 5:379–385.
3. Sipos G, Kuchler K (2006) Fungal ATP-binding cassette (ABC) transporters in drug resistance & detoxification. *Curr Drug Targets* 7:471–481.
4. DeRisi J, *et al.* (2000) Genome microarray analysis of transcriptional activation in multidrug resistance yeast mutants. *FEBS Lett* 470:156–160.
5. Egner R, Rosenthal FE, Kralli A, Sanglard D, Kuchler K (1998) Genetic separation of FK506 susceptibility and drug transport in the yeast Pdr5 ATP-binding cassette multidrug resistance transporter. *Mol Biol Cell* 9:523–543.
6. Golin J, Ambudkar SV, Gottesman MM, Habib AD, Sczepanski J, Ziccardi W, May L (2003) Studies with novel Pdr5p substrates demonstrate a strong size dependence for xenobiotic efflux. *J Biol Chem* 278:5963–5969.
7. Kolaczkowski M, *et al.* (1996) Anticancer drugs, ionophoric peptides, and steroids as substrates of the yeast multidrug transporter Pdr5p. *J Biol Chem* 271:31543–31548.
8. Conseil G, *et al.* (2000) Prenyl-flavonoids as potent inhibitors of the Pdr5p multidrug ABC transporter from *Saccharomyces cerevisiae*. *Biochemistry* 39:6910–6917.
9. Schuller C, *et al.* (2007) Membrane-active compounds activate the transcription factors Pdr1 and Pdr3 connecting pleiotropic drug resistance and membrane lipid homeostasis in *Saccharomyces cerevisiae*. *Mol Biol Cell* 18:4932–4944.
10. Schmitt L, Tampé R (2002) Structure and mechanism of ABC-transporters. *Cur Opin Struc Biol* 12:754–760.
11. Oswald C, Holland IB, Schmitt L (2006) The motor domains of ABC-transporters. What can structures tell us? *Naunyn Schmiedebergs Arch Pharmacol* 372:385–399.
12. Dawson RJ, Locher KP (2006) Structure of a bacterial multidrug ABC transporter. *Nature* 443:180–185.
13. Orelle C, Dalmas O, Gros P, Di Pietro A, Jault JM (2003) The conserved glutamate residue adjacent to the Walker-B motif is the catalytic base for ATP hydrolysis in the ATP-binding cassette transporter BmrA. *J Biol Chem* 278:47002–47008.
14. Zaitseva J, Jenewein S, Jumpertz T, Holland IB, Schmitt L (2005) H662 is the linchpin of ATP hydrolysis in the nucleotide-binding domain of the ABC transporter HlyB. *EMBO J* 24:1901–1910.
15. Ernst R, Koch J, Horn C, Tampe R, Schmitt L (2006) Engineering ATPase activity in the isolated ABC cassette of human TAP1. *J Biol Chem* 281:27471–27480.
16. Moody JE, Millen L, Binns D, Hunt JF, Thomas PJ (2002) Cooperative, ATP-dependent association of the nucleotide binding cassettes during the catalytic cycle of ATP-binding cassette transporters. *J Biol Chem* 277:21111–21114.
17. Al-Shawi MK, Omote H (2005) The remarkable transport mechanism of P-glycoprotein: A multidrug transporter. *J Bioenerg Biomembr* 37:489–496.
18. Davidson AL, Shuman HA, Nikaido H (1992) Mechanism of maltose transport in *Escherichia coli*: Transmembrane signaling by periplasmic binding proteins. *Proc Natl Acad Sci USA* 89:2360–2364.
19. Liu CE, Liu PQ, Ames GF (1997) Characterization of the adenosine triphosphatase activity of the periplasmic histidine permease, a traffic ATPase (ABC transporter). *J Biol Chem* 272:21883–21891.
20. Balzi E, Wang M, Leterme S, Van Dyck L, Goffeau A (1994) *PDR5*, a novel yeast multidrug resistance conferring transporter controlled by the transcription regulator *PDR1*. *J Biol Chem* 269:2206–2214.
21. Bissinger PH, Kuchler K (1994) Molecular cloning and expression of the *Saccharomyces cerevisiae STS1* gene product. A yeast ABC transporter conferring mycotoxin resistance. *J Biol Chem* 269:4180–4186.
22. Jha S, *et al.* (2003) Purification and characterization of the N-terminal nucleotide binding domain of an ABC drug transporter of *Candida albicans*: Uncommon cysteine 193 of Walker A is critical for ATP hydrolysis. *Biochemistry* 42:10822–10832.
23. Shukla S, Rai V, Banerjee D, Prasad R (2006) Characterization of Cdr1p, a major multidrug efflux protein of *Candida albicans*: Purified protein is amenable to intrinsic fluorescence analysis. *Biochemistry* 45:2425–2435.
24. Wada S, *et al.* (2005) Phosphorylation of *candida glabrata* ATP-binding cassette transporter Cdr1p regulates drug efflux activity and ATPase stability. *J Biol Chem* 280:94–103.
25. Procko E, Ferrin-O'Connell I, Ng SL, Gaudet R (2006) Distinct structural and functional properties of the ATPase sites in an asymmetric ABC transporter. *Mol Cell* 24:51–62.
26. Szabo K, *et al.* (1998) Drug-stimulated nucleotide trapping in the human multidrug transporter MDR1. Cooperation of the nucleotide binding domains. *J Biol Chem* 273:10132–10138.
27. Goffeau A, Dufour JP (1988) Plasma membrane ATPase from the yeast *Saccharomyces cerevisiae*. *Methods Enzymol* 157:528–533.
28. Smith PC, *et al.* (2002) ATP binding to the motor domain from an ABC transporter drives formation of a nucleotide sandwich dimer. *Mol Cell* 10:139–149.
29. Sauna ZE, Smith MM, Muller M, Kerr KM, Ambudkar SV (2001) The mechanism of action of multidrug-resistance-linked P-glycoprotein. *J Bioenerg Biomembr* 33:481–491.
30. Al-Shawi MK, Polar MK, Omote H, Figler RA (2003) Transition state analysis of the coupling of drug transport to ATP hydrolysis by P-glycoprotein. *J Biol Chem* 278:52629–52640.
31. Golin J, Ambudkar SV, May L (2007) The yeast Pdr5p multidrug transporter: How does it recognize so many substrates? *Biochem Biophys Res Commun* 356:1–5.
32. Jha S, Dabas N, Karnani N, Saini P, Prasad R (2004) ABC multidrug transporter Cdr1p of *Candida albicans* has divergent nucleotide-binding domains which display functional asymmetry. *FEMS Yeast Res* 5:63–72.
33. Gadsby DC, Vergani P, Csanady L (2006) The ABC protein turned chloride channel whose failure causes cystic fibrosis. *Nature* 440:477–483.
34. Payen LF, Gao M, Westlake CJ, Cole SP, Deeley RG (2003) Role of carboxylate residues adjacent to the conserved core Walker B motifs in the catalytic cycle of multidrug resistance protein 1 (ABCC1). *J Biol Chem* 278:38537–38547.
35. Davidson AL, Sharma S (1997) Mutation of a single MalK subunit severely impairs maltose transport activity in *Escherichia coli*. *J Bacteriol* 179:5458–5464.
36. Hofacker M, *et al.* (2007) Structural and functional fingerprint of the mitochondrial ATP-binding cassette transporter Mdl1 from *Saccharomyces cerevisiae*. *J Biol Chem* 282:3951–3961.
37. Tutulan-Cunita AC, Mikoshi M, Mizunuma M, Hirata D, Miyakawa T (2005) Mutational analysis of the yeast multidrug resistance ABC transporter Pdr5p with altered drug specificity. *Genes Cells* 10:409–420.
38. Golin J, *et al.* (2007) Complete inhibition of the Pdr5p multidrug efflux pump ATPase activity by its transport substrate clotrimazole suggests that GTP as well as ATP may be used as an energy source. *Biochemistry* 46:13109–13119.
39. Egner R, Bauer BE, Kuchler K (2000) The transmembrane domain 10 of the yeast Pdr5p ABC antifungal efflux pump determines both substrate specificity and inhibitor susceptibility. *Mol Microbiol* 35:1255–1263.
40. Decottignies A, Kolaczkowski M, Balzi E, Goffeau A (1994) Solubilization and characterization of the overexpressed *PDR5* multidrug resistance nucleotide triphosphatase of yeast. *J Biol Chem* 269:12797–12803.
41. Wada S, *et al.* (2002) Candida glabrata ATP-binding cassette transporters Cdr1p and Pdh1p expressed in a *Saccharomyces cerevisiae* strain deficient in membrane transporters show phosphorylation-dependent pumping properties. *J Biol Chem* 277:46809–46821.

10 Acknowledgements

I would like to thank the following persons:

First of all, I want to thank Karl Kuchler for the opportunity to do my PhD work in his laboratory.

All (former) members of the “Kaku” lab for their help, advice, teaching, discussions, coffee breaks, ice cream on the roof top terrace, good and hard times, Glühwein, Badminton and listening to “Discard Flowthrough”.

I want to thank Suzanne Noble and Alexander Johnson (UCSF) for two weeks in San Francisco teaching me fusion PCR, Biao Ma and Brendan Cormack for strains and discussion, and all the people who use my strains and put me on their paper.
Further, Mads and Andrea for climbing and occasional concert excursions, Heli for his dirty jokes, Niki, Chris and Luise for supporting me psychologically, the C-WG from Regensburg and all non-biology friends from Munich and Garmisch-Partenkirchen, although they don’t have a single clue about what I do. And anybody else I might have forgotten.

Especially, I want to thank Maria for all her love, her endurance to bear my bad mood and all the time I can spend with her. Hopefully more in the future.
And finally, I want to thank my parents, who supported me during all my studies and my two sisters.

Some things in life are bad
They can really make you mad
Other things just make you swear and curse.
When you're chewing on life's gristle
Don't grumble, give a whistle
And this'll help things turn out for the best...

(Eric Idle)

11 Curriculum Vitae

PERSONAL DATA

Name:	Tobias Schwarzmüller
Date of Birth:	9th of October 1976
Place of Birth:	Garmisch-Partenkirchen, Germany

EDUCATION

1983 – 1987	Primary School Garmisch – Partenkirchen (Germany)
1987 – 1996	Secondary School Garmisch – Partenkirchen (Germany)
28th of June 1996	Graduation from Secondary School

STUDIES

1998 – 2003	Studies of Biology at the University of Regensburg (Germany)
2003	Diploma Thesis, University of Regensburg (Germany), PD Dr. J. Stolz, Dept. of Cell Biology & Plant Physiology (Prof. Dr. Tanner): "Regulation of the *S. cerevisiae* Pyridoxin Transporter Tpn1p"
12th of Dec. 2003	Graduation to Dipl. Biol. Univ., University of Regensburg (First Class Honours)
2004 - 2009	PhD Thesis, Laboratory of Prof. Dr. Karl Kuchler, Max F. Perutz Laboratories, University of Vienna (Austria)

CAREER-RELATED ACTIVITIES

2001	Internship, Biochemical Laboratory of the ENT-Division, Klinikum Rechts der Isar, Munich (Germany)
2001 – 2002	Internship with Dr. Tim Hoey and Dr. Songzhu An, Department of Biology, Tularik Inc, South San Francisco (USA)
2004	Research Associate Tularik GmbH, Regensburg (Germany)
2005	Research Stay, Laboratory of Prof. Dr. Alexander Johnson, UCSF, San Francisco (USA)

AWARDS & FELLOWSHIPS

2000	Oskar-Karl-Forster Stipend
2001	DAAD travel grant
2007	YTF grant FEBS Advanced Lecture Course "Human Fungal Pathogens"
2009	Eukaryotic Cell Outstanding Young Investigator Award

EXPERIENCE IN CONGRESS ORGANIZATION

2005	1st FEBS Advanced Lecture Course “Systems Biology”, 350 Participants, Gosau, (Austria)
2006	1st FEBS Special Meeting on ABC Proteins, 350 Participants, Innsbruck (Austria)
2007	32nd FEBS Congress “Molecular Machines”, ~2000 participants Vienna (Austria)

MEMBERSHIP IN PROFESSIONAL SOCIETIES

since 2005	Austrian Society for Biochemistry and Molecular Biology

SCIENTIFIC PRESENTATIONS

2005	Poster Presentation,1st FEBS Advanced Lecture Course “Human Fungal Pathogens”
2005	Poster Presentation, 22nd International Conference on Yeast Genetics and Molecular Biology”
2007	Poster Presentation, 2nd FEBS Advanced Lecture Course “Human Fungal Pathogens”
2007	Oral Presentation, 3rd PhD-Symposium, Medical University of Vienna
2008	Oral Presentation, 9th ASM Conference on Candida and Candidiasis, Jersey City (USA)
2009	Oral Presentation, 3rd FEBS Advanced Lecture Course “Human Fungal Pathogens”